Towards a Better Understanding of Coastal Cliff Erosion in Waitemata Group Rock; Auckland, New Zealand

A thesis submitted in partial fulfilment

of the requirements for the

Degree of

Master of Science in Earth and Ocean Sciences

at the

University of Waikato

by

Jessica Emily Bell

THE UNIVERSITY OF
WAIKATO
Te Whare Wānanga o Waikato

University of Waikato

2007

If the coast is bold and rocky, it speaks a language easy to be interpreted. Its broken and abrupt contour, the deep gulfs and salient promontories by which it is indented, and the proportion which these irregularities bear the force of the waves, combined with the inequality of hardness in the rocks, prove, that the present line of the shore has been determined by the action of the sea…It is true, we do not see the successive steps of this progress exemplified in the states of the same individual rock, but we see them clearly in different individuals; and the conviction thus produced, when the phenomena are sufficiently multiplied and varied, is as irresistible, as if we saw the changes actually effected in the moment of observation.
(Playfair, 1802)

Acknowledgements

First and foremost, my biggest thanks go to my supervisors Dr Vicki Moon and Professor Cam Nelson. Vicki, thank you for the scientific knowledge and the writing wisdom that helped me to improve my story. Cam, thank you for being my mentor from the first ERTH103 lecture and for teaching me to continually analyse and critique my work…It was annoying at the time but I'm sure it's made me a better scientist.

To the staff of the Department of Earth and Ocean Sciences who helped with technical work: Renat Radosinsky, for you help during lab and fieldwork (I still owe you that geological hammer I lost at Leigh!); Dave Palmer, you're my GIS hero; Judi McWhirter, my on-call statistician; and the lecturers - Roger Briggs, Richard Smith, Dave Lowe, Dave Campbell, Steve Hood, Willem de Lange - who have continued to encourage all of us beyond teaching years.

Also, thanks go to staff at the Department of Geology at Auckland University, in particular Paul Williams, for chasing up my queries about their rocks.

Thanks to all of the JAFA's who kept me feed and watered, and provided a bed, while I was doing my fieldwork: Aunty Debi and Uncle Jeff; Aunty Dianne and John; Nana; Anna and Andrew; Ann Long; and The Bell's for having a bach so appropriately placed at Martins Bay. How convenient!

To the uni gang: Miss Anna Marie, Big D, J-hovah, Kate-ahontas, Neil 'inappropriate' Jelley, Natalie, Lauren, Lisa and Nigel – we made it!! Thanks for your support and humour, and the call-up for a social event just when we all needed one. Nig – would it be too cheesy if I said that you are MY rock??

Lastly, to my whantastic whanau! Mum and Dad, you guys are the best!! I've made it out the other side in one piece and that's all thanks to you. Thanks Mel (and Blair) (and Megan) for…hmmm…I guess for just being able to call you all my family, and for giving me the most amazing day off on July 7. Also, to my girls, Lou and Jenn, who have kept me true.

Abstract

The soft sedimentary deposits of the Waitemata Group which outcrop on the eastern coastline of the Auckland region are a coastal cliff erosion hazard. The determination of the rate that these cliffs erode for hazard zonation purposes still requires research. A database has been collated of a range of structural, geological, geomorphic and climate parameters from 16 representative cliff sites in order to statistically assess what parameters influence cliff erosion and why erosion rates vary within the relatively uniform geology.

Four different lithological units have been defined: sandstone beds of turbidites; sandstone beds of densites (contain rip-up clasts); sand to gravel beds of debrites; and siltstone beds. Cliff rock has very weak to weak intact rock strength; apertures of 0.1 to 15 mm; infill types are soft clay and grit, and hard calcite and iron; spacing of discontinuities are smaller in siltstone beds (≥ 5 mm), and up to 5 m in sandstone and debrite beds; bedding and fault planes are continuous, joints are non-continuous; block size is dictated by bed thickness and non-continuous joints. Shore platform widths were used to determine long-term erosion rates which range from 1.2 to 53.0 mm y^{-1}. Platform morphologies are either sloping or horizontal or are a combination of both. Higher platform benches found at some sites are considered to be the result of a higher period of sea-level or are high-tide benches. Intact and rock mass strength increases northwards. Cliff heights are 8 to 38 m; cliff angles are 51 to 79°. Conditions for sporadic planar and wedge failure were determined at some sites; frittered siltstone and low durability sandstone allow smaller-scale, continual erosion. Castor Bay, Army Bay, Waiwera Beach and Leigh Marine Reserve have the lowest rock mass quality. Musick Point, Narrowneck Beach and Waiake Bay have good rock mass quality.

A conceptual model for coastal cliff erosion has been developed for Waitemata Group coastal cliffs, based on the dominant processes that act on the cliffs determined from statistical analysis (student t-test, correlation and regression) and field observations. The primary factor for cliff erosion is bed dip, whereby seaward dipping beds have higher erosion rates than landward dipping beds. The secondary factors for cliff erosion include: the intact and rock mass strength of the rock; the rock mass quality; strength of the siltstone beds; strength and structure of the sandstone beds; and orientation of the bedding planes with respect to the cliff face. Shear stresses are enhanced when beds dip seaward and thus shear failure along continuous surfaces is achievable. When beds dip landward the influence of shear stresses along bedding planes, and their contribution to the removal of individual blocks of rock, is severely inhibited resulting in reduced rates of erosion. There is no relationship between cliff height and erosion rates and cliff heights are mainly controlled by the pre-existing landscape. Cliff angle is controlled by the proportion of sandstone and siltstone (whereby lower cliff angles are more siltstone-dominated), rock mass strength and weathering. Erosion rates do vary in Waitemata Group rock of the Auckland region because of the variation in structural and geomorphic conditions of the cliff, most strongly controlled by the dip angle of bedding planes.

TABLE OF CONTENTS

List of tables

List of figures

CHAPTER ONE

INTRODUCTION

1.1 Coastal Cliff Erosion in the Auckland Region

Coastal cliff erosion is a hazard whereby continual retreat and sudden collapse of the cliff face and cliff top poses a risk to both people and their property. Coastal cliffs are the product of erosion processes that degrade, loosen and strip away the rock and soil material that makes up the exposed land mass. Erosion processes can be both marine and subaerial, and the power of these processes plus the structure and geology of the rock mass itself determine the way in which the cliff erodes. Because of the properties of coastal cliffs however, in certain areas there is a need to appreciate the hazard of the erosion and the level of risk to those who utilize such areas. Cliff-top land provides scenic and panoramic views which get utilized by residential and other properties. Sudden collapse of the cliff can create a hazard to those in the collapse zone, and gradual retreat creates a challenge to the planning of future development on cliff-top land and of the level of risk to already-developed land. Shoreline areas at the base of coastal cliffs can be popular recreational zones and this also creates a risk to people in the event of sudden collapse of the cliff.

In the Auckland region of New Zealand, coastal cliff erosion is a hazard. The Auckland Region (as defined by the territorial boundaries of the Auckland Regional Council) is New Zealand's most populated area, with a booming central city isthmus and northward-sprawling urban development. The Auckland Region (Figure 1.1) houses 1.3 million people, or almost one third of New Zealand's total population, and between 2002 and 2006 the Auckland Region experienced the largest growth for all urban centres of 12.4 % (Census data for usually resident population count; Statistics NZ, 2006).

The Region is bound entirely on the west and east by coastline of which a significant proportion is steep cliff land and coastal cliff erosion is recognised and treated by territorial authorities as a significant hazard (Tonkin and Taylor, 2005a). The Auckland Regional Council governs the hazard assessment and public awareness of coastal cliff erosion for the entire Auckland Region through requirements of the Resource Management Act of 1991.

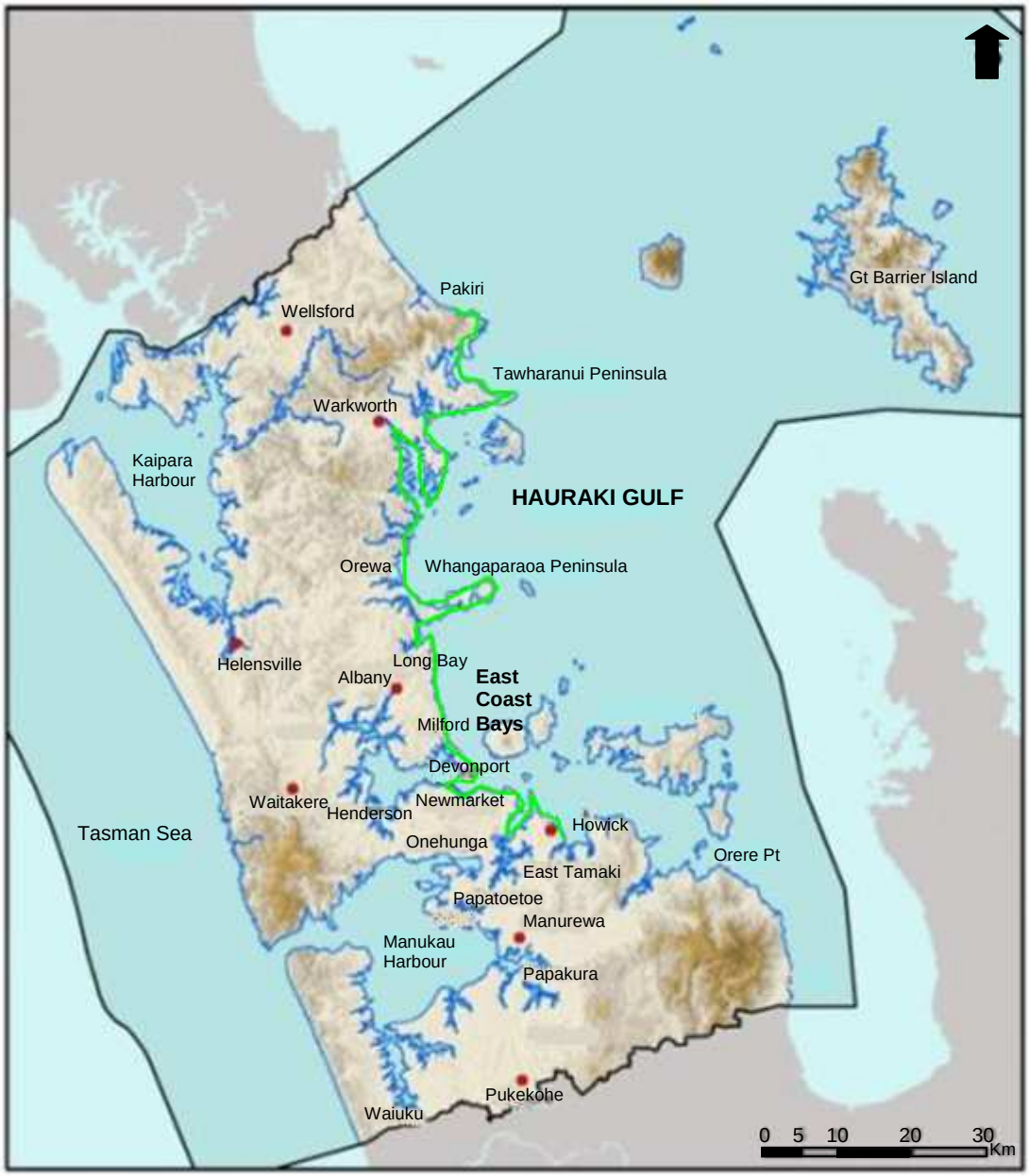

Figure 1.1: Map of Auckland Region as a territorial authority; the study area along the eastern coastline is shown by the green line. Modified from ARC (2007).

Of particular concern and interest are the early Miocene Waitemata Group rocks which crop out on most of the eastern coastline of the Auckland Region. These coastal cliffs comprise weak, alternating sandstone and siltstone flysch beds and volcaniclastic, debris flow beds termed the Parnell Grit (Ballance, 1974). The informal term "Auckland region" will now be used to denote the study area.

The population is especially concentrated along the eastern coastline offering a significant reason why much work has been done on researching the processes and rate of cliff erosion. As a result of such research on coastal cliffs in the Auckland region (Healy, 1967; Healy, 1968; Simpson, 1987; Brodnax, 1991; de la Mare, 1992; Gordon, 1993; Moon and Healy, 1994; Buckeridge, 1995; Glassey *et al.* 2003; de Lange and Moon, 2005; Gulyaev and Buckeridge, 2004; Paterson and Prebble, 2004; Tonkin and Taylor, 2005a; Jongens *et al.* 2007), as well as internationally (Trenhaile, 1973; Sunamura, 1977; Emery and Kuhn, 1982; Trenhaile, 1987; Jones and Williams, 1991; Sunamura, 1992; Benumof and Griggs, 1999; Mano and Suzuki, 1999; Budetta *et al.* 2000; Benumof *et al.* 2000; Woodroffe, 2002; Lahousse and Pierre, 2003; Masselink and Hughes, 2003; Runyan and Griggs, 2003; Zviely and Klein, 2004; Pierre, 2006; Pierre and Lahousse, 2006), many models of the way in which cliffs erode, and a range of methodologies to determine the future extent of erosion, have been established. However, such results often have limited wider applicability, particularly when work is restricted to a particular lithology or is carried out through private consultancies and therefore not published.

With regards to the Waitemata Group, the dominant erosive processes and general geomechanical properties of the various lithologies are reasonably well understood. However, erosion rates vary considerably within this formation and there still appears to be a need to understand what processes influence and affect the rate at which individual cliff sites erode. Subaerial processes have been highlighted as the dominant form of erosion on Waitemata Group coastal cliffs (de Lange and Moon, 2005) and the structure of any coastal cliff has a strong influence on the nature of the erosion (Sunamura, 1992; Selby, 1993; Woodroffe, 2002). Bearing this in mind, it seems necessary to determine whether there are any structural and geological properties of the Waitemata Group coastal cliffs which have a tendency to influence the rate of cliff erosion.

1.2 Research Objectives

Sixteen sites have been selected along the eastern coastline of the Auckland region in a representative range of Waitemata Group rock and a database has been collated of various geological, structural, geomorphic and climate properties at each of these sites. Through comprehensive data collection and statistical analysis of the database **this project aims to determine relationships between cliff erosion rates and geological and structural properties** of the Waitemata Group coastal cliffs with the overall theme of working towards a better understanding of coastal cliff erosion in this region.

The aim of this research will be achieved through the following objectives:

1. Develop a database of geological and structural properties of a representative range of Waitemata Group coastal cliffs through field work, laboratory work and further derived properties.

2. Review GIS databases for basic climate parameters and additional geomorphic and terrain properties at the coastal cliff sites and add these to the data base.

3. Statistically analyse the database to determine the influential processes on the key determinants of a hazard assessment which include coastal cliff erosion rates, cliff height and cliff angle.

4. Review the definitions of sediment gravity flows with respect to the structural properties of the cliffs and compare these to field observations.

5. Review Holocene sea level trends with respect to shore platform development in the Auckland region and compare these to field observations.

6. Develop a conceptual model for coastal cliff erosion based on the statistically significant parameters that influence erosion rates.

7. Determine the influential properties on cliff height and cliff angle from results of the statistical analysis.

1.3 Thesis Structure

Chapter One introduces the topic of coastal cliff erosion in Waitemata Group rock of the Auckland region and outlines the aims for this research. Chapter Two presents a literature review of the Auckland region environment, coastal cliff erosion research and methodologies for determining erosion rates. The methodologies for the field work, laboratory work and further derived properties used in this study are presented in Chapter Three.

Results are given in Chapters Four, Five and Six. Chapter Four details the sites used in this study and presents the results of geotechnical field work. Chapter Five further presents the results of laboratory work and the results of the data analysis that was required to determine additional properties of the Waitemata Group coastal cliffs. Chapter Six presents the statistical analysis of the entire collated database of the properties for Waitemata Group rocks to determine what properties have a major influence on coastal cliff erosion rates.

Based on the analysis of the database, a conceptual model for coastal cliff erosion is presented in Chapter Seven. The main conclusions drawn from this research are outlined in Chapter Eight followed by a discussion of future cliff erosion work that may be done in the Auckland region. All original field, laboratory and statistical data are presented in the Appendices. These include: laboratory test results; rock strength test results; scanline data; stereographic projection; geomorphology parameters; rock mass classification values; the collated database and statistical analysis results.

CHAPTER TWO

LITERATURE REVIEW

2.1 Introduction

This chapter reviews literature regarding coastal cliff erosion, particularly of the Waitemata Group. The geological setting of the Auckland region is first reviewed, followed by discussion of the marine and terrestrial environment in which Waitemata Group coastal cliffs have developed. A new method for classifying the various lithologies in flysch rock is critically analysed with respect to better determining the geomechanical properties that lead to varying forms of erosion. The processes that lead to coastal cliff erosion are presented together with discussion of the methodologies that have been developed to assess the rate and hazard of erosion from international and national literature. Lastly, Quaternary sea-level trends in the Auckland region are discussed with respect to determining long-term erosion rates in Waitemata Group cliffs.

2.2 Geological Setting

2.2.1 Geological history of the Auckland region

There are five main geological groups that coastal cliffs develop in within the Auckland region as illustrated in Figure 2.1, and these include: Mesozoic greywacke basement rock of the Waipapa Group; the Early Miocene western Waitakere Group and Manukau Subgroup; Early Miocene eastern Waitemata Group; the Northland Allochthon; and Holocene volcanic deposits from the Auckland Volcanic Field (Edbrooke, 2001; Edbrooke *et al.* 2003).

During the Rangitata Orogeny in the Jurassic period, greywacke and argillite rocks were uplifted and exposed to erosion and formed the base of the North Island land mass of New Zealand (Searle, 1981). The early Miocene Kaikoura Orogeny saw

downwarping and partial submergence across the North Island as New Zealand was cleaved by two plate boundaries (Searle, 1981) and at this stage the Waitemata Basin, situated in the vicinity of today's Auckland region, subsided and began to be infilled with volcanic and sedimentary material known as Waitemata Group rock.

The Waitemata Basin was a shallow, enclosed, elongate basin, approximately 130 km by 60 km, which was bound on the west and east by two separate volcanic ridges and to the north and south by basement horst (Ballance, 1974). Also during this period, the Northland Allochthon was emplaced as thrust sheets of Cretaceous and Oligocene sedimentary and igneous rocks, and volcanic and volcaniclastic material was deposited in the west as the Waitakere Group. The region experienced uplift following the Miocene events and exposed a new landscape to erosion and weathering; this landscape has since been partially covered by Quaternary volcanic products.

2.2.2 The Waitemata Group

The evolution of the Waitemata Basin has produced a range of subgroups and facies (collectively termed the Waitemata Group) which are classified based on their location within the basin and their lithological content. Three subgroups resulted from the infilling of the Waitemata Basin with sediment largely derived from erosion of an andesitic volcanic arc to the west of the basin (Figure 2.2): the Kaipara Subgroup comprises the north-western shelf of the basin; the central Warkworth Subgroup comprises predominantly flysch sequences of bathyal marine depths; and the eastern Kawau Subgroup comprises a basal, shallow-marine facies that unconformably overlies greywacke basement rock (Allen, 2004). The Warkworth Subgroup rocks outcrop along most of the eastern coastline of the Auckland region, from Beachlands in the south to Mangawhai in the north, a north/south distance of approximately 130 km (Edbrooke, 2001; Thompson, 1961). The sediments of the Warkworth Subgroup were fed from the northwest volcanic ridge down a south-easterly paleoslope (Allen, 2004). Following the sedimentation of the Waitemata Basin there was a period of regional uplift and gentle tilting to the west which created open folds and normal faults (Edbrooke *et al.*, 2003) and exposed the Waitemata Group rocks and the underlying greywacke basement in select places to erosion by subaerial and marine processes.

Figure 2.1: Geological map of the Auckland region. Only the geological units discussed in this research are presented in the legend; the predominant formations are broadly represented. Modified from Edbrooke (2001).

The 1000 m thick section of the Warkworth Subgroup comprises a northern volcanic-rich flysch facies, a mixed flysch facies, and a southern volcanic-poor flysch facies (Allen, 2004). These facies are known geologically as the Pakiri Formation, the Blockhouse Bay Formation, and the East Coast Bays Formation respectively (Allen, 2004). Both the Pakiri and East Coast Bays Formations outcrop along the eastern coastline of the Auckland region and are the main focus of coastal cliff erosion in this area; the Blockhouse Bay Formation is situated further inland and is not affected by coastal cliff erosion.

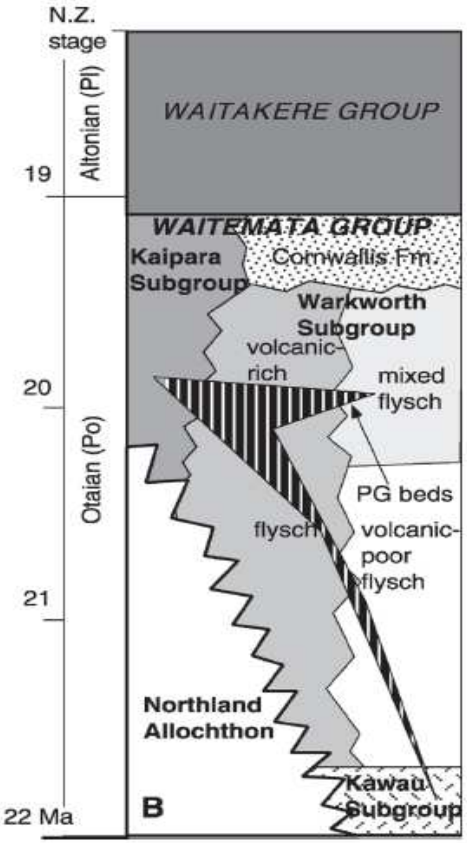

Figure 2.2: Stratigraphic section of the extent of the Waitemata Group. Formations that outcrop on the eastern coastline of the Auckland region include the volcanic-rich flysch facies (Pakiri Formation), and the volcanic-poor flysch facies (East Coast Bays Formation). Sourced from Allen (2004).

The boundary between the East Coast Bays Formation and Pakiri Formation is not definitive and has been variously mapped on either side of the Whangaparaoa Peninsula (northern side of the Peninsula by Edbrooke, 2001; southern side of the Peninsula by Allen, 2004). However, most authors consider the boundary to be to the north of Whangaparaoa Peninsula following the map of Edbrooke (2001).

There are three distinct lithological units within the East Coast Bays and Pakiri Formation: sandstone beds; siltstone beds; and interfingered andesitic breccia beds of the Parnell Grit (Moon and Healy, 1994). The primary units are poorly sorted sandstone beds and secondary units are thinner siltstone beds intercalated with the sandstone beds. The Parnell Grit deposits tend to be thick (> 10 m) homogenous beds (Moon and Healy, 1994) containing lava and pumice clasts imbedded in a crystal-rich sand and clay matrix (Allen, 2004). Ballance (1974), Hayward (1979) and Ballance and Williams (1992) report a regional tilt and younging of the strata to the west.

2.3 Environment of the Auckland Region

The Auckland region environment is one of generally mild and moderate conditions owing to its northern location in New Zealand and due to being surrounded by the sea (Hurnard, 1979). In the following sections the soil types, weather and climate patterns, coastline types and morphology, and offshore marine characteristics of the eastern Auckland region are presented.

2.3.1 Soil type

Soils of the Auckland region are characterised by yellow-brown earths (Morton, 1993). In general Waitemata Group rocks weather to soft or very soft silty clay with high shear strength and generally low plasticity, to depths of about 10 m (Edbrooke *et al.*, 2003). Specific soil types on the eastern coastline are different depending on whether they have formed on flysch beds or Parnell Grit (Moon and Healy, 1994). Soils developed on flysch beds are very firm, yellow, clayey soil with kaolinite as the dominant clay mineral, and significant abundances of smectite and vermiculite as secondary clay minerals (McLeod, 1988). Soils developed on Parnell Grit deposits are a firm, silty clay and are dominated by both kaolinite and smectite (McLeod, 1988).

2.3.2 Weather and climate

Auckland's climate is warm temperate, but close to subtropical, with a mean summer temperature of 19 °C and mean winter temperature of 12 °C (Searle, 1981; Edbrooke

et al., 2003). There is little extreme between temperatures, further exemplified by the relatively few frosts and fogs Auckland receives (Searle, 1981).

Mean annual rainfall ranges from 1200 to 1600 mm (Hurnard, 1979). A rainfall distribution map of the Auckland region in Hurnard (1979) shows that along the eastern coastline annual rainfall south of the East Coast Bays is about 1200 mm whereas north of the East Coast Bays annual rainfall increases and ranges between 1400 and 1600 mm (Figure 2.3). Regionally, rainfall is greatest in the winter months; there is the least rainfall in the summer months and this can contribute to periods when evaporation exceeds precipitation (Hurnard, 1979; Searle, 1981).

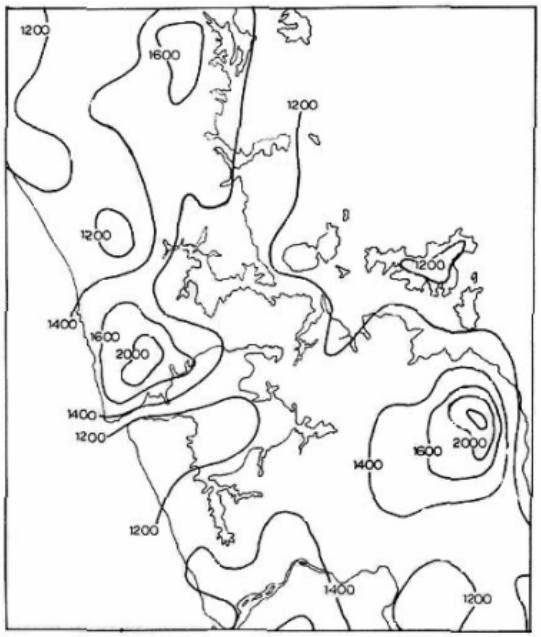

Figure 2.3: Map of mean annual rainfall (mm) for 1941-70. Sourced from Hurnard (1979).

Depressions of a tropical or northern Tasman Sea origin bring periods of moderate or heavy rain and may also be accompanied by north-easterly gales and warm, humid conditions (Hurnard, 1979). Such wind directions would blow directly onto a large proportion of eastern coastline cliff faces. However, prevailing wind flow over northern New Zealand is from the west to southwest for all seasons (Hurnard, 1979). Such winds may blow straight over the cliff-top, resulting in fairly sheltered cliff face zones. The north-facing cliff faces receive relatively more sun during all months as well as being sheltered from the prevailing southwest winds (Searle, 1981).

2.3.3 Marine environment

The offshore environment may play an important role in developing shore platforms and coastal cliffs through the orientation and strength of wave processes. The offshore environment of the eastern Auckland region broadly comprises an indented lee shore that is sheltered from the prevailing westerly and southerly waves (Pickrill and Mitchell, 1979). The Waitemata Harbour and inner Hauraki Gulf areas are further protected by offshore islands and, to a certain extent, the Coromandel Peninsula to the far east which gives a maximum fetch of 25 km (Moon and Healy, 1994). City Design (1996) reported a maximum fetch of 6.5 km from the inner islands of the Hauraki Gulf. North of Whangaparaoa Peninsula the coastline becomes a more open environment where wind strength and wave energy could potentially increase due to less indentation along the coastline and fewer offshore islands.

Waves acting on the Hauraki Gulf coastline are locally wind generated (Moon and Healy, 1994) and maximum wave heights recorded range from 0.49 to 2.25 m (Wells-Green, 1975; Robinson, 1985; Tonkin and Taylor, 2005b). The largest waves tend to be generated by north to east winds (Wells-Green, 1975; Riley Consultants Ltd, 2001; BECA, 2003).

2.4 Coastline and Shore Platform Morphology

Cliff coasts make up about 80 % of the worlds coastline (Emery and Kuhn, 1982) and are the evidence for past or current erosion of a landmass. Cliff coastlines vary in accordance with geological, structural and marine characteristics, specifically resulting in features such as beaches, coastal cliffs and shore platforms.

2.4.1 Beaches

Beaches play an important role when present at the base of coastal cliffs, for the most part as a buffer to wave attack of the cliff base. A study by Sunamura (1976) found that initial sediment accumulation at the base of a cliff can enhance erosion due to the abrasive power of sediment-laden water, however as beaches further

develop waves begin to break on the beach thereby creating the buffer zone between cliff and waves.

The location of the coastline and thus the energy of the waves (compare quiet harbour environments to open coastline) also has an influence on the type of beaches that can develop at cliff bases. Beaches on open coastlines, with dynamic sand exchange, have relatively steep slopes for wave attack (Morton, 1993). In quieter marine environments, the protected shores described by Morton (1993), which seem to depict the pocket and harbour beaches of Tonkin and Taylor (2005a), have finer grained sediments which form flats that are very expansive between high and low tide levels. These extensive flat beaches would tend to cover shore platforms and act as further protection from erosion. Beaches on the eastern coastline of the Auckland region are described by Moon and Healy (1994) as being usually re-entrant "angles pointing inward" valleys that are truncated by the shoreline or are only a thin veneer of sand over a pre-existing shore platform.

2.4.2 Cliffs

Cliff profiles develop in relation to the strength of the rock and beds that the cliff has developed in, (stronger rock produces more vertical cliffs (Woodroffe, 2002)), and the strength of marine and subaerial processes. A classic model developed by Emery and Kuhn (1982) and repeated by Trenhaile (1987), Woodroffe (2002), and Masselink and Hughes (2003), illustrate the cliff profile likely to develop based on the relative strengths of subaerial and marine processes, and the placement of stronger beds of rock with respect to cliff height (Figure 2.4).

In this model, cliff profiles become near-vertical as marine processes predominate over subaerial processes. As subaerial processes become more dominant, cliffs begin to develop a convex profile, merging to a concave profile at the base when marine processes are relatively insignificant. More durable beds will always result in a near-vertical type profile no matter the location within in the cliff profile. Waitemata group coastal cliffs that were protected by seawalls do not appear to have relatively lower erosion rates than other sites observed by Brodnax (1991) which suggests that wave action has little effect on cliff erosion rates.

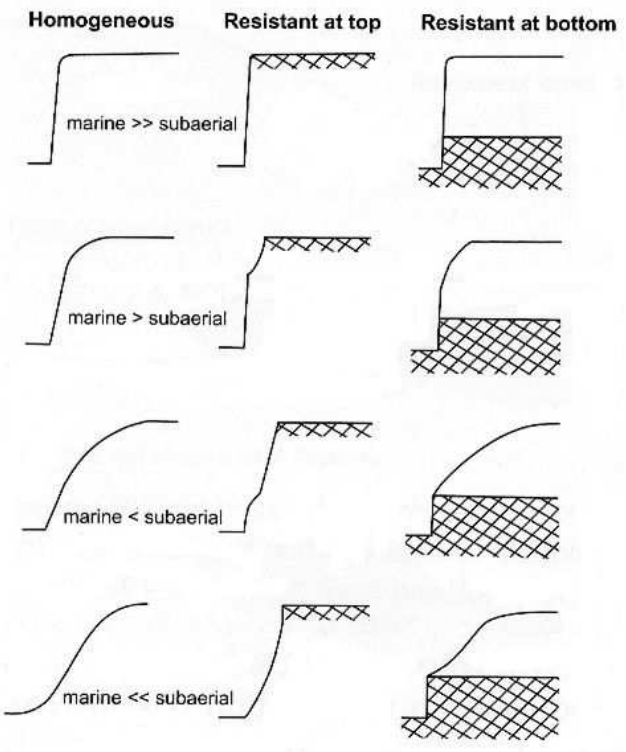

Figure 2.4: Model for coastal cliff profiles. The hash pattern indicates relatively resistant beds of rock (From Masselink and Hughes, 2003; modified from Emery and Kuhn, 1982).

Cliffs can also be classified in terms of their state of activity (Figure 2.5). Active cliffs (Figure 2.5A) are subject to wave action at their base. Talus slopes can develop at the base of some cliffs when supply of debris exceeds removal by wave action (Figure 2.5B); this talus acts as toe-support for the cliff and renders the cliff inactive. Cliffs will become 'relict' features when wave action is lost and the only processes that can then degrade the cliff are subaerial; this results in a more convex profile (Figure 2.5C). A cliff can however be reactivated when wave processes can again act on the cliff, such as if sea-level were to rise, and this tends to steepen cliffs again (Figure 2.5D).

Lastly, the dip angle and direction of discontinuities, particularly in heterogeneous materials, can have an influence on the stability of cliffs, and subsequently the profile of the cliff. Cliffs are relatively stable where the dip is away from the coast but much less stable if the bids dip seaward, with slide-type failure able to occur along structural bedding planes (Trenhaile, 1987). Where strata do dip seaward the cliff profile tends to follow the dip (Masselink and Hughes, 2003).

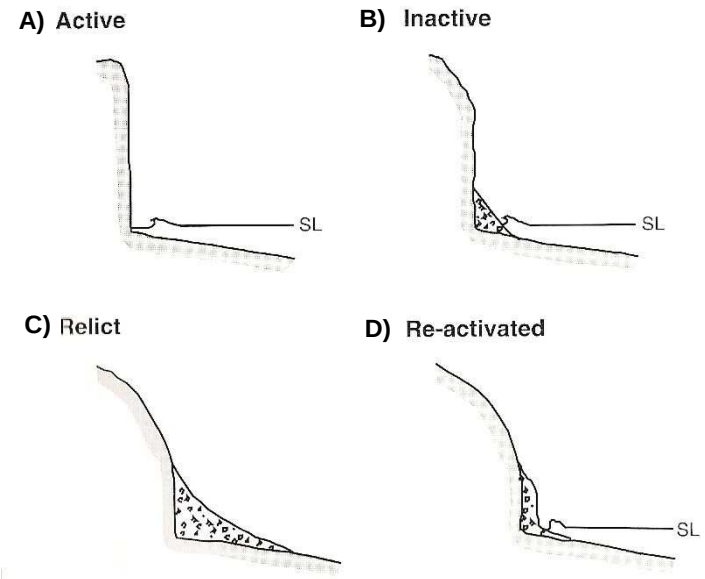

Figure 2.5: State of activity of a cliff with respect to cliff profile. Sourced from Woodroffe (2002).

2.4.3 Shore platforms

The morphology of shore platforms can be divided into two general types (Figure 2.6) based on whether the platform is sloping gently into the sea, which are termed "Type A" platforms (Bird, 1968; Sunamura, 1992; Masselink and Hughes, 2003), or the platform is sub-horizontal, which are termed "Type B" platforms (Bird, 1968; Sunamura, 1992). Type A platforms (Figure 2.6A) have a slope of approximately 1-5^{o} and extend from the cliff-platform junction to below low-tide level (Woodroffe, 2002; Masselink and Hughes, 2003). Type B platforms (Figure 2.6B), conversely, are sub-horizontal with an abrupt seaward ledge that is exposed at the low-tide level; these sub-horizontal platforms can develop at the high-tide or low-tide level according to Woodroffe (2002) and can be supra-, inter- or subtidal according to Masselink and Hughes (2003).

Healy and Kirk (1992) defined platform morphology of New Zealand coasts into high-tidal benches (similar to Figure 2.6B) and broad intertidal platforms (Figure 2.6C). High-tidal benches are similar to the aforementioned Type B platforms but are classified for development at the high-tide level and occur in more indurated lithologies (Healy and Kirk, 1992). These benches have been noted to occur in the Waitemata Harbour where 2 - 3 m thick massive sandstone beds are exposed at the cliff (Healy and Kirk, 1992). Broad intertidal platforms develop in more porous, less-indurated rock than for high-tidal benches, and are gently sloped with a seaward

edge; their broad width is associated with its higher susceptibility to erosion (Healy and Kirk, 1992). According to Moon and Healy (1994), Waitemata Group shore platforms are typically a gently sloping surface about 40 - 200 m wide which ends abruptly in a bio-eroded sea cliff. From the aforementioned definitions, the Waitemata Group platforms appear to fit the description of broad intertidal platforms of Healy and Kirk (1992), in Figure 2.6C.

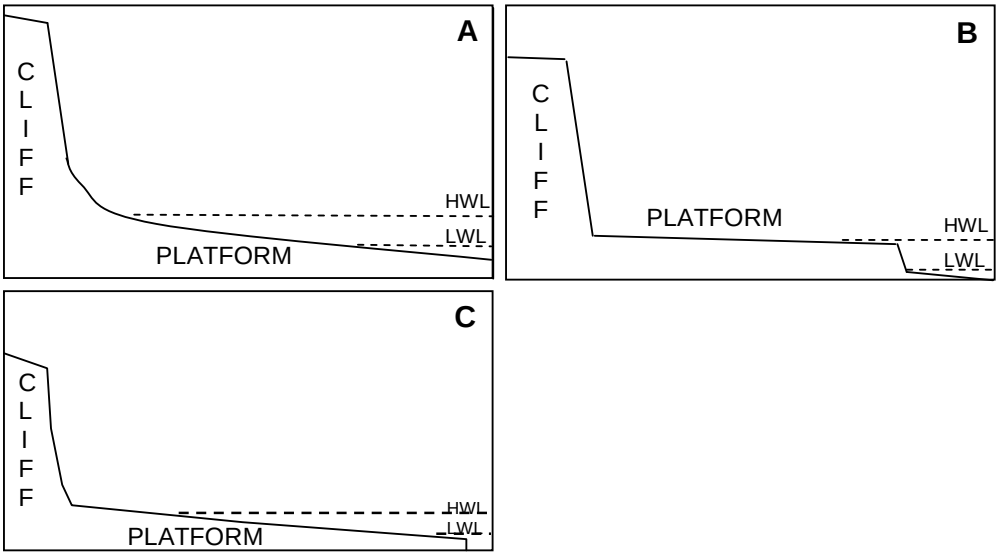

Figure 2.6: Schematic sketches of shore platform types. A is a sloping 'Type A' platform and B is a sub-horizontal 'Type B' platform which has a low tide cliff at its edge (modified from Sunamura, 1992). C is a broad intertidal platform (interpreted from Healy and Kirk, 1992)

2.5 Sedimentary Flows and Rheology

The Waitemata Group cliffs comprise various types of sediment gravity flows and the geomechanical nature (such as strength and durability) of the different flow types may have an effect on their susceptibility to erosion. The Waitemata Group coastal cliffs comprise gravity flow deposits described by authors as turbidity current deposits, debris flow deposits, and most simply alternating sandstone and siltstone beds (Healy, 1967; Healy, 1968; Moon and Healy, 1994; Gulyaev and Buckeridge, 2004). Other authors simply present the various lithologies found in the Waitemata Group as thick-bedded and thin-bedded sandstone, siltstone, and volcaniclastic (Parnell Grit) units (Simpson, 1987; Brodnax, 1991). With regards to the sandstone

beds, the distinction between thick-bedded and thin-bedded units may mean they are the result of different gravity flow types, and thus have different erosion characteristics.

The definition of a turbidity current is a sediment gravity flow where sediments are supported by upward turbulence of the fluid within the flow and the flow is propelled by gravity rather than any interaction between the fluid and the grains (Prothero and Schwab, 1996). The deposits of a turbidity current typically produce normal graded bedding which usually results from the settling of a single poorly sorted suspension of sand, silt and clay into heavier grains first, followed by the finer fractions, following Stokes' law (Prothero and Schwab, 1996). The grading and sedimentary structures of a turbidite have been modelled by Bouma (1962), as shown in Figure 2.7, from which it is noted that the whole sequence of units may be observed or certain units may be missing or have merged together.

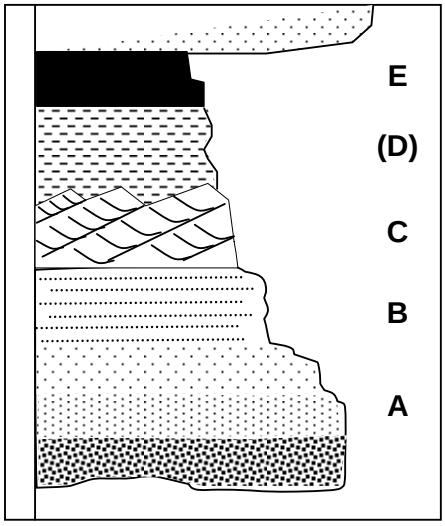

UNITS

E = pelitic division, partly deposited by the turbidity current, partly hemipelagic

D = faint parallel laminations of silt and mud, bracketed to emphasize that weathered or tectonized outcrops cannot be separated from E

C = ripple cross-laminated fine sandstone, traction in lower flow regime

B = Parallel laminated sandstone, traction in upper flow regime

A = graded or massive sandstone, rapid deposition

Figure 2.7: Bouma sequence structure of an ideal turbidite deposit. Adapted from Walker (1979).

Debris flows are considerably denser than turbidity currents and have the ability to carry larger particles downslope (Prothero and Schwab, 1996). The Parnell Grit is classified by Allen (2004) as a high particle concentration gravity flow transitional between a turbidity current and a debris flow.

A recent paper by Gani (2004) documents a new approach for determining different types of sedimentary flow deposits based on their rheology. Gani (2004) implies that there is no universal agreement over which of the four parameters that are used to categorize sediment gravity flows, namely sediment concentration, sediment-support mechanism, flow state and, rheology, should be the decisive one. His paper establishes rheology as the one parameter that can be used to distinctly differentiate between the various sediment gravity flow types. The principal model produced (Figure 2.8) illustrates that 'turbidity currents' behave purely as a Newtonian fluid whilst 'debris flows' behave as a non-Newtonian fluid. Newtonian fluids deform instantly and linearly with applied stress while non-Newtonian fluids are classified as anything deviating from this description (Gani, 2004). A 'non-cohesive debris flow' is commonly known as a grain flow, while a 'cohesive debris flow' has the rheology of a characteristic mud flow according to Gani (2004). Perhaps the most substantial outcome of this paper is the development of a separate category for deposits from mixed rheology flows that have a lower zone of non-Newtonian dilatant fluid with an overlying Newtonian fluid counterpart. It is these types of beds that may be being misinterpreted as turbidites in the cliff face of Waitemata Group rocks. The nomenclature for these various sediment gravity flows are collectively termed gravites. Turbidity current deposits are termed turbidites; debris flows are termed debrites; and mixed rheology flows are termed densites.

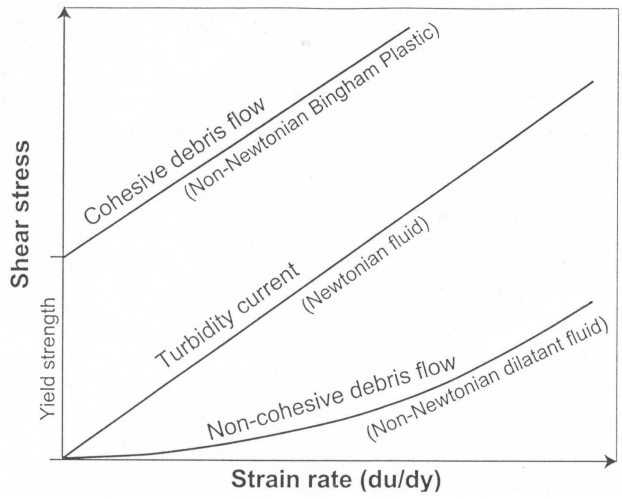

Sediment gravity flows = Gravites

Turbidity currents = Turbidites
Debris flows = Debrites
Mixed rheology flows = Densites

Figure 2.8: Types of rheology in sediment gravity flows and their terminology. Sourced from Gani (2004).

The rheology of turbidity currents means that sandstone beds (as the heavier grains) are deposited first followed by gradational depositing of finer hemipelagic silt and mud; the resulting product is the same as the Bouma structure presented in Figure 2.7. The lower component of a 'densite' flow has non-Newtonian laminar flow and is dense enough to support larger clasts; it appears as a massive sandstone bed with rip-up clasts of commonly different lithology. The upper component of the densite has turbulent flow and settles out gradationally much as the turbidity currents do. Debrite beds are derived entirely from non-Newtonian flows and experience mostly sluggish laminar flow which supports sediments dominantly through dispersive grain pressure. Debrites take the form of poorly sorted, massive or faintly laminated beds which contain larger clasts throughout the deposit, in a mud matrix (Prothero and Schwab, 1996). Thus, sandstone and siltstone beds are the products of both turbidites and densites from different rheology states, while Parnell Grit beds fit the description of debrites.

2.6 Coastal Cliff Erosion Processes

The processes that act on coastlines to erode and develop shore platforms and cliffs can be divided into: marine processes that act on the shore platform, and potentially the cliff base, in the littoral zone; and subaerial processes that work on the upper zones of the shore platform and the cliff face that are not reached by the tide. The international and national literature that regularly adds to, and advances on, knowledge of the processes of cliff erosion is summarised in Table 2.1. The mass wasting processes that occur specifically in the Waitemata Group coastal cliffs will be reviewed in further detail.

Table 2.1: Summary of literature on the processes of coastal cliff erosion and sea-cliff and shore platform development.

Year	Author	Location/lithology	Research
1968	Healy	Auckland, New Zealand Waitemata Group flysch and Parnell Grit	Researched the significance of bioerosion on shore platforms, using the Whangaparaoa Peninsula as a study site. Found that both grazing and boring organisms act to break down rock material and listed the commonly observed organisms specifically found on the Waitemata Group substrate.
1982	Emery and Kuhn	California, USA Shale, alluvium and sands	Developed profiles of active sea-cliffs based on the relative rates of marine and subaerial erosion processes. Highlighted that the characteristics for shaping sea-cliffs were homogeneity, structure of the rock mass and topography landward of the sea-cliff.
1983	Sunamura	-	The ultimate factors affecting wave-induced cliff erosion are the assailing force of the waves (f_w) and the resisting force of the cliff material (f_r) through lithology, mechanical structure and geological structure. Cliff erosion occurs when $f_r < f_w$.
1984	Pethick	-	General textbook on coastal geomorphology. Encourages the idea that cliff erosion is due in part to marine processes but subaerial processes also play a significant role. Models are illustrated for variation between inputs and outputs which result in the maintenance of vertical cliffs, the maintenance of slope angles, and the decrease in slope angles.
1987	Trenhaile	-	General textbook on geomorphology of rock coasts. Discusses types of coastal cliffs and erosion processes on an international scale with mathematical and graphical explanation.
1987	Simpson KA	Auckland, New Zealand Waitemata Group flysch and Parnell Grit	Different lithologies (thick sandstone, thin sandstone, siltstone, volcaniclastic units) of the Waitemata Group flysch show different geomechanical characteristics. Physical properties are primarily controlled by microfabric. Slope processes include slabbing and spalling, bedding and fault parallel slides and complex failures which are controlled by rock defects and properties of the rock substance which is primarily a function of microfabric and mineralogy.
1991	Jones and Williams	West Wales Alternating greywacke and mudstone beds	Wave-refraction modelling and longshore beach surveys indicated the presence of 'high' and 'low' beaches. Factors influencing variation in recession rates include the morphogenetic (wave-shaping) environment, beach parameters, coastline orientation, predicted and actual beach levels, beach profile, height of the cliff base, strength of cliff material, and protective features. Regression analysis suggested that the volume of beach material was the dominant explanatory variable of short-term erosion rates.
1992	Sunamura	-	Develops on the ideas by Sunamura in 1983 of the assailing force of waves and the resisting force of cliff material and presents them mathematically and graphically. Focuses on wave action eroding the cliff base, and not subaerial processes to interpret spatial and temporal variations in erosion rates.
1993	Jones et al.	Massachusetts, USA Glacial sediment	Shoreline and cliff erosion rates measured in order to determine the influence of textural and shear strength properties with respect to directions of the most frequent storm approaches. Multiple regression showed that the most resistant cliffs should have the lowest average sand : mud ratios, low gravel content and high shear strengths.
1999	Benumof and Griggs	San Diego County, USA Sandstone and unlithified sand	Highlight a lack of understanding of the role that cliff materials have on erosion processes and erosion rates. Erosion rates varied from 3 cm y^{-1} in well-lithified sandstone to 43 cm y^{-1} in unlithified Pleistocene sands. A classification system was designed to assess mass strength of the cliffs and found that stability of the cliffs is highly dependent on physical properties of the material (intact rock strength and structure), secondary to wave action.
2000	Benumof et al.	San Diego County, USA Sandstone and unlithified sand	Investigated the relationship between wave energy and sea-cliff erosion as confirmation of the findings in the 1999 paper by Benumof and Griggs. Distribution of wave power from 10 m water depth to the cliff-toe was inversely related to historical cliff erosion rates and this helped to confirm that waves are a secondary mechanism to subaerial erosion processes
2002	Woodroffe	-	General textbook on the form, processes and evolution of coasts. Ties in the major understandings of coastal cliff erosion and the form of cliffs from publishings to date, with a particular focus on Australasian examples.
2002	Trenhaile	-	Review of rock coast processes to date with particular emphasis on shore platform development and cliff inheritance due to sea-level changes over the Quaternary.
2003	Masselink and Hughes	-	General textbook on coastal processes and geomorphology. Also ties together the major ideas to date with a particular focus on work by Sunamura (1992), Trenhaile (1987) and Emery and Kuhn (1982).
2003	Lahousse and Pierre	Boulonnais, France Chalk	Three failure mechanisms are interpreted (collapses, flows-and-landfalls, and gullies) as a result of an erosional crisis following heavy rainfall and storm conditions. Failure mechanisms were dependent on the cliff shape and height, and its structural and hydrogeological behaviour.
2005	Pierre	Boulonnais, France Clay and sandstone	Retreat of clay and sandstone cliffs was measured by stereophotogrammetry and was found to be closely related to shore platform morphology and dynamics. Low recession rates in otherwise weak material are explained by down-cutting of the bedrock immediately in front of the cliff having to occur before the cliff face can recede as a result of the landward shore platform morphology.
2006	Pierre and Lahousse	Boulonnais, France	Amount of cliff retreat is related to structural and topographic factors which control the infiltration-runoff balance and therefore the mechanical behaviour of the rock. Temporal variability is difficult to explain and is impeding the ability to develop effective risk management of the area.

2.6.1 Marine processes

Marine processes that act to erode coastal cliffs are considered here to be any process acting in the littoral zone, and where normal tide levels reach. Thus, marine processes are predominantly to do with tides and offshore waves (Masselink and Hughes, 2003). Table 2.2 highlights the general marine processes that act on rocky coasts.

Table 2.2: Marine erosion processes acting on rocky coasts. Adapted from Masselink and Hughes (2003)

Process	**Result**
Mechanical wave erosion	Removal of loose material by waves, the level of greatest wear is associated with the elevation most frequently occupied by the water surface
Mechanical wave abrasion	Scouring of rock surfaces by wave-induced flow with mixture of water and sediment
Hydraulic action	Wave-induced pressure variations within the rock causes and widens rock capillaries and cracks
Water-layer weathering	Physical, salt and chemical weathering working together along the edges of rock pools
Bioerosion	Physical removal of rock by grazing and boring organisms and chemical removal by dissolution through metabolic processes

Sunamura (1983; 1992) developed the concept that erosion rates of coastal cliffs were affected by the relative intensity of the assailing force of waves and the resistant force of the cliff material. That is, if the force of waves is stronger than the strength (erodability) of the cliff material then erosion will occur and likewise, erosion will not occur if the cliff material is durable and the force of the waves is small. Waves always exert hydraulic action on a cliff face but when the water is "armed" with sediment this gives the ability for mechanical action to occur (Sunamura, 1992) in the form of abrasion.

Water-layer weathering is a process that occurs on the shore platform and is thought to aid in loosening material for the removal by wave action (Woodroffe, 2002). The weathering occurs by the alternate wetting and drying of the platform over tidal cycles due to the chemical and physical processes that occur between the seawater and the rock material and is most effective in tropical settings (Pethick, 1984).

The effect of bioerosion on overall erosion rates is mainly dependent upon the setting of the coastline (bioerosion occurs more readily in tropical, calcareous substrates); the availability of moisture which controls organism distribution; and tidal characteristics which determine how long the substrate is inundated or exposed (Trenhaile, 1987). With respect to cliff erosion, the closer bioerosion occurred at the cliff base, the more effect it would have as a process to erode (and to a certain degree, destabilise) the cliff rather than just the platform material. Healy (1968) found that bioerosion may be a significant active process in developing the broad intertidal platforms formed in Waitemata Group rock, with a range of boring and browsing organisms that can be attributed to the degradation.

2.6.1 Subaerial processes

Subaerial processes work on the cliff surface and may also work to erode the cliff base area that is not reached at high tides. This results in the movement of sediments down the cliff slope to the sea (Masselink and Hughes, 2003). The rate at which subaerial processes can degrade, loosen, and remove sediment in the form of single grains or blocks of rock is, to a great degree, dependent upon the lithology of the cliff face and the structure of the rock mass. Secondly, the climate and local physical conditions (such as amount of shade, wind exposure, and temperature) at the cliff site have an influence on the rate of weathering which determines the resistance of the rock or sediment (Ollier, 1984). Healy (1967) emphasised (through research on shore platforms on the Whangaparaoa Peninsula) that subaerial weathering, above the permanent saturation zone, played a major role in the development of cliffs and platforms in Waitemata Group rock. The subaerial processes that are recognised by Masselink and Hughes (2003) to act on rocky coasts are listed in Table 2.3.

Salt weathering acts to weaken rock by volumetric growth of salt crystals, and subsequent expansion in the capillaries of the rock (Trenhaile, 1987). While the effectiveness of salt weathering increases as porosity and permeability increase, meaning sandstone rock is particularly susceptible, salt weathering is most effective in semi-arid environments with low rainfall and high temperatures (Masselink and Hughes, 2003), unlike the Auckland region.

Table 2.3: Subaerial erosion processes acting on rocky coasts. Adapted from Masselink and Hughes (2003)

Process	**Result**
Salt weathering	Growth of salt crystals causes and widens rock capillaries and cracks
Chemical weathering	Processes such as hydrolysis, oxidation, hydration and solution remove rock material
Wetting and drying (physical weathering)	Frost action and cycles of wetting and drying causes and widens rock capillaries and cracks
Mass movement	- Rock falls and toppling due to well-jointed rocks - Slides due to deeply weathered rock - Flows due to unconsolidated material - All mass movement types are affected by undercutting of the cliff

Chemical weathering rates are influenced by the amount of water available and the ability to remove the soluble products, thereby keeping the chemical process out of a state of equilibrium (Masselink and Hughes, 2003). Colder, drier climates experience slower rates of chemical weathering but this process may still be effective where the substrate experiences frequent wetting and drying (Masselink and Hughes, 2003). With regards to subaerial zones, the spray zone of a cliff face consisting of calcareous material can induce pitting on the rock surface as a result of chemical weathering (Bird, 1974).

Wetting and drying processes can also occur in the spray zone of a cliff face as well as wherever the cliff face is exposed to rainfall. This is a form of mechanical weathering whereby wetting of the substrate causes expansion or swelling of the grains (particularly clay minerals such as smectite) and subsequent drying of the cliff surface causes expanded grains to shrink, from which cracks can develop (Sunamura, 1992). Cycles of wetting and drying act to progressively degrade the rock substrate over time (Sunamura, 1992).

Mass wasting processes are mechanisms for failure. They are important to understand in the cliff zone to be studied because the lithology and structure of the rock mass, and weathering status of the cliff rock and overburden, will influence how the cliff may fail. Slope movements in Waitemata Group rock were classified by Simpson (1987) and fitted into all groups of the classification scheme of Varnes

(1958) including rock and soil falls, flows, slides, topples and complexes. Five mechanisms for cliff retreat in Waitemata Group coastal cliffs were later determined by Moon and Healy (1994) and greatly simplify the work by Simpson (1987). The mechanisms for failure are more specific to the Waitemata Group study area, rather than being classified from a general mass movement scheme, and also continue to be referred to in related research and reports today.

The five mechanisms summarised from Moon and Healy (1994) include:

Joint block fall — occurs in sandstone blocks when support is lost underneath from loose frittered siltstone being removed; collapse is simply influenced by gravity and failure from this mechanism is the most common form of instability of these cliffs. The common situation in Auckland with stratified sedimentary rocks is to observe continuous bedding planes with essentially perpendicular cross-joints creating regular blocks that will fall out when loosened.

Fault plane failure — occurs along the weak fault planes in the cliff face; the crushed gouge rock has minimal frictional strength providing little resistance to failure.

Fault planes normal to the cliff face conditions are more stable and sliding is unlikely to be able to occur, however the weak zones of the plane are preferentially washed resulting in the development of narrow gullies.

Fault planes sub-parallel to the cliff face are less stable due to the capability of planar failure along the fault plane. Removal of material at the cliff base can remove the support of the overlying rock mass. An event by this mechanism may be very large involving tens of metres of cliff face.

Bedding plane failure — may occur along the bedding planes in the cliff when they dip seaward at a sufficient angle for shear failure. Water entering these planes reduces friction and stability of the rock mass.

Failure of folded strata — occurs by the same mechanisms as mentioned above but is dependent upon the inclination of the individual beds. Discontinuity surfaces that are daylighting from the cliff face have the propensity for planar failure and joint block fall is dependent upon erosion from underlying strata.

Failure of overlying soils — is the most immediate hazard to dwellings. Any rock failure which results in cliff retreat will lead to oversteepening of the soils which will be matched by failure of the soil zone to maintain a stable angle. Failure appears different in soils developed on flysch (deep, curved rotational failure) compared to Parnell Grit (steep, straight translational failure). Creep may also occur in overlying soils, and is a particular problem when lateral support is lost.

2.7 Review of Published Work on Assessing Coastal Cliff Erosion

In the last 3 - 4 decades much international and national research (summarised in Table 2.4) has been carried out to:

A) develop relationships between observed erosion processes and erosion rates;
B) develop methodologies for estimating erosion rates of coastal cliffs; and
C) determine the hazard associated with erosion of the cliff.

International literature tends to publish work on the erosion processes that act on soft coastal cliffs, and provide new and revised methods for assessing coastal cliff erosion rates, some principles of which may be able to be applied to Waitemata Group coastal cliffs. National research also contributes to the knowledge base of cliff erosion processes and methods for determining erosion rates. Many studies on Waitemata Group coastal cliffs have worked on determining erosion rates as well as developing models for assessing the hazard level of erosion for planning purposes. National studies have the particular advantage of being more comparative with research in the Waitemata Group as they are often in the context of New Zealand engineering standards and government legislation such as the Resource Management Act and New Zealand Coastal Policy Statement.

2.7.1 The relation of erosion processes to erosion rates

A number of authors have related observed erosion processes to the rates of erosion calculated at their coastal cliff study sites (Table 2.3A). Often the relationships found are purely from site specific work due to consistency in lithology, structure or marine characteristics, but this shows that numerical and computer-based modelling can be used to predict statistically-significant models of erosion processes versus erosion rates.

The Fukushima Coast in Japan has been the site of continual coastal cliff work as it consists of soft rock which suffers from "severe wave-induced erosion" (Mano and Suzuki, 1999). An equation model has been developed by Mano and Suzuki (1999) which determines the erosion rate of cliffs from parameters including wave energy flux, Young's modulus and cliff height.

Table 2.4: Summary of the methodologies developed and published for the assessment of the hazard of coastal cliff erosion.

Year	Author	Location/lithology	Methodology
A	Relationships between erosion processes and erosion rates		
1964	Yamanouchi	Ohmika Coast, Japan	Explained local differences in recession rate by the rock hardness tested by a penetrometer.
1967	Horikawa & Sunamura	Ohkuma Coast, Japan	The recession rate of cliffs was measured through aerial photographs; the authors found this was significantly related to uniaxial compressive yield stress of cliff-forming rocks.
1973	Toyoshima et al.	Fukushima Coast, Japan	Used the direction of the coastline and radius of pocket beaches as a measure of wave intensity and compared these quantities with recession rates obtained by aerial photographs.
1973	Gelinas and Quigley	Great Lake Erie, USA	Chose the wave energy flux at breaking points for a measure of wave intensity and obtained a linear relationship between the recession rate and energy flux. The geological materials of this study could not be sourced.
1977	Sunamura	-	Determined that recession rate was a function of a dimensionless parameter defined by the ratio of wave pressure at the cliff base to the yield stress of the cliff rock.
1987	Kamphuis	Great Lake Erie, USA	Re-analysed the data from Gelinas and Quigley (1973) and obtained a weakly nonlinear relationship between recession rate and wave energy flux. The geological materials of this study could not be sourced.
1991	Brodnax	Auckland, New Zealand Waitemata Group flysch and Parnell Grit	Developed a multiple linear regression model of the most statistically influential processes on Waitemata Group cliffs. The parameters included shore platform width measured through aerial photography, Rock Mass Strength classification number for groundwater from Selby (1993), aspect of the cliff, presence of a beach, the proximity of the geological strike to the cliff orientation, the wave regime, and the presence of Parnell Grit rock. Five of the parameters used in the model are given a 1 or 0 as to whether the parameter exists at the cliff site or not e.g. a beach at the base of the cliff, so that they are in a linear form.
1991	Jones and Williams	Cardigan Bay, West Wales. Greywacke & mudstone, clay, glacial deposits	Cliff erosion over a two-year period is measured and described. Wave refraction modelling and longshore surveys highlight 'high' and 'low' beaches. These measurements combined in a regression analysis suggest that the volume of beach-face material was the dominant explanatory variable in short-term cliff erosion.
1999	Mano and Suzuki	Fukushima Coast, Japan Tuff, mudstone and sandstone	Erosion of soft rock cliffs is due to high wave attacks and weak rocks. The recession rate, q, is equal to 0.082F/EL, where F = wave energy flux at the breaking point through refraction analysis, E = Young's modulus, and L = cliff height.
2000	Budetta et al.	Cilento, Italy Sedimentary rock	Made estimates of the destructive force of waves at the base of cliffs where no accurate bathymetric data are available, by means of correlation between the erosion rate of rocky coasts and the mechanical strength of soils and rock masses. This has a semi-logarithmic relationship.
2002	Hall et al.	UK Soft rock	Developed an episodic stochastic simulation model which models the duration between cliff falls as a gamma process and fall size as a log-normal distribution and is applied to cliff recession data from a coastal site in the UK
B	Methodologies for determining erosion rates		
1993	Gordon	Auckland, New Zealand Waitemata Group	Determined erosion rates in Waitemata harbour coastal cliffs from historic engineering structures
2004	Zviely and Klein	Israeli Mediterranean coastline Aeolianite	A combination of satellite geodesy, photogrammetry and mapping produces more highly accurate data than aerial photography, regarding cliff erosion rates. Thus the use of computer digitising appears to improve the error associated with deducing erosion rates from aerial photographs.
2004	Gulyaev and Buckeridge,	Auckland, New Zealand Waitemata Group sandstone and siltstone	Modern airborne laser scanning technique provides higher horizontal accuracy (from 20 cm). Terrestrial methods such as terrestrial laser scanning and terrestrial photogrammetry methods may be used to quantify erosion rates and provide higher accuracy than the standard method of studying aerial photographs.
2005	de Lange and Moon	Auckland, New Zealand Waitemata Group sandstone and siltstone	Use shore platform widths as an estimate of long term cliff recession rates, where the seaward edge of the platform is a static feature and platform development has occurred over one erosion cycle of sea level of 7120 ± 70 years. Long term erosion measurements will account for continual retreat and larger sporadic collapse which shorter term measurements may not be able to establish.
C	Hazard zone delineation of erosion rates		
1994	Moon and Healy	Auckland, New Zealand Waitemata Group sandstone and siltstone	A hazard zone of 16 m is initially established for cliffs in Waitemata Group flysch rock; 10 m accounts for the most hazardous mechanism (planar failure along faults), plus 6 m for the point taken back from the cliff face at which the bevelled edge of soil approximately begins. The authors see this as possibly being too small for some areas which have unique and complicated structures e.g. numerous faults or folded strata and thus added a safety factor (as suggested by Gibb and Aburn, 1986) which is 2/3 the width derived from a 100 year retreat rate (7 m).
1994	Gibb	Wainui Beach, Gisborne and Mount Maunganui, Bay of Plenty. No geology information given.	The methodology to define Areas Sensitive to Coastal Hazards (ASCH's) and Coastal Hazard Zones (CHZ's) to control subdivision use and development of coastal land is described. ASCH's are used to forewarn both public and territorial authorities so that further assessment of those areas can be made. $CHZ = [(X + R)T + S + D]F$ X = rate of shore retreat F = safety factor that accommodates errors of X, R, S, and D T = planning horizon of 100 years S = magnitude of max observed short-term shoreline fluctuations D = horizontal distance of retreat to attain a stable slope R = rate of long-term (historic) trend of net shoreline advance, retreat or dynamic equilibrium
2003	Glassey et al.	Auckland, New Zealand Waitemata Group sandstone and siltstone	**CLHZ = (S + R.T) F + SF** CLHZ = Coastal Landslide Hazard Zone S =extent of sea-cliff subject to relatively sudden failure from landslip T = hazard assessment period R = net long-term rate of sea-cliff retreat F = safety factor as a provision for uncertainties in the parameters
2005	Walkden and Hall	Naze Peninsula, England Soft mud to clay	Developed a predictive mesoscale model of the erosion and profile development of soft rock shores which required the inputs of shore platform, beach, tidal range, wave transformation, cliff and talus.
2005a	Tonkin and Taylor	Auckland, New Zealand Greywacke, Miocene flysch and volcaniclastic deposits, alluvium, Quaternary volcanic deposits, displaced units (Northland Allochthon)	Auckland Regional Council commissioned Tonkin & Taylor to complete a coastal erosion hazard assessment for the entire region. The extent of coastal erosion hazard has been determined based on a review of existing published data and information, supplemented by field validations, to derive erosion hazard zones. The erosion hazard zone for cliffs is determined by : $EHZ_{Cliffs} = \left[(LTR_H \times T) \times F + \left(\frac{H_t + 2.5}{\tan \alpha} \right) \right]$ Where, LTR_H = Historic long-term retreat (m yr^{-1}) T = Timeframe of study (100 years) F = Allowance for uncertainty associated with long-term retreat rates H_t = Height of cliff (m) 2.5 = Error associated with height of cliff (m) α = Characteristic slope angle of the cliff surface Hazard zones are calculated for cliff top land and are categorised into Likely, Possible, Unlikely or Rare as a distance measure based on the value of the EHZ.
2007	Jongens et al.	Auckland, New Zealand Waitemata Group sandstone and siltstone	A revised hazard zonation methodology is presented which advances on the methodology established by Glassey et al. (2003), and is established for the application to areas with very low erosion rates such as in the East Coast Bays area of Auckland. CLHZ = S + (RT) + F Where: CHLZ = Coastal Landslide Hazard Zone T = Hazard assessment period of 100 years F = Factor of safety S = Amount of horizontal retreat expected (simplified) R = Amount of sea-cliff retreat over the hazard assessment period

Initial studies found the strength of the cliff material on Fukushima Coast was related to erosion rates; wave conditions were later analysed, particularly using numerical models, to appreciate how erosion rates, cliff strength and wave attack relate. Wave energy flux was found to have a relationship with erosion rates and so was incorporated into the model by Mano and Suzuki (1999). This model was developed from previous work by Yamanouchi (1964), Horikawa and Sunamura (1967), Toyoshima *et al.* (1973), Gelinas and Quigley (1973), Sunamura (1977), and Kamphuis (1987), as sited by Mano and Suzuki (1999).

Multiple linear regression analysis was used by Brodnax (1991) and Jones and Williams (1991) to determine the dominant independent variables that influenced cliff erosion rates. Jones and Williams (1991) found that only 27 % of their measured variables could explain the control on erosion rates, but the volume of beach material was highlighted as the most significant independent variable. The regression analysis by Brodnax (1991) found seven of 25 parameters that have a statistically-significant influence on erosion rates of Waitemata Group coastal cliffs. Brodnax (1991) discounted the significance of the findings of Jones and Williams (1991) due to the low percentage of influence on cliff erosion rates and aimed to provide a significant explanation for variation in erosion rates from his regression analysis work.

2.7.2 Methodologies for assessing coastal cliff erosion rates

Methods for determining erosion rates (Table 2.3B) have varying levels of accuracy and can determine the erosion over short term periods (few years) to long term periods (hundreds to thousands of years). Advances in these methodologies aim to increase the accuracy of the measurements especially when projecting a yearly erosion rate to the commonly-used planning period of 100 years (Tonkin and Taylor, 2005a). Work also continually aims to improve the ease and time of collecting data from which to calculate the erosion rates. Methods used for measuring erosion rates in the East Coast Bays of the Auckland region include aerial photography, cadastral surveys, from man-made structures, from geological markers such as shore platform widths, and laser cliff face topographic surveys (Glassey *et al.*, 2003). Latest advances in these methodologies include the use of laser technology (Gulyaev and Buckeridge,

2001; 2004) and satellite imagery and computer digitising (Zviely and Klein, 2004) as a means of reducing the error of the measurements of cliff retreat.

According to Brodnax (1991), only scattered attempts had been made to measure rates of cliff erosion in coastal cliffs of the Hauraki Gulf and Waitemata Harbour. Brodnax (1991) used aerial photographs and fixed structures on the coastline to measure short to medium term erosion rates and found that erosion rates ranged between 20-350 mm y^{-1}. Gordon (1993) also determined erosion rates from historic engineering structures and found erosion rates for cliff retreat to average 3.49 mm y^{-1}. Gordon (1993) discounted Brodnax's measured values due to the large error associated with determining erosion rates from aerial photography. For instance, the mean rate of erosion on the open coast of the East Coast Bays was measured by Brodnax as 180 mm y^{-1}, which can be extrapolated to 18 m over a 100 year period; erosion at this rate is not seen from cadastral surveys. Brodnax's calculated error was 100 mm y^{-1} which is very high (55 %) compared to the average erosion rate. Furthermore, Gordon (1993) suggests that if this were the erosion rate and cliff retreat had occurred since the present sea-level highstand 6500 years B.P. then shore platforms should be > 800 m wide.

Gulyaev and Buckeridge (2004) used terrestrial laser scanning and terrestrial photogrammetry to monitor cliff erosion more accurately than other methods, with a pilot study carried out in the North Shore area of Auckland. The advantages of these methods include: a much smaller margin of error (< 1 cm for terrestrial laser scanning and 10 cm for terrestrial photogrammetry) in terms of the calculated erosion rate; a smaller period of time over which to measure the erosion; being quick and cost effective; being non site-specific thereby having universal application; and being able to be used in difficult areas such as undercut cliffs and overhanging trees.

Other methods that they compared the efficiency of were aerial photography (accuracy of 1 - 5 m), airborne laser scanning (0.2 - 1 m), cartography-sequential historical maps (3 - 5 m) and direct field measurements (0.2 - 1 m). When working with erosion periods of less than 100 years these margins of error are often a significant percentage of the total erosion rate.

Another method for determining erosion rates was suggested and examined on two Waitemata Group sites by de Lange and Moon (2005). Their method was to use shore platform widths to calculate long-term erosion rates on the proviso that the shore platform edge was a static feature that had not experienced significant erosion and the time period for shore platform development (and thus cliff erosion) was 7120 ± 70 years. This is the time during which sea-level in the Auckland region (measured from the Weiti River mouth) has been at its present level according to Gibb (1986). This method determined erosion rates of 1.4 to 14.3 mm y^{-1} (or 0.0014 to 0.0143 m y^{-1}) which are said to be, "consistent with the lower end of the average range of cliff-top and face recession rates published for Waitemata Group rocks using different methods" (de Lange and Moon, 2005). Indeed, other authors have determined erosion rates of up to 50 mm y^{-1} (Glassey *et al.* 2003), 100 mm y^{-1} (Riley, 2001), and 300 mm y^{-1} (Brodnax, 1991) which are comparably higher than those determine by de Lange and Moon (2005).

Jongens *et al.* (2007) mention the use of 6500 years as the period for shore platform development in Waitemata Group coastal cliffs. Gibb (1986) determined the time period of the culmination of postglacial marine transgression in the Auckland region as 7120 ± 70 years ago, which was used by de Lange and Moon (2005) as the time period for shore platform development. Gibb was a co-author of the recent paper by Jongens *et al.* (2007) and yet the paper did mention the date of 7120 years when discussing erosion rates in the Waitemata Group coastal cliffs. As long as the shore platforms have all developed over the same period of time then they will still produce internally consistent results because one site will have a higher rate of erosion than another by the same proportion.

Based on the range of data measured in Waitemata group coastal cliffs, there does not seem to be any distinction between measuring erosion rates over a short, medium or long term. Because coastal cliff erosion occurs as both a continual steady process and as larger sporadic events, long-term erosion rates would determine the average of both of these processes. Shorter term measured erosion rates would likely only determine the rate of continual retreat and medium term erosion rates would determine continual retreat plus possible larger sporadic collapse events. There is a bias towards short-medium term erosion rates in that the period of measurement

may be less than the frequency of larger mass wasting events at the site of measurement. It is more accurate to determine erosion rates over a long period of time (such as one erosion cycle of sea-level) and then calculate an estimated erosion rate for a 100 year planning period from the long term measurement, rather than to extrapolate an erosion rate for a 100 year planning period from data measured over a shorter period than this.

2.7.3 Methodologies for hazard zone delineation of coastal cliffs

The measurement of erosion rates and understanding of erosion processes on the Waitemata Group coastal cliffs have been applied to the development of methodologies for hazard zonation of cliff-top land (Table 2.3C). Much of this work has occurred in the last decade as the need to more accurately determine how far cliffs will recede over a specified period is required by local territorial authorities for planning purposes. For the Auckland region, a planning period of 100 years is used by Regional and Territorial Local Authorities (Tonkin and Taylor, 2005a).

In Waitemata Group coastal cliff studies, hazard zone delineation commonly takes the form of an equation which uses calculated erosion rates, mechanisms for failure, and a safety factor to determine a horizontal distance from the cliff-top edge which is potentially at risk of failing in the specified planning period.

Hazard zone delineation was carried out in the East Coast Bays area of the Auckland region by Moon and Healy (1994). The total hazard zone of 23 m was calculated from a minimum 16 m distance for the riskiest failure mechanism (fault plane failure) and the stable angle of overlying soil, plus a 7 m safety factor.

Glassey *et al.* (2003) developed a methodology for coastal cliff hazard mapping, also using the East Coast Bays area as a study site. They determined that a Coastal Landslide Hazard Zone (CLHZ) could be calculated from the measurements of four different parameters including: Factor S, the extent (normal to the cliff face) of the sea-cliff subject or likely to be subject to relatively sudden failure from landslip; Factor R, net historic/long-term rate of sea cliff retreat; Factor T, hazard assessment period; and Factor F, a safety factor that makes provision for uncertainties in the parameters. Glassey *et al.* (2003) found that along the cliff coastline of J.F. Kennedy

Memorial Park, CLHZ widths ranged between 23 and 52 m inland from the cliff-toe and are proportionate to the degree of risk to cliff-top land over the next 100 years. They mention that this is somewhat wider than the 15-25 m development setback implemented by North Shore City Council.

A number of organisations also carry out research in this area including Tonkin and Taylor, Riley Consultants, and BECA Amec, often through contract with Regional Councils (Tonkin and Taylor, 2005b). Auckland Regional Council employed Tonkin and Taylor to undertake a regional coastal erosion hazard assessment, the purpose of which was to provide information for the consideration and use of both Regional and Territorial Local Authorities (Tonkin and Taylor, 2005a). The report presented an equation for the calculation of the area susceptible to erosion (Erosion Hazard Zone, EHZ) for cliffs which uses the parameters of historic long-term retreat, a study timeframe of 100 years, an allowance for uncertainty associated with long-term retreat rates, cliff height, an error of 2.5 m associated with cliff height measurement, and a characteristic slope angle of the cliff surface. The calculated EHZ was used in combination with characteristic slope angles to construct hazard lines that estimate the likely, possible, unlikely and rare events of erosion based on a 100 year timeframe (Figure 2.9).

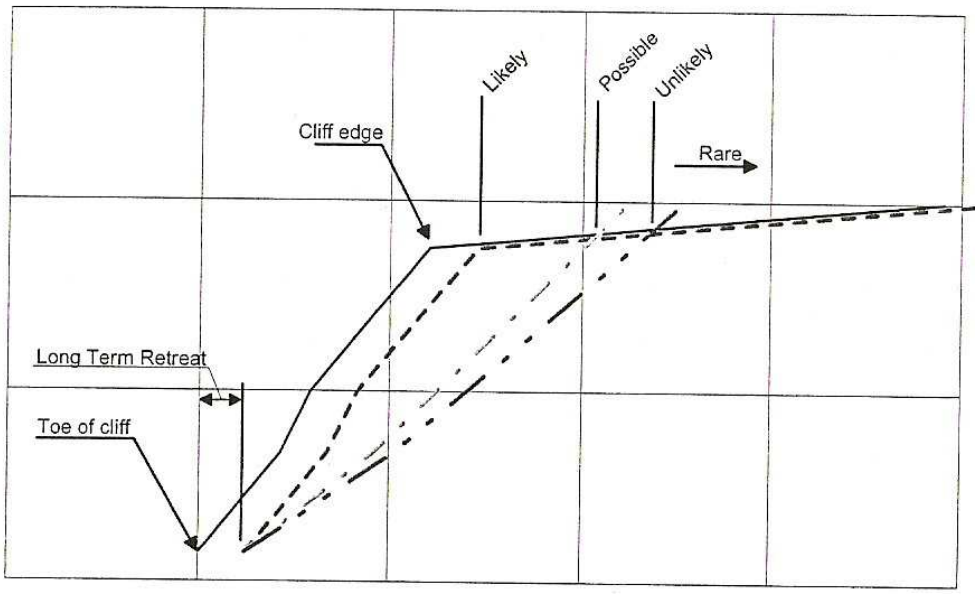

Figure 2.9: Diagram of a cliff profile showing the derived Erosion Hazard Zones. Sourced from Tonkin and Taylor (2005a).

Most recently, Jongens *et al.* (2007) have revised the CLHZ that was first developed by Glassey *et al.* (2003) to now have particular application to coastal cliffs with very low erosion rates; their study area was the East Coast Bays which was deemed to have suitably low cliff erosion rates. The revised CLHZ uses parameters of: Factor S, horizontal distance representing the potential average sudden horizontal retreat of the cliff-top from either rock fall, fault plane failure or bedding-plane failure (S_2) coupled with amount of horizontal retreat resulting from slumping of the cliff-top weathered layer to achieve a stable slope angle of 26° in the upper bevelled zone (S_1); Factor R, amount of sea cliff retreat over the hazard assessment period inferred from a Sea-cliff Vulnerability Index ("an internally consistent measure of the relative vulnerability of sea-cliffs to natural hazards"); Factor T, hazard assessment period of 100 years; Factor F, safety factor in meters. The calculated CLHZ widths along the East Coast Bays range from 13 to 34 m over a time frame of 100 years from coastal erosion and landslips.

2.8 Sea-level Trends in Relation to Quaternary Marine Terraces and Shore Platform Development

Shore platforms develop concurrently with coastal cliff recession. Shore platforms are constructed when sea-level is at a stillstand, the period in between a transgression of the sea toward land, and a regression of the sea away from land (Allaby and Allaby, 1991). The Auckland region shows evidence of numerous periods of stillstand, in the morphological form of marine terraces that step repeatedly up the inland ranges, particularly on the eastern coast (Ballance and Williams, 1992). If cliff erosion rates are to be determined from shore platform widths, as done so by de Lange and Moon (2005), then there must be verification of the time at which the current shore platform began to develop and agreement that the seaward edge of the platform has remained relatively static over this period of erosion.

2.8.1 Auckland sea-level fluctuations

The Auckland region landscape displays a flight of marine terraces which mark the various periods of stillstand in which shore platforms have developed throughout the Quaternary, the broad history of which is displayed in Table 2.4. In the current situation, the shore platform that exists at present sea-level along the eastern

coastline of the Auckland region has been understood by some researchers to have developed over one erosion cycle, such as de Lange and Moon (2005). Gibb (1986) developed a regional Holocene eustatic sea-level curve which presents a time period over which the current shore platform has been developing on the eastern coastline of the Auckland region; the start of this period thereby indicates when shore platform development began. Eighteen dated eustatic paleosea-levels represent the culmination of the postglacial marine transgression (6500 ka) from which the Weiti River is classed as the zero-datum level for the Auckland region (Gibb, 1986). The calibrated age at the Weiti River site is 7120 ± 70 (calendar) years and this date is used by de Lange and Moon (2005) as the period over which the present shore platform has developed in the Auckland region. Some authors (Brodnax, 1991; Jongens *et al.*, 2007) quote the period for shore platform development as 6500 ka which is possibly a generalised age for New Zealand rather than a specific value for the east coast of the Auckland region.

Table 2.5: Sea-level history of the Auckland region for the Quaternary period.

Period		Time (ka)	Event
QUATERNARY	Holocene	0.5	[e] Maximum age of Rangitoto lava flows in which no platforms exist
		1-2	[c] Sea receded to present level
		3-4	[c] Maximum sea-level reached resulting in low coastal terraces above current shore platform
		6.5	[b] Culmination of the postglacial marine transgression
		7.1	[b] Beginning of Auckland shore platform development
		10	[c] Slow sea-level rise to within 30 m of the present level, then rapid rise to as much as 2 m above present level
	Pleistocene	30	[c] Sea-level rose to almost present level then fell again with renewed glacial growth
		100	[c] **Ice Age 4** Gradual sea-level fall >100 m below present sea-level with intermittent warmer periods and stillstands at 11 m and 6 m above present level.
		140	[f] Lake Pupuke basalts erupted
		160	[d] Beginning of volcanism in Auckland Volcanic Field
		200-300	[c] **Ice Age 3** Stillstand remained until the onset of the next glaciation 200-300 ka which ended with sea-levels about 12-20 m above present.
		700	[c] **Ice Age 2** Period of stillstand ended 700 ka followed by sea-level fall brought on by the next glaciation. The ice age ended with sea-levels about 30 m above present level.
		1600	[c] **Ice Age 1** Period of sea-level fall, continued over about 100,000 years; sea-levels later rose to only about 75 m above the present sea-level
		1800	[a,c] End of Pliocene / Beginning of Pleistocene, highest recorded marine terrace in Auckland region of 170 m

(a) Ballance, 1968; (b) Gibb, 1986; (c) Searle, 1991; (d) Ballance and Williams, 1992; (e) Nichol, 1992; (f) Williams (pers. comm.), 2006

2.8.2 Static evolution of a shore platform

To determine long term erosion rates from shore platform widths, as has been done recently by Paterson and Prebble (2004) and de Lange and Moon (2005), not only does the platform development have to occur over one erosion cycle, but the seaward edge of the platform also needs to be assumed to be a static feature, as modelled in Figure 2.10.

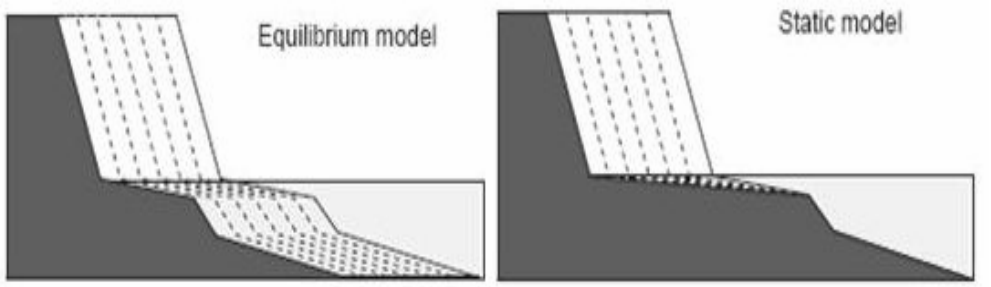

Figure 2.10: Diagram of the equilibrium and static models of shore platform evolution. Sourced from de Lange and Moon, 2005.

According to de Lange and Moon (2005) the static model of evolution sees the seaward edge of the shore platform remain relatively fixed while the platform width increases over time with cliff erosion. Equilibrium models see the whole shore platform migrate landward at a rate controlled by the recession of the coastal cliffs (de Lange and Moon, 2005). For the East Coast Bays sites measured by de Lange and Moon (2005), platform development has been assumed to behave like that modelled in Kaikoura by Stephenson and Kirk (1996) whereby the seaward edge of the platforms remains static and evolution occurs through cliff erosion and platform lowering.

2.8.3 Discussion of the origin of a higher platform bench

Several authors (Ballance, 1968; Searle, 1981; Ballance and Williams, 1992; Ballance, 1993; Williams, pers. comm. 2006) have discussed the origin of a platform bench that exists 2 - 4 m above the current shore platform on the east coast of the Auckland region. If the 'current' shore platform is to be used to determine erosion rates it is necessary to distinguish it from the higher platform bench. Three possible origins of the higher platform include tectonic movement, a higher period of sea-level, and storm wave attack.

2.8.3.1 High platforms as a result of tectonic movement

Tectonic movement is a common theory for the creation of marine terraces that sit slightly above the modern platform surface. Indeed, Searle (1981) notes that tectonic movement of the land during sea-level stillstand, "would produce exactly comparable results". The dating work of the culmination of the postglacial marine transgression by Gibb (1986) implies that while the Weiti River site has been tectonically stable for the last 120 - 125 ka, Kellys Beach on the north-eastern Firth of Thames has experienced 0.10 m ka^{-1} uplift. Pillans (1984) also reports a tectonic uplift of 0.15 m ka^{-1} from the Firth of Thames to approximately Auckland City and tectonic stability from about the East Coast Bays area to Leigh. Such uplift rates work out as about 0.7 - 1.1 m over the shore platform development period of 7120 ± 70 years which fits with the height of the observed higher platforms which range from 1 to 4 m (Ballance 1968; Ballance and Williams, 1992).

Gibb (1986) suggests that while the Kellys Beach site has experienced uplift, tectonic stability for the Holocene can be inferred if there is a platform less than 3 ± 3 m above the present sea-level and that, furthermore, all of the sites measured in his study can be classified as tectonically stable. Other authors suggest that while these higher benches may not be a result of tectonic movement, a general regional uplift has occurred of about 0.10 - 0.15 m ka^{-1} (Ballance and Williams, 1992; Ballance, 1993).

2.8.3.2 High platforms as a result of higher sea-level

Sea-level reached its maximum height 3 - 4 ka and then fell back to the current level (Searle, 1981) following which it is assumed that shore platforms continued to be eroded from their previous stillstand level. The maximum sea-level reached is believed by some authors to be marked by a low coastal terrace about 3-4 m above the current shore platform (Searle, 1981; Williams, pers. comm. 2006). Williams (pers. comm. 2006) believes that modern platforms that cut across Waitemata Group rock (and in places, greywacke) are trimming down and replacing a former higher platform - covered at high tide - that was about 1 m higher than the modern inter-tidal surface. This higher platform is considered to be a sea-level maximum from about 7-5 ka (Williams, pers. comm..2006).

A ~ 140 ka basalt platform (sourced from Lake Pupuke) that stands just above the high tide level near Takapuna in the North Shore may provide evidence to solve the question of sea-level oscillations, as dating of the basalts will give a maximum age for the platform (Ballance and Williams, 1992; Williams, pers comm. 2006). Gibb (1986) infers that the eustatic sea-level at the Last Interglacial climax was 4 - 6 m above present sea-level. The Lake Pupuke basalt platform has two benches cut into it, one of which is in the present inter-tidal zone, and the other is about 3 m higher (just below the predicted height of the Last Interglacial climax) (Williams, pers. comm. 2006).

2.8.3.3 High platforms as a result of storm wave attack

Higher level platforms exist in Manukau Breccia on the west coast of the Auckland Region which are generally believed to be the result of storm wave attack reaching higher levels and developing a separate platform from the predominant tidal platform (Searle, 1981). Similar higher benches are seen in the East Coast Bays Formation on the east coast of the Auckland Region and could be attributed to the same processes. However, due to the shelter from offshore islands and the Coromandel Peninsula, similar high-energy, erosive storm waves as those believed to have carved into the Manukau Breccia do not occur on the east coast and so the possibility of high platforms being a result of storm waves is questionable. The rock of the Waitemata Group is less resistant to erosion than the west coast volcanic rocks and so perhaps do not require as strong waves during storm conditions to develop higher shore platforms (Searle, 1981). Or, the benches are simply developed at the present-day high-tide mark and are the high-tidal platforms of Healy and Kirk (1992).

Gibb's (1986) conclusion that a marine bench found within a few metres of the modern analogue is likely to represent tectonic stability, therefore probably holds true for benches found in the southern sites of this research. Ages of formation of Holocene coastal landforms younger than 6.5 ka can be explained by a period of coastal erosion immediately following the postglacial transgression and at Kellys Beach the age of the highest Holocene shoreline is about 4 ka, suggesting coastal erosion from 6.5 - 4 ka (Gibb, 1986).

From the evaluation of the past research it seems that higher benches observed at the described sites are not the result of tectonic uplift, and there is too little evidence to prove storm wave attack. Platform benches at higher levels seem likely to be the result of periods of higher eustatic sea-level and/or are the present-day high-tide marker.

2.9 Summary

- Along the eastern coastline of the Auckland region, coastal cliffs have developed in the weak flysch beds of the Waitemata Group; namely the southern East Coast Bays Formation and northern Pakiri Formation.
- The Auckland region is within a marine environment which has a temperate climate with few extremes. Winds are predominantly from the south east which means the eastern coastline is sheltered, however north to east winds bring storm conditions and higher wave heights. The indented lee shoreline has a relatively low energy wave climate.
- Coastal cliff morphology in general is dependent upon a combination of marine and subaerial processes but on the eastern coastline of the Auckland region subaerial processes dominate cliff erosion. Shore platforms are commonly defined as either Type A (gently sloping) or Type B (horizontal with a seaward edge) profiles.
- Four lithological units can be distinguished in Waitemata Group rock and are classified on the basis of rheology of the flow by Gani, 2004. The units include sandstone and siltstone beds of turbidites, densite beds and debrite beds.
- Numerous research on coastal cliff erosion and methods for determining erosion rates has been carried out internationally, nationally and on Waitemata Group rocks in the Auckland region. A recent method for measuring long-term erosion rates involves using the width of a shore platform as the period over which recession of the cliff has occurred. The period over which cliff erosion in the Auckland region has occurred is 1720 $\pm$ 70 years based on the assumption that the seaward edge of platform has experienced insignificant erosion.

CHAPTER THREE

METHODOLOGY

3.1 Introduction

This chapter describes the methodology for data collection. Field work included rock mass descriptions and scanline surveys, conducting *in situ* strength measurements, determining the geomorphology of the site, and determining the Geological Strength Index of the rock mass. Laboratory work involved determining bulk density and porosity of sandstone rock, the modified jar slake test, and determining intact rock strength.

Some of the original data from field and laboratory work was then used for the calculation of other parameters including four different rock mass classification systems, rock mass strength parameters and for the construction of stereonets. A further set of data were sourced from GIS surfaces. This developed a complete database of parameters, which could be used to determine the influences on erosion rates through statistical analysis.

While it is understood by the author that the siltstone beds may in some areas classify as mudrocks (which include proportions of silt- and clay-sized sediments), the term 'siltstone' will be used in this study from here on in. This is because grain-size analysis on the rock was not undertaken in this study and also because there are many classifications for defining what is claystone, siltstone or collectively, mudstone between engineering and geology realms; choosing one classification system over another would serve no purpose to the aims of this study. Therefore, the 'siltstone' term which is most frequently used in research on Waitemata Group rocks is chosen.

3.2 Fieldwork

At each selected site a 30 - 50 m wide section of cliff and adjacent shore platform was described and measured for the geological and structural properties of the rock mass. All data are recorded from within the chosen section to ensure that any relationships made between the properties of the rock mass are comparable and consistent between sites.

3.2.1 Rock mass description

The geotechnical description of the cliff face was carried out following the guidelines of NZGS (2005). The features that were recorded are from:

1) Rock material descriptions including rock type (colour, fabric and grain size), weathering, bedding (inclination and thickness), and strength (intact rock); and
2) Discontinuity descriptions including type (joint, fault, bed), orientation (dip and dip direction), spacing, persistence, roughness, wall strength (of joint surfaces), aperture, infill, seepage, number of joint sets, block size and shape.

The rock name, colour, weathering, fabric and bedding were determined subjectively from a categorical list and wall strength was determined qualitatively by the degree of indentation from blows of a geological hammer. For the discontinuity parameters a categorical value was determined using the NZGS (2005) guidelines. The tilt of the beds and discontinuity orientations were measured using a Clar geological compass and joint roughness was measured with a profile gauge and recorded as a Joint Roughness Coefficient (JRC). Block size and shape were determined using the ISRM (1981) classification because this method better described the Waitemata Group rocks than the NZGS (2005) method.

At each site, the following information was also recorded:

- geomorphic profile sketches of the cliff section and shore platform including bedding orientation and thickness, bed dip angle, lithology type, cliff face orientation, vegetation cover, plus any outstanding features such as faults;
- location (NZ Map Grid co-ordinates) of the described site using a Garmin E-Trek 12 channel hand-held GPS; and
- photographs of the geology, structure and general site conditions.

3.2.2 Scanline survey

A scanline survey is a field method for collecting detailed statistical data of all aspects of discontinuities passing through a cliff section. A tape measure is stretched across a cliff face section and the properties of every discontinuity that passes through that tape is recorded. Various authors have made suggestions as to the length of tape required, or the number of discontinuities to record (for example, Priest and Hudson, 1976; Hoek and Bray, 1977; Brady and Brown, 2004) and it is a case of finding a balance between the time constraints of a research project and gathering enough data to be statistically sound. Based on this advice, approximately 100 discontinuities were recorded for both a horizontal and a vertical scanline at the sites and followed the method outlined in Brady and Brown (2004). A typical scanline set up is illustrated in Figure 3.1.

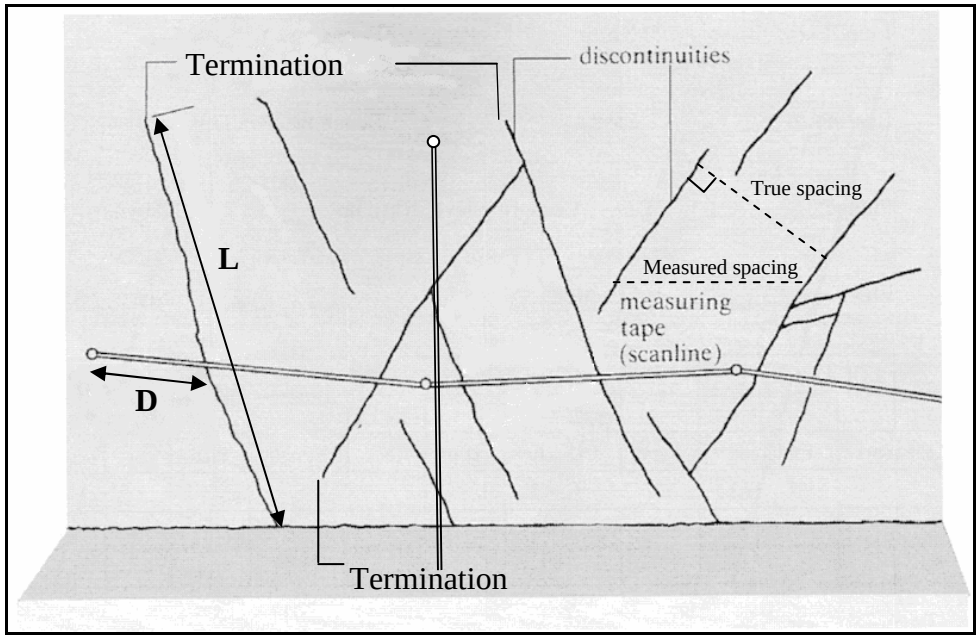

Figure 3.1: Scanline survey of a cliff face. 'L' is the length of the discontinuity; 'D' is the measured distance at which the discontinuity passes through the scanline. Modified from Brady and Brown (2004).

Firstly, a 30 m measuring tape was stretched and secured horizontally along a cliff face, in the vicinity of the described cliff section for that site. The point at which a discontinuity passed through the tape was recorded as the distance, D. The type of discontinuity was recorded (that is, joint, fault, fracture or bedding plane).

The following parameters were then recorded for each discontinuity using the same methods and equipment as for the rock mass descriptions: dip and dip direction of the discontinuity; the persistence of the discontinuity from one end to the other; the termination of the discontinuities both in their upper extent and their lower extent; the aperture and infill of the discontinuity; and the surface roughness of the discontinuity face if exposed enough for measurement. A second scanline is done at the same location in a vertical direction, because in heterogeneous rock masses a horizontal scanline often only surveys the discontinuities of one bed. True spacing has not been calculated for this research because regular, definite joint sets could not be determined at most sites. True spacing is the perpendicular distance between two joints, compared to a spacing measured horizontally (Figure 3.4). For the purposes of this research, and because there is too much variability in the joint orientations, it was deemed unnecessary to calculate the true spacing of the joint sets.

3.2.3 Strength measurements

The wall strength of the discontinuity surfaces was recorded at each site using an 'N' type Schmidt Hammer. 3 - 5 different beds were tested at each site, both vertically on the top of the bed, and horizontally on the joint face (Figure 3.2). Strength measurements were predominantly taken on sandstone beds as the siltstone beds were too highly fractured, but where siltstone beds were fresh and unfractured, strength measurements were taken. The tests were carried out following the methods outlined in ISRM (1981) and a measurement error of 1R (rebound number) was recorded as the highest error.

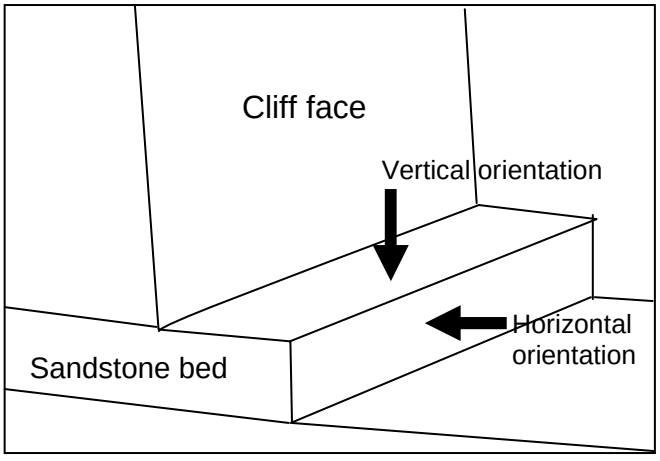

Figure 3.2: Orientation of the 'N' Type Schmidt hammer for measuring the wall strength of discontinuity surfaces. Arrows indicate the orientation of the Schmidt hammer on the sandstone bed.

3.2.4 Geomorphology

3.2.4.1 Cliff height and angle

A geomorphological profile of each site was constructed. The cliff face angle (angle C) was measured by lying down at the cliff base and sighting up to a defined cliff-top (Figure 3.3A). The angle to the top of the cliff was then measured at a recorded distance (angle D and distance B) from the cliff base, once again lying down. Lastly, the angle of the shore platform was measured (angle E) from the point where angle D was recorded to the point where angle C was recorded. All angle measurements were taken using a hand-held clinometer and the location and name of each measurement are illustrated in Figure 3.3B and 3.3C. Using the three measured angles (C, D and E), distance B, plus trigonometry calculations, the cliff height and cliff length could be determined (see the calculated example in Table 3.1).

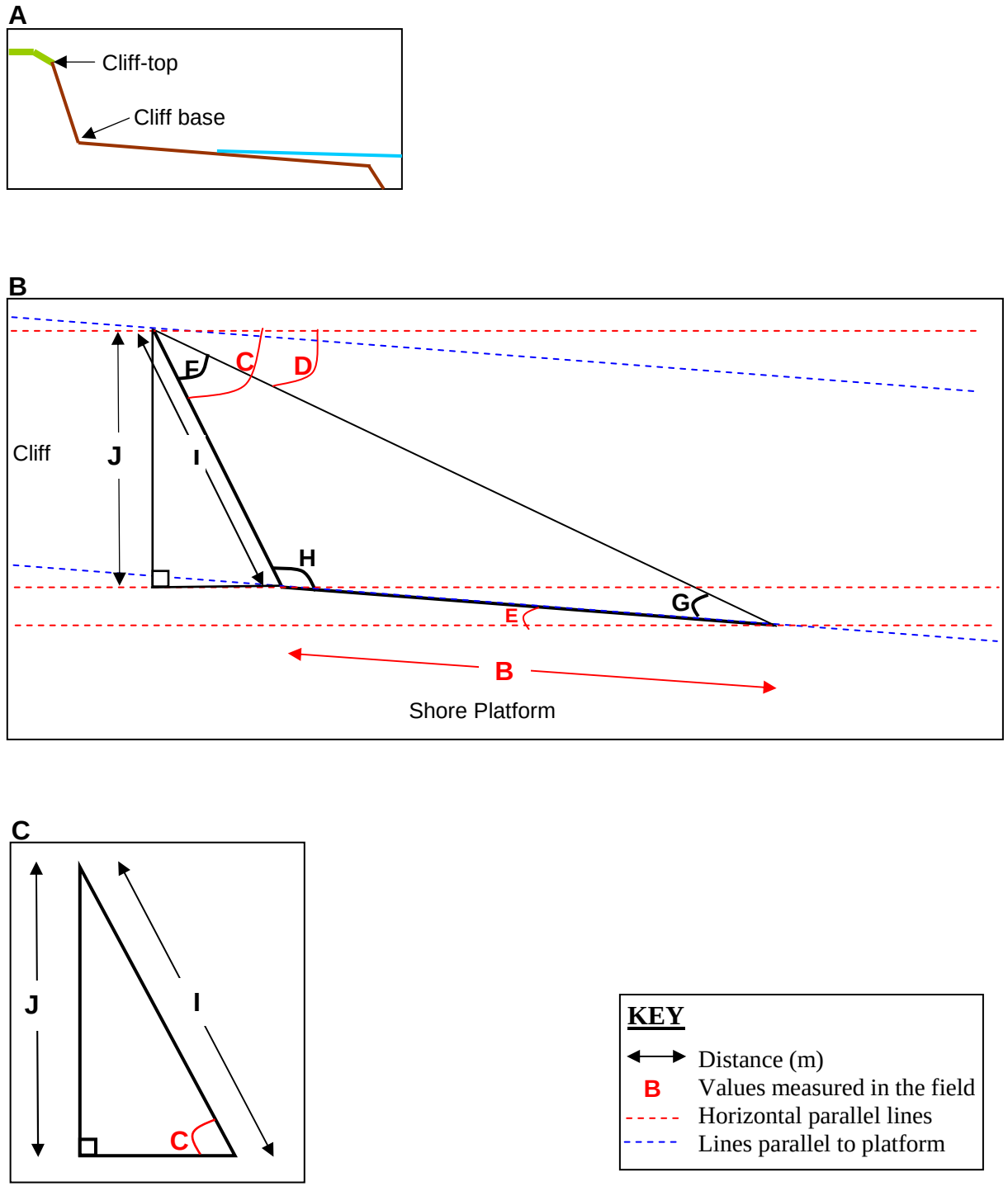

Figure 3.3: Angles and distances measured of the cliff face and shore platform area in order to calculate cliff heights and lengths for each site. **A:** The top of the cliff (marked by a black arrow) is taken as the point at which the bottom of the beveled edge and the top of the cliff scarp meet. **B:** The letters A-J represent the various measurements and calculations required to calculate the cliff height and length. An example calculation is shown in Table 3.1. **C:** 'J' represents the cliff height and 'I' represents the cliff length.

Table 3.1: Working example of the calculation of cliff height and cliff length.

A	B	C	D	E	F	G	H	I	J
Location (example)	distance B (m)	cliff base angle (°)	angle at distance (°)	platform angle (°)	angle F (°)	angle G (°)	angle H (°)	Length I (m)	Height J (m)
Example Bay	10	65	51	13	14	38	128	25.45	23.1
Error	0.2	0.5	0.5	0.5					

B (distance B) = 10 m
C (cliff base angle) = 65°
D (angle at distance) = 51°
E (platform angle) = 13°

F (angle F) = cliff base angle – angle at distance
= C-D
= 65 – 51
= 14°

H (angle H) = (180 - cliff base angle) + platform angle
= (180 - C) + E
= (180 - 65) + 13
= 128°

G (angle G) = 180 – angle F – angle H
= 180 - F - H
= 180 - 14 - 128
= 38°

Trigonometry formula used: $\frac{\sin a}{A} = \frac{\sin b}{B} = \frac{\sin c}{C}$ where a, b, c are angles and A, B, C are lengths of an isosceles triangle

Cockle Bay example: $\frac{\sin F}{B} = \frac{\sin G}{I} \longrightarrow I = B(\sin G) / (\sin F)$

I (Length I) = [distance B * SIN (angle F * PI( )/180)] / SIN (angle G * PI( )/180)
= [B * SIN(F*PI( )/180)] / (SIN(G*PI( )/180)
= B * SIN F / SIN G
= 10 * sin38 / sin14
= 25.45 m

*PI( )/180 = conversion of radians to degrees in Microsoft Excel spreadsheet

J (Height J) = distance I x sin (cliff base angle)
= I x sinC
= 25.45 x sin65°
= 23.06 m

3.2.4.2 Shore platform geometry

The geometry of the shore platform at each cliff site was determined using a hand-held GPS unit which recorded northing and easting co-ordinates of the New Zealand Map Grid. Mapping the geometry of the shore platform allowed the width of the platform to be determined, from the cliff base to the seaward margin of the shore platform, because the distance (in metres) between 2 points on land can be determined. These width measurements were later used to calculate the long term erosion rates of the cliffs.

Mapping the geometry of the shore platform involved walking and wading around the seaward margin of the shore platform then back along the cliff base to complete a circuit, encompassing the described cliff section. Waypoints were entered/recorded at regular intervals (every few seconds or at notable changes in orientation of the cliff base or platform edge) whilst walking around the circuit. The GPS data were downloaded to computer and formatted in a spreadsheet as cliff base coordinates and platform edge co-ordinates; the two sets of coordinates were graphed as separate lines to verify their geometry. Both sets of coordinates were then entered into a MATLAB routine which determined the width of the platform based on a line normal to the tangent from one cliff base coordinate to where it crossed the platform edge line of coordinates (Figure 3.4). A platform width value was determined from each cliff base coordinate from which the average shore platform width from each site's set of data were calculated.

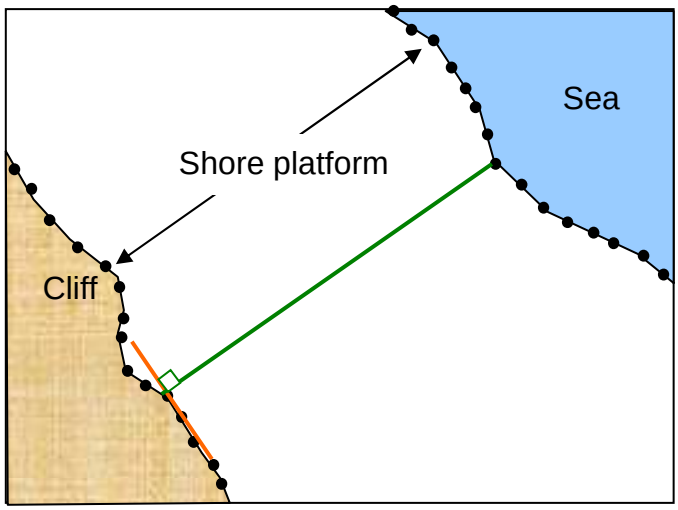

Figure 3.4: Plan view of the geometry of a shore platform, the width of which is measured using GPS coordinates. The marked coordinates are represented by black dots. The orange line represents the tangent of the GPS coordinate. The green line represents the normal to the tangent which intersects with the shore platform edge coordinates; this distance is the shore platform width.

3.2.5 Geological Strength Index

The Geological Strength Index (GSI) is a rock mass classification system which uses the surface conditions and structure of a rock mass to determine geological strength. Unlike other classification systems the GSI can be determined entirely in the field. The GSI value was recorded at each site using the standard chart for jointed rock masses (Table 3.1) for both sandstone and siltstone, and then using the more recently developed chart for heterogeneous rock masses (Table 3.2). Thus, two GSI values are obtained from Table 3.1, one for sandstone rock masses and one for siltstone rock masses individually, and a single value is obtained from Table 3.2 as an overall value of the heterogeneous rock mass.

Table 3.2: The GSI chart for jointed rock masses. Sourced from Marinos and Hoek (2001).

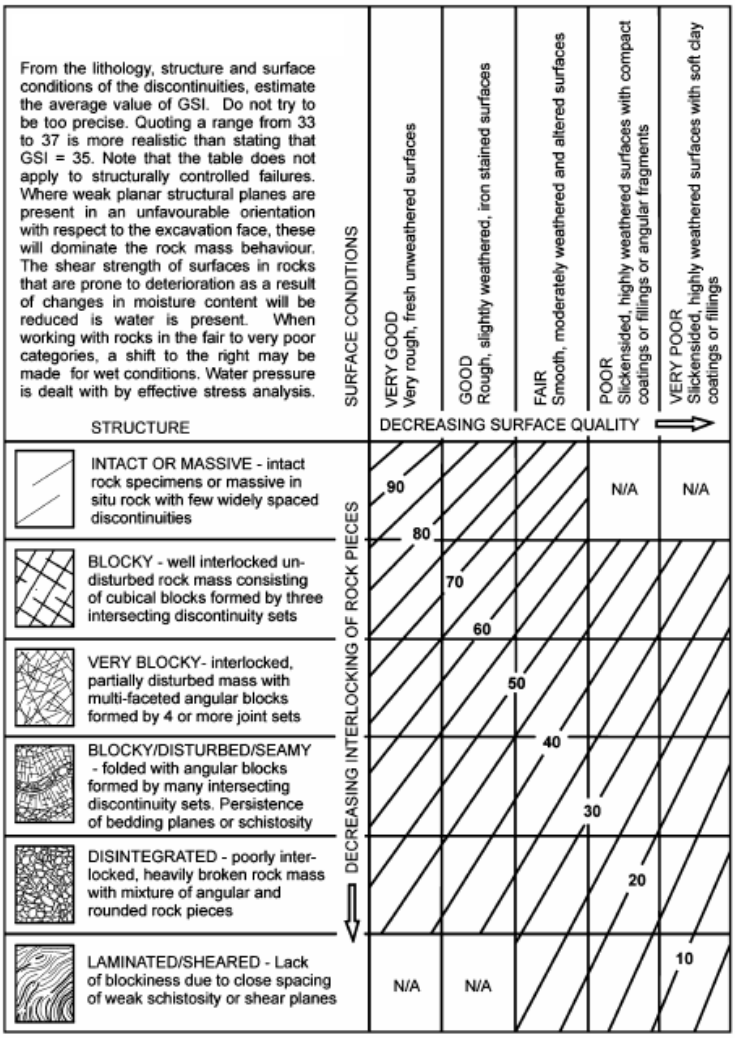

Table 3.3: The GSI chart for heterogeneous rock masses such as flysch. Sourced from Marinos and Hoek (2001).

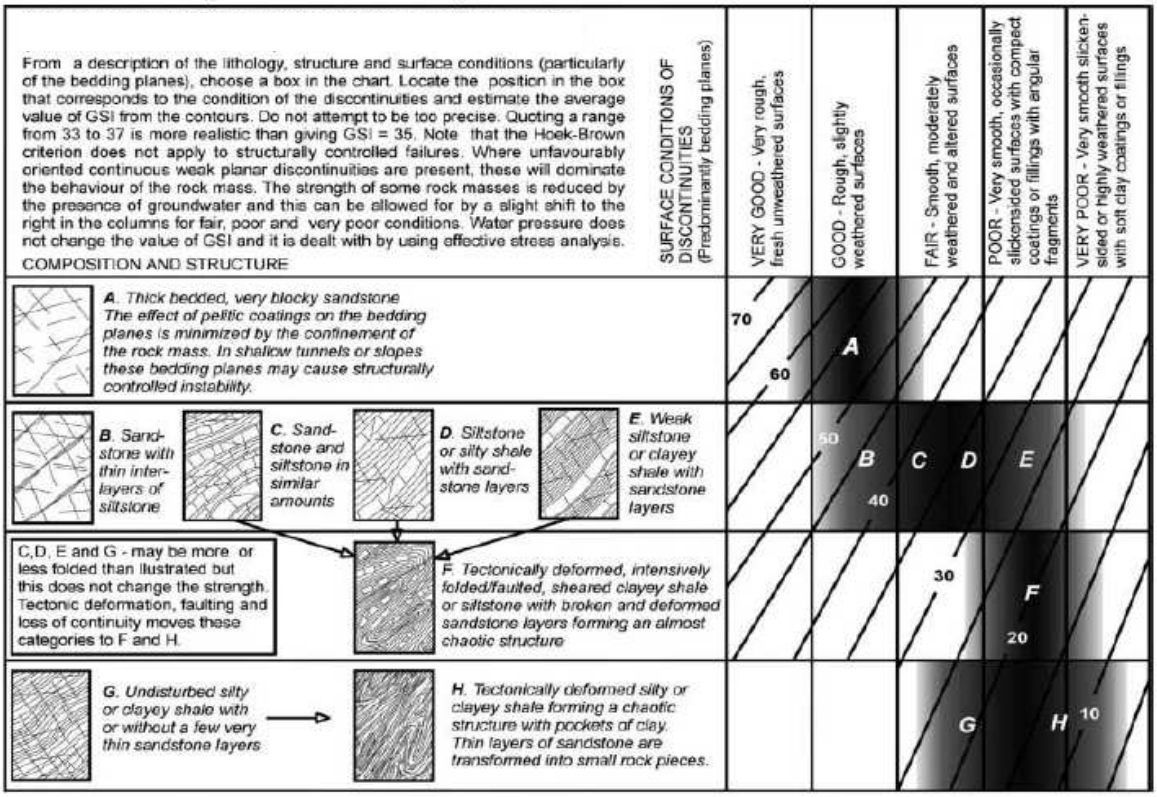

3.3 Laboratory Work

Laboratory work was carried out to determine some of the geomechanical properties of the sandstone and siltstone rock. Bulk density and porosity were measured in the sandstone samples for comparison with other related values, and for the determination of Hoek-Brown parameters. The modified jar slake test was used to observe slaking behaviour of the sandstone blocks. Intact strength tests were carried out on sandstone blocks and siltstone chips separately using the point load test and the NCB Cone Indenter respectively.

3.3.1 Sample preparation

3.3.1.1 Selecting samples

Sandstone and siltstone samples from turbidite beds were collected from every site for the laboratory tests. Twenty sandstone blocks (approximately 0.001 m^3 each) and a representative sample of siltstone (similar size to one sandstone sample) were collected from each site. The samples were taken from loose debris at the cliff base, broken off from larger debris with a geological hammer, or where possible were broken off from the cliff itself. The blocks were picked to be as fresh and unweathered as possible, free from cracks and normal discontinuities, and were collected at or within 50 m of the described cliff section.

The samples were stored in sealed plastic bags prior to testing; samples were chosen to be tested under air dry conditions because the natural moisture content of the rock is spoiled when the samples are cut into blocks with a wet saw. Also samples were collected on different days and so represented very different moisture conditions from site to site. All the samples were left in the same laboratory environment for 48 hours to air dry in order for samples from all sites to represent similar moisture conditions

3.3.1.2 Sample preparation

Sandstone samples were prepared for the laboratory tests by cutting into fist-sized blocks with regular and equal sides using a diamond-tip wet saw and following the guidelines set by ISRM (1981). The following procedure was used for sample preparation:

- using a rock saw, approximately 20 samples were cut to blocks such that the block had sides of a minimum of 27 mm (ISRM, 1981);
- for each block, each dimension was measured three times using calipers and an average dimension was calculated;
- the average values of each of the three dimensions were used to calculate the volume of the rock specimen, specimen bulk volume;
- the samples were left for 48 hours to air dry;
- half of the samples (~ 10) for each site were used for point load testing, and the other half (~ 10) were used to determine bulk density and porosity.

3.3.2 Bulk density and porosity

Bulk density and porosity of sandstone were measured using the saturation and caliper technique outlined in ISRM (1981). Masses of the cut, air-dried sandstone blocks (M_a) were measured first giving the air-dried bulk density of the samples (ρ_a). The samples were then saturated under vacuum pressure and the masses of the saturated-surface-dry blocks determined (M_{sat}). Because of the weak, incoherent nature of the sandstone, the block was weighed in an aluminium container of mass (M_{cont}). The samples were then oven-dried and their oven-dried grain masses determined (M_S). The bulk density (ρ_d) and porosity (V_v) for each rock sample were calculated from these measurements. An average was taken of the 10 samples for each site. The bulk density of siltstone was unable to be measured as samples were too frittered for testing. Selby (1993) quotes unit weight values for uniform inorganic silt as 12.6 - 18.5 kN m^{-3}. The average of this quoted range (15.6 kN m^{-3}) is used as the bulk density value for all the siltstone samples.

3.3.3 Modified Jar Slake test

The jar slake test was first proposed by Lutton (1977) as a means of determining the slake durability of very low and very high durability mudrocks, compared to the ISRM (1981) suggested methods which are intended for less friable rock. The modified jar slake test of Czerewko and Cripps (2001) is an updated version of Lutton's test which allows the rate at which a sample is degrading to be assigned independently of the physical disintegration (Table 3.4).

For the bulk density and porosity test, a few samples from each site were tested to begin with to see how they withstood the saturation under vacuum pressure. A number of the sandstone blocks showed signs of slaking whilst under saturation, and for these sites three untested blocks were kept aside for slake durability testing in order to better quantify the durability. Waitemata Group siltstone is already known to show signs of slaking *in situ* (Simpson, 1987; Brodnax, 1991), and the intact rock fragments from the collected samples were not large enough for this test, so the slake durability of the siltstone rock was not determined in this study.

For the sandstone samples a block with sides of 40 - 50 mm was brushed clean to remove any dust and oven dried at 60° for 72 hrs. Once the sample had cooled in a desiccator it was placed in a 500 ml or 1000 ml beaker, covered to a level 50 mm above its top with distilled water, and the stopwatch was started (Figure 3.5).

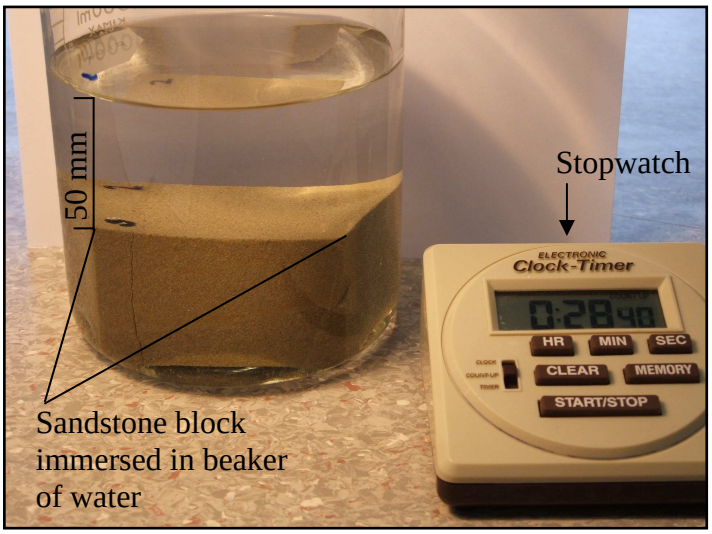

Figure 3.5: Modified jar slake test set-up for observing the durability of rocks when immersed in water.

Descriptions of the samples and the associated modified jar slake value (Ij') were recorded at elapsed time intervals of 1 min, 10 min, 30 min, 1 hr, 2 hr, 3 hr, 4 hr, 6 hr, 8 hr, and 24 hr (Table 3.4). Samples were viewed in good light from several different aspects. If no change was observed in the sample after 24 hours, it was left for a further 24 hours and again described. Samples were tested in triplicate and then averaged for each site.

Table 3.4: Modified jar slake classification scheme. Adapted from Czerewko and Cripps (2001).

Ij'	Sample behaviour	Classification
1	No visible sign of specimen deterioration - air bubbles may be emitted from the sample.	**Extremely Durable**
2	No notable specimen deterioration, development of occasional hairline fractures (usually bedding fractures, or parallel to bedding), air bubbles generally emitted from these fractures.	
3	Slight specimen deterioration, consisting of closely spaced (10 - 20 mm), up to 1 mm open fractures, usually parallel to bedding. Sample may exhibit up to 5 % slaking, usually from the sample corners.	
3i	Same as 3, but fractures tend to be randomly orientated.	
4	Moderate specimen deterioration, generally consisting of many very closely spaced (5 - 10 mm) fractures which are open up to 2 mm. Sample may exhibit up to 15 % slaking producing gravel sized fragments and shards.	**Durable**
4i	Same as 4, but fractures tend to be randomly orientated.	
5	Moderate to high specimen deterioration, consisting of many extremely closely spaced (2 - 5 mm) fractures which are open up to 4 mm and generally parallel to bedding. Sample block integrity is maintained, although the block may have split into a few free standing columns. Sample block/s have a heavily desiccated appearance. Sample may exhibit up to 25 % slaking producing gravel sized fragments and shards.	
5i	Same as 5, but fractures tend to be randomly orientated.	
6	High degree of sample deterioration. The specimen block shape is only partially retained, either in the form of multiple free-standing columns, or as a column supported within a pile of slaked debris. Sample block/s have a heavily desiccated and unstable appearance. Horizontal fractures are extremely closely spaced (2 - 6 mm) and generally open 2 - 4 mm with many crossing fractures. Sample may exhibit up to 75 % mass slaking.	**Non Durable**
7	The sample block shape is largely or completely destroyed. The slaked debris (75 - 100 % of the block) generally consists of a pile of angular gravel sized shards or blocky fragments occasionally supported with free-standing fragments of the original sample block.	
8	Total sample disintegration consisting of a pile of soil like debris, i.e. high proportion of sub-gravel sized debris and some fine to medium gravel sized fragments	

3.3.4 Point Load Strength testing

The Point Load Strength test was used to determine the intact uniaxial compressive strength (UCS) of the Waitemata Group sandstone following the ISRM (1985) suggested method for block and irregular lump tests. Rock specimens were in the form of a cut block (Section 3.3.1) and the test was performed using a Point Load Strength laboratory testing machine (Figure 3.6). The rock sample was placed between the two steel platens of the machine and the hydraulic ram consistently pumped until the rock sample failed, from which the load, P, required to break the sample was recorded from the digital

display. The digital display gave a P value that was unit-less and was converted to a force value by the formula:

$$\mathbf{P\,(N) = \frac{(P\,(unit-less) \times 1000\,N) - 0.1427}{0.8775}}$$

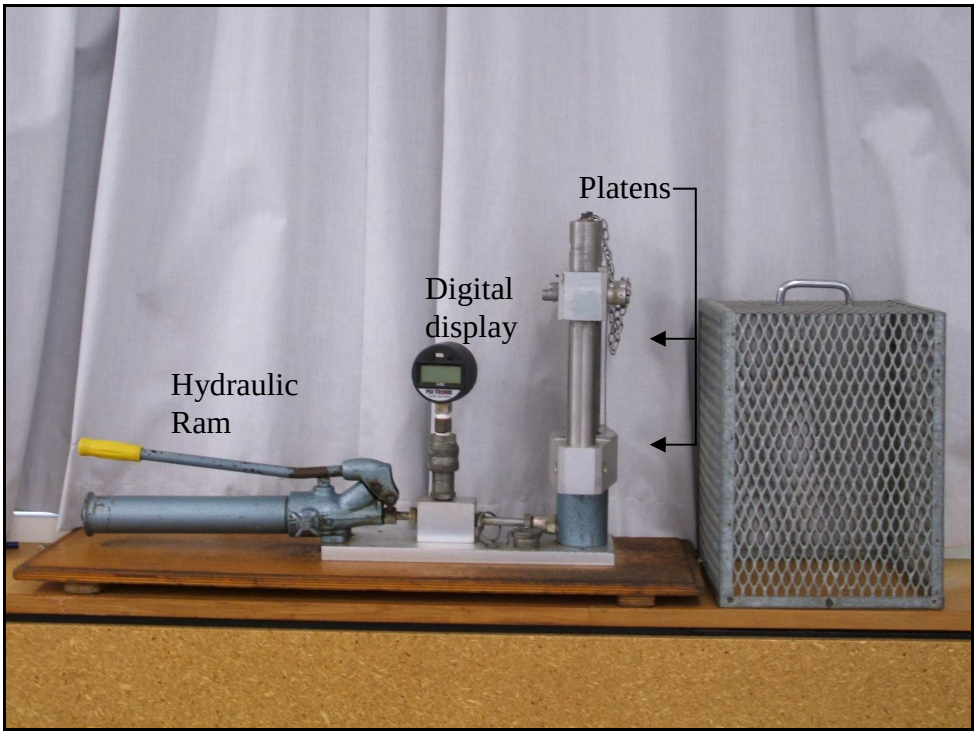

Figure 3.6: Point Load Strength testing machine.

The maximum uncorrected strength, I_S, exerted on the centre of the block is calculated as:

$$\mathbf{I_S = P/D^2_e}$$

where: P = applied force at failure (dimensionless)

D_e (mm) = the equivalent core diameter

The equivalent core diameter (Figure 3.7) is given by:

$$\mathbf{D^2_e = 4A / \pi}$$

where: A (mm^2) = minimum cross sectional area of a plane through the platen contact points

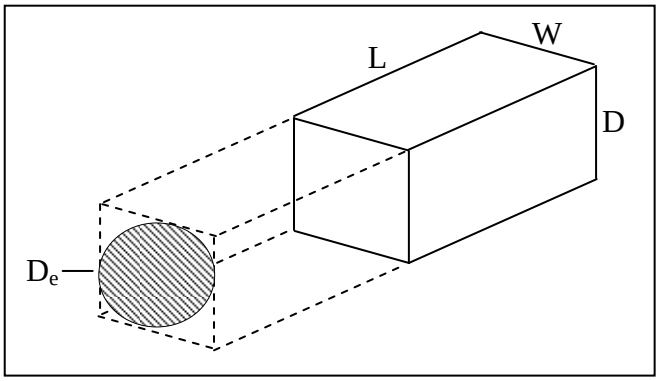

Figure 3.7: Aspects of cut block used in the Point Load Strength test. L = length of the block. W = width of the block. D = depth of the block. D_e = equivalent core diameter. The diagram is adapted from ISRM (1985).

I_S varies as a function of D_e for the block and irregular lump test and as such a size correction needs to be applied to acquire a unique point load strength value for every rock sample. For these samples the size correction is calculated by:

$$\mathbf{I_{s(50)} = F \times I_S,}$$

where: $F = (D_e/50)^{0.45}$

For each site the average corrected point load strength value ($I_{S(50)}$) was calculated by deleting the two highest and lowest values obtained from all the samples and then calculating a mean from the remaining values. The average $I_{S(50)}$ value for each site was then converted to a UCS value by multiplying by 22. This factor of 22 has been determined by Brook (1985) as the relationship between a given point load strength value and uniaxial compressive strength and has commonly been used by other studies on weak Tertiary rocks in New Zealand (Russell, 1996; Roy, 1997).

3.3.5 NCB Cone Indenter

The NCB Cone Indenter (Figure 3.8) determines the hardness of rock by measuring its resistance to indentation from a hardened tungsten carbide cone (MRDE, 1977) and was chosen as the method for determining the uniaxial compressive strength (UCS) of siltstone rock. The NCB Cone Indenter only needs very small samples (maximum 12 mm x 12 mm x 6 mm) so was the most appropriate equipment to use on the frittered siltstone. For each site, 15 specimens were tested for each sample and the highest and lowest values of the specimens were discarded before calculating an average UCS value (as for the Point Load Strength test). Specimens chosen were free from cracks and other defects and were dusted clean before testing.

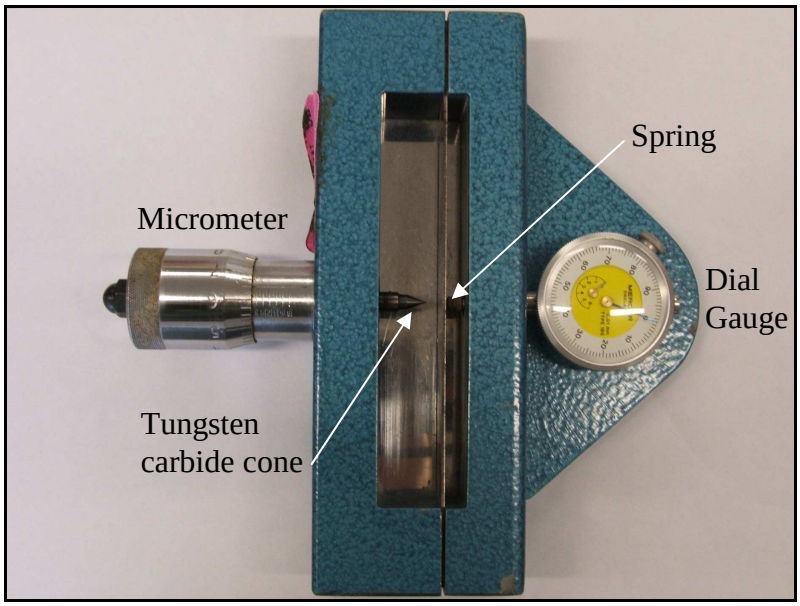

Figure 3.8: NCB Cone Indenter.

The micrometer is used to measure the amount of indentation into the siltstone fragment and the gauge indicates the distance the spring has deflected; both are measured in millimeters. The specimen was set on the steel bar of the cone indenter and the micrometer was screwed until the specimen was just held in position by the cone. The dial gauge was reset to zero and the initial micrometer reading (M_0) was taken. Because the siltstone specimens were weak the applied load was set at 12 N (MRDE, 1977). The micrometer screw was turned clockwise until the spring deflection was equivalent to a load of 12 N and the amount of deflection on the spring, read from the

dial gauge, recorded (D_1). At this stage the final micrometer reading (M_1) was also taken. The siltstone rock was classified as weak rock so a conversion factor was applied to obtain the weak rock cone indenter number following the guidelines of MRDE (1977).

The penetration of the cone into the siltstone specimen is calculated as:

$$\mathbf{P_W\ (mm) = (M_1 - M_0) - D_1}$$

The weak rock cone indenter number is then calculated as:

$$\mathbf{I_W\ (mm) = 0.23/P_W}$$

The UCS value of the siltstone (MPa) is equal to I_W x 16.5 (MRDE, 1977)

3.4 Data Manipulation and Analysis

Some of the data collected from field work and laboratory work was required for the calculation of additional properties of Waitemata Group coastal cliffs. These properties included: four rock mass classification systems (the Rock Quality Designation (RQD), the Rock Mass Rating (RMR), the Slope Mass Rating (SMR), and Rock Mass Strength (RMS)); rock mass parameters of cohesion, friction angle and strength; and structural analysis from stereographic projections. These properties were only determined for the sites where scanline surveys were carried out as they require the detailed discontinuity data.

3.4.1 Rock Quality Designation

RQD was originally established as a means of finding the frequency of discontinuities within a core of rock, calculated as the proportion of core that consists of intact lengths that are 0.1 m or longer (Priest and Hudson, 1976). Because coring of rock is not always feasible due to time, money and accessibility constraints, Priest and Hudson (1976) established a method for calculating RQD from scanline survey data. Priest and Hudson (1976) considered the possible distributions of discontinuity spacing along a straight line

through a rock mass and found that any combination of evenly spaced, clustered and randomly positioned discontinuities leads to a negative exponential form of a frequency versus spacing curve. A relationship was thus developed between the RQD and the mean discontinuity frequency per meter by incorporating the negative exponential form. This relationship is (Priest and Hudson, 1976):

$$\mathbf{RQD = 100e^{-0.1\lambda}\,(0.1\lambda + 1)}$$

where: λ = average number of discontinuities (that persist > 0.1 m) per meter.

For each site where scanline surveys were carried out the number of discontinuities recorded that persisted > 0.1 m was divided by the total scanline length to determine the mean discontinuity frequency per meter.

3.4.2 Rock Mass Rating system

The RMR was developed by Bieniawski (1973) to assess and predict the behaviour of a rock mass for tunnel design (Bieniawski, 1979). It has since been adjusted for use in a number of different engineering applications including the stability of natural slopes.

3.4.2.1 Basic RMR

The basic RMR (bRMR) considers five parameters of the rock mass (Bieniawski, 1989) including: intact rock strength rating; RQD rating; joint spacing rating; discontinuity condition rating; and groundwater rating. For each of these parameters, ratings are determined from the charts illustrated in Bieniawski (1989) and are presented in Tables 3.5 and 3.6. Summation of the five rating values gives the bRMR (a value out of 100). The description of the rock mass is given in Table 3.6C (from Bieniawski, 1989).

For this study the following methods were used to determine the ratings for each parameter:

1) Intact rock strength values for sandstone and siltstone were measured from the point load strength test and NCB cone indenter test respectively as UCS values.

2) RQD values were determined from scanline survey data as detailed in Section 3.4.1.

3) The spacing of discontinuities was calculated from scanline data as the reciprocal of the mean discontinuity frequency; that is, scanline length divided by the number of discontinuities recorded in the scanline.

4) Five discontinuity properties are individually given RMR ratings using the chart (Table 3.5) of Bieniawski (1989); they were calculated from scanline data and then added together to provide an overall condition of the discontinuities for every site (Table 3.6A).

Table 3.5: Classification of discontinuity orientations. Adapted from Bieniawski (1989).

Parameter	Ratings				
Discontinuity length (persistence/continuity)	<1 m	1-3 m	3-10 m	10-20 m	>20 m
	6	4	2	1	0
Separation (aperture)	None	<0.1 mm	0.1-1.0 mm	1-5 mm	>5 mm
	6	5	4	1	0
Roughness	Very rough	Rough	Slightly rough	Smooth	Slickensided
	6	5	3	1	0
		Hard filling		Soft filling	
Infilling (gouge)	None	<5 mm	>5 mm	<5 mm	>5 mm
	6	4	2	2	0
Weathering	Unweathered	Slightly weathered	Moderately weathered	Highly weathered	Decomposed
	6	5	3	1	0

Persistence and aperture were calculated as the average discontinuity persistence of all discontinuities measured in the scanline. Roughness and infill were qualitatively determined as the predominant or average roughness of all discontinuities measured in the scanline. Weathering was qualitatively determined as the state of weathering recorded during the geotechnical site descriptions.

5) Observations of the seepage from the cliff face and shore platform area were made during geotechnical rock mass descriptions (Table 3.6A).

3.4.2.2 Adjusted RMR

The adjusted RMR (aRMR) is calculated by subtracting a rating for the favourability of discontinuity orientation (Table 3.6B) from the basic RMR value. The predominant discontinuity sets (dip and dip direction) were determined from scanline data then converted to a rating based on favourability for strength of the rock mass.

Table 3.6: RMR classification parameters and their ratings. Adapted from Bieniawski (1989).

A. CLASSIFICATION PARAMETERS AND THEIR RATINGS

Parameter			Range of values						
1	Strength of intact rock material	Point-load strength index (MPa)	>10	4-10	2-4	1-2	For this low range, uniaxial compressive test is preferred		
		Uniaxial compressive strength (MPa)	>250	100-250	50-100	25-50	5-25	1-5	<1
	Rating		15	12	7	4	2	1	0
2	Drill core quality RQD (%)		90-100	75-90	50-75	25-50	<25		
	Rating		20	17	13	8	3		
3	Spacing of discontinuities		>2 m	0.6-2 m	200-600 mm	60-200 mm	<60 mm		
	Rating		20	15	10	8	5		
4	Condition of discontinuities		Very rough surfaces Not continuous No separation Unweathered wall rock	Slightly rough surfaces Separation <1 mm Slightly weathered walls	Slightly rough surfaces Separation <1 mm Highly weathered wall	Slickensided surfaces or Gouge <5 mm thick or Separation 1-5 mm Continuous	Soft gouge >5 mm thick or Separation >5 mm Continuous		
	Rating		30	25	20	10	0		
5	Groundwater General conditions		Completely dry	Damp	Wet	Dripping	Flowing		
	Rating		15	10	7	4	0		

B. RATING ADJUSTMENT FOR DISCONTINUITY ORIENTATIONS

Strike and Dip Direction of Discontinuities		Very Favourable	Favourable	Fair	Unfavourable	Very Unfavourable
Ratings	Tunnels and mines	0	-2	-5	-10	-12
	Foundations	0	-2	-7	-15	-25
	Slopes	0	-5	-25	-50	-60

C. ROCK MASS CLASSES DETERMINED FROM TOTAL RATINGS

Rating	100-81	80-61	41-60	40-21	<20
Class No.	I	II	III	IV	V
Description	Very good rock	Good rock	Fair rock	Poor rock	Very poor rock

3.4.3 Slope Mass Rating system

The Slope Mass Rating (SMR) was developed by Romana (1985) as a new geomechanical classification for slopes in rock intended as a tool for the preliminary assessment of slope stability and stemming from the development and use of the RMR (Romana, 1993). The classification is calculated from five parameters including (Romana, 1993): the bRMR of Bieniawski (1989); a factor that depends on the parallelism between joints and the strike of the slope face; a factor that refers to joint dip angle in the planar mode of failure; a factor that reflects the relationship between the slope face and joint dip; and an adjustment factor for the method of excavation of the slope. The ratings of the four factors are given in Table 3.7.

Table 3.7: Adjustment ratings for F_1, F_2, and F_3 of the SMR. Adapted from Romana (1993).

Case	*Very favourable*	*Favourable*	*Fair*	*Unfavourable*	*Very unfavourable*
P $\lvert\alpha_j - \alpha_s\rvert$ T $\lvert(\alpha_j - \alpha_s) - 180°\rvert$	> 30°	30-20°	20-10°	10-5°	< 5°
P/T F_1	0.15	0.40	0.70	0.85	1.00
P $\lvert\beta_j\rvert$	< 20°	20-30°	30-35°	35-45°	> 45°
P F_2	0.15	0.40	0.70	0.85	1.00
T F_2	1	1	1	1	1
P $\beta_j - \beta_s$	> 10°	10-0°	0°	0° to -10°	< -10°
T $\beta_j + \beta_s$	<110°	110-120°	>120°	n/a	n/a
P/T F_3	0	-6	-25	-50	-60

Where: P, plane failure; T, toppling failure; α_s, slope dip direction; β_s, slope dip; α_j, discontinuity dip direction; β_j, discontinuity dip; n/a, not applicable.

With regards to slope failure, bedding plane failure is noted by Moon and Healy (1994) as one of the most prominent failure mechanisms in Waitemata Group cliffs and this is supported by the knowledge that in sedimentary rock the major joints are usually along bedding planes and are hence, essentially planar (Selby, 1993). Therefore, only the planar discontinuities of the bedding surfaces were considered and compared to the orientation of the cliff face. Factors 1, 2 and 3 were calculated from the dip and dip directions of the prominent bedding planes and the cliff face at each site. Factor 4 was consistently a value of +15 for each site as it is the rating for natural slopes.

3.4.4 Rock Mass Strength system

The RMS was developed by Selby (1980) to predict the overall rock mass strength for engineering purposes (Selby, 1993). The RMS system considers seven parameters of the rock mass (Selby, 1993): intact rock strength rating; weathering rating; joint spacing rating; joint orientation rating; joint width rating; joint continuity and infill material rating; and groundwater outflow rating.

Similarly to the RMR system, field and laboratory data are converted to ratings from the chart in Selby (1993) which is presented in Table 3.8. Summation of the seven rating values gives the RMS (a value out of 100) for which the description is also given in Table 3.8.

Table 3.8: Rock Mass Strength classification system. Adapted from Selby (1993).

Parameter	(1)	(2)	(3)	(4)	(5)
	Very Strong	Strong	Moderate	Weak	Very Weak
Intact rock strength (N-type Schmidt Hammer 'R')	100-60 r : 20	60-50 r : 18	50-40 r : 14	40-35 r : 10	35-10 r : 5
Weathering	Unweathered r : 10	Slightly weathered r : 9	Moderately weathered r : 7	Highly weathered r : 5	Completely weathered r : 3
Spacing of joints	>3 m r : 30	3-1 m r : 28	1-0.3 m r : 21	300-50 mm r : 15	<50 mm r : 8
Joint orientations	Very favourable. Steep dips into slope, cross joints interlock r : 20	Favourable. Moderate dips into slope r : 18	Fair. Horizontal dips, or nearly vertical (hard rocks only) r : 14	Unfavourable. Moderate dips out of slope r : 9	Very unfavourable. Steep dips out of slope r : 5
Width of joints	<0.1 mm r : 7	0.1-1 mm r : 6	1-5 mm r : 5	5-20 mm r : 4	>20 mm r : 2
Continuity of joints	None continuous r : 7	Few continuous r : 6	Continuous, no infill r : 5	Continuous, thin infill r : 4	Continuous, thick infill r : 1
Outflow of groundwater	None R : 6	Trace R : 5	Slight <25 //min/10m^2 R : 4	Moderate 25-125 //min/10m^2 R : 3	Great >125 //min/10m^2 R : 1
TOTAL RATING	100-91	90-71	70-51	50-26	<26

For this study the following methods were used to determine the ratings for Each parameter:

1) Intact rock strength was measured from an N-Type Schmidt Hammer and the rebound (R) number was converted to a UCS value using the conversion chart of Deere and Miller (1966).

2) The state of weathering was recorded during the geotechnical rock mass description.

3) Joint spacing was calculated as the scanline length divided by the number of discontinuities recorded in that scanline survey.

4) Joint orientations are determined based on their favourability for strength of the rock mass. Major discontinuity sets were determined from the scanline data and assessed using the chart of Selby (1993) which is presented in Table 3.9.

Table 3.9: Classification of discontinuity orientations. Adapted from Selby (1993).

	Mode of joint formation	
	Tensile (rough)	Shear (smooth)
Very unfavourable	Joints dip out of the slope: planar joints 30-80°; random joints >70°.	Joints dip out of slope; planar joints >20°; random joints >30°.
Unfavourable	Joints dip out of the slope; planar joints 10-30°; random joints 10-70°.	Joints dip out of the slope; planar joints 10-20°; random joints 10-30°.
Fair	Horizontal to 10° dip out of the slope. Nearly vertical (80-90°) in hard rocks with planar joints.	Horizontal to 10° dip out of the slope.
Favourable	Joints dip from horizontal to 30° into the slope: cross joints not always interlocked.	
Very Favourable	Joints dip at more than 30° into the slope: cross joints are weakly developed and interlocking.	

5) Joint width (aperture) was taken from the scanline survey data and an average value was calculated.

6) Continuity of predominant discontinuity sets was estimated from the scanline survey data and infill material was qualitatively assessed for the average thickness and type at the cliff section.

7) Observations of the seepage from the cliff face and shore platform area were made during geotechnical site descriptions.

3.4.5 Analysis of rock mass strength

Field data was used in the RocLab 1.0 program to determine rock strength parameters, derived from the generalized Hoek-Brown failure criterion (Rocscience, 2002). This program is designed for jointed rock masses based on the principles of Hoek and Brown (1980) and requires the following inputs from each cliff site: UCS values of intact rock (sig_{ci}) measured in MPa as in section 3.3.4 and 3.3.5; GSI values; a material constant related to the frictional properties of the rock (m_i); and a disturbance factor (D) which ranges from 0 for undisturbed rock masses to 1 for disturbed rock masses (Hoek *et al.*, 2002). For slopes the cliff face height is also required, and the unit weight of the rock material is calculated from an average of the air-dried bulk density measures of sandstone and the average bulk density value of siltstone sourced from Selby (1993). The series of equations developed by Hoek *et al.* (2002) determine the cohesion and friction

angle of the rock mass plus rock mass parameters of tensile strength (sig_t), compressive strength (sig_c), global strength (sig_{cm}), and the deformation modulus (E_m).

This analysis was done for the sites where scanline surveys were conducted. Because GSI classification was undertaken using the chart for jointed rocks (sandstone and siltstone as separate rock masses) and the chart for heterogeneous rock masses, separate analyses were undertaken for the three variants (see Tables 3.2 and 3.3). The material constant was determined from the chart of Hoek and Brown (1997) and the average values for sandstone (17) and siltstone (7) were used. The disturbance factor is a qualitative measure of the degree of disturbance to which the rock mass has been, or will potentially be, subjected and originated from experience in the design of slopes in large mines (Thomas *et al.*, 2004). There were applicable published guidelines describing which D value to use for natural slopes and as such, the D value used for this study was chosen as 0.5, which is the mid-range of the values available for D. It is appreciated however that the disturbance factor is a very sensitive parameter when determining rock mass parameters (Hoek and Brown, 2002; Thomas *et al.* 2004).

Estimating the rock mass properties using the GSI chart for heterogeneous rock masses requires the sig_{ci}, m_i and unit weight values to be adjusted according to the proportion of sandstone and siltstone in the rock mass, as determined by the recorded flysch type for a particular site (Table 3.10).

Table 3.10: Suggested proportions of parameters sig_{ci}, m_i and unit weight for estimating heterogeneous rock mass properties. Modified from Table 4 of Marinos and Hoek (2001).

Flysch type (see Table 3.3)	Proportions of values for each rock type to be included in rock mass property determination
A and B	Use values for sandstone beds
B-C	Reduce sandstone values by 10% and use full values for siltstone
C	Reduce sandstone values by 20% and use full values for siltstone
D	Reduce sandstone values by 40% and use full values for siltstone
E	Reduce sandstone values by 40% and use full values for siltstone
E-F	Reduce sandstone values by 50% and use full values for siltstone
F	Reduce sandstone values by 60% and use full values for siltstone
G	Use values for siltstone or shale
H	Use values for siltstone or shale

3.4.6 Stereographic analysis of structural geology

Stereographic projection of discontinuity orientations allows three-dimensional data to be represented and analysed in two dimensions (Wyllie and Mah, 2004). Scanline surveys provided a detailed view of the orientations of joint sets, faults, and bedding surfaces. Stereonets were constructed in RockWorks02 (RockWare Inc., 2002) to estimate the modes of failure in Waitemata Group cliffs. The stereonets were analysed following the guidelines of Wyllie and Mah (2004) which outline specific conditions to determining various mechanisms of failure. These are summarised in Figure 3.9.

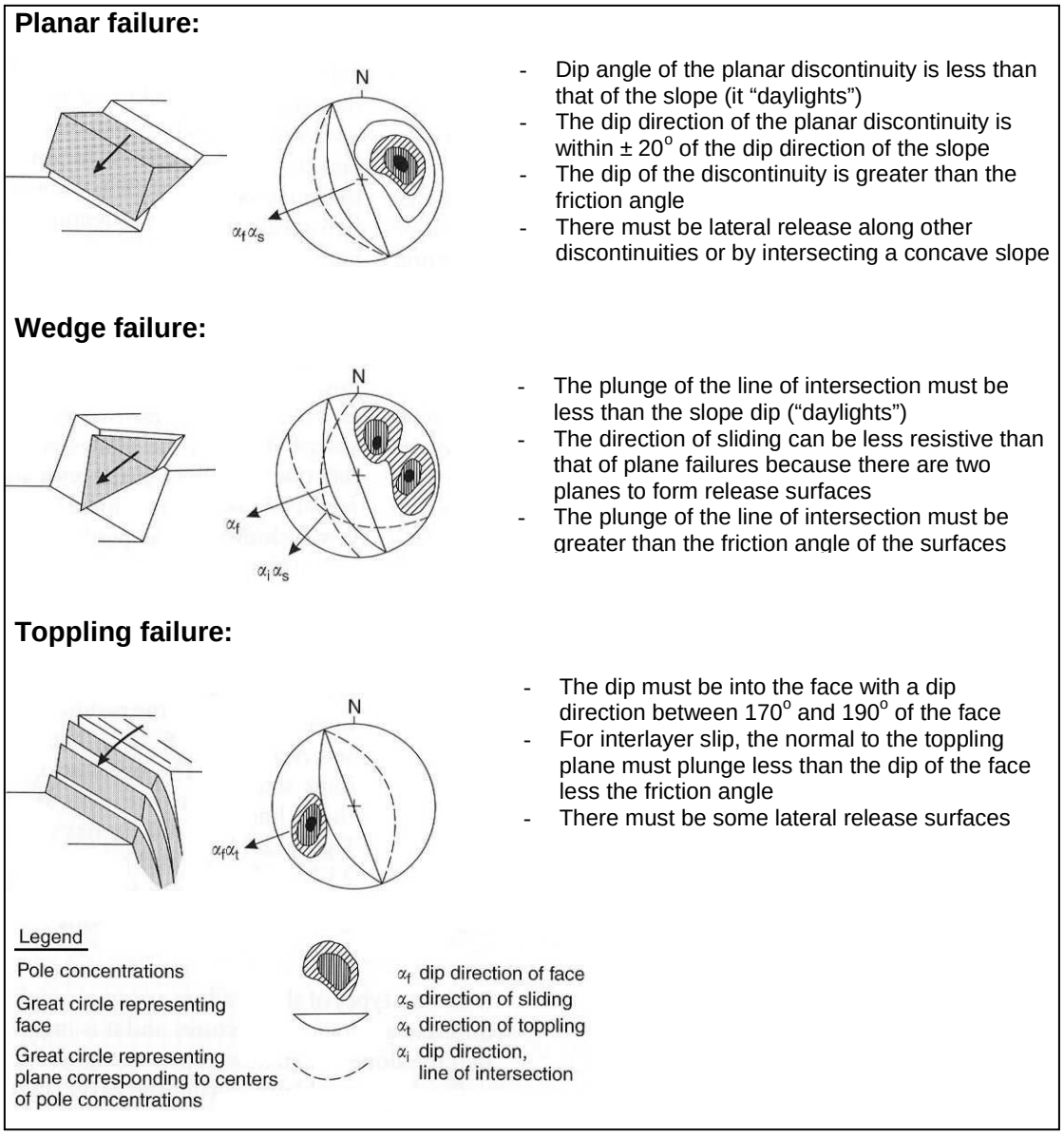

Figure 3.9: Mechanisms for failure predicted from the kinematic analysis of stereonets. Modified from Wyllie and Mah (2004).

3.5 GIS Source of Additional Data

A range of climate, geomorphology and terrain attributes were sourced from GIS surfaces for each of the selected sites to contribute in addition to the collection of data from field work and laboratory work and the other derived properties. The selected parameters (to be used in later statistical analysis) are detailed in Appendix 7.

Data were extracted from the GIS surfaces for each site using the New Zealand Map Grid (NZMG) coordinates measured along the cliff base at each of the 16 cliff sections (Figure 3.10). The cell that a coordinate is in can be linked with data for all the available parameters that exist in that cell. Where a GPS coordinate did not fit into a cell, the coordinate was altered by a small margin to fit within the closest cell.

Various parameters were extracted from three different cell resolutions (widths): 1000 m, 100 m, and 25 m. The shore platform widths calculated for each site were added in as a data set for later statistical analysis. Once the data had been extracted for each coordinate at each site, all of the values had to be transformed in order to develop central tendency of the data sets and convert the values to proper units of measure. This involved a three stage process of scaling the value through division, revaluing zeros, and transforming the value with an exponent. For instance:

- For the extracted value from a cell for mean annual temperature the following information was given:
  The value of that cell was 149 (no units),
  Scale by (divide by): 10
  Revalue zeros: 0
  Power transformations: 1
- This value needed to be scaled by 10 = 149 / 10 = 14.9
- Any mean annual temperature values that were zero did not need to be revalued because 0 ^{o}C is an actual value
- The power transformation for mean annual temperature was 1.
  $14.9^{\wedge 1} = 14.9$ (^{o}C)

These calculations were carried out on all the parameters that were found in a cell that had a marked GPS coordinate in it. Thus for every site location, there were a series of values (for each parameter) from which an average could be taken to represent the likely conditions at that site. The resulting dataset is presented in Appendix 7.

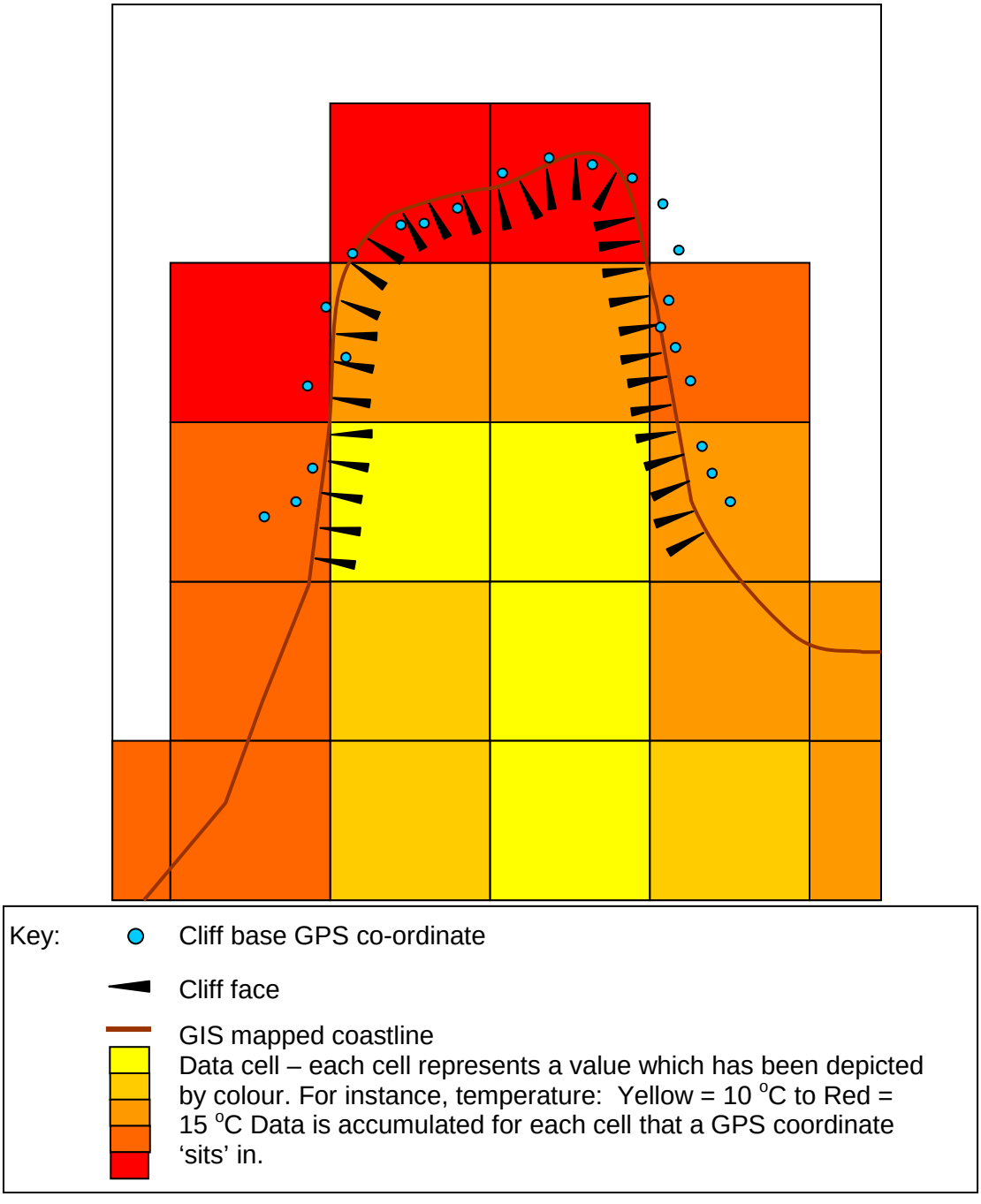

Figure 3.10: Plan view of a GIS surface illustrating the placement of cliff base coordinates measured in this study on the GIS mapped coastline. The surface is divided into cells for which each holds separate measured values.

CHAPTER FOUR

GEOTECHNICAL and LITHOLOGICAL PROPERTIES

4.1 Introduction

This chapter presents the geotechnical and lithological properties of the coastal cliff sites selected in this study. Sixteen sites were selected based on lithological and geographic criteria to represent the extent of the Waitemata Group rock. Each site is described and presented individually. Geomorphology results and the lithological properties of the coastal cliffs (with respect to the bedding characteristics and grain size) are then described. The data regarding the discontinuities measured during site descriptions and from scanline surveys are presented last.

4.2 Site Selection

4.2.1 Site location

Sixteen sites were chosen along the eastern coastline of the Auckland region to quantitatively and qualitatively record the structural and geological properties of Waitemata Group coastal cliffs (Figure 4.1). The sites are spread from the southern extent of the Waitemata Group to the northern extent where the basal contact of the Waitemata Group with Jurassic basement rock is exposed.

Ten sites are in East Coast Bays Formation rock and include (from south to north): Cockle Bay, Eastern Beach, Musick Point, Achilles Point, Narrowneck Beach, St Leonard's Beach, Castor Bay, Mairangi Bay, Waiake Bay and Army Bay. Six sites are in the Pakiri Formation rock and include (from south to north): Waiwera Beach, Opahi

Bay, Martins Bay, Buckleton Beach, Matheson Bay, and Leigh Marine Reserve. The abovementioned location names indicate the geographic area in which field work on cliff sections were carried out and these names will be used for comparative purposes for the remainder of this report.

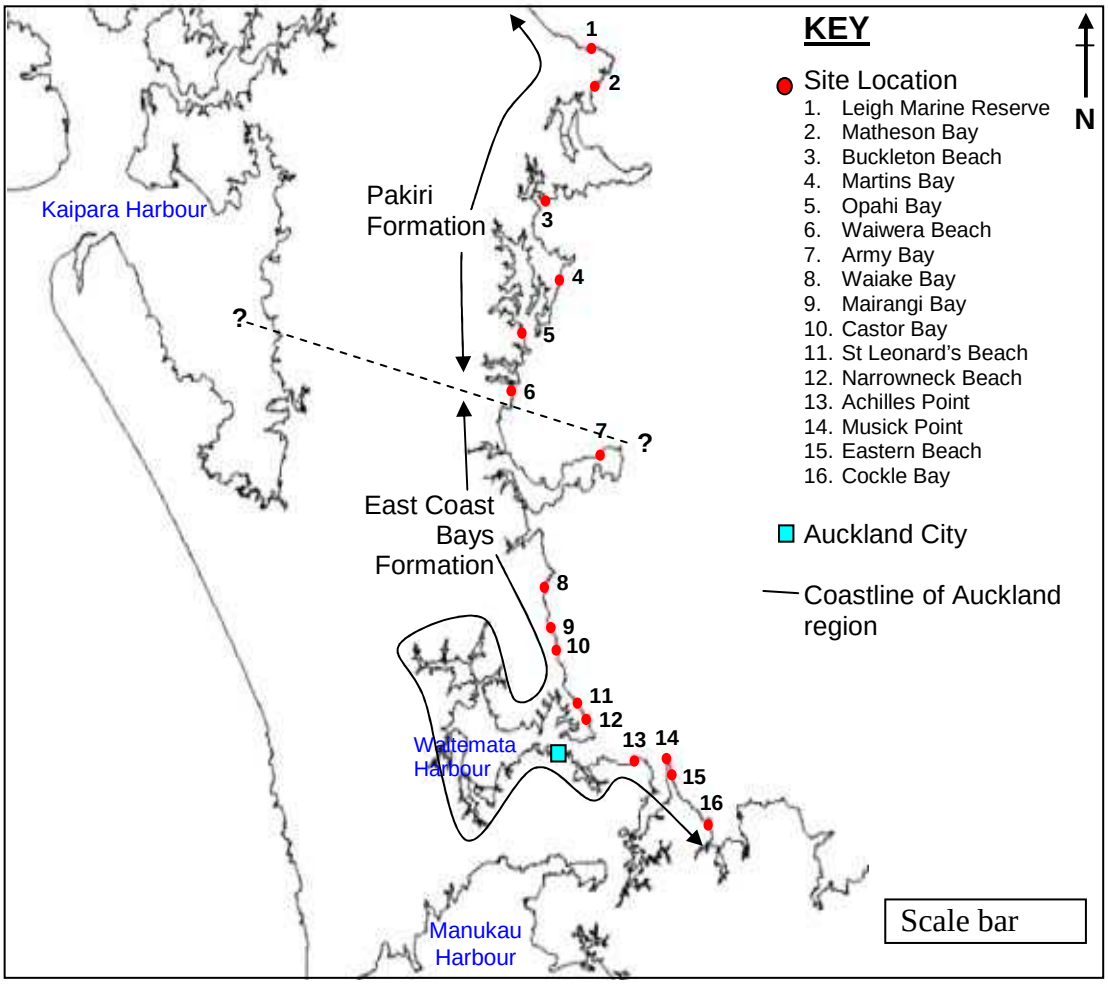

Figure 4.1: Map of the location of the sixteen sites used in this research. Sites 1 to 6 exist in Pakiri Formation rock and sites 7 to 16 exist in East Coast Bays Formation rock. The dashed line represents the boundary between these two formations from Edbrooke (2001). Arrows along the coastline trace the extent of each Formation outcropping along the coastline.

4.2.2 Selection criteria for choosing sites

The ultimate purpose of choosing the 16 sites was to be able to gather and analyse data from a representative range of Waitemata Group coastal cliffs, with a particular focus on the cliffs' structure and geology, and the ability to determine erosion rates from a cliff's associated shore platform. The criteria for site selection were based on lithological spread and geographic spread, as well as good cliff exposure and the safety of working at the cliff base and shoreline.

Site selection needed to represent the variation and change in lithology throughout the coastal exposures of the Waitemata Group, and as such, sites were chosen from the volcanic-poor East Coast Bays Formation and volcanic-rich Pakiri Formation, and were spread from their southern to northern extents. Sites also represented the structural changes in the Waitemata Group including both relatively undeformed strata where cliffs exhibit few and minor faulting and beds were near-horizontal with respect to the cliff face (Cockle Bay, Eastern Beach, Musick Point, Achilles Point, Narrowneck Beach, St Leonard's Beach, Mairangi Bay, Waiake Bay, Martins Bay, and Buckleton Beach), and deformed strata where cliff exposures are considerably faulted and/or folded, and beds are tilted (Castor Bay, Army Bay, Waiwera Beach, Opahi Bay, Matheson Bay and Leigh Marine Reserve). Cliff sections were selected in predominantly sandstone and siltstone bedded cliff exposures, without dominant inclusion of large Parnell Grit deposits.

Site selection represented a geographic spread too, with sites spread across a north/south distance of approximately 70 km (Edbrooke, 2001). Sites are more sheltered in the southern Auckland region as the inner Hauraki Gulf Islands and Coromandel Peninsula provide some protection and wind energy increases further north as the coastline becomes more exposed to the open ocean (Hurnard, 1979). The majority of the coastal cliffs at each site have an easterly aspect for which the cliff provides shelter from the predominant southwesterly winds. Sites such as Army Bay, which is situated on the northern side and tip of the Whangaparaoa Peninsula and has a westerly aspect, are more exposed to the coastal elements and need to be represented with respect to examining coastal cliff erosion rates.

Cliff sections of 30 - 50 m width, within the chosen sites, were then selected based on the exposure and also the safety of, and accessibility to, the cliff face and shore platform (Figure 4.2). The section of cliff to be described was representative of the surrounding coastline, and displayed well the bedding and structure of the rock without masses of loose debris covering the slope.

Lastly, site selection was based upon the safety of being able to work at the cliff base for long periods of time. Sites were not selected where there were precarious overhanging rocks or trees, or large loosened blocks within the cliff face. Field work had to be carried out over periods of low tide both for access to the cliff section and for assessment of the shore platform at that site. Where platforms are near horizontal, an incoming tide can move landward very quickly and tides and platforms may be just exposed at low tide. Also, the height that the tide reaches at the cliff base strongly influences accessibility and ease of working for periods of time at the cliff base.

4.2.3 Field work

The same details and measurements were consistently recorded at all sixteen sites as outlined in Section 3.2.5. Scanline surveys were carried out additionally at 8 of the sites to provide a concentrated and detailed view of rock mass structure. The scanline surveys were taken at both relatively undeformed and deformed cliff sites in both East Coast Bays Formation (Musick Point, Narrowneck Beach, Castor Bay, Waiake Bay, Waiwera Beach) and Pakiri Formation (Army Bay, Martins Bay, Leigh Marine Reserve).

4.3 Site Descriptions

Observations made at each individual site are presented for the selected cliff and shore platform section, as well as notable features of the broader coastline. Graphs display the plan morphology of the shore platform and their variation in width, and annotated photographs and sketches provide a visual display of the described sites. The key for each site description is given in Table 4.1; sites are described from south to north.

Table 4.1: Key for individual site descriptions.

Symbol	Description
	Location of described cliff section, marked at the base of the cliff
	Sandstone
	Siltstone
	Densite
	Debrite (Parnell Grit)
LWL	Low Water Level
HWL	High Water Level
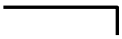	Horizontal platform with seaward edge
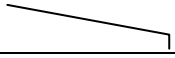	Sloping platform with a seaward edge
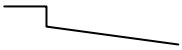	Horizontal platform and sloping platform with no seaward edge
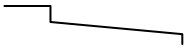	Horizontal platform and sloping platform with a seaward edge
	Sand beach
	Cobbles/debris

4.3.1 Cockle Bay

Cliff height: 23.1 m	Cliff angle: 65°	Cliff strike: 115°	Bed dip: 1° landward
GSI:	Flysch 45 ± 5	Sandstone 60 ± 5	Siltstone 37 ± 5
Schmidt Hammer Rebound number:		Sandstone 11 - 19	Siltstone not measured

Sandstone dominates and beds are mostly of medium thickness (< 0.5 m); a few beds are about 1 m thick. Siltstone appears to be mostly 10 - 30 cm thick but some sections of the cliff face are covered by weathered material making visibility of the structure poor. At the cliff base are 2 thick densite deposits which are medium-coarse sand-dominated with rip-up clasts and grade into upper siltstone. There is a lack of vertical joints in sandstone beds of turbidites and densites. The shore platform is very narrow, high and stepped, and has many prominent concretions. There is a lot of burrowing (bioerosion) in lower densite bed and joints are only visible on top surface. Many large boulders and cobbles litter the platform just below the defined cliff base.

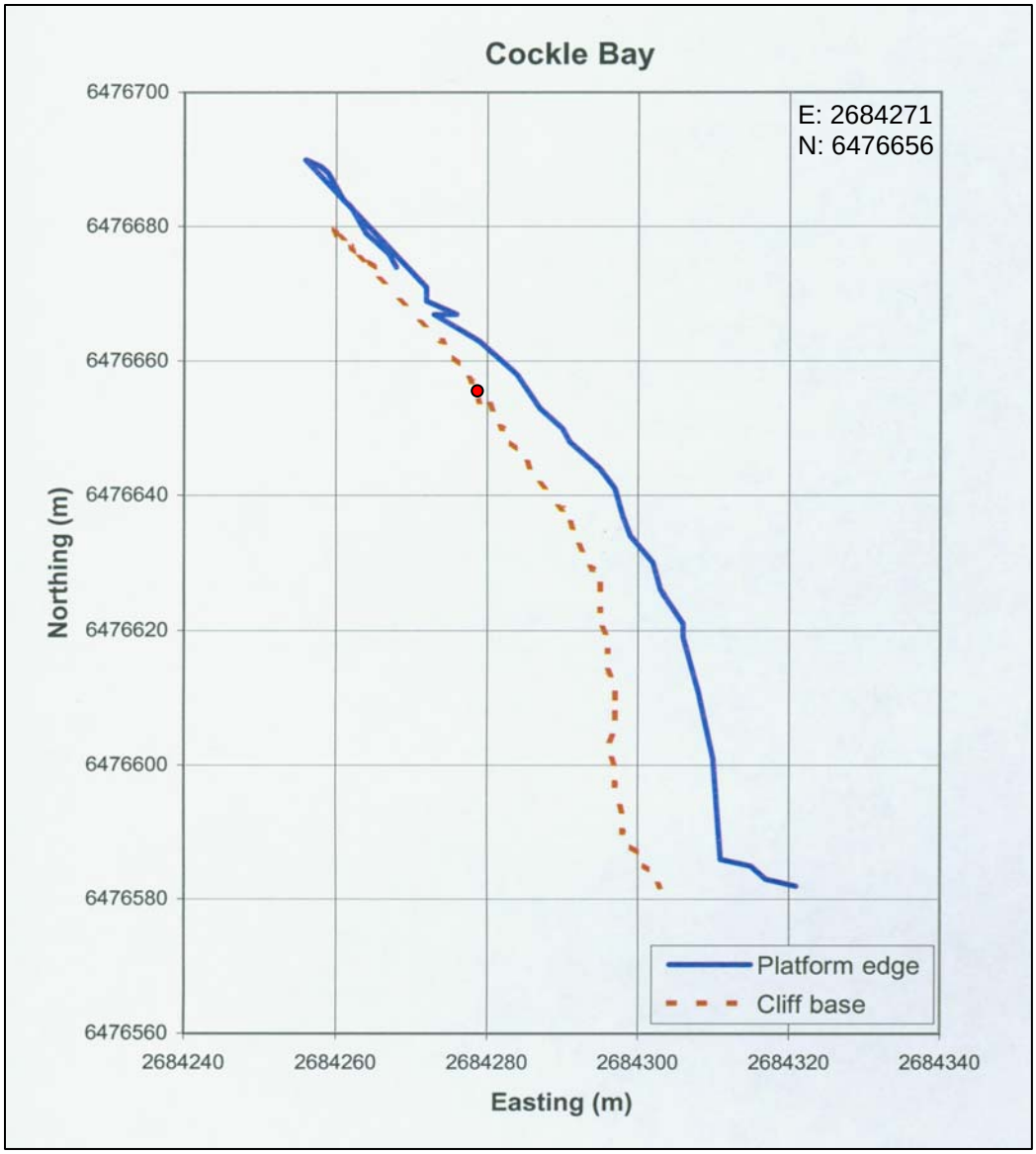

Figure 4.2: Shore platform plan morphology of Cockle Bay.

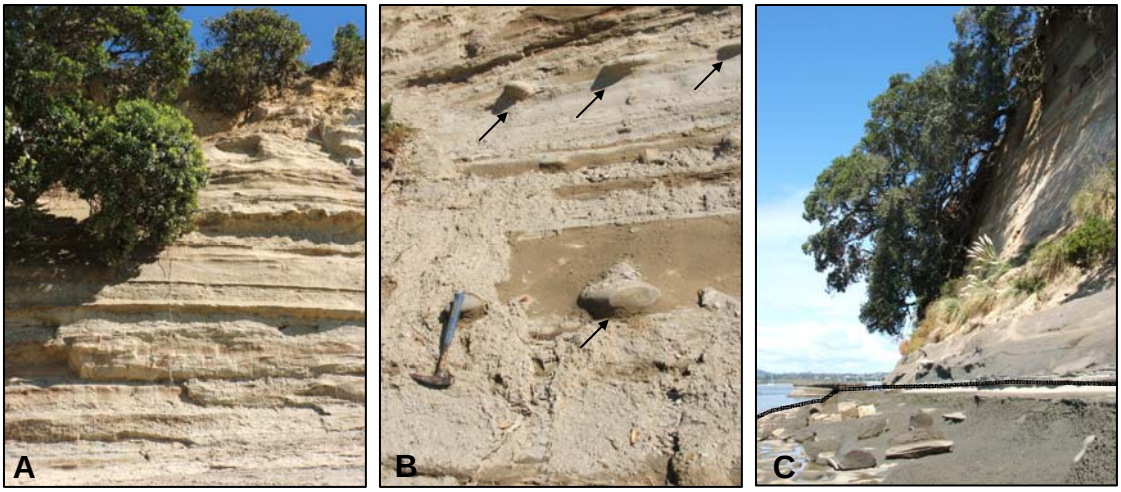

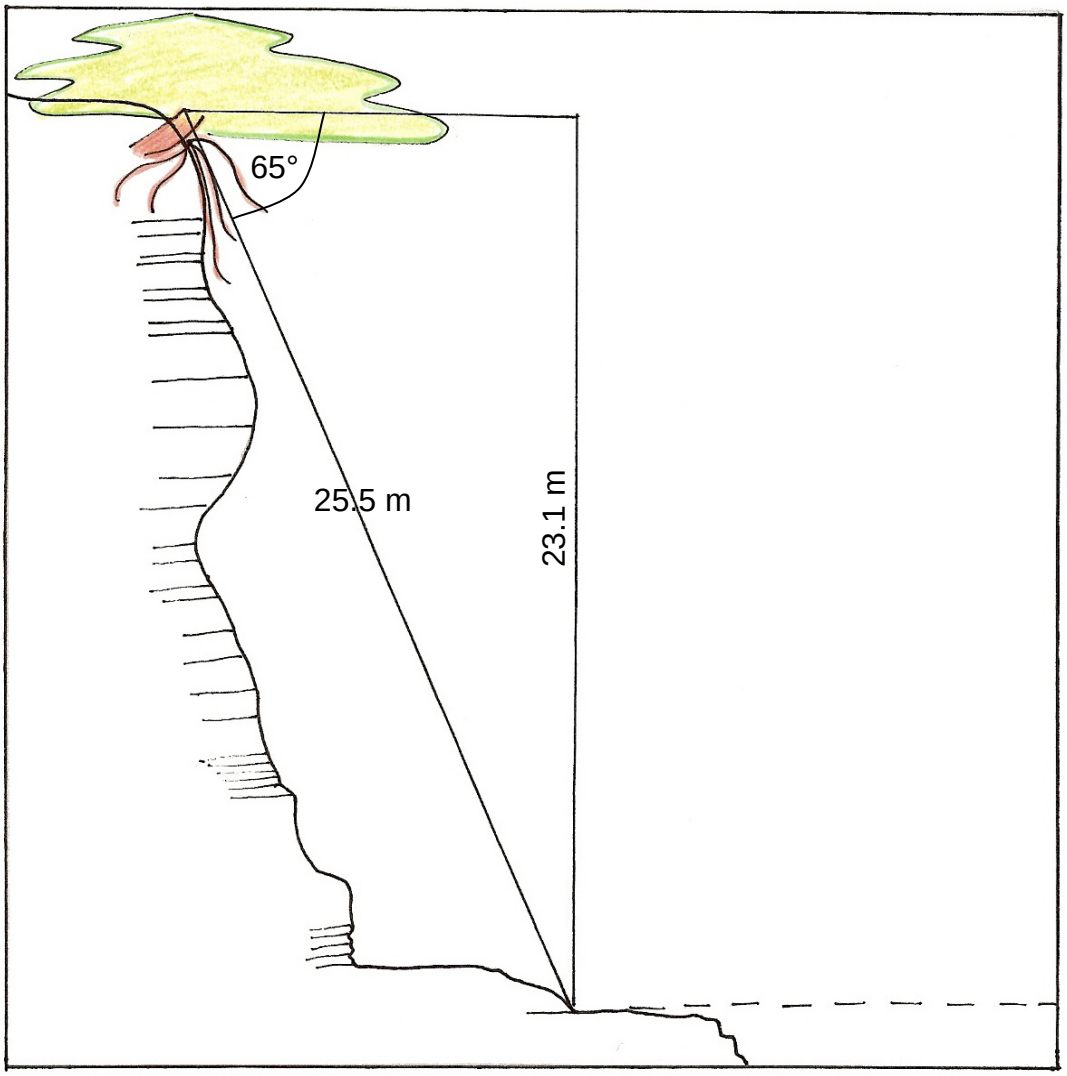

Figure 4.3: Photographs and sketch of the described Cockle Bay cliff section. A: Cliff face. B: Moderately weathered cliff face with concretions (black arrow) in sandstone beds. C: Cliff profile and narrow shore platform (black outline). D: Sketch of bedding and shore platform characteristics.

4.3.2 Eastern Beach

Cliff height: 22.4 m	Cliff angle: 62°	Cliff strike: 140°	Bed dip: 17° seaward
GSI:	Flysch 42 ± 5	Sandstone 50 ± 5	Siltstone 37 ± 5
Schmidt Hammer Rebound number:		Sandstone 13 - 14	Siltstone 17

At the described site the cliff strikes parallel to the axis of an anticline so that beds are dipping out of the slope toward sea. Bed dip ranges from 10 - 42° as a result of the anticline fold. A number of zones (particularly in siltstone) are weathered to a soil and vegetation is growing in soil talus slopes. Siltstone grades up into a coarser, laminated and sometimes cross-bedded sandstone which then grades back into siltstone. Many fallen blocks litter the cliff base. Honeycomb and pockmark weathering is exhibited in the high platform bench that extends from the cliff base. Some thick sandstone beds contain rip-up clasts about 10 cm diameter with coarse sand grading upwards to medium sand; these are densite deposits. There are faults in the limb of the anticline with a throw of up to 0.5 m.

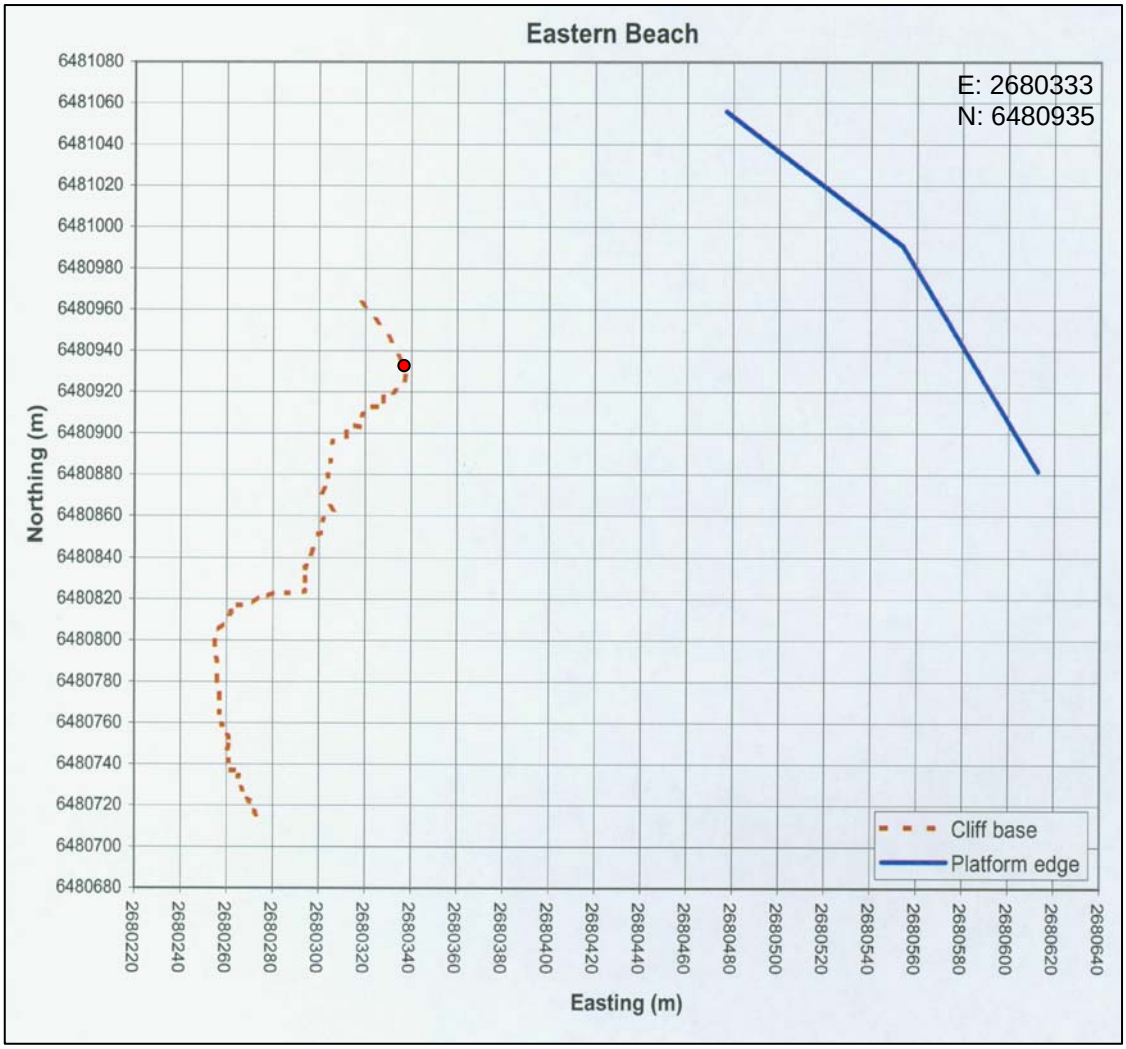

Figure 4.4: Shore platform plan morphology of Eastern Beach.

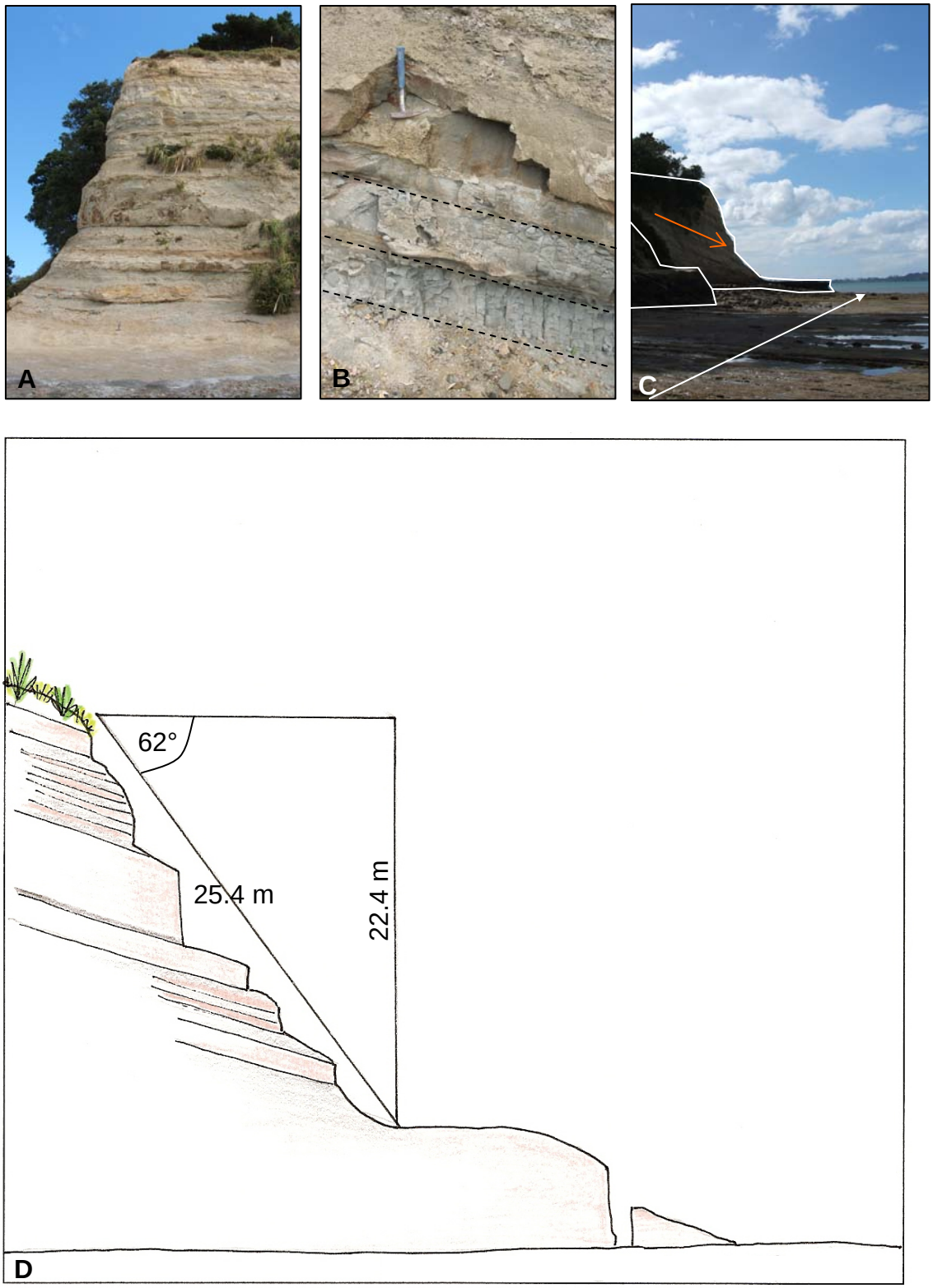

Figure 4.5: Photographs and sketch of the described Eastern Beach cliff section. A: Cliff face and profile. B: Bedding, note the regular near-vertical joints in the siltstone beds. C: View from beach showing higher platform bench and extensive lower platform (white arrow), and bedding dip (orange arrow) D: Sketch of bedding and shore platform characteristics.

3.4.3 Musick Point

Cliff height: 18.9 m	Cliff angle: 79°	Cliff strike: 076°	Bed dip: 10° seaward
GSI:	Flysch 45 ± 5	Sandstone 65 ± 5	Siltstone 45 ± 5
Schmidt Hammer Rebound number:		Sandstone 14 - 18	Siltstone not measured

The site has very thick sandstone beds which dominate the cliff face; siltstone beds inbetween are very thin and laminated, and have carbonaceous material at their base. Siltstone beds are thicker (~ 30 - 50 cm) in the upper part of the cliff section. The thickest sandstone bed which extends beyond the base of the cliff has a lower part that is massive and an upper part that is thicker and faintly laminated. The flame structures between the upper and lower parts of the thickest sandstone bed are about 40 cm in height, and indicate synsedimentary slumping. There is no debris at base of cliff. A sandy beach about 10 m wide exists at the cliff base although the width is variable due to tidal and storm events.

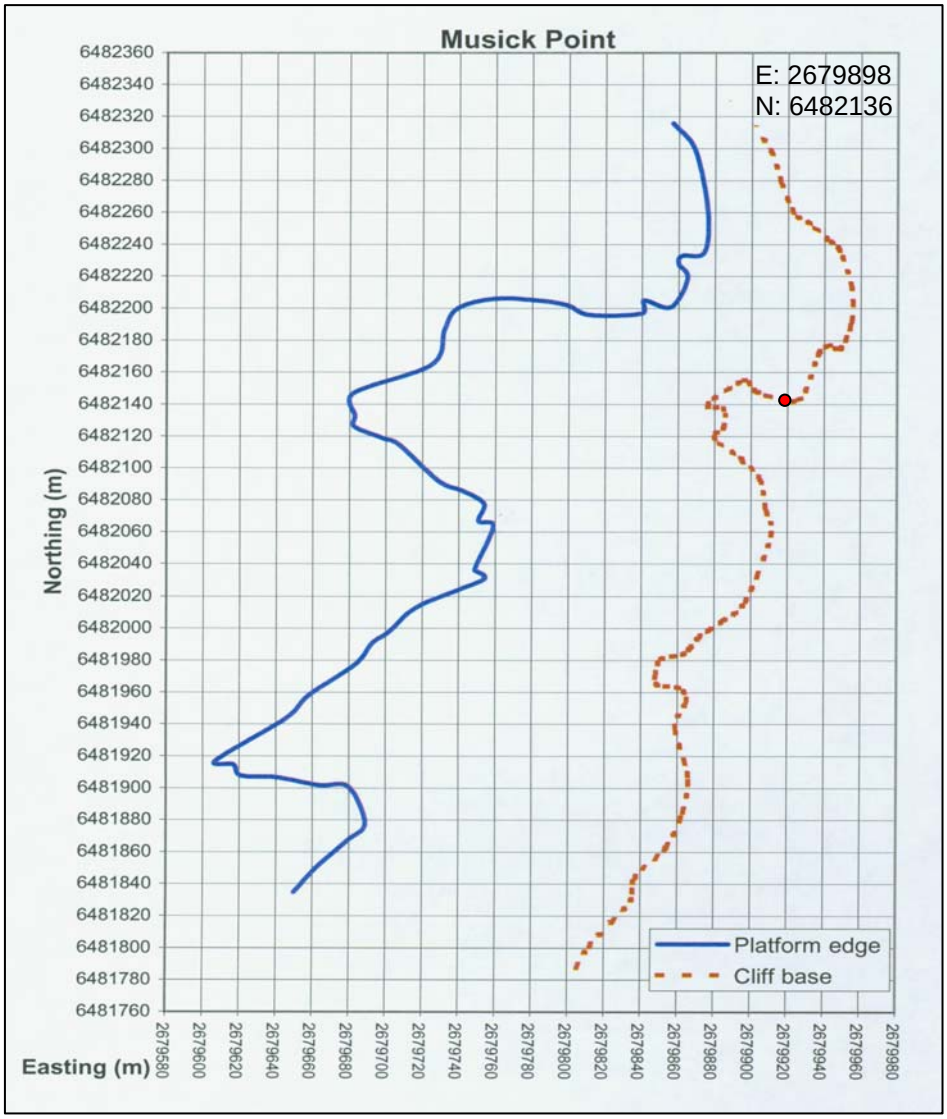

Figure 4.6: Shore platform plan morphology of Musick Point.

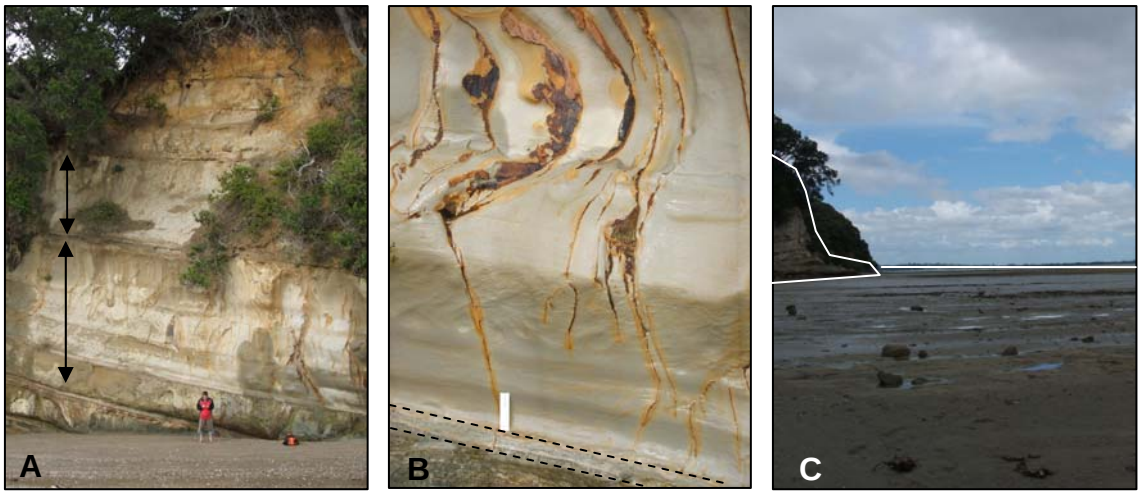

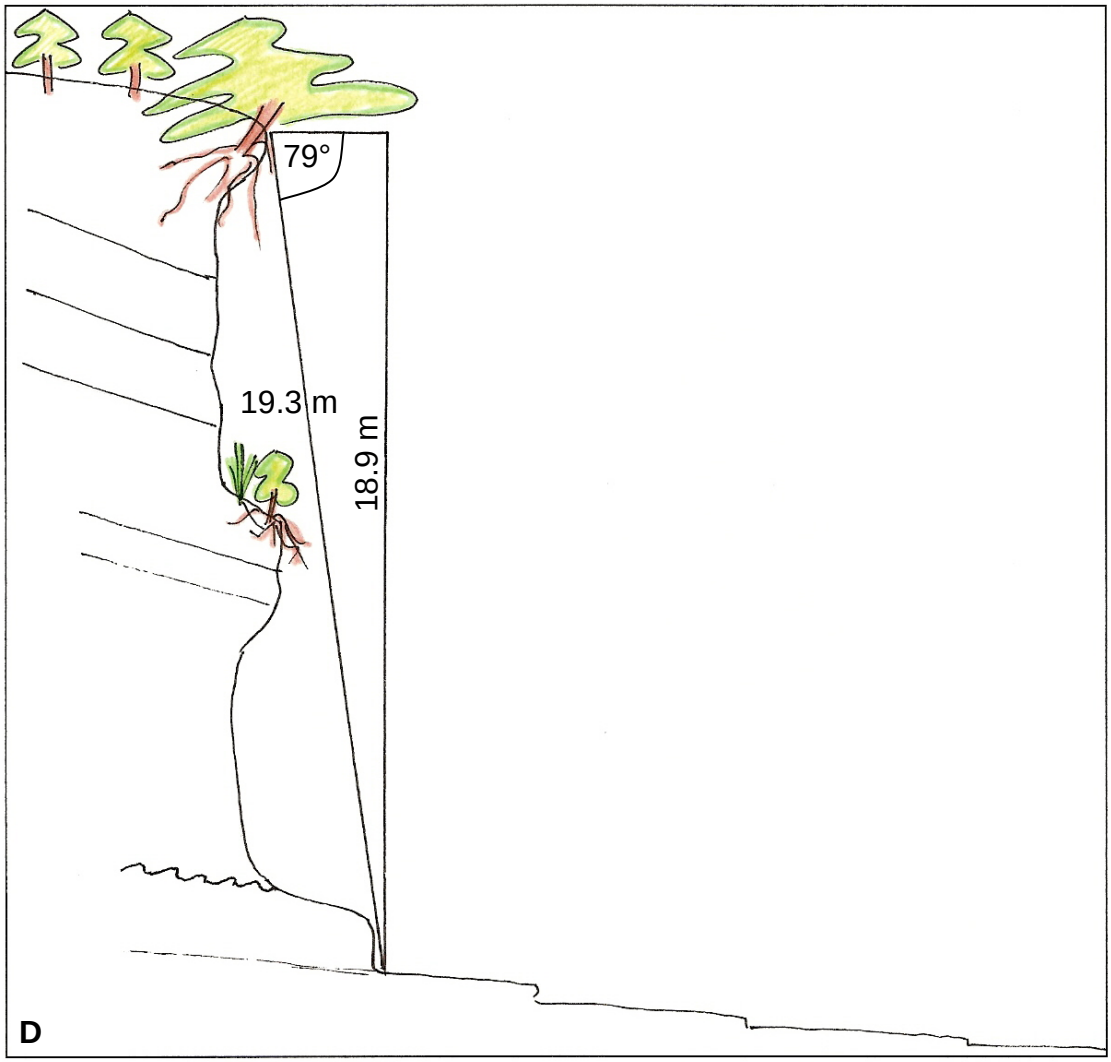

Figure 4.7: Photographs and sketch of the described Musick Point cliff section. A: Cliff face. B: Very thick sandstone bed with near-vertical joints and lower thin siltstone bed. C: Wide shore platform with higher platform benches at headlands. D: Sketch of bedding and shore platform characteristics.

4.3.4 Achilles Point

Cliff height: 23.3 m	Cliff angle: 65°	Cliff strike: 020°	Bed dip: 3° landward
GSI:	Flysch 40 ± 5	Sandstone 65 ± 5	Siltstone 40 ± 5
Schmidt Hammer Rebound number:		Sandstone 19-20	Siltstone not measured

The lower half of the cliff section has medium sandstone beds with thin siltstone and the upper half of the cliff is siltstone dominated. There are areas of slumping (~ 3 x 3 m) consisting of soil material and crushed rock in which scrub vegetation is growing. Scrub is also growing in zones of weathered rock. The main platform is high and stepped in Parnell Grit rock, and there is a lower sloped platform. There are concretions, carbonaceous material and convolutions in the platform beds. Seepage was observed outside of the cliff section and there are drain pipes hanging over cliff-top which were regularly draining water. There are many faults and localised tilting. The platform is not covered in scattered blocks, but has accumulating piles of both sandstone and siltstone debris.

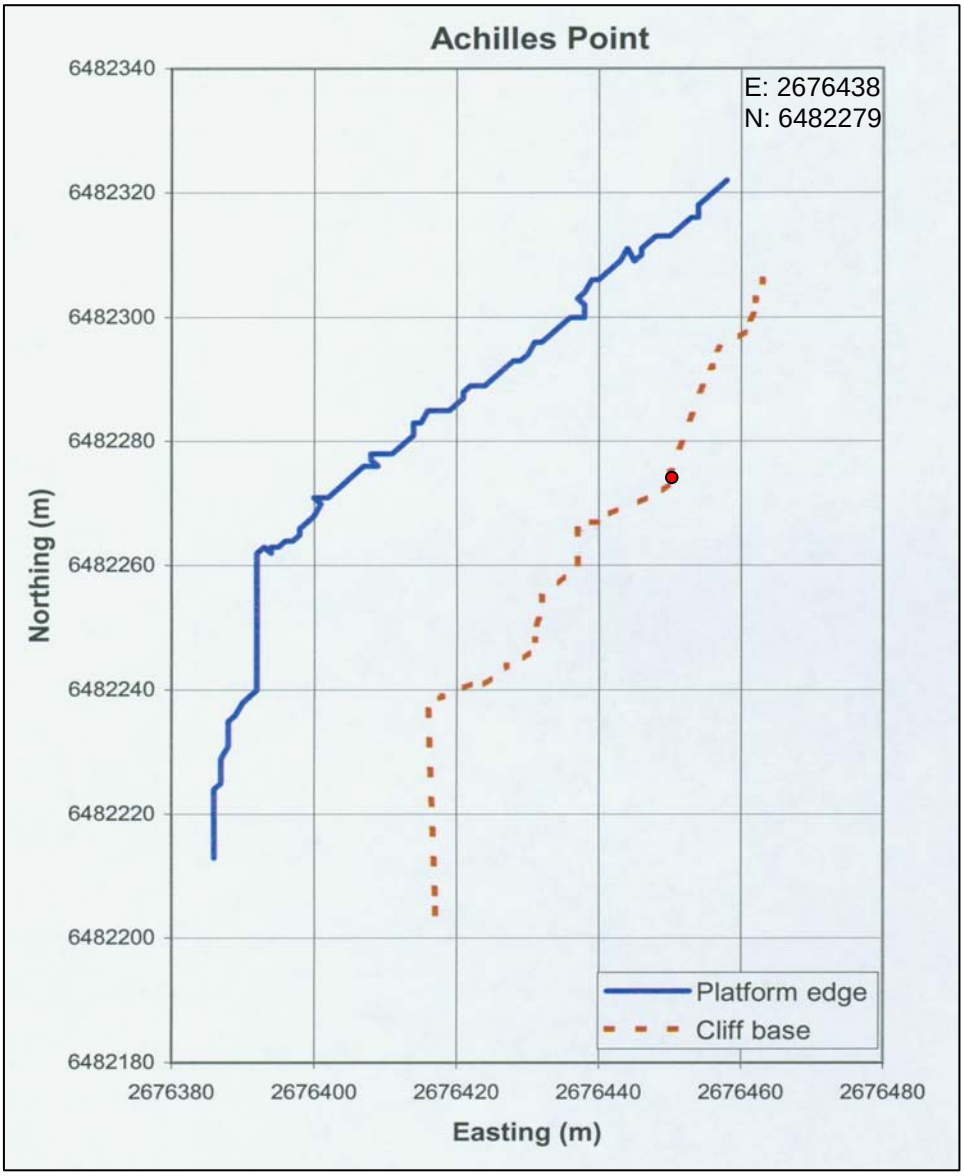

Figure 4.8: Shore platform plan morphology of Achilles Point.

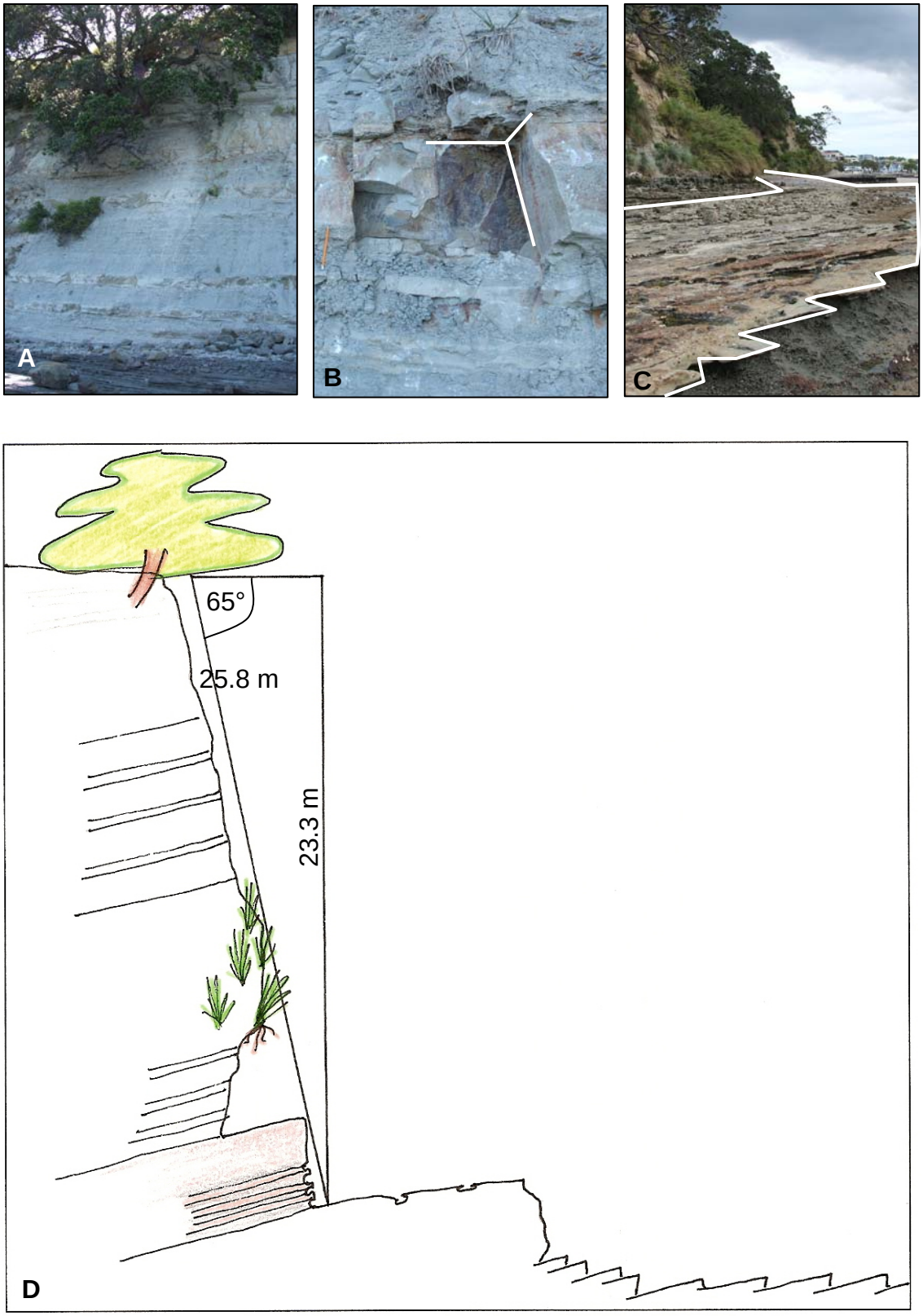

Figure 4.9: Photographs and sketch of the described Achilles Point cliff section. A: Cliff face. B: Bedding, note 3 joint sets leading to block fall in sandstone bed. C: Shore platform in Parnell Grit rock. D: Sketch of bedding and shore platform characteristics.

4.3.5 Narrowneck Beach

Cliff height: 15.0 m	Cliff angle: 65°	Cliff strike: 100°	Bed dip: 15° landward
GSI:	Flysch 35 ± 5	Sandstone 50 ± 5	Siltstone 35 ± 5
Schmidt Hammer Rebound number:		Sandstone 16 - 19	Siltstone 21

The cliff section is quite siltstone dominated apart from a few medium thick sandstone beds and siltstone beds are noticeably eroded out underneath sandstone beds. Some beds are densites containing silt rip-up clasts which have an elongated shape up to 5 cm in length plus reddish pebbles of volcanic origin. A few zones are highly weathered and small talus piles have formed in which scrub is growing. Regular concreted drainage pipes exist down the cliff face and drain water out at the base of the cliff. Regular faulting occurs along the whole cliff site. The shore platform is stepped due to the landward-tilting of the beds and consists of iron-crusted, blocky sandstone beds with siltstone beds eroded out. The platform is occasionally covered by sand forming a beach at cliff base.

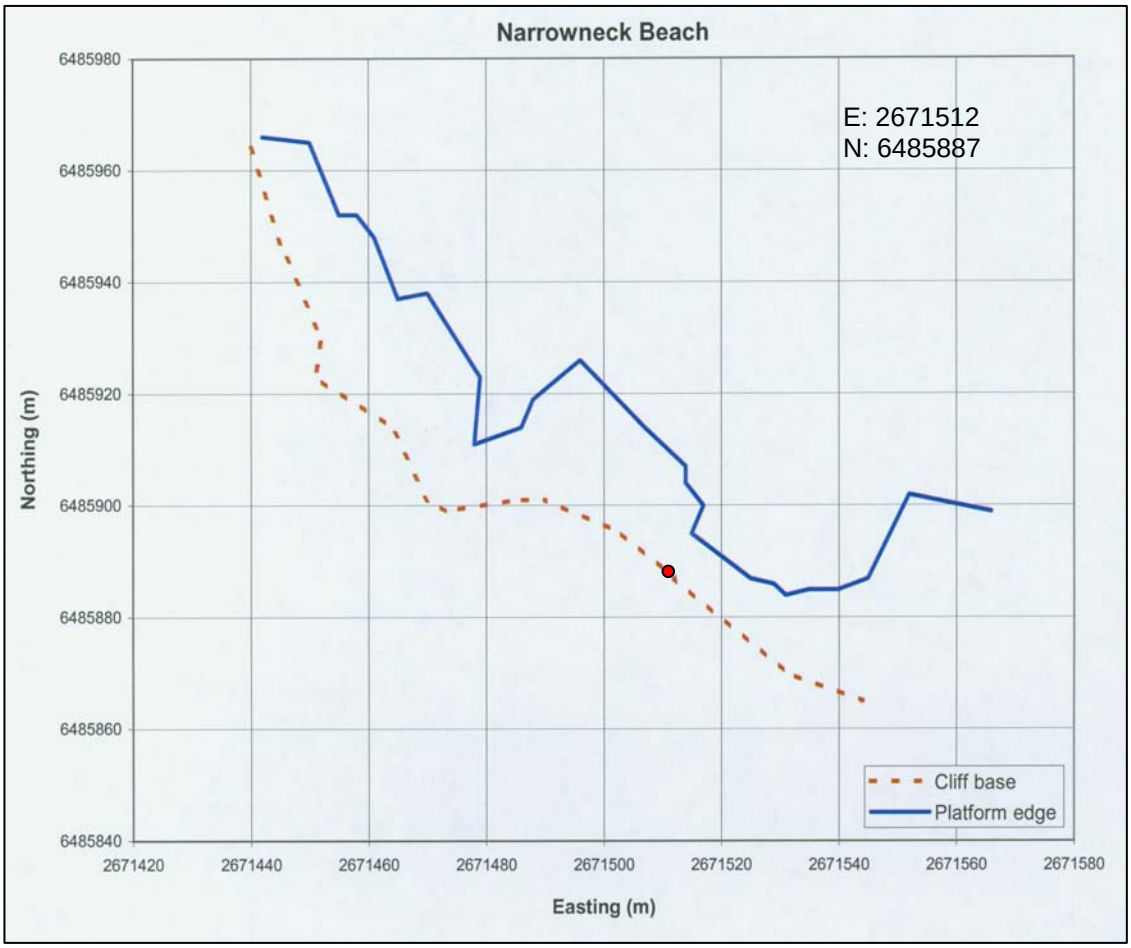

Figure 4.10: Shore platform plan morphology of Narrowneck Beach.

Figure 4.11: Photographs and sketch of the described Narrowneck Beach cliff section. A: Cliff profile and narrow shore platform; beds dip is marked by black arrow. B: Cliff face; flysch beds with fallen sandstone blocks. C: Close up of iron-stained joints; dashed line indicates boundary between sandstone & siltstone. D: Sketch of bedding and shore platform characteristics.

4.3.6 St Leonard's Beach

Cliff height: 23.8 m	Cliff angle: 61°	Cliff strike: 133°	Bed dip: 3° landward
GSI:	Flysch 40 ± 5	Sandstone 65 ± 5	Siltstone 45 ± 5
Schmidt Hammer Rebound number:		Sandstone 20 - 25	Siltstone 22

The cliff site has a high prominent face with many faults. A few grasses and small shrubs are scattered across the cliff but are fairly sparse, Pohutukawa trees overhang the cliff top. Gully erosion is observed at the cliff top along weaker discontinuities which are probably faults. The cliff has predominantly equal amounts of siltstone and sandstone and beds are < 30 cm thick, except for the upper top 10 m of the cliff where there are 3 thick sandstone beds (~ 1 m thick each, light silvery grey, no orangey/yellow staining). The wind was observed to continually clean away small broken (mainly siltstone) fragments. The sandstone beds are laminated and some show convolutions. There is some waviness between the boundary of the lower siltstone and upper sandstone, and a sharp contact with the top of the siltstone and base of the upper sandstone. The sandstone beds tend to grade into upper siltstone. The sandstone beds in the shore platform have a massive base with a convoluted upper which also grades into siltstone (classic Bouma sequence). The shore platform has about three levels (a high narrow platform that is around the base of some of the cliff, a lower ledge which is stepped and strongly dipping, and a lowermost platform which has a sloping profile covered by varying amounts of rock and sand. The shore platform changes noticeably where a fault or series of faults cuts through.

Figure 4.12: Shore platform plan morphology of St Leonard's Beach.

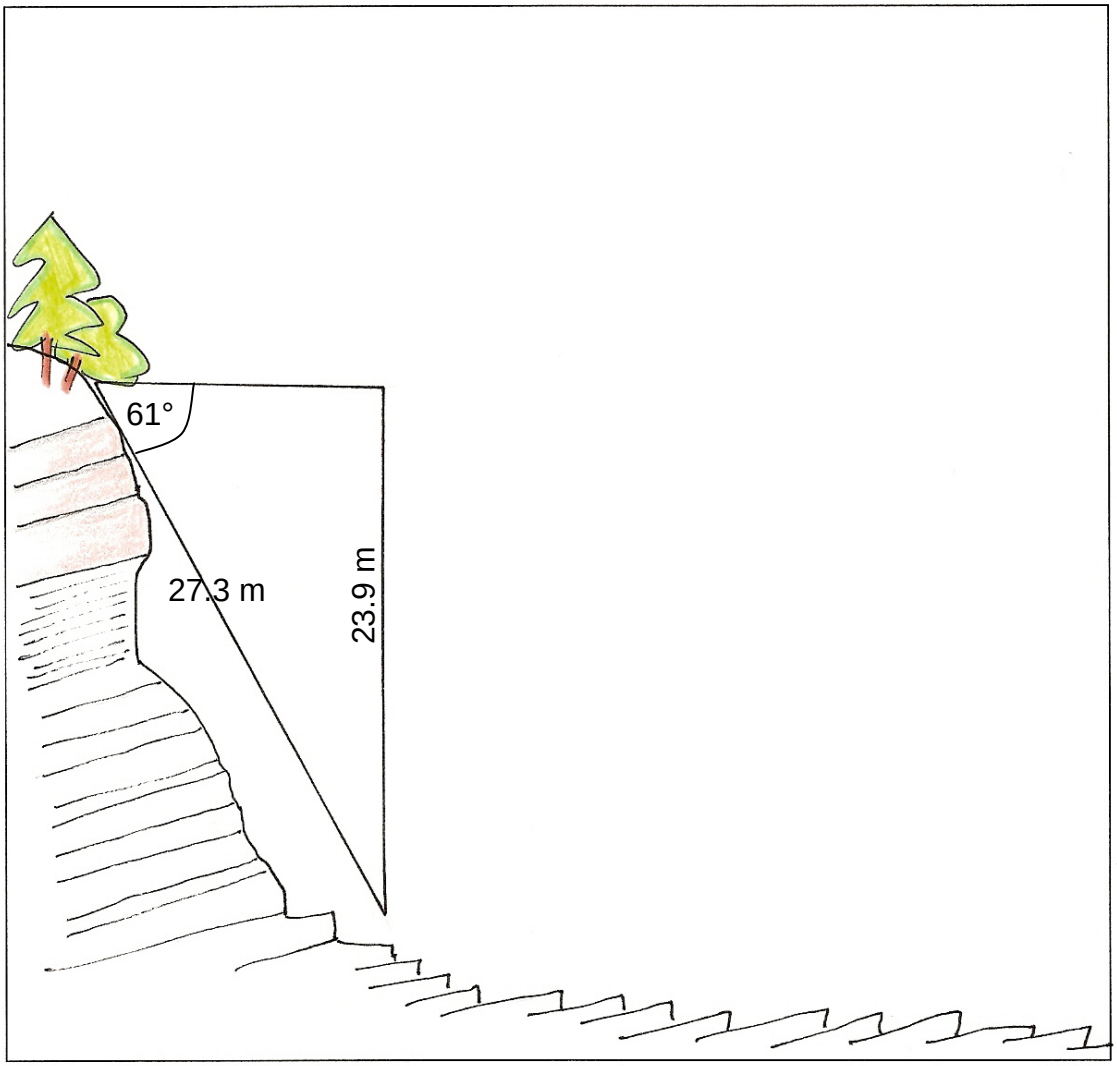

Figure 4.13: Photographs and sketch of the described St Leonard's Beach cliff section. A: Cliff face with upper gully erosion. B: Cliff profile and shore platform. C: Sandstone and siltstone beds; note sharp contact of sandstone base and grading into upper siltstone. D: Sketch of bedding and shore platform characteristics.

4.3.7 Castor Bay

Cliff height: 18.7 m	Cliff angle: 73°	Cliff strike: 117°	Bed dip: 26° seaward
GSI:	Flysch 24 ± 5	Sandstone 42 ± 5	Siltstone 42 ± 5
Schmidt Hammer Rebound number:		Sandstone 18 - 20	Siltstone not measured

A very thick densite bed exists at the cliff base which has been gently eroded back from cliff to a lower angle than the whole slope face. It appears that thin sandstone beds (which have high joint frequency) and medium siltstone beds readily erode which weakens the overlying support of massive sandstone beds. The sandstone beds appear to be coarse-medium sand and siltstone beds are gritty both overall and just at base of the individual deposit. There is no significant soil development on the cliff face. The bed dip is variable due to folding and tilting but is approximately moderately to steeply inclined. Seepage is observed in some areas at the base of sandstone beds. The shore platform is regularly and gently stepped but overall horizontal, with a steep drop-off at the seaward edge. Major joints are well developed and scoured out in the shore platform.

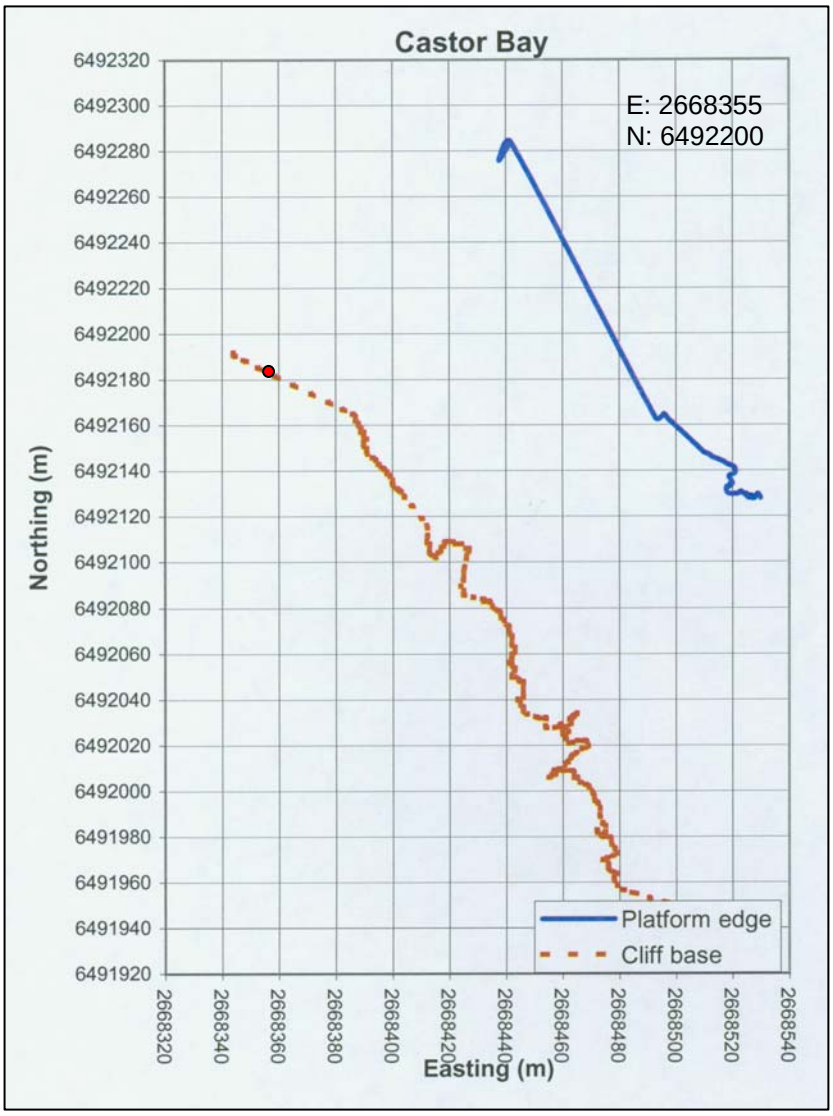

Figure 4.14: Shore platform plan morphology of Castor Bay.

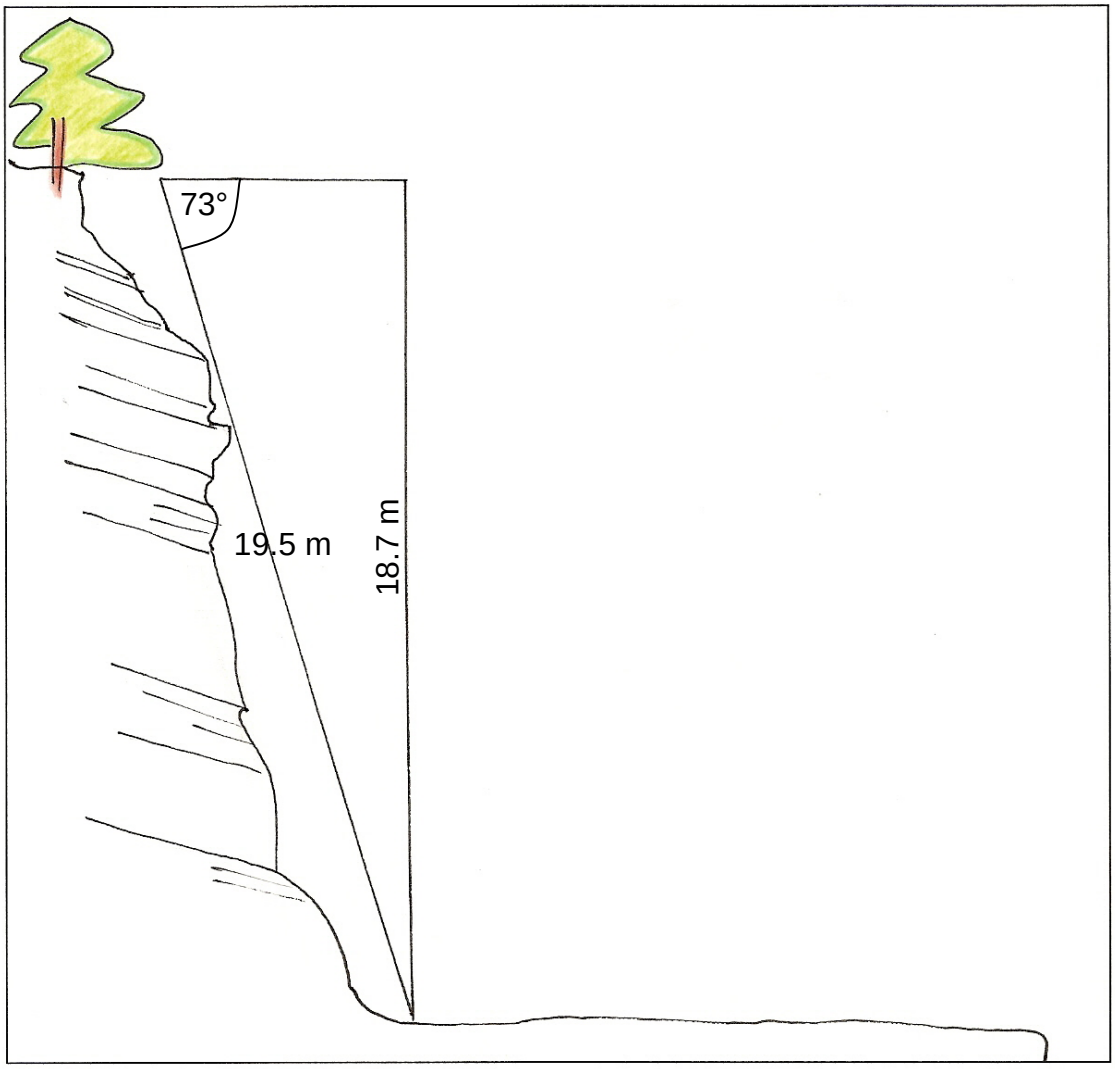

Figure 4.15: Photographs and sketch of the described Castor Bay cliff section. A: Close up of sandstone and siltstone beds; tape sits on fault plane. B: Cliff face; beds dip steeply seaward. C: Cliff profile and shore platform. D: Sketch of bedding and shore platform characteristics.

4.3.8 Mairangi Bay

Cliff height: 8.6 m	Cliff angle: 79°	Cliff strike: 117°	Bed dip: 5° seaward
GSI:	Flysch 45 ± 5	Sandstone 65 ± 5	Siltstone 45 ± 5
Schmidt Hammer Rebound number:		Sandstone 16 - 19	Siltstone not measured

The site has a very steep cliff face and very low height. Thick sandstone beds (~50 cm, up to 1 m) dominate with thin siltstone beds in between (~ 10 - 20 cm thick) and sandstone block fall seems to be main erosion method. The siltstone beds at the site have regular vertical joints and horizontal beds/laminations which result in a tabular block shape. Seepage is observed in some areas. An encased sewer pipe about 4 - 5 m from cliff base acts as a sea wall and high tide does not reach the cliff base; blocks fallen out from cliff face are piling-up between the cliff and the sea wall. The platform is very horizontal with a sharp drop off at the seaward edge.

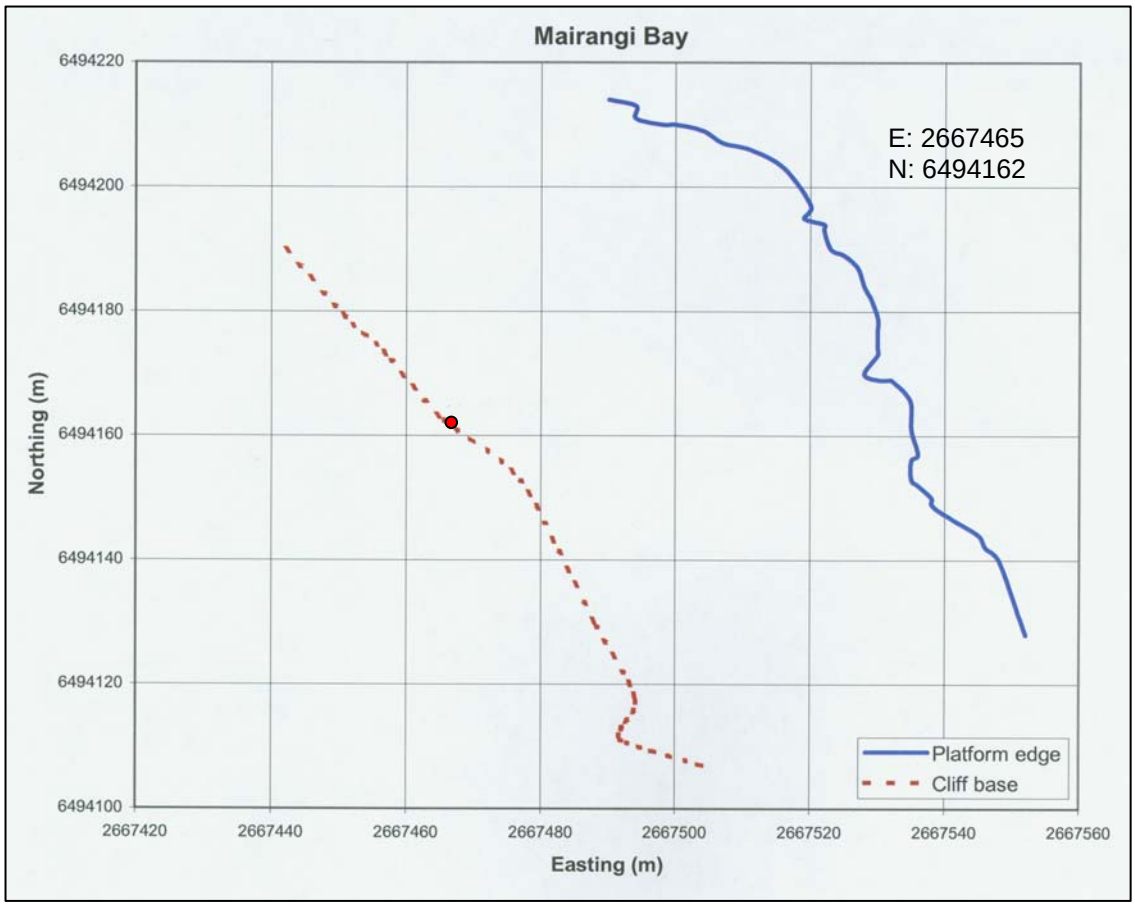

Figure 4.16: Shore platform plan morphology of Mairangi Bay.

Figure 4.17: Photographs and sketch of the described Mairangi Bay cliff section. A: Cliff face with lower encased sewer pipe (red bracket) which acts as a sea wall. B: Dark iron-stained sandstone joint faces; thin siltstone bed is between dashed lines. C: Cliff profile and shore platform (extent is marked by white arrow); sewer pipe is marked by red line. D: Sketch of bedding and shore platform characteristics.

4.3.9 Waiake Bay

Cliff height: 23.8 m	Cliff angle: 79°	Cliff strike: 149°	Bed dip: 6° landward
GSI:	Flysch 40 ± 5	Sandstone 63 ± 5	Siltstone 30 ± 5
Schmidt Hammer Rebound number:		Sandstone 14 - 15	Siltstone 19 - 20

The entire cliff section is fairly uniform and horizontal, only offset by some faults and a small overall dip of the beds. There are at least 6 - 8 faults along the entire cliff section with a throw of up to about 1 m. The cliff site has fairly equal amounts of sandstone and siltstone. The presence of a thick sandstone bed in the upper section of the cliff has resulted in approximately the upper third of the cliff protruding out past the cliff face. Thin sandstone beds appear laminated and grade upward into siltstone. The lower sloping platform from Tipau Point to Waiake Bay is a sandy densite full of siltstone rip-up clasts, Parnell Grit clasts and carbonaceous material. To the south of Waiake Bay a Parnell Grit bed exists about 3 m thick.

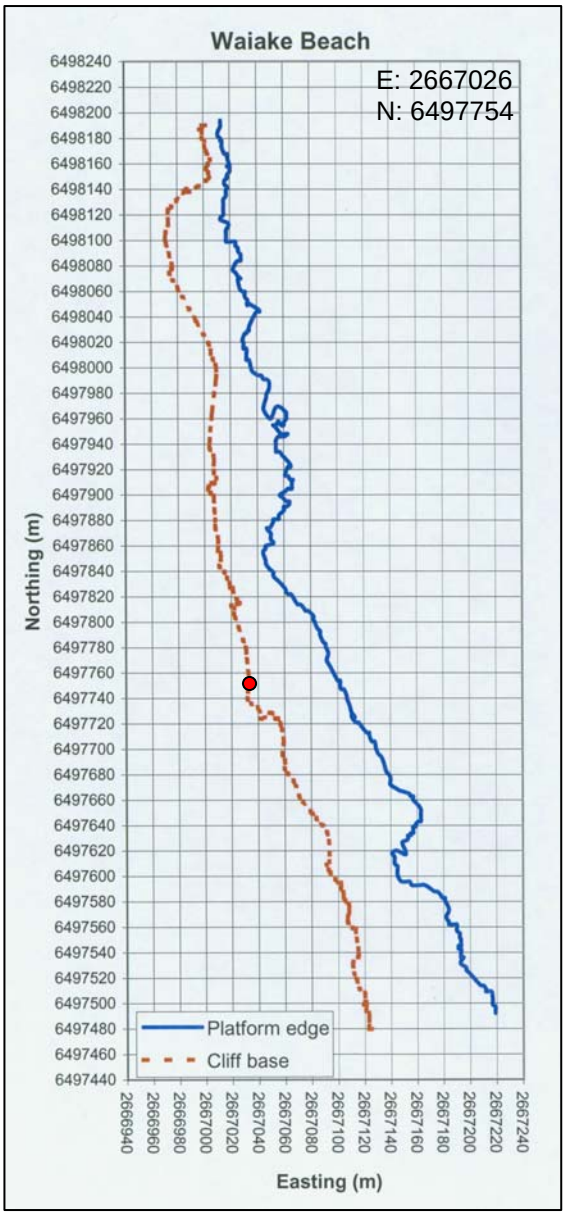

Figure 4.18: Shore platform plan morphology of Waiake Bay.

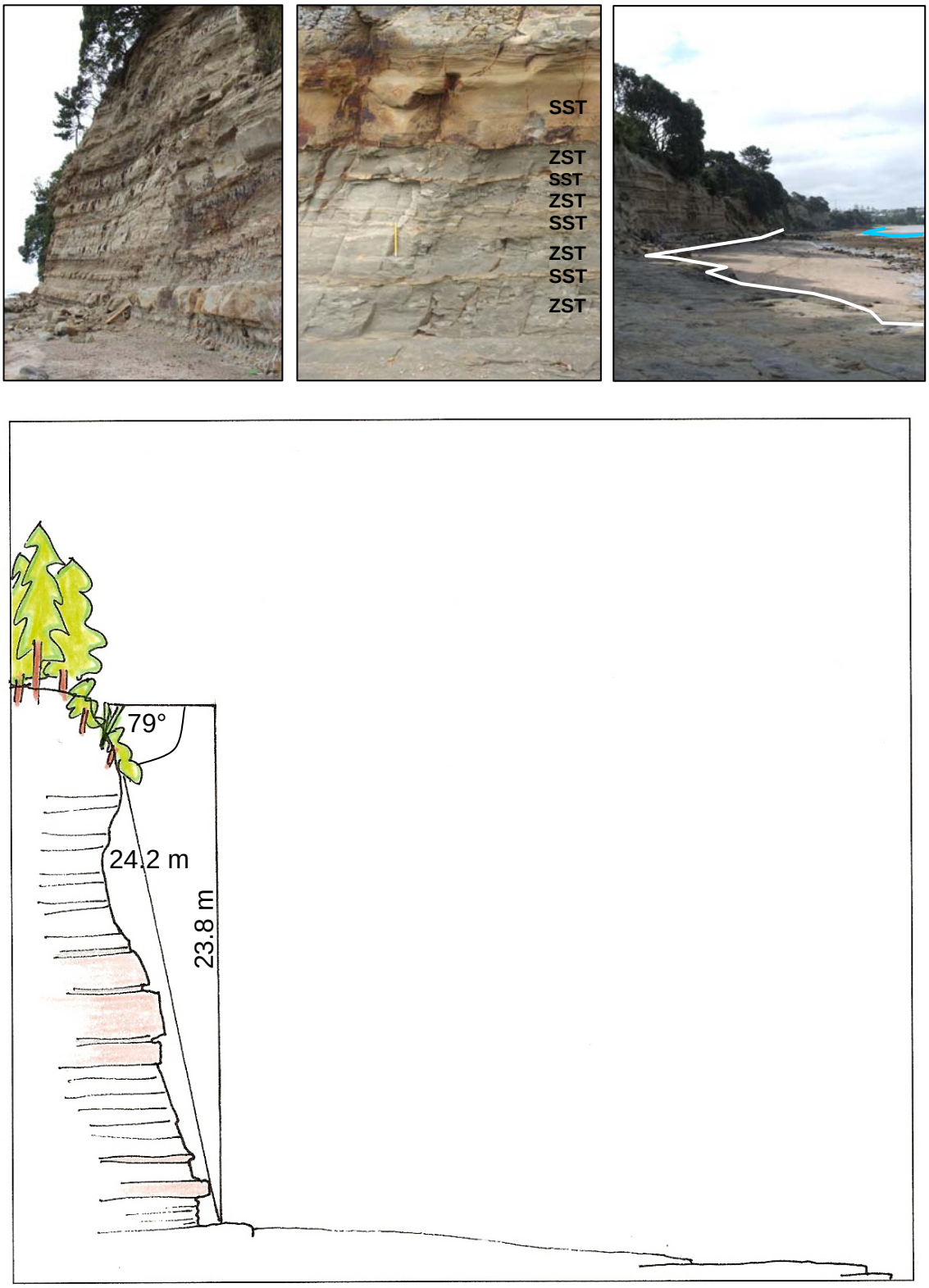

Figure 4.19: Photographs and sketch of the described Waiake Bay cliff section. A: Cliff profile and cliff face. B: Medium thick sandstone bed with lower zone of thin-medium siltstone with interbedded thin sandstone (iron-stained). C: Shore platform; white line marks the seaward extent of the high horizontal bench and the blue line marks the seaward extent of the lower sloping platform. D: Sketch of bedding and shore platform characteristics.

4.3.10 Army Bay

Cliff height: 38.3 m	Cliff angle: 62°	Cliff strike: 004°	Bed dip: 25° seaward
GSI:	Flysch 20 ± 5	Sandstone 45 ± 5	Siltstone 33 ± 5
Schmidt Hammer Rebound number:		Sandstone 18 - 27	Siltstone not measured

The scanline survey had to be carried out about 30 m west of the description site and had medium sandstone beds interbedded between thin sandstone and siltstone sequences. Beds are heavily iron-stained and weathered in places and calcite infill is also common. The cliff site is overall highly folded and faulted with a large Parnell Grit bed midway up the cliff section. Beds tilt both seaward and landward but are dipping seaward at the described cliff section. Seepage is observed in a number of areas along the entire cliff. The platform is repeatedly and regularly stepped and reflects the folding pattern and tilting of the strata in the cliff face.

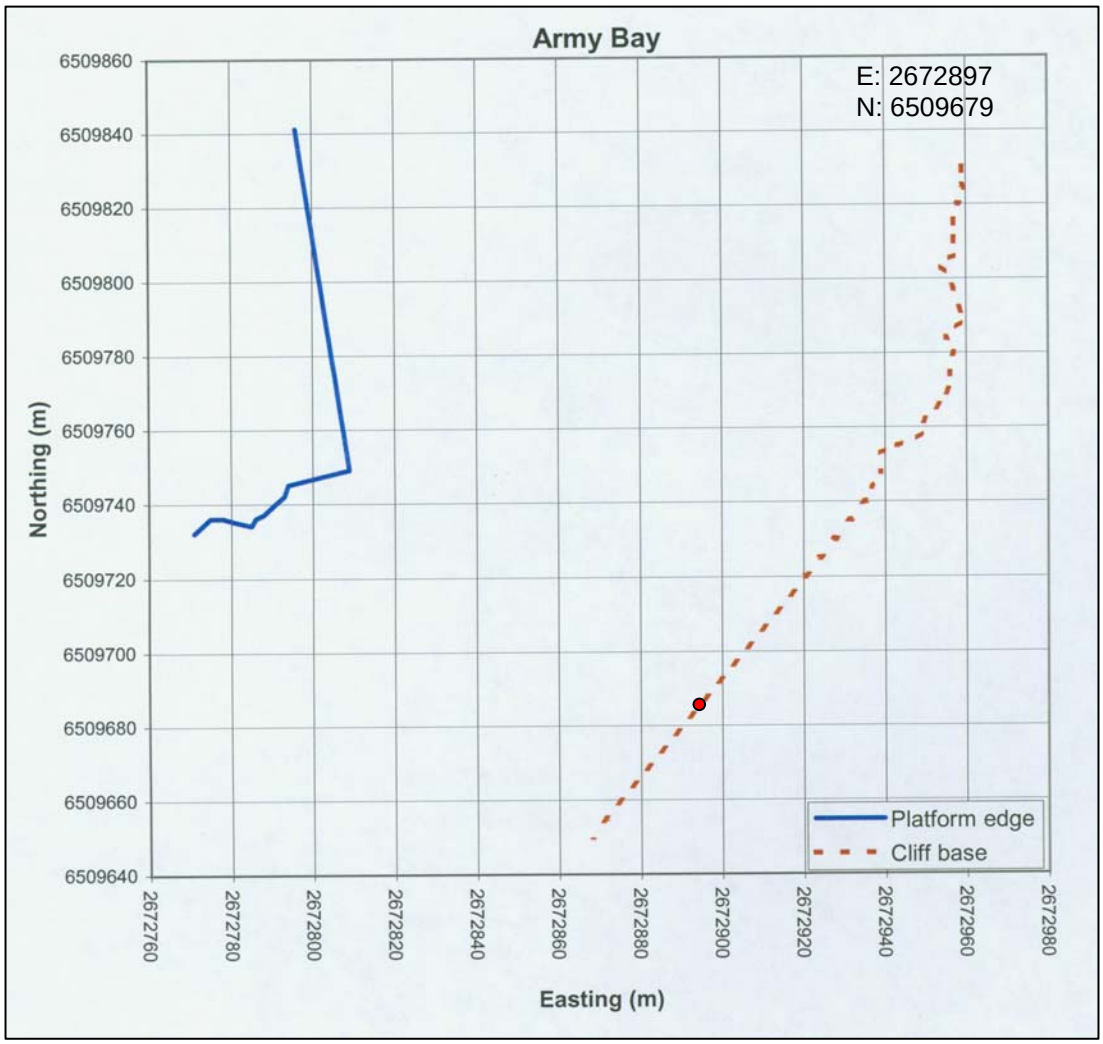

Figure 4.20: Shore platform plan morphology of Army Bay.

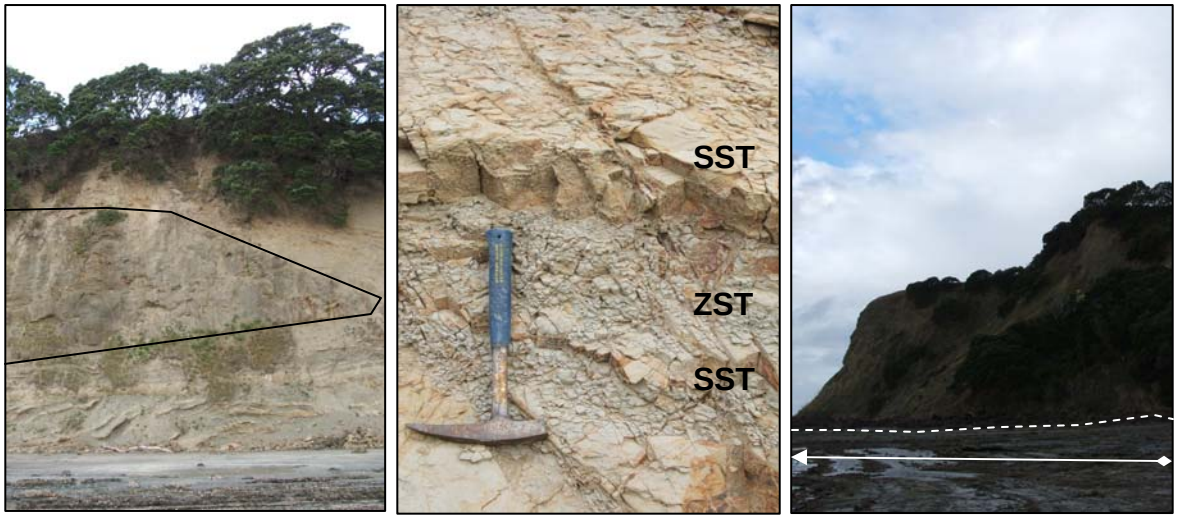

Figure 4.21: Photographs and sketch of the described Army Bay cliff section. A: Cliff face with very thick Parnell Grit mid-section (outlined by black line). B: Heavily jointed, seaward dipping beds. C: Cliff profile and shore platform; dashed line marks the cliff base and the arrow marks the direction from the described cliff base (dot) to the seaward margin of the platform (arrowhead). D: Sketch of bedding and shore platform characteristics.

4.3.11 Waiwera Beach

Cliff height: 34.8 m	Cliff angle: 67°	Cliff strike: 106°	Bed dip: 20° seaward
GSI:	Flysch 24 ± 5	Sandstone 39 ± 5	Siltstone 43 ± 5
Schmidt Hammer Rebound number:		Sandstone 24 - 27	Siltstone 30

The cliff site is highly faulted and folded with the presence of an extremely thick Parnell Grit bed (up to 15 m). The shore platform surface reflects the dip of beds but is overall horizontal with a steep drop-off at the seaward edge; beds are dipping seaward at the described cliff site. Beds in the cliff face are very steep due to thrust faulting. The main fault sets have orientations of 89/099, 88/262, and 05/149, and the main thrust fault is oriented 44/104.

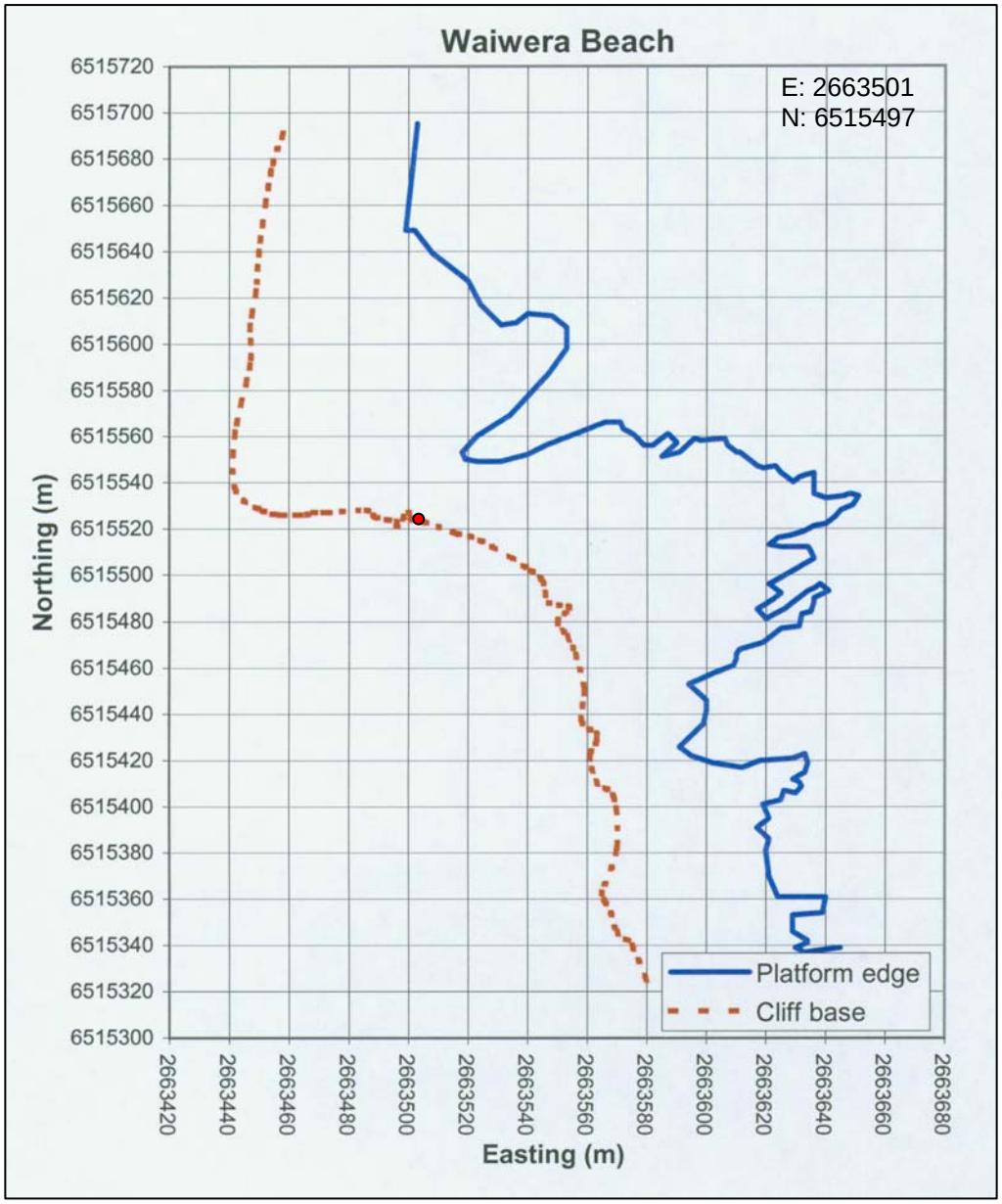

Figure 4.22: Shore platform plan morphology of Waiwera Beach.

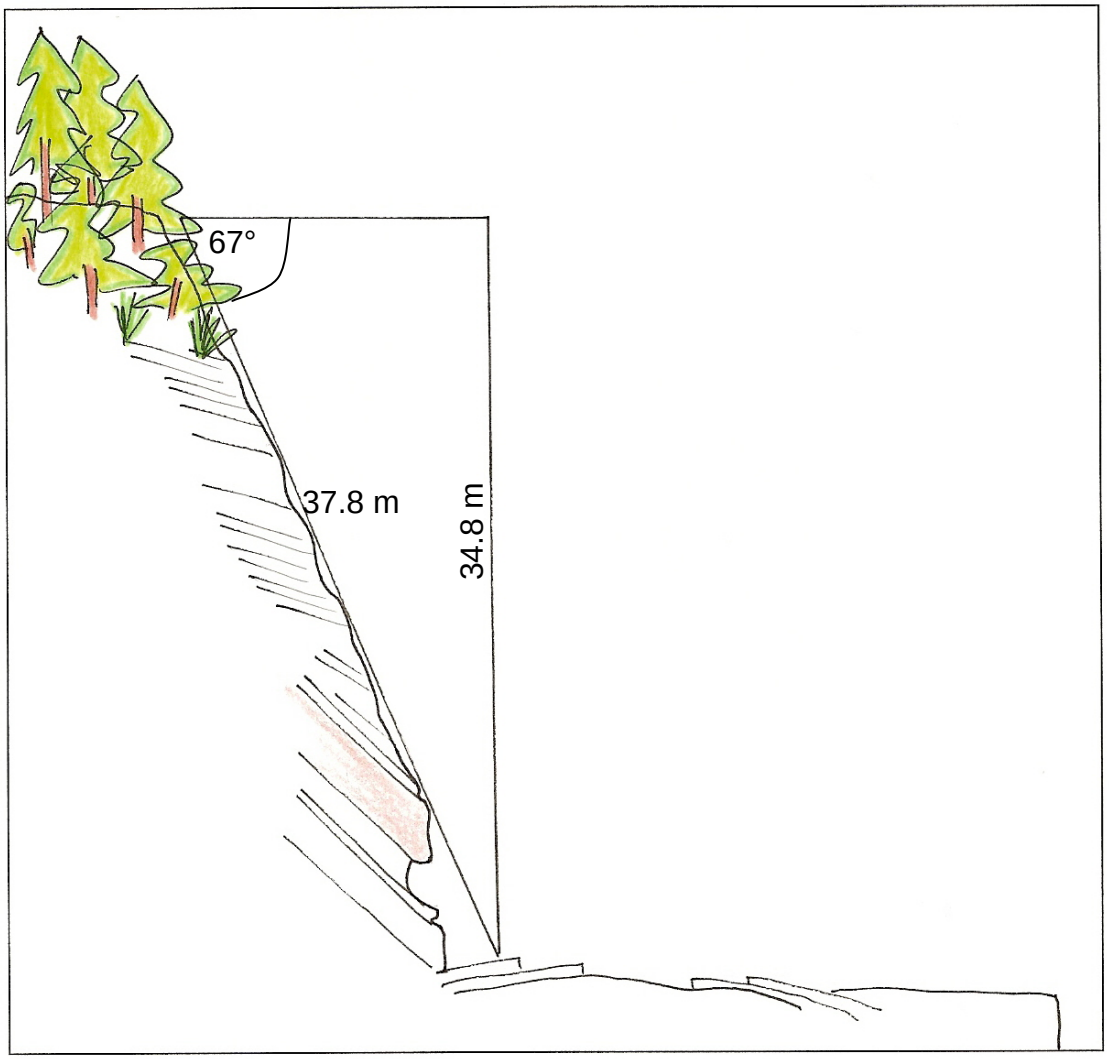

Figure 4.23: Photographs and sketch of the described Waiwera Beach cliff section. A: Cliff profile showing the intensely folded beds also evident in the shore platform. B: Shore platform with seaward dipping beds; dip direction is marked by the white arrow. C: Sandstone and siltstone beds of the described section; note undercutting of sandstone beds by siltstone. D: Sketch of bedding and shore platform characteristics.

4.3.12 Opahi Bay

Cliff height: 21.0 m	Cliff angle: 74°	Cliff strike: 062°	Bed dip: 3° seaward
GSI:	Flysch 45 ± 5	Sandstone 55 ± 5	Siltstone 40 ± 5
Schmidt Hammer Rebound number:		Sandstone 20 - 25	Siltstone not measured

The shore platform and cliff are highly faulted, slumped and folded and thus the shore platform exhibits a wide range of tilt and dip both seaward and landward; beds are dipping seaward at the described cliff section. The cliff has very thick sandstone beds with thin interbedded siltstone and block fall appears to be the dominant form of erosion. A 1 - 1.5 m high talus slope exists around the base of the cliff but at this stage does not seem to inhibit rock fall processes. A Parnell Grit bed exists through part of the cliff (outside the described section) and on the shore platform. The platform is near-horizontal with a sharp drop-off at the seaward edge.

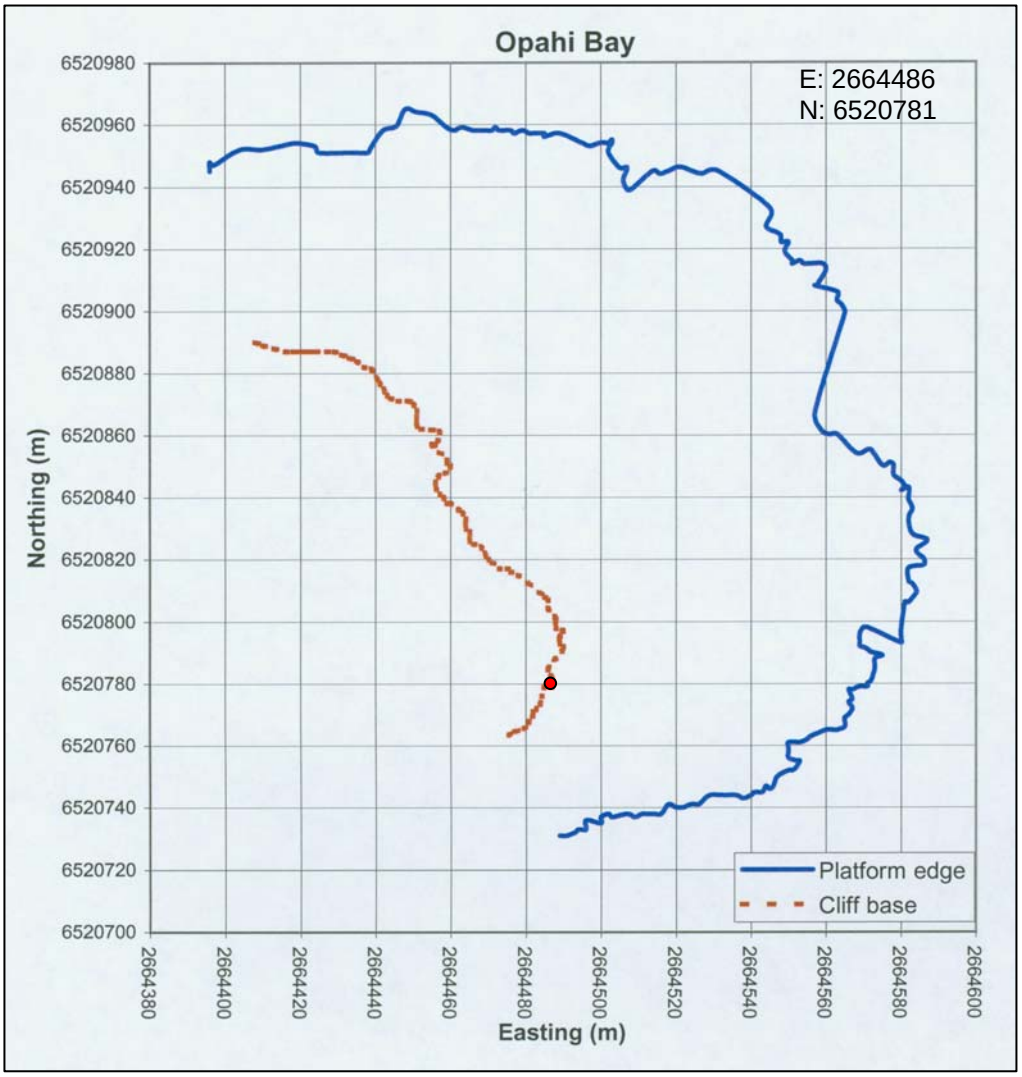

Figure 4.24: Shore platform plan morphology of Opahi Bay.

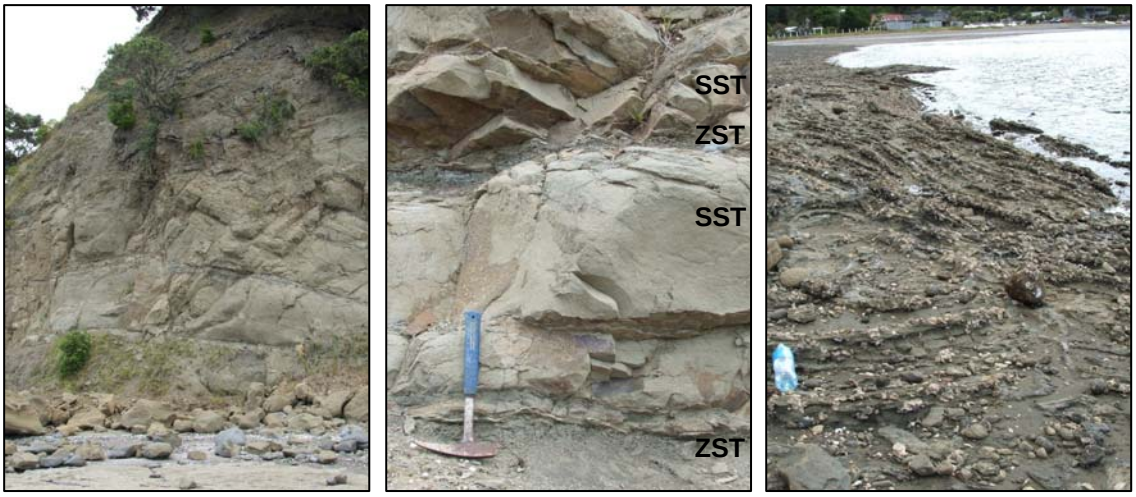

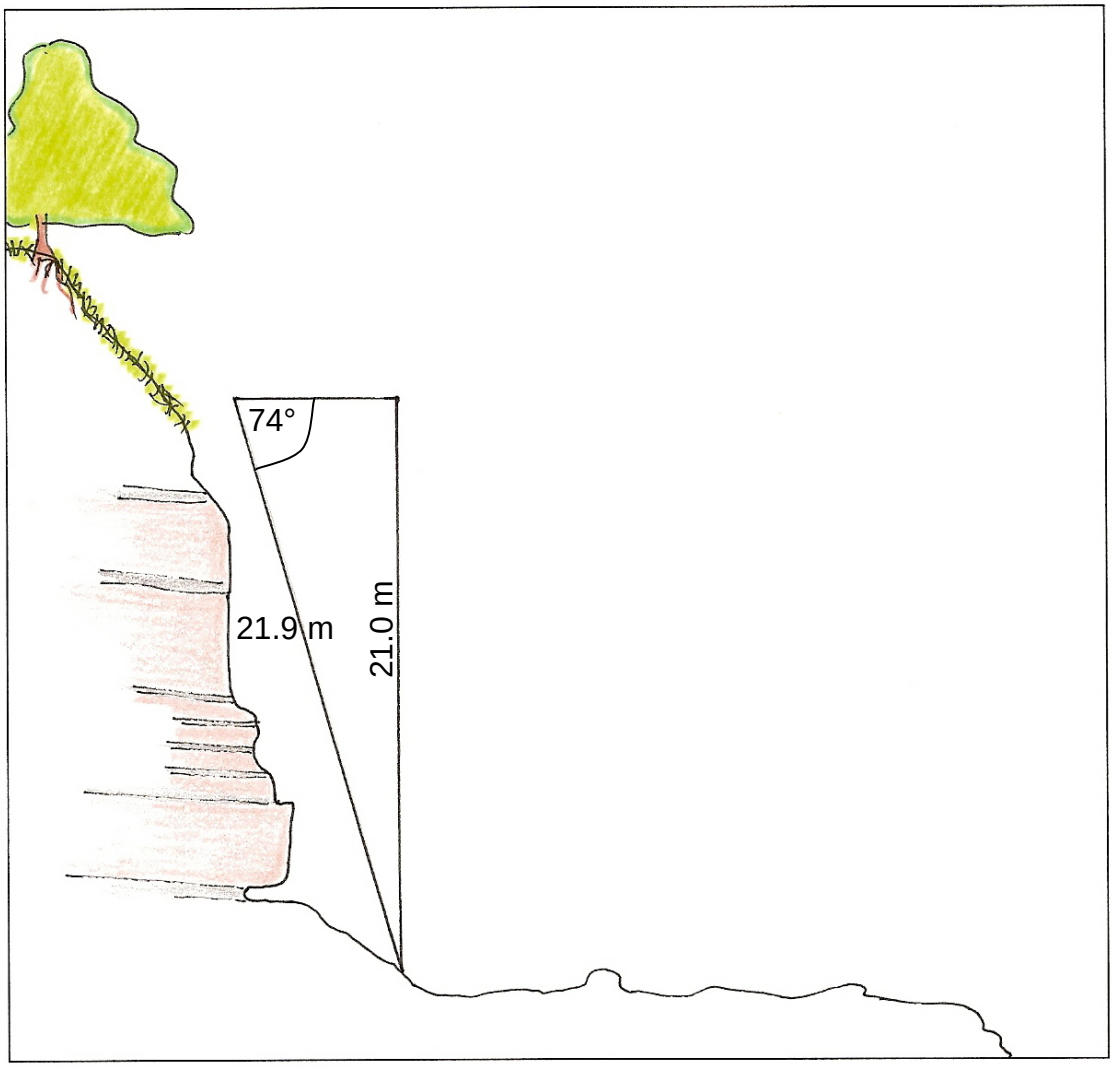

Figure 4.25: Photographs and sketch of the described Opahi Bay cliff section. A: Cliff profile; note the cliff debris covering the cliff base B: Medium to thick sandstone beds with thin siltstone interbeds. C: Shore platform constructed of heavily folded Parnell Grit; the northern part of the platform edge has a sloped profile. D: Sketch of bedding and shore platform characteristics.

4.3.13 Martins Bay

Cliff height: 23.4 m	Cliff angle: 67°	Cliff strike: 144°	Bed dip: 3° seaward
GSI:	Flysch 40 ± 5	Sandstone 65 ± 5	Siltstone 45 ± 5
Schmidt Hammer Rebound number:		Sandstone 25 - 26	Siltstone 30

Thin sandstone and thin siltstone beds are in successions of ~ 1 - 2 m, interrupted by thick-medium sandstone beds. Lower thick sandstone beds are faintly laminated to massive and grade into upper siltstone; basal sandstone and upper siltstone contacts are sharp. The beds have a purple and orange staining on the surface but joints are not iron-lined. Successions of thin siltstone and sandstone are highly degraded and siltstone continually falls out in very small blocks, clearly weakening the support of upper sandstone beds. There are numerous slumps and normal faulting along the entire cliff site. The platform is stepped, steadily into sea and steps are wide (0.5 - 1.5 m) and about 5 - 20 cm deep due to the near horizontal dip of the beds. There are regular joint patterns in the beds on the shore platform and the platform surface is predominantly sandstone. Medium-flow seepage was observed following heavy rainfall and was readily washing out smaller rock particles and clay/soil.

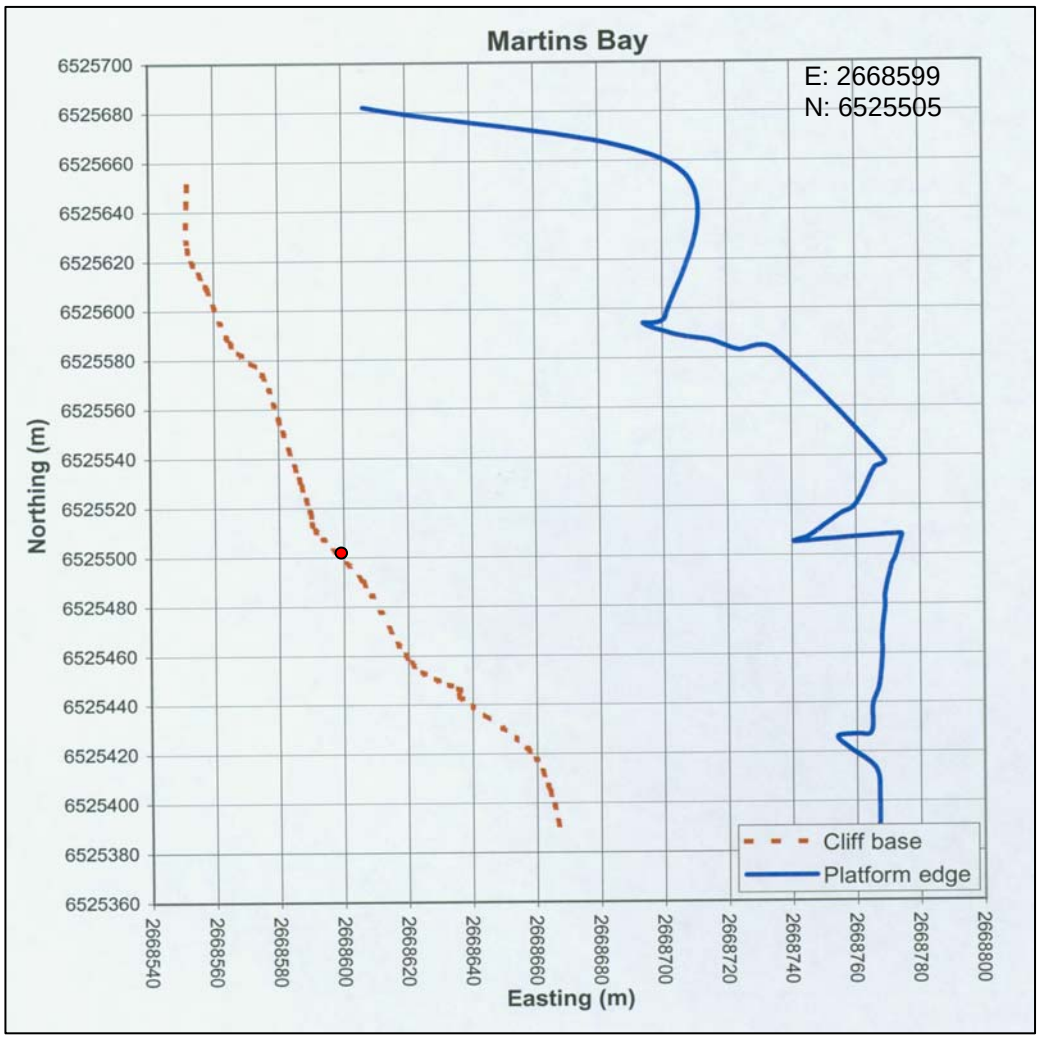

Figure 4.26: Shore platform plan morphology of Martins Bay.

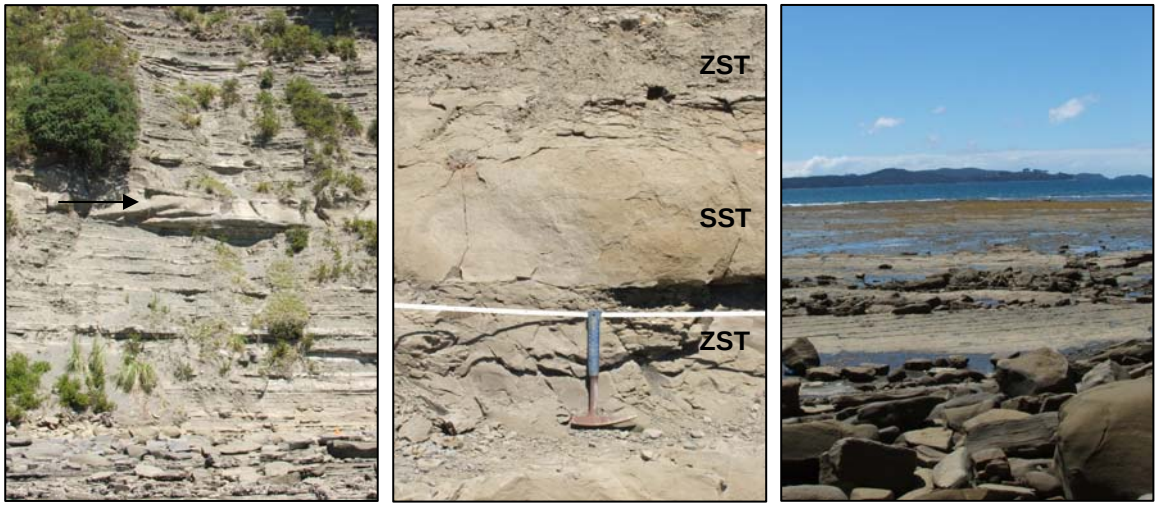

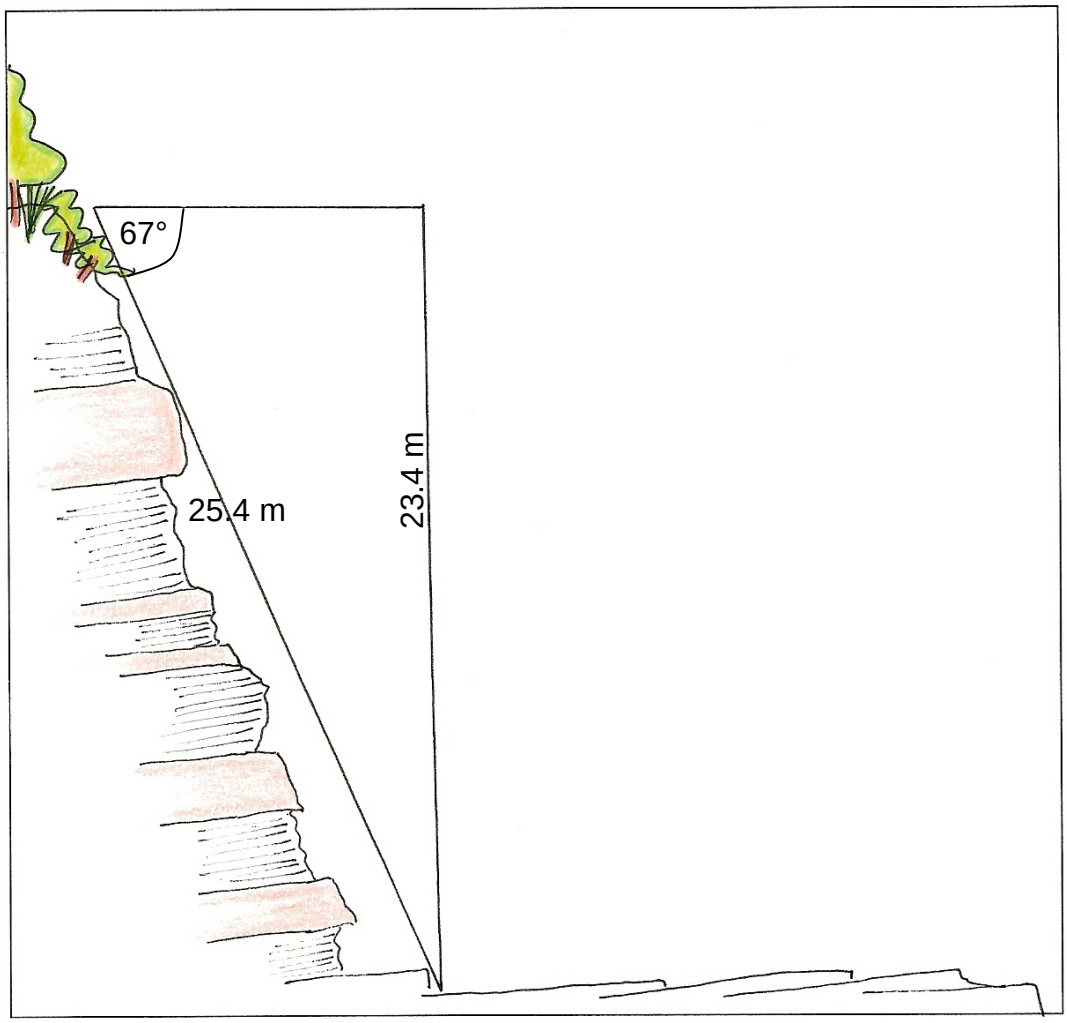

Figure 4.27: Photographs and sketch of the described Martins Bay cliff section. A: Cliff face with prominent thick sandstone bed mid-section (black arrow). B: Sandstone and siltstone beds; base of sandstone bed has a sharp contact (just above white tape measure) and the upper sandstone bed grades into siltstone. C: Shore platform with boulder-littered cliff base in the foreground. D: Sketch of bedding and shore platform characteristics.

4.3.14 Buckleton Beach

Cliff height: 19.0 m	Cliff angle: 73°	Cliff strike: 028°	Bed dip: 9° landward
GSI:	Flysch 48 ± 5	Sandstone 65 ± 5	Siltstone 45 ± 5
Schmidt Hammer Rebound number:		Sandstone 22 - 32	Siltstone not measured

Very thick, coarse-sand beds exhibit channelised flow with variable amplitudes and lensing. Below the thick sandstone beds, a section of thin siltstone beds with thin interbedded sandstone exists at the cliff base. The thin sandstone beds in this lower zone are massive to convoluted and grade upward into siltstone. Seepage was observed following a 2 day period of showers; the seepage was a dripping to continuous flow at about medium pressure. The platform is gently stepped and littered with many cobbles and boulders. Spheroidal weathering persists on the shore platform and cliff face at the northern end of the cliff site.

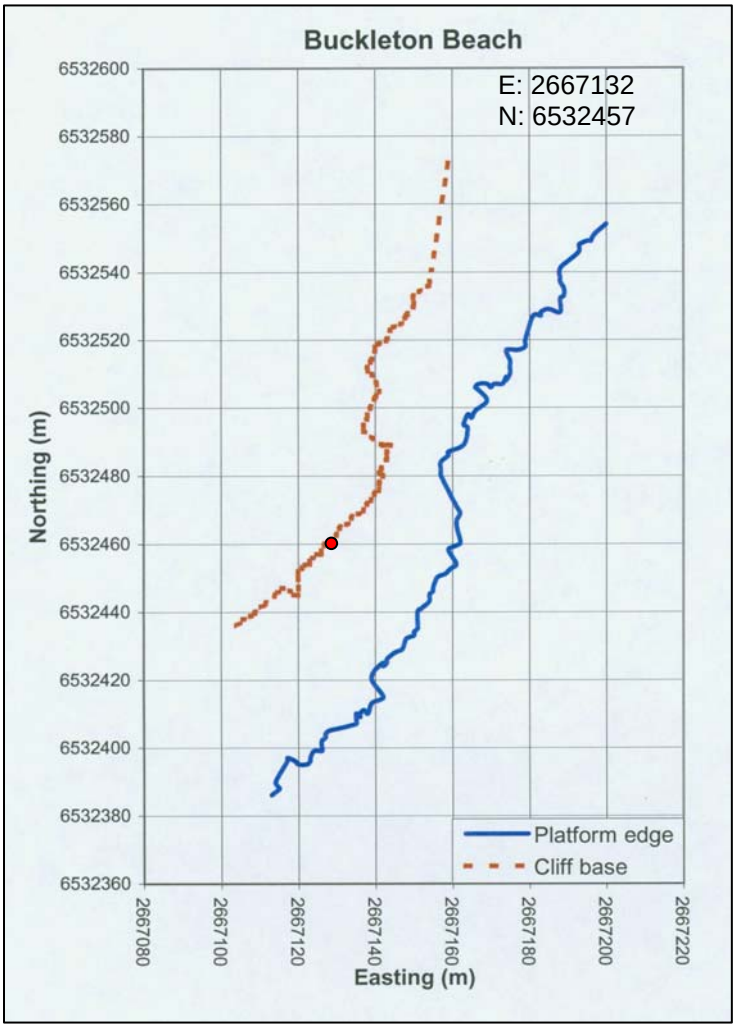

Figure 4.28: Shore platform plan morphology of Buckleton Beach.

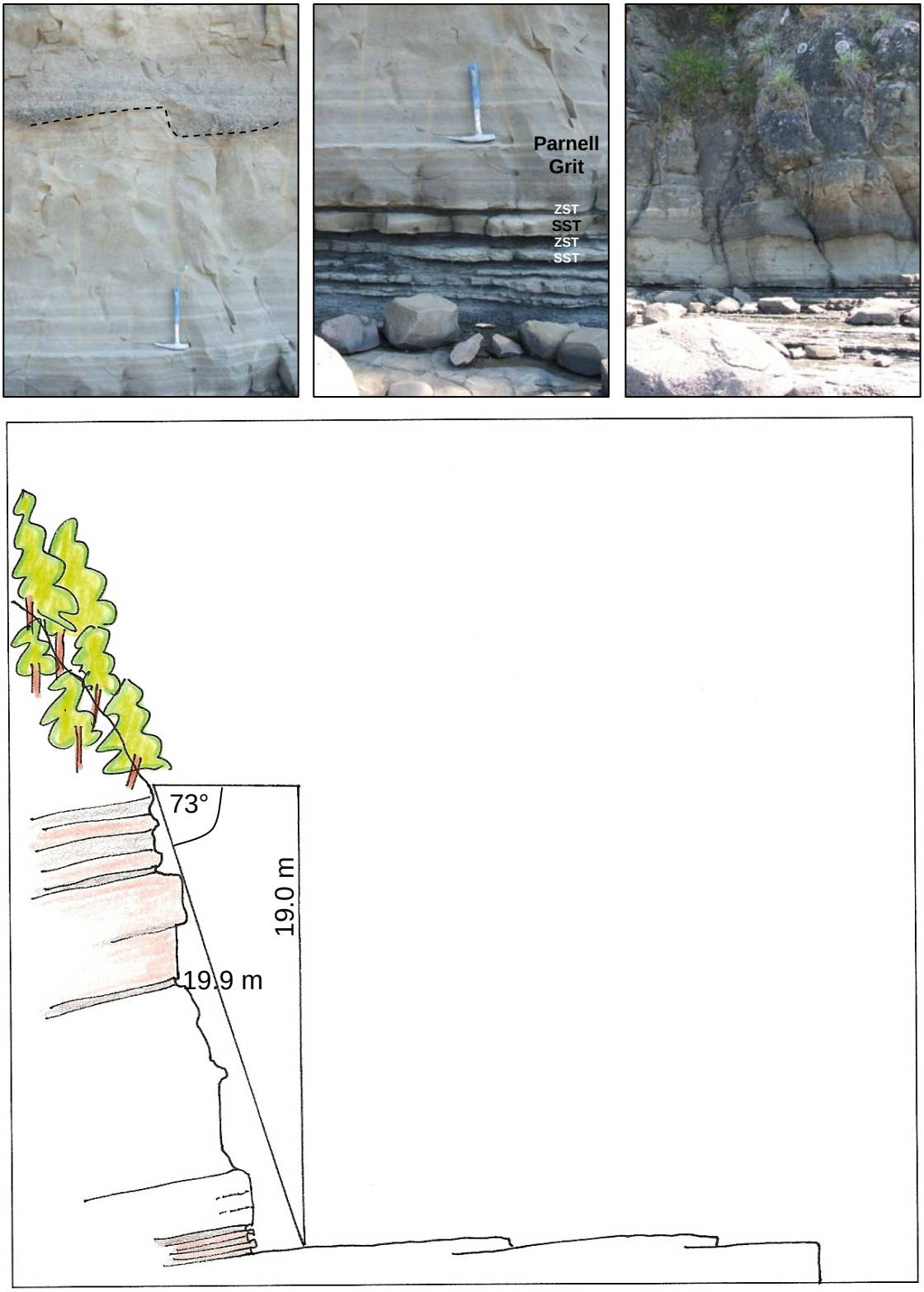

Figure 4.29: Photographs and sketch of the described Buckleton Beach cliff section. A: Very thick sandstone beds with lower laminated zones and coarser Parnell Grit-like zones which have a convoluted base (dashed line). B: Cliff base consisting of alternating thin sandstone and siltstone beds. C: Cliff face showing the prominent, very thick sandstone beds; the platform is gently-stepped and littered with numerous boulders. D: Sketch of bedding and shore platform characteristics.

4.3.15 Matheson Bay

Cliff height: 25.1 m	Cliff angle: 51°	Cliff strike: 170°	Bed dip: 3° seaward
GSI:	Flysch 25 ± 5	Sandstone 45 ± 5	Siltstone 37 ± 5
Schmidt Hammer Rebound number:		Sandstone 39 - 41	Siltstone not measured

Siltstone layers dominate the entire cliff section with a few thick sandstone units at higher elevation; sandstone beds which are about 30 cm thickness exist approximately every metre between the siltstone beds. Apart from the heavily frittered exterior of the siltstone, there are major primary joints that run through all of these units plus the strong sandstone beds have their own secondary and tertiary joint sets. The shore platform is covered (and protected) by abundant sandstone boulders and accumulate sheets of siltstone. The shore platform steps down gradually from the cliff base due to the thin siltstone bedding of ~ 1.5 cm and drops off sharply at the seaward edge.

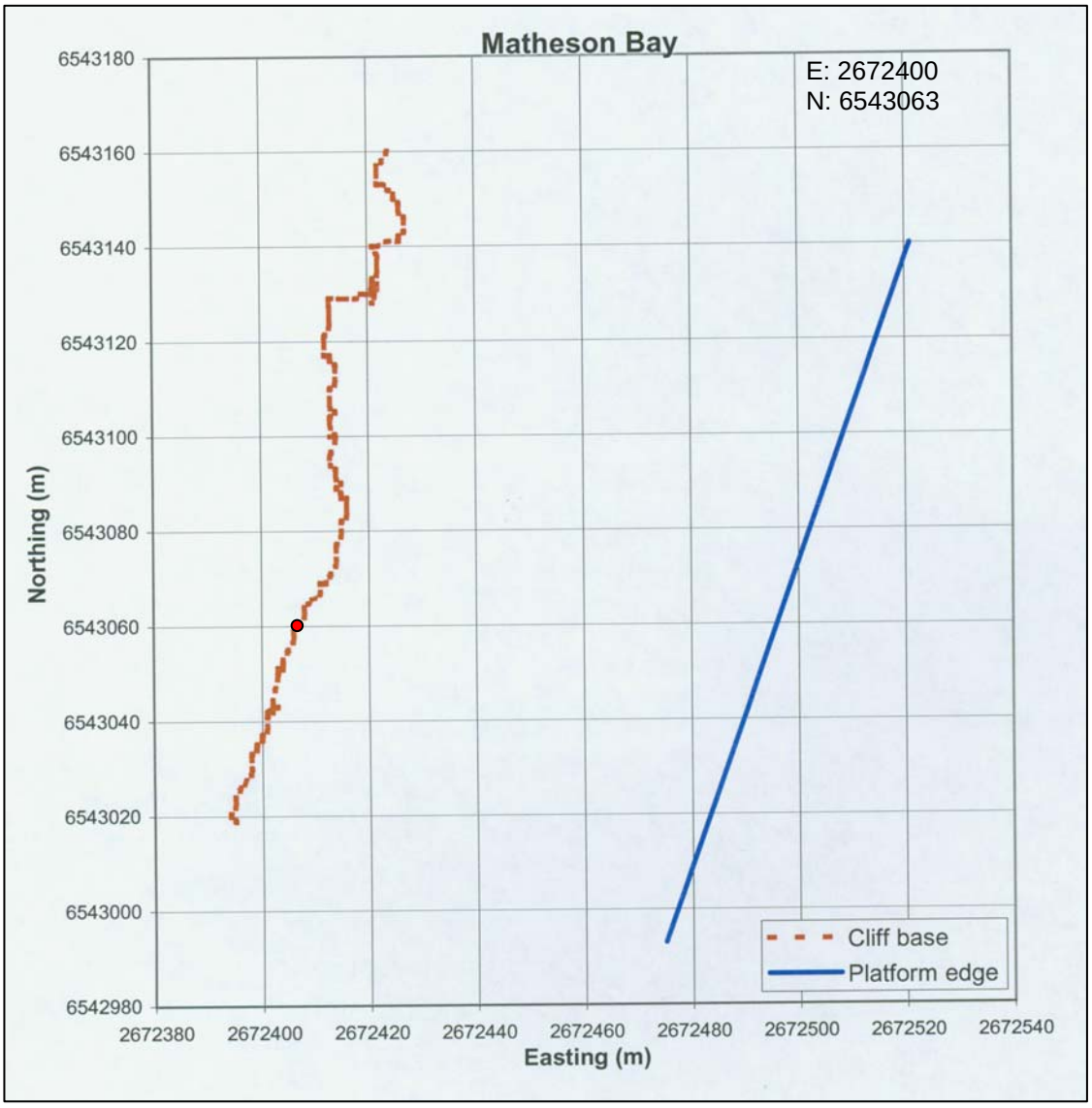

Figure 4.30: Shore platform plan morphology of Matheson Bay.

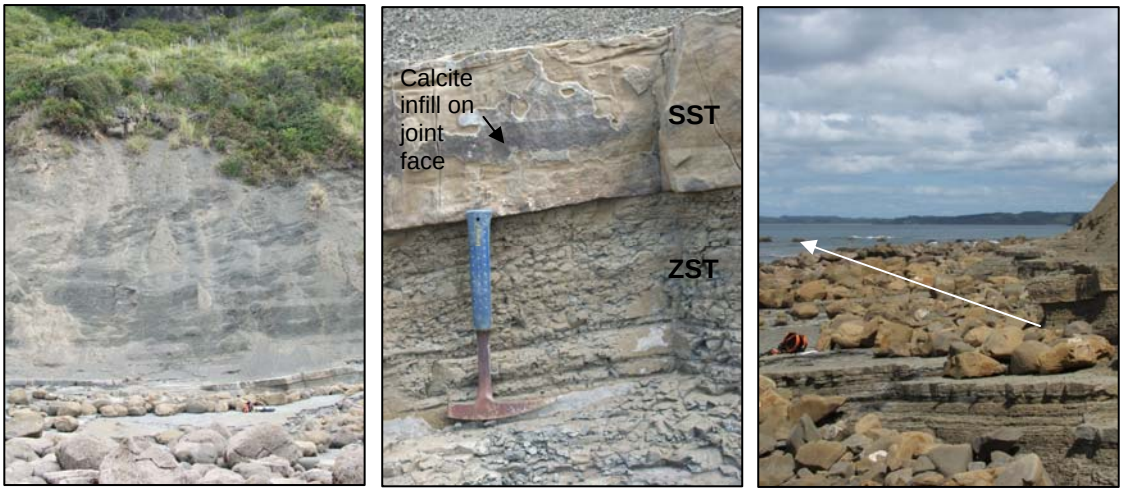

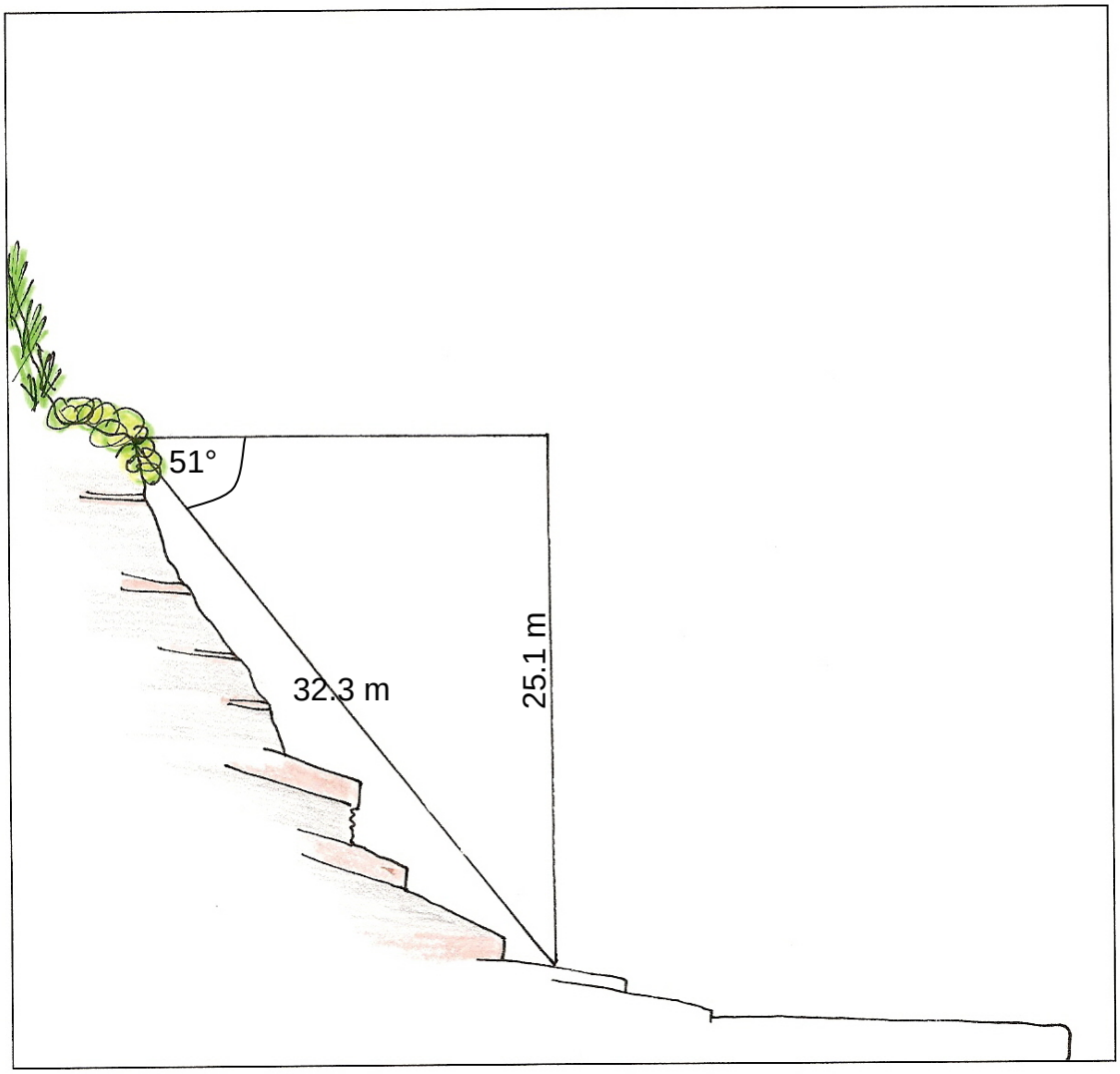

Figure 4.31: Photographs and sketch of the described Matheson Bay cliff section. A: Cliff face dominated by tumbling siltstone fragments. B: Close up of prominent sandstone bed and lower siltstone beds. C: Shore platform, the extent of which is marked by the white arrow. D: Sketch of bedding and shore platform characteristics.

4.3.16 Leigh Marine Reserve

Cliff height: 14.8 m	Cliff angle: 51°	Cliff strike: 062°	Bed dip: 10° seaward
GSI:	Flysch 20 ± 5	Sandstone 45 ± 5	Siltstone 45 ± 5
Schmidt Hammer Rebound number:		Sandstone 20 - 24	Siltstone 41

Siltstone dominates in this cliff site and is heavily frittered and numerous faults cross cut each other through the rock mass. A steep, coarse-sand beach exists between the base of the cliff and the shore platform with no cliff debris. There is also no cliff debris larger than a 1 - 5 cm directly the cliff base, indicating it is regularly removed at high tides. Frittered particles are continually falling down the cliff face. The shore platform is free of cliff debris, presumably because the platform is covered for much of a tidal cycle and the small-sized cliff debris and beach sand become highly mobile. About 9 boulders protrude on top of the shore platform and appear be attached to the cliff base (these may be the Albany Conglomerate or concretions). The platform is folded and dipped particularly toward the western side of the section.

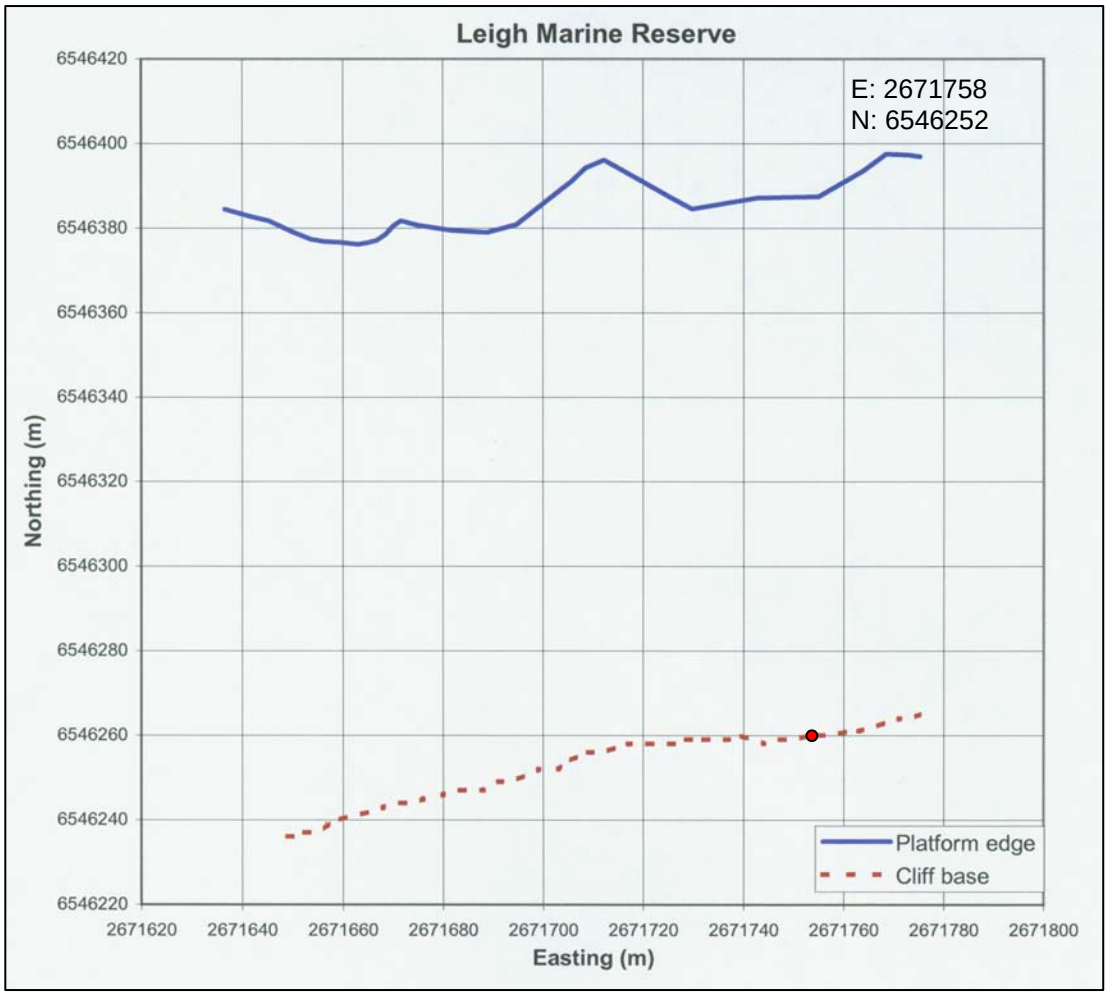

Figure 4.32: Shore platform plan morphology of Leigh Marine Reserve

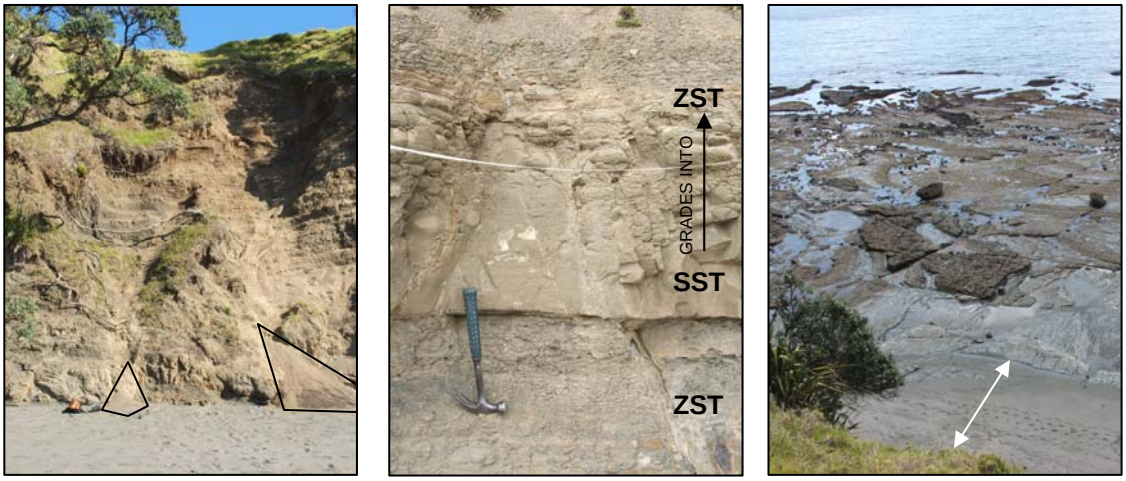

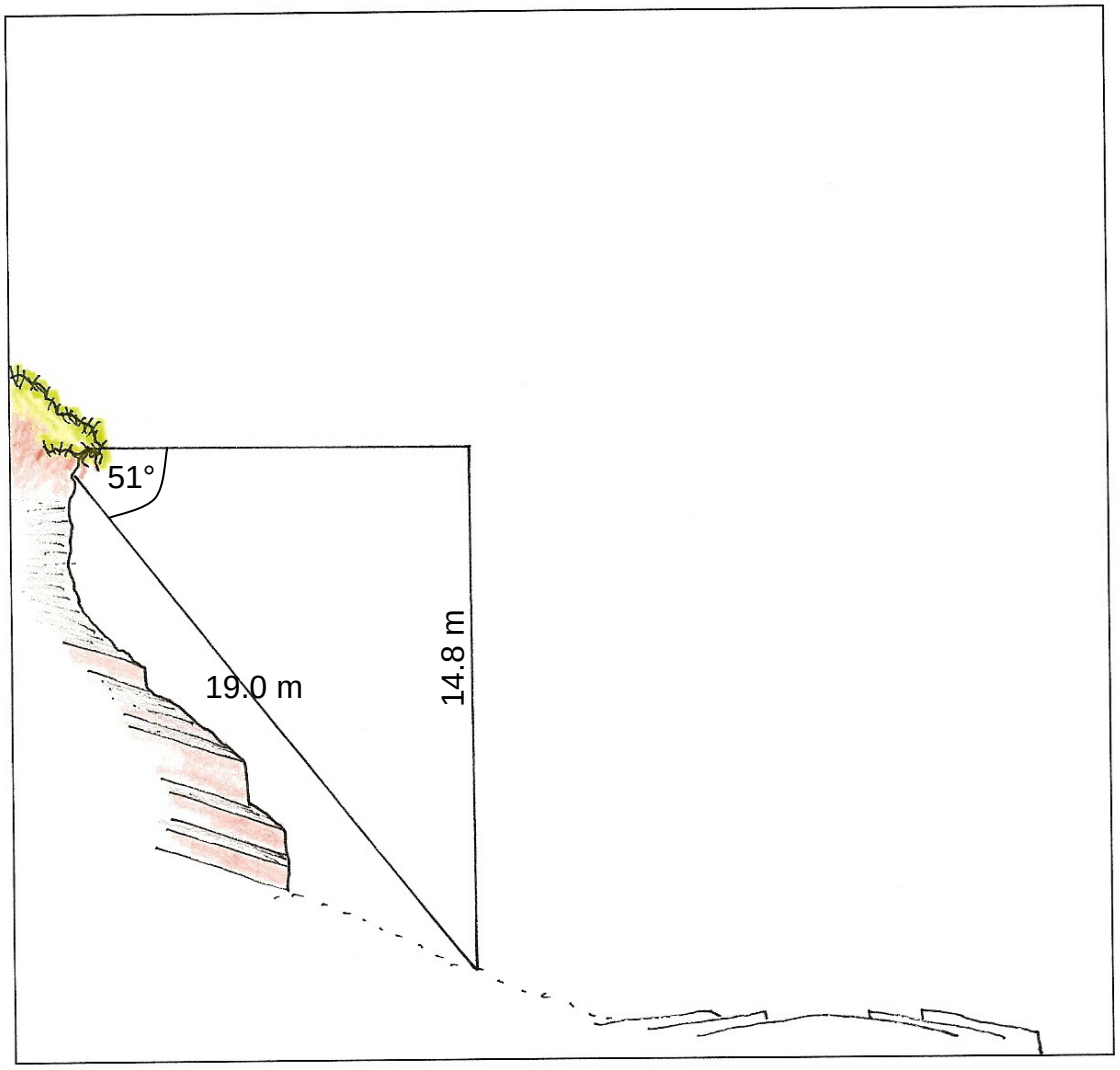

Figure 4.33: Photographs and sketch of the described Leigh Marine Reserve cliff section. A: Cliff face with talus cones at the cliff base (black outline). B: Sandstone bed grading into a siltstone bed. C: Shore platform; taken from cliff top (~ 15 m above sea level) at low tide; the extent of the beach is marked by a white arrow. D: Sketch of bedding and shore platform characteristics.

4.4 Geomorphology Summary

The geomorphologic variations between sites are illustrated and discussed here including cliff height and length, cliff angle, and shore platform type and width.

4.4.1 Cliff height and length

Cliff height is the vertical distance to the top of the cliff whereas cliff length is the actual distance of the cliff face from the base to the top (see Section 3.2.4.1), and is thus slightly longer than the cliff height, as illustrated in Figure 4.34. Cliff height is used in the database (rather than cliff length) to compare with other parameters because cliff height is an independent measure compared to cliff length which is dependent upon slope angle.

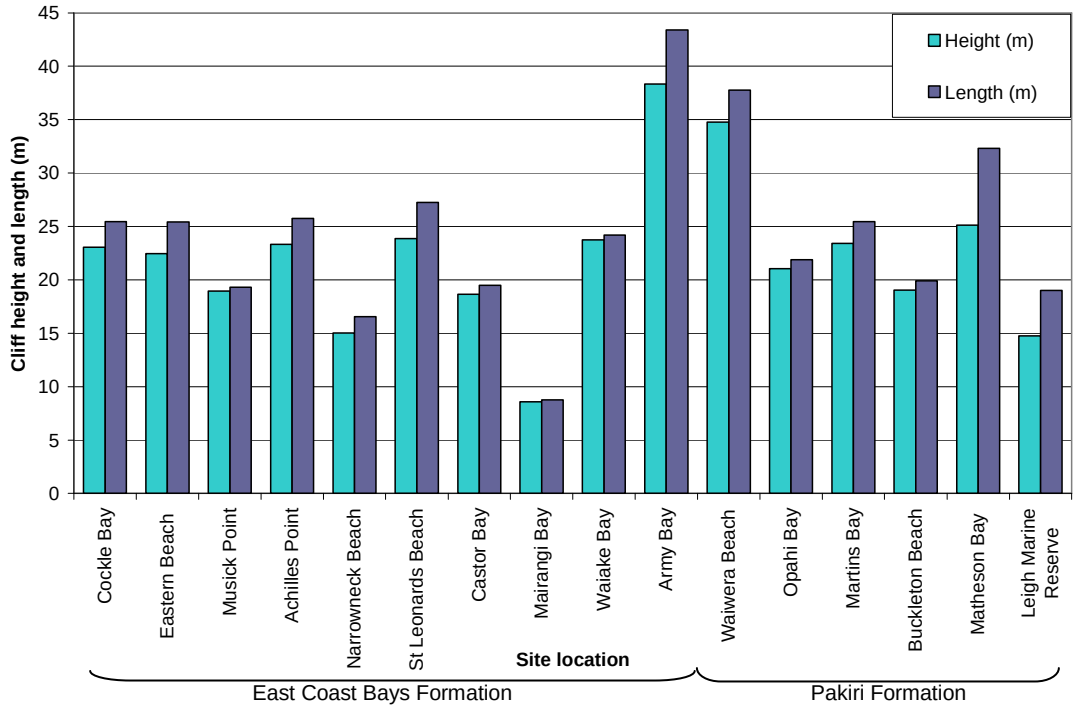

Figure 4.34: Cliff heights and their associated lengths for southern to northern cliff sites.

Cliff height ranges from 8.6 ± 1.3 m to 38.3 ± 6.2 m between the 16 sites, with the average for East Coast Bays Formation rock being 21.6 ± 11.3 m and for Pakiri Formation rock being 23.0 ± 11.6 m. Based on these results, cliff heights do not seem significantly lower in the East Coast Bays Formation compared to the Pakiri Formation rock. From observations, cliffs are higher at headlands, and lower in embayments; there appears to be no relationship between cliff height and site location (Figure 4.34) except that the two highest sites occur in the central Whangaparaoa - Waiwera part of the study area. Cliff height is thus interpreted as being merely due to the geomorphology of the section of existing, previously-eroded landscape in which coastal erosion is occurring. Comparatively, Tonkin and Taylor (2005a) quote that Pakiri Formation cliff heights range from ~ 45 - 140 m and East Coast Bays Formation cliff heights are overall lower and range from ~ 18 - 30 m. Data in this study suggest that while the Pakiri Formation may exhibit a wide range of cliff heights, due perhaps to an overall steeper, more incised topography, in this part of the study area, there is nothing to suggest that the average cliff height is significantly greater than in the East Coast Bays Formation.

4.4.2 Cliff angle

Cliff angles vary between 51° and 79° (all sites have a measurement error of ± 2.5°) and are presented for each site in Figure 4.35. From observation, cliff angles are lower where siltstone dominates the cliff section, for instance Matheson Bay (51°) and Leigh Marine Reserve (51°). Thick bedded sandstone units, with very thin siltstone beds in a cliff section result in higher cliff angles, for instance Musick Point (79°) and Mairangi Bay (79°). As with cliff height, there was no consistent variation between the East Coast Bays Formation cliff angles (average 68 ± 8°) and the Pakiri Formation (average 64 ± 6°).

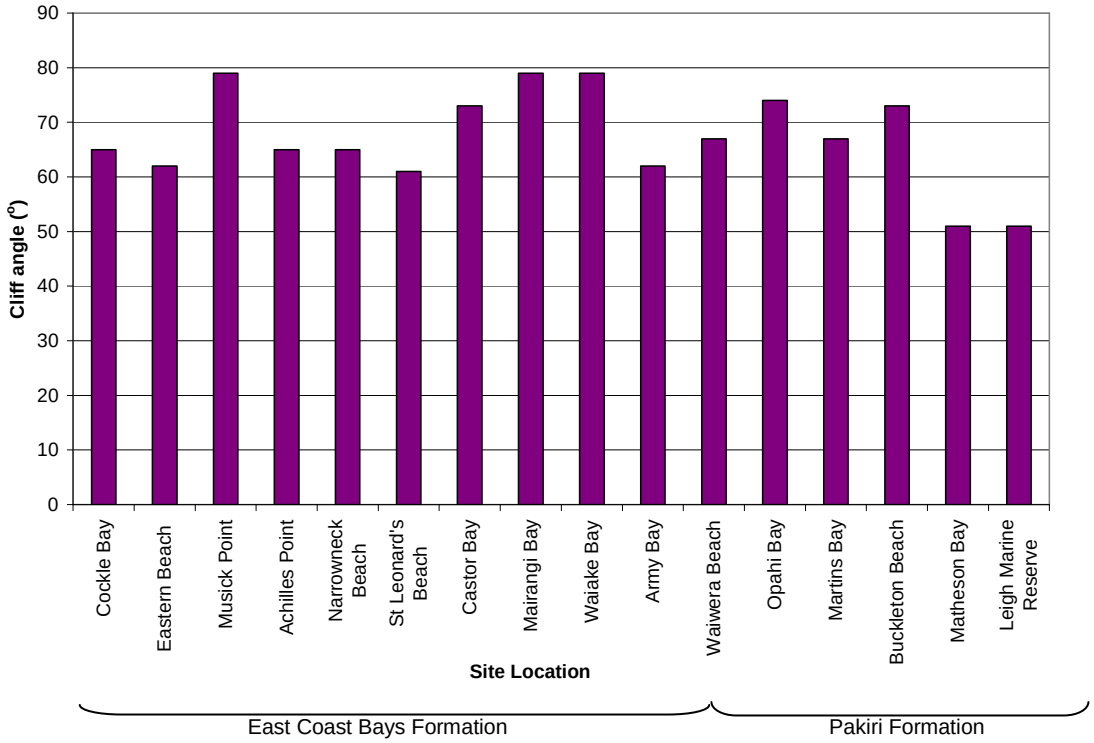

Figure 4.35: Cliff face angle for southern to northern cliff sites.

4.4.3 Bed dip and orientation

The dip angles of bedding planes are predominantly seaward at most sites ranging from nearly horizontal to +26°; the maximum seaward-dipping angle recorded was > +40° (refer to Section 4.3; Figure 4.36). These sites included Eastern Beach, Musick Point, Castor, Mairangi Bay, Army Bay, Waiwera Beach, Opahi Bay, Martins Bay, Matheson Bay and Leigh Marine Reserve. The sites at which beds dipped landward (near horizontal to -15°) included Cockle Bay, Achilles Point, Narrowneck Beach, St Leonard's Beach, Waiake Bay, and Buckleton Beach. While the dip direction value determines whether beds were dipping seaward or landward with respect to the strike of the cliff face, the dip angle value means that some of the beds dipping seaward could effectively be buttressed. Dip angle is included as a parameter in the collated database for this study, recorded as positive values for beds that dip seaward and negative values for beds that dip landward.

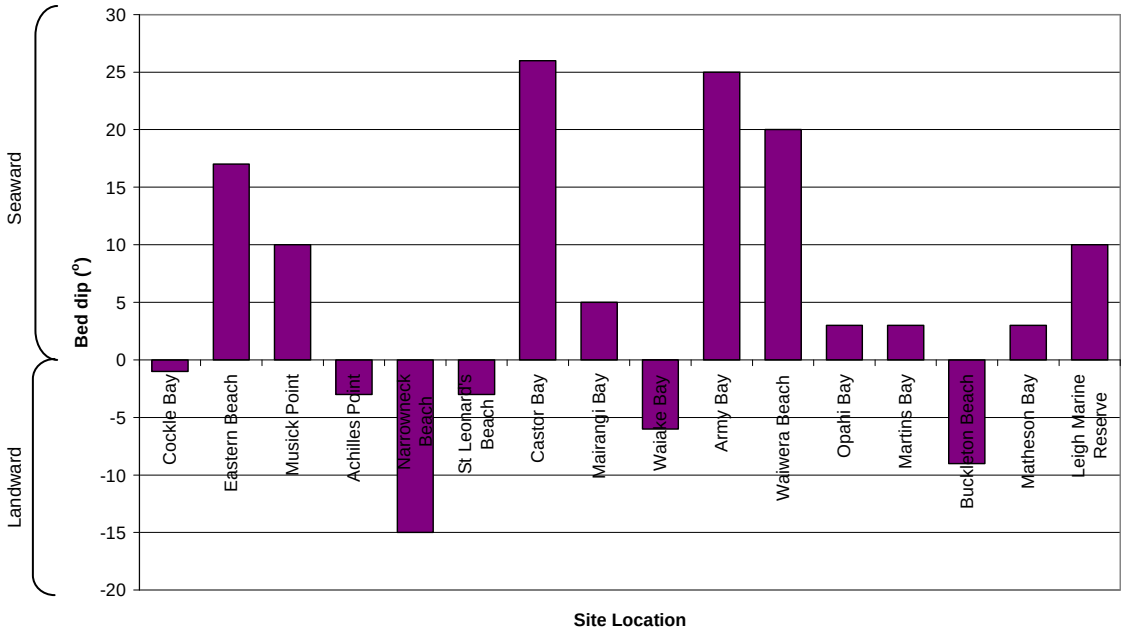

Figure 4.36: Approximate dip angle of the prominent bedding planes in the described cliff sites.

4.4.4 Shore platform type

The sketches drawn for each site (Section 4.3) illustrate the basic morphology of the shore platform that has developed within the cliff section area. The platforms fit into four different classified morphologies including: the Type B platforms of Sunamura (1992) and the synonymous high-tidal platforms of Healy and Kirk (1992); the broad intertidal platforms of Healy and Kirk (1992); a combination of both Type A and Type B platforms of Sunamura (1992); and a combination broad intertidal (Healy and Kirk, 1992) and Type B (Sunamura, 1992) platforms (Table 4.2). Section 2.4.3 defines and illustrates each platform type individually; a designated symbol for each platform morphology type, including the two combined morphologies defined in this study, is illustrated on each cliff site sketch in Section 4.3.

Table 4.2: Shore platform morphology types categorized from observations made of the 16 described sites. Intertidal and high-tidal platforms are from Healy and Kirk (1992); Type A and Type B platforms are from Sunamura (1992).

1. Intertidal (sloping with edge)	**2.** Type B / High-tidal (horizontal)	**3.** Combination of Intertidal and Type B	**4.** Combination of Type A and Type B
Narrowneck Beach	Castor Bay	Musick Point	Cockle Bay
St Leonard's Beach	Mairangi Bay	Waiake Bay	Eastern Beach
Army Bay	Opahi Bay		Achilles Point
	Martins Bay		Waiwera Beach
	Buckleton Beach		
	Matheson Bay		
	Leigh Marine Reserve		

The sloping, Type A platform morphology was not observed as a solo feature at any of the cliff sites. However, the broad intertidal platforms which are sloping but end with a seaward edge were observed at three of the cliff sites. The Narrowneck Beach and St Leonard's Beach sites both had similar highly-stepped platforms with beds dipping landward, and the stepped nature of the platforms were defined as having an overall sloping profile. The Army Bay site displayed a broad platform which was defined as being overall sloping due to the significant elevation of the cliff base above the platform surface with a sloped beach in between (Section 4.3.10).

Horizontal platforms with clearly defined seaward edges (Type B or high-tide platforms) were observed at seven of the cliff sites. This platform type is displayed in both the deformed and relatively-undeformed cliff sites. All of the platforms are just exposed at low tide and so presumably are underwater for a significant period of a tidal cycle. Because of their horizontal nature they are covered by an incoming tide fairly quickly, potentially giving more time for the cliff base to be affected by marine erosion processes. Buckleton Beach has a relatively narrow platform width and no beach so the cliff base was reached at high tide. If Mairangi Bay was not protected by an encased sewer pipe then presumably the high tide would have also reached the cliff base. There is evidence of this from a notch at the base of the cliff. All of the other sites with horizontal platforms had beaches or rock cover at the cliff base and were not reached at high tide.

The other observed platforms have a combination of horizontal and sloping platforms (Figure 4.37). There were two sites observed that have high, narrow horizontal benches,

with lower sloping platforms that terminate in a seaward edge; these are Musick Point and Waiake Bay. At Musick Point, the high benches are only around headland areas or convex parts of the coastline. They are relatively small and, with no evidence of organisms on them, they do not appear to be significantly covered or even reached by the high tide. The lower sloping platform is very broad and, within the described area, has a seaward edge. At Waiake Bay, prominent high benches were observed at both ends of the cliff coastline (between north Browns Bay and south Waiake Bay), as well as a narrower ledge existing at the same level which runs along the majority of the cliff in between. The headland benches are reached and partially covered at high tide. The coastline often has a beach at the cliff base, which temporally prevents it from being reached at high tide. The lower platform has a sloping profile that ends in a low seaward edge.

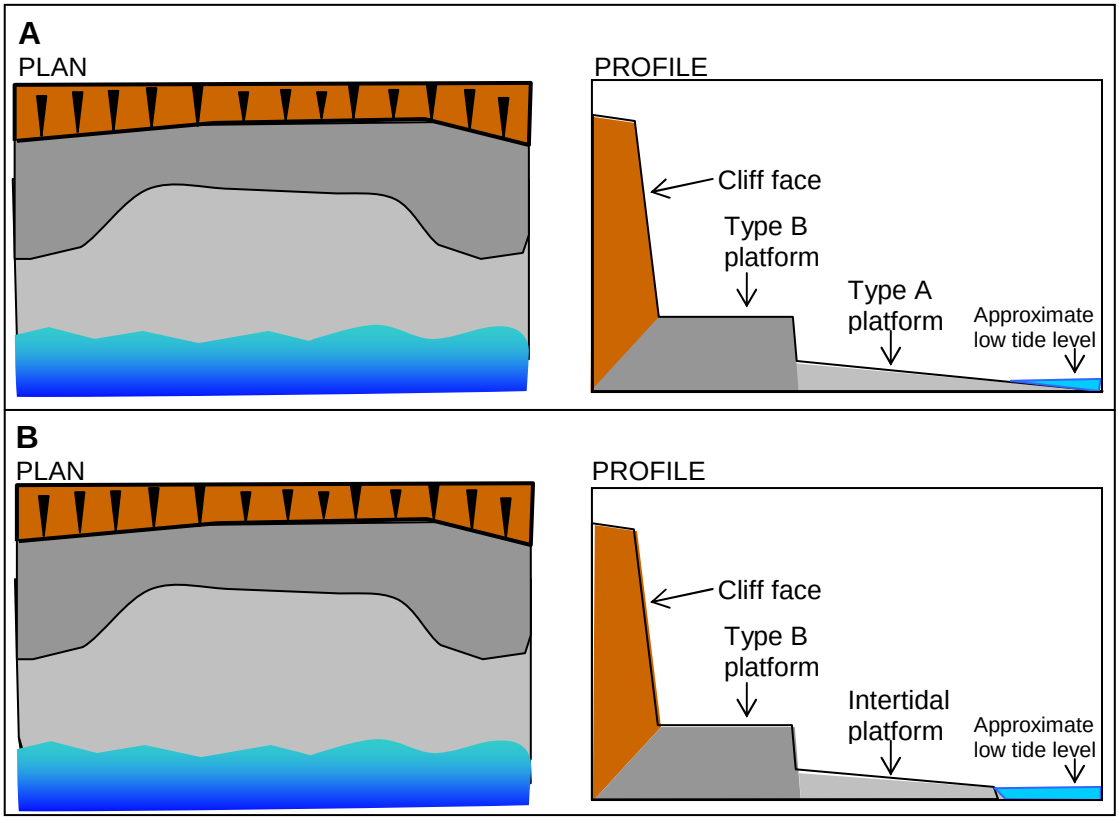

Figure 4.37: Sketch of the plan view and profile view of combined shore platform types observed in the described cliff sites. The solid arrow heads in the plan view indicate the sloping cliff face. **A**: Combination of Type A (no seaward edge) and Type B platforms. **B**: Combination of intertidal (terminates in a seaward edge) and Type B platforms.

There were four sites observed that have similar high, narrow horizontal benches but have lower sloping platforms with no notable seaward edge. At the Waiwera Beach site the majority of the platform has a horizontal profile with a steep seaward edge developed in Parnell Grit rock; low tide was noted to reach just below the seaward edge. Toward the beach the platform became a sloping profile with no defined edge and this appears to be due to either the shallowing of the bay or the loss of the Parnell Grit bed. At Achilles Point, the high horizontal platform has also developed in Parnell Grit rock. At low tide however, the entire bench is exposed and a lower sloping profile can be seen persisting from the base.

At Eastern Beach, higher benches are only prominent on the headland or convex parts of the coastline, similarly to Musick Point. They did appear to be reached at high tide however. The lower sloping platform was very broad and its seaward edge was not found after wading out about 200 m from the coastline. The end of the platform could be seen through the water about 40 m from this point and, with the use of Google Earth satellite maps, the platform's extent was determined. The GPS coordinates were extrapolated to this distance in order to calculate its full width. At Cockle Bay a horizontal, and relatively narrow, bench is observed at the base of the cliff but no lower sloping platform is exposed at low tide. The embayment of Cockle Bay (which is not cliffed) however does exhibit a lower, wide sloping platform with no notable edge. This lower platform may also exist at the base of the horizontal bench at the cliff site but is just not exposed at low, or even spring-low, tides.

The headland areas can be associated with a slightly higher, more prominent and horizontal platform that terminates with a definite edge, while the embayment areas exhibit lower platforms that slope more steeply into the nearshore sea floor to low tide level or beyond. However, at some of these sites the higher platform appears to be relatively narrow, has sporadic occurrence or is significantly above the tidal range and thus suggests that it is not part of the continual erosion and development of the lower sloping platform. The platforms were measured based on the assumption that the platform that is exposed at low tide is the platform in which cliff erosion has been occurring for the past 7120 $\pm$ 70 years.

4.5 Lithology

Following observations made in the field, it was found that the lithology of Waitemata Group beds could be classified into four different types based on the classification system by Gani (2004) which differentiates flow deposits by their rheology during transport and deposition and also their broad grain size (Section 2.4). The four lithological types are sandstone beds from turbidite deposits, sandstone beds from densite deposits, sand to gravel beds of debrites, and siltstone beds.

4.5.1 Sandstone – turbidite deposits

Sandstone beds from turbidite units in Waitemata Group rock are recognized in the field as prominent beds of the cliff section that, most simply, do not contain clasts larger than sand-size (Figure 4.38). The sandstone is commonly light orange-yellow grey and beds range in thickness from thin (20 - 60 mm) to very thick (> 2 m) following the NZGS (2005) classification. Bed thickness varies between sites and within one cliff section. The sandstone beds are the basal portion of a turbidite unit and grade normally into finer grained sands then hemipelagic silt and mud, although the main bulk of the sandstone bed is often massive. The base of the sandstone unit is a sharp boundary (Figure 4.38A). At the majority of sites sandstone blocks are lined with limonite and at three sites had a hard calcite lining. More incoherent and/or weathered sandstone blocks and were covered in dust, and occasionally halite. The sandstone beds are porous (Simpson, 1987). Joints sets predominantly include a sub-horizontal bedding plane plus 2 - 3 sub-vertical joints at various orientations, perpendicular and parallel to the strike of the cliff face. Grain size was noted by de la Mare (1992), who carried out detailed grain analysis on Waitemata Group sandstones, as fine to medium sand and generally well sorted. Simpson (1987) measured that the sandstones contain up to 10 % clay and are non-calcareous. Fizzing from weak hydrochloric acid on joint surfaces at the sites of this research confirms calcite infill rather than calcareous sandstone material.

Figure 4.38: Sandstone beds of turbidite deposits. A: sandstone beds (base marked by arrows) grading upwards into siltstone from the Leigh Marine Reserve cliff site. Note hammer for scale. B: Sandstone bed transitioning from lower massive zone, to mid parallel laminated zone to upper convoluted zone at St Leonard's Beach; boundaries marked by dashed lines; 15 cm pencil length for scale.

4.5.2 Sandstone – densite deposit

Densite deposits (Figure 4.39) are found in Waitemata Group beds (including Castor Bay, Army Bay and Waiwera Beach) whereby the lower part of a flow unit is a relatively thick sandstone that contains rip-up clasts (non-Newtonian flow) that grades into an overlying siltstone counterpart (Newtonian flow). At first glance, these can appear to be turbidite sequences as the sandstone beds may have noticeable upper laminar and convoluted zones associated with the classic Bouma sequence model (Figure 2.7). However, the densite unit cannot be associated with a turbidity current flow because the sandstone bed contains rip-up clasts; the fluid flow of a turbidity current theoretically cannot support large clasts and therefore by definition cannot contain rip-up clasts. Bedding thicknesses are in the upper range of thicknesses observed in turbidite deposits, commonly 0.6 to 2 m and joint spacing tends to be wider with limited block development created by orthogonal joint sets.

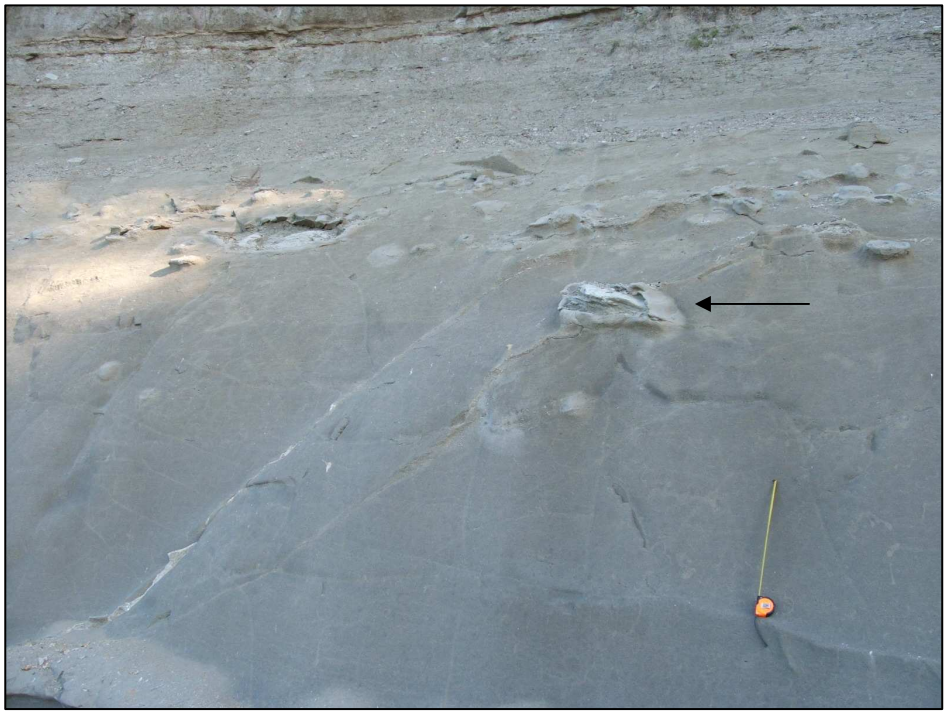

Figure 4.39: Sandstone bed of a densite deposit at Castor Bay. Note siltstone clasts in the mid to upper portions of the bed (marked by an arrow) and lack of joints. Tape measure indicates 80 cm.

4.5.3 Sand to gravel - debrite deposits

Debrite beds are a distinguishable lithology in Waitemata Group coastal cliffs, best represented by the Parnell Grit (Figure 4.40). Debrite deposits observed at the sites are generally thicker beds than the sandstone deposits of turbidites and densites and have irregular joint spacing. They are the result of an entirely non-Newtonian fluid flow which was dense enough to support very large clasts. Parnell Grit beds have been deposited intermittently throughout the Waitemata Group sequence and were observed at Achilles Point, Narrowneck Beach, Army Bay, Waiwera Beach, Opahi Bay and Buckleton Beach. Parnell Grit beds are also located at Eastern Beach, Musick Point and Waiake Bay according to Allen (2004) but were not observed within the vicinity of the described cliff sections for this study. Allen (2004) notes that Parnell Grit beds are up to 20 m in thickness; clasts are mostly 1 - 50 cm in diameter (Ballance, 1974; Allen, 2004) although some observed are many metres across such as at the Waiwera Beach site. The Parnell Grit beds often form prominent headlands and extensions from the cliff face.

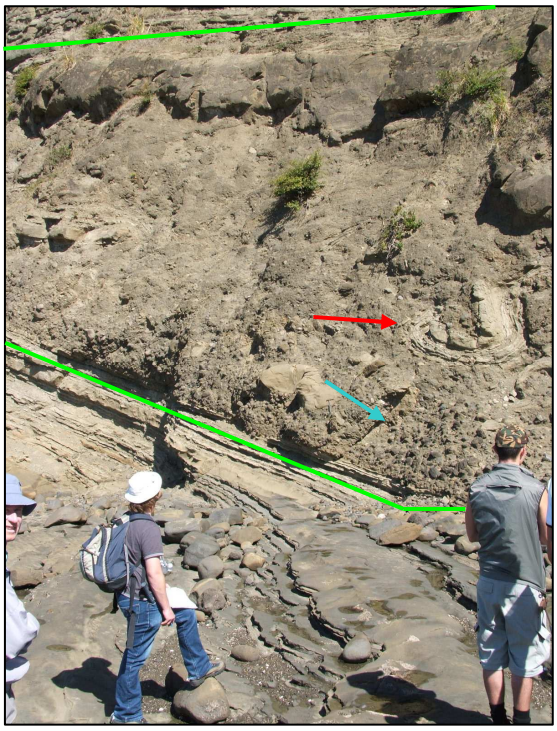

Figure 4.40: Debrite beds of the Parnell Grit at Waiwera Beach, marked by the green line. Debrite beds contain large rip-up clasts (red arrow) and gravel clasts set in a finer grained matrix (blue arrow).

4.5.4 Siltstone

Siltstone beds in Waitemata Group rock are recognized in the field as heavily-frittered, light grey beds which tend to have receded further back than adjacent sandstone beds. Many beds are laminated with total thicknesses from very thin (6 - 20 mm) to moderately thick (0.2 - 0.6 m). The weathered zone of the siltstone beds, resulting from exhumation and stress release, and wetting/drying processes, can extend up to 0.25 m into the cliff face according to Simpson (1987) and this acts to mask the true joint spacing. The siltstone units do have bedding planes (formed during accumulation of deposit) generally with orthogonal joints formed at right angles to the bedding planes (Arnould, 2006). Siltstone joint faces rarely exhibit limonite staining but are commonly covered in dust and grit from weathering.

Siltstone beds exist as either the hemipelagic component of a turbidite or densite deposit (black arrow in Figure 4.41) or as pelagic mud that has settled out of suspension onto the sea floor during quiescent times (green arrow in Figure 4.41). There are no notable differences in the structure of the siltstone beds between these two different sources.

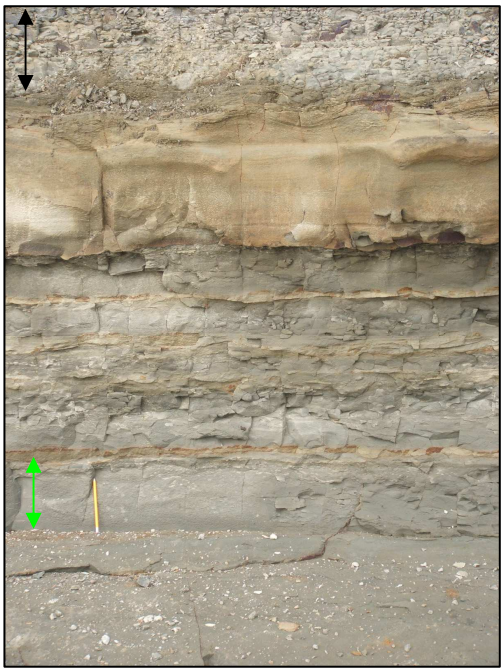

Figure 4.41: Siltstone beds from the Waiake Bay cliff site. Lower deposits (green arrow) are siltstone from hemipelagic deposition between very thin, iron-stained sandstone beds. The upper deposit (black arrow) is siltstone from the last stages of a turbidite overlying the convoluted portion of a sandstone bed. Pencil (15 cm) for scale.

4.6 Summary of Geotechnical Data

A summary of the data for the geotechnical properties of the selected sites using both scanline data (Table 4.3) and description data (Table 4.4) is presented.

Table 4.3: Summary data measured from horizontal and vertical scanline surveys. H = horizontal scanline survey; V = vertical scanline survey; j = joints.

Site		Aperture (mm)	Spacing (m)	Persistence (m j^{-1})	Joint frequency (j m^{-1})
Musick Point	H	1.8 ± 0.4	0.23 ± 0.01	1.29 ± 0.13	4.28 ± 0.04
	V	1.5 ± 0.7	0.25 ± 0.01	3.09 ± 1.39	4.07 ± 0.04
Narrow Neck Beach	H	3.8 ± 0.8	0.11 ± 0.01	0.71 ± 0.06	8.83 ± 0.07
	V	1.2 ± 0.6	0.14 ± 0.002	6.14 ± 1.77	7.33 ± 0.18
Castor Bay	H	0.2 ± 0.03	0.055 ± 0.004	0.41 ± 0.15	18.07 ± 0.13
	V	0.2 ± 0.03	0.034 ± 0.003	2.59 ± 0.46	29.31 ± 0.10
Waiake Bay	H	1.1 ± 0.2	0.14 ± 0.01	0.48 ± 0.03	7.25 ± 0.10
	V	0.1 ± 0.01	0.081 ± 0.002	7.71 ± 1.85	12.28 ± 0.22
Army Bay	H	0.3 ± 0.04	0.039 ± 0.004	0.58 ± 0.13	25.44 ± 0.17
	V	0.2 ± 0.04	0.018 ± 0.001	0.61 ± 0.07	55.41 ± 0.53
Waiwera Beach	H	0.5 ± 0.06	0.094 ± 0.002	1.11 ± 0.12	10.59 ± 0.64
	V	0.1 ± 0.004	0.045 ± 0.001	0.55 ± 0.09	22.31 ± 2.06
Martins Bay	H	3.3 ± 1.1	0.18 ± 0.002	0.56 ± 0.08	5.54 ± 0.38
	V	0.3 ± 0.1	0.091 ± 0.001	6.16 ± 1.68	10.99 ± 0.79
Leigh Marine Reserve	H	0.8 ± 0.2	0.036 ± 0.002	0.84 ± 0.27	27.48 ± 0.72
	V	0.3 ± 0.02	0.015 ± 0.001	0.17 ± 0.02	68.24 ± 2.82

Table 4.4: Properties of cliff rock masses from geotechnical site descriptions (NZGS, 2005; ISRM; 1981). 1. = primary joint; 2. = secondary joint; 3. = tertiary (minor) joint; major joints include primary and secondary joints; ⊥ = perpendicular to cliff face compared to parallel to cliff face.

SANDSTONE

SITE	Colour	Weathering	Grain size	Wall strength	Orientation	Roughness (JRC)	Aperture	Infill	Spacing	Persistence	No. joint sets	Block size and shape	Seepage
Cockle Bay	Light yellowish brown	Slightly	Medium sand	Weak rock		3-5	Could not observe	Could not observe	1-5 m (estimated)	Parallel joints >5 m No perpendicular joints	3	Irregular, some columnar Medium	None evident
Eastern Beach	Light orangey grey	Slightly, moderately in some zones	Medium sand	Very weak to weak rock	1. 74/280, 2. 84//348 3. 10/009	3-5	Tight, up to 15 mm where loosened	Clean	Vertical 1°1 m 2°11 cm Horizontal 22 cm	Parallel joints >1 m Perpendicular joints plus 3rd set 10-30 cm	4	Irregular, columnar or tabular Small	None observed but shows evidence
Musick Point	Light yellowish brown	Slightly	Coarse sand, gravel clasts	Weak rock		Could not measure	Tight, up to 10 mm	Clean or clay, some had Fe lining of variable thickness	10 cm to 2 m	Most 1-3 m Major joints persisted up to 10 m	3 + random	Presumed to be columnar Medium	Yes after rainfall plus shows evidence
Achilles Point	Light orangey grey	Slightly	Fine to medium sand	Weak rock		Could not measure, rough & undulating	Tight to 0.5 mm, up to >1 cm where loosened	Clean	20-60 cm Areas of 10 cm	<1 m	3 + random	Irregular and tabular Medium	None observed but shows evidence
Narrowneck Beach	Light yellowish grey	Slightly	Fine to medium sand	Weak rock		12-14	0.5-2.5 mm, up to 15 mm where loosened	Clean or grit, all Fe lined	Vertical 15-45 cm Minor joints 4-12 cm	Major joints ≥1 m through to siltstone Others only persist bed thickness	3 +random	Columnar to blocky Medium	None observed but shows evidence
St Leonard's Beach	Light orangey grey	Slightly	Medium sand	Weak rock		Could not measure, rough & undulating	Tight to 0.5 mm, >1 cm where loosened	Clean	Perpendicular ~20 cm	Perpendicular <1m up to bed thickness Parallel may be > 1m	3	Blocky, some columnar Medium	None observed but shows evidence
Castor Bay	Light yellow grey to light orange brown	Slightly	Medium to coarse sand	Weak rock	1. 74/132 2. 70/284 Bed 26/006	8-10	Tight to 1 mm	Calcite in debrite, clay & Fe in turbidite	1. 15-65 cm 2. 45-85 cm Bed 2-5 cm	Major joints ~1 m Debrites have different joint sets >1 m	4 + random	Irregular, some equidimensional or tabular Small to medium	Yes, dripping flow
Mairangi Bay	Dark grey to dark brownish red	Slightly	Fine to medium sand, some coarse sand	Weak rock		Could not measure, rough & undulating	<0.5 mm, up to 1 cm where loosened	Loosened blocks are partially opened & have clay	Mostly <20cm, up to 60 cm	Perpendicular <1 m Parallel joints up to 3 m	3	Blocky, some irregular Small to medium	Damp, some have very low pressure continuous flow
Waiake Bay	Light yellowish/ orangey brown	Slightly	Medium sand	Weak rock		Joint 8-10 Bed 18-20	0.3-10 mm, very few tight	Fe stained and clean	20-60 cm Random joints result in <20 cm spacing	Vertical joints >1 m	3 + random	Blocky Medium	None observed but shows evidence
Army Bay	Light orangey brown	Slightly	Fine to medium sand	Weak to medium weak rock	⊥ 84/183 Parallel 76/248 Bed 25/073	⊥ 16-18 Parallel 6-8	Tight, up to 5 mm where loosened	Calcite, loosened blocks are clean	⊥ 5-20 cm Parallel 5-25 cm Beds and fractures 4-14 cm	⊥ joints >1 m Parallel joints <1 m Beds persist 3-10 m but stopped by faults	4+	Irregular, tabular or columnar Small, some very small	Dry with evidence of seepage, some have low pressure flow
Waiwera Beach	Light orangey brown	Slightly	Medium to coarse sand	Weak rock	Bed 07/186	4-6	Tight, up to 4 mm where loosened	Clean and calcite	30-60 cm	Most 30-60 cm Some persist through to other beds >1 m	3	Irregular, some tabular or blocky Medium	None evident
Opahi Bay	Light greyish brown	Slightly	Medium sand	Weak to medium weak rock		4-6	Tight to 1 mm, up to 15 mm where loosened	Clay in most joints	1°0.8-1.4 m 2°10-20 cm 3°~3 cm	Up to 10 m	3 + random	Irregular, some columnar Medium	None observed but shows evidence
Martins Bay	Light brownish grey	Slightly	Medium sand	Weak rock	1. 89/005 2. 76/073	⊥ 14-16 Parallel 3-5	Tight to 2.5 mm Clay infills ~1 mm of many joints	Clay	1. 1-2 m 2. 10-50 cm	1. limited to bed thickness ~60-80 cm 2. persist through to other beds >3 m	3	Tabular Medium	Dry, evidence of seepage, high pressure flow observed after a storm event
Buckleton Beach	Light yellowish grey	Slightly	Fine to medium sand	Weak to medium weak rock		8-10	Tight to 0.5, up to 1.5 mm where loosened	Clean, clay in loosened joints	3-10 cm	Vertical >1 m but maximum of bed thickness Beds >20 m if not stopped by vertical joints	3	Columnar or tabular Very small to small	None observed but shows evidence
Matheson Bay	Light yellowish/ orangey brown	Slightly	Medium to coarse sand	Weak rock	1. 83/343 2. 80/084 3. 06/124	10-12	2-3 mm	Calcite, silt and gouge in some	20-30 cm	Vertical joints persist only to bed thickness Major joints/faults >2 m. Beds >20 m if not faulted	3 + random	Irregular to blocky, few massive Medium	None observed but shows evidence, low pressure flow at base of sandstone beds
Leigh Marine Reserve	Dark orangey brown to grey	Slightly	Medium sand	Weak to medium weak rock		6-8	0.5 mm	Clean, some grit, major joints have calcite	Major joints 4-9 cm, horizontal 2-7 cm	Vertical at least bed thickness ~65 cm Major joints >2 m Horizontal 2-50 cm	4+	Irregular Small	Dry to damp, dripping observed in some zones

SILTSTONE

SITE	Colour	Weathering	Grain size	Wall strength	Orientation	Roughness	Aperture	Infill	Spacing	Persistence	No. joint sets	Block size and shape	Seepage
Cockle Bay	Light creamy grey	Slightly, moderately in some zones	Silt	Very weak rock		Could not measure, smooth	Tight	None	Vertical 4-8 cm Horizontal 1-2 cm	Persist bed thickness Vertical ~15 cm Horizontal ~4-8 cm	3 + random	Irregular to columnar Small - very small	None evident
Eastern Beach	Light yellowish grey	Slightly to moderately	Silt	Very weak to weak rock	Parallel 75/168 ⊥ 82/090	4-6	Mostly tight, up to 1 mm	None	Vertical 2-5 cm Horizontal <2 cm	Vertical persist to bed thickness <0.5 m Horizontal bound by vertical Few major joints >1 m	3 + random	Irregular, columnar or tabular Very small	None observed but shows evidence
Musick Point	Light orangey grey	Slightly	Silt	Weak rock	⊥ 87/091 Beds 10/277	Could not measure	Tight, some up to 0.5 mm	Clean or clay, major joints Fe lined	Vertical 1-3 cm + small fractures Horizontal fractures 2 cm	Only persist bed thickness Major joints pass through siltstone beds	3 + random, some 4	Crushed Very small	Yes after rainfall plus shows evidence
Achilles Point	Light yellowish grey	Slightly	Silt	Very weak rock		Could not measure, rough & undulating	Tight to 1 mm, a few up to 3 mm	Clean	Vertical 2-6 cm Horizontal <1 cm	< 5 cm Joints that pass into siltstone are <1 m	3 + random, some 4	Tabular to crushed Very small	None observed but fresh rock is damp
Narrowneck Beach	Light grey	Slightly	Silt	Weak rock	Semi-vertical 86/266 & 63/356, semi-horizontal 04/200	3-5 (vertical) 9-11 (horizontal)	Semi-vertical up to 1 mm Minor joints 0.2 mm	Fe lined & clean, some major joints have clay	1°1 m 2°10-50 cm 3°~1 cm	1°and 2° 2-4 m (poor visibility) 3°1-2 cm	Major 3 Minor 4	Irregular blocky or tabular Very small	None observed but shows evidence
St Leonard's Beach	Light yellowish grey	Slightly	Silt	Very weak rock		Could not measure, smooth & undulating	Tight to 0.5 mm, up to 2 mm where loosened	Clean	Vertical ~2 cm up to 6 cm Laminations ~0.8 mm	Persist bed thickness, <0.5 m	4+ or crushed	Irregular to crushed Very small	None observed but shows small evidence
Castor Bay	Light grey to light yellow grey	Slightly	Silt	Very weak rock	One joint set is 62/025	7-9	Tight, some loosened, major joints up to 1 mm	Clay and Fe	1°35-50 cm 2°6-12 cm, 3°1-2.5 cm	1°>1 m Other joints up to 20 cm	3 + random	Irregular Very small	Yes, dripping flow
Mairangi Bay	Light yellowish grey	Slightly	Silt	Very weak rock		Could not measure, slightly rough & undulating	Tight – 2.5 mm	Clean, some have silt	2-6 cm	Vertical <30 cm Horizontal <1 m	4+	Irregular Very small	Dry to damp, some joints have low pressure flow
Waiake Bay	Light grey	Slightly	Silt	Very weak to weak rock		Could not measure	Tight to 10 mm	Clean	<2 mm where highly frittered Lower beds up to 30 cm	1°>1 m Other joints <1 m	4+	Irregular Small	None observed but shows evidence
Army Bay	Light yellowish grey	Slightly to moderately	Silt	Weak to medium weak rock	1. 78/011 2. 80/127 3. 32/229	12-14	Tight, up to 10 mm where loosened	Fe lined but clean	Horizontal 1-4 cm	Vertical <1m Major joints persist through to sandstone >1 m	3 + random	Irregular Very small	None observed but shows evidence
Waiwera Beach	Light greyish brown	Slightly	Silt	Weak rock		2-4	Tight to 2 mm	Clean, salt in open joints	0.7-7 cm	1°>1 m 2° ~40 cm 3°1-2 cm	3	Tabular Very small	None evident
Opahi Bay	Light grey	Slightly	Silt	Very weak rock		10-12	Tight to 1 mm	Clean	Vertical 5-10 cm Horizontal <0.3 cm	Persist only thickness of bed <10 cm	3 + random	Irregular and tabular Very small	None evident
Martins Bay	Light grey	Slightly	Silt	Weak to medium weak rock	Major joints 76/073	2-4	Tight to 0.5 mm, up to 5 mm where loosened	Clean	Vertical 4-20 cm Horizontal 1-3 cm	Major joints >3 m Other vertical 10-20 cm Horizontal >1 m	3 + random	Irregular and tabular Very small - small	Dry, high pressure flow observed after a storm event
Buckleton Beach	Light yellowish grey	Slightly	Silt	Weak to medium weak rock	Vertical 84/214 Beds 09/310	Could not measure	Tight	Clean	Vertical 0.5-2 cm Horizontal laminations 0.2 cm	Vertical persist bed thickness 5-10 cm Horizontal persist along entire bed	3 + random	Irregular to tabular Very small	None evident
Matheson Bay	Light brownish grey	Slightly, moderately in some zones	Silt	Medium weak rock		2-3	Tight to 0.5 mm	Calcite ≤2 mm, clean where joints open >2 mm	Vertical 0.5-1 cm Horizontal 2 cm	Major joints up to 1 m Minor joints ~30 cm	4 + random	Tabular, some irregular Very small	Yes, low pressure flow at sandstone/ siltstone boundary
Leigh Marine Reserve	Light yellowish grey	Slightly to moderately	Silt	Very weak to weak rock	Major vertical 87/281, minor vertical 76/254	7-9	Tight to 0.5 mm, up to 2 mm at surface	Clean, major joints have calcite	Vertical 1-3 cm Major joints 20-30 cm Beds 0.4-1 cm	Major joints >2 m Vertical joints up to bed thickness Beds >2-3 m	3 + random	Irregular Very small	Dry to damp, dripping observed in some zones

4.6.1 Weathering, strength, and grain size

Weathering of the cliff face varies between slightly weathered and moderately weathered. Frittering and iron staining of joint surfaces indicate slight weathering; zones of siltstone that have weathered to soil-like material, and scrub growing in small talus piles that have accumulated on the cliff face, are evidence of more advanced (moderate) weathering.

Wall strength, assessed in the field, is predominantly weak in sandstone and very weak in siltstone. Schmidt hammer rebound values of the intact rock wall strength show a general increasing trend toward the north, with East Coast Bays Formation rock ranging from 11-27 and Pakiri Formation rock ranging from 20-41 (Figure 4.42). Siltstone rebound values are higher than sandstone values for each site and overall ranged from 17-41, still maintaining a general increasing trend northwards. The highest measured values for sandstone and siltstone, at Matheson Bay and Leigh Marine Reserve respectively, are sites where the basal contact of the Waitemata Group is exposed. Simpson (1987) found higher rebound values in siltstone compared to thin sandstone beds. Brodnax (1991) also noted that the siltstones usually have greater compressive strengths than the sandstones.

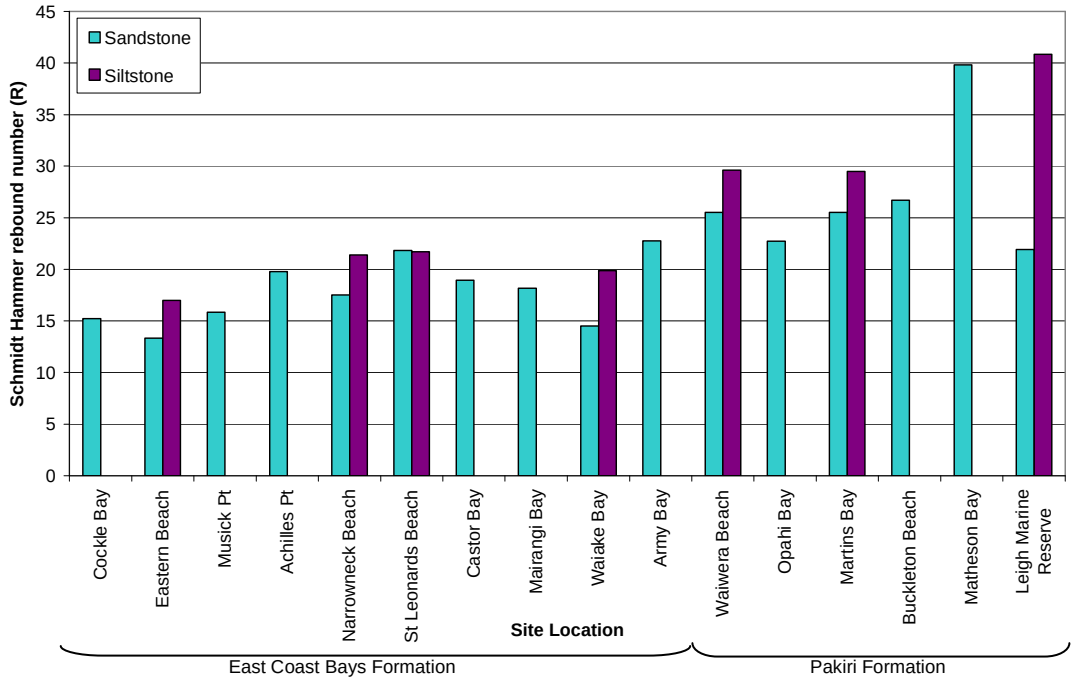

Figure 4.42: Wall strength of sandstone and siltstone measured by 'N' type Schmidt hammer.

Grain size was not directly measured for this research, however data have been sourced from de la Mare (1992) through particle size analysis on sandstone beds from five different sites across the Waitemata Group (East Coast Bays to Cape Rodney). The results indicate that the sandstones are dominated by sand sized grains 49.9-76.5 % and all have a low clay fraction ranging from 5.7-9.4 %. Silt-size grains are also prominent in the sandstones with sandstone from Tipau Point (between Waiake Bay and Browns Bay) having 49.9 % sand and 43.5 % silt (classified as a sandy silt), and all others having 18-26 % silt (classified as silty sands). Siltstones analysed by Simpson (1987) vary from muddy silt to sandy silt; no data is available for sand-silt-clay ratios in siltstone rock of the Waitemata Group. For this study, a range of grain sizes were observed within the same lithology, particularly in some sandstone beds where sand grains graded upward from coarse to fine. The Buckleton Beach cliff section displayed the effects of dynamic changes within a gravity flow event with repeated normal-graded banding of one thickly-bedded deposit.

4.6.2 Discontinuities

The various properties of the discontinuities in Waitemata Group rock are summarised in this section and presented in Table 4.4. For easy distinction between the various joint sets in one cliff section the discontinuities are classified in terms of their persistence through the cliff section. Primary (1^o) joints persist through the entire cliff section, including bedding planes and faults, and are the most widely spaced. Secondary joints (2^o) persist between bedding planes and may extend partially into the bed above or below it; these joints are less widely spaced than primary discontinuities. Minor tertiary joints (3^o) then exist between the secondary joints and make up the framework for the block size of the beds of sandstone or siltstone.

4.6.2.1 Roughness

Across all the sites, the Joint Roughness Coefficient (JRC) ranged the full scale, from 1-20. The majority of joints had JRC values between 4 and 12 with siltstone joints having a broadly lower JRC compared to the rougher sandstone.

4.6.2.2 Aperture and Infill

The average site values of aperture measured from scanline surveys ranges from 0.1 mm to 3.8 mm. The measured aperture values from site descriptions are mostly tight (0.1 mm) to 1 mm, but aperture becomes much larger when blocks were loosened from the cliff face. Such apertures are as large as 15 mm.

Infill varieties include: soft clay; soft fault gouge which looks similar to the clay infill but is found in faulted discontinuities; grit which tends to be a coarser grained, often loose, sediment and is thought to have been sourced from the surrounding cliffs and washed or blown into the discontinuity; hard iron is present in many discontinuities as a thin lining but on occasion forms a thick crust that fills in all or some of the aperture; and a hard calcite infill that is exhibited at a few sites and either entirely fills the discontinuity or now only partly fills open discontinuities. An aperture that is classified as tight, which means it is less than 0.1 mm wide is assumed to have no infill.

4.6.2.3 Spacing and persistence

The average site values of discontinuity spacing measured from scanline surveys is 0.015 m to 0.25 m. Spacing values measured at site descriptions have a wider range from < 0.005 m to 5 m. Minimum spacing is < 5 mm for siltstone beds and 20 mm for sandstone beds. Maximum spacing is in the order of tens of centimetres to a few metres in siltstone for primary and secondary joints that persist through the siltstone to upper and lower beds. Sandstone beds have a maximum spacing of about 5 m observed in thick, durable debrite beds.

The average site values of persistence measured from scanline surveys is from 0.17 m to 7.71 m. Persistence values measured at site descriptions range from 0.02 m to > 1 m for joints and > 20 m for bedding planes. In siltstone beds tertiary joints persist only a few to 300 mm and primary and secondary joints may persist decimetres to several metres. In sandstone beds tertiary joints persist up to 100 mm between parallel joints (commonly bedding planes) but the majority of joints have a persistence of decimetres to commonly over a metre. Bedding planes can persist > 20 m where other joints do not dissect them.

4.6.2.4 Joint sets, block size and shape

All sites have a minimum of 3 joint sets with many sites having clearly defined joint sets plus random fractures, or messy joint sets that were hard to differentiate.

Irregular block shape became the default group during site descriptions due to the wide range of shapes observed within one cliff section. This is particularly the case when there is a range of different bed thicknesses. Vertical joint sets often remain regular but the bed thickness provides a variable horizontal joint set and can produce columnar through to blocky through to tabular shapes. Tabular, columnar and blocky shapes are however, the most common shape at some sites such as Narrowneck Beach and Martins Bay, while equidimensional shapes were only observed in Castor Bay. Where siltstone beds are heavily frittered they were classified as having an irregular shape. Siltstones that have a discernable block shape were classified as crushed and tend to be at the sites that display moderate weathering. Only where joint sets are well preserved and the face of the bed is smooth could the true persistent block shape be determined.

Sandstone blocks are overall larger than siltstone blocks; the majority of siltstone blocks are very small. Sandstone blocks are predominantly medium-size with particular beds (differing in thickness, proportion of grain sizes or mineralogy) allowing for much larger or very small blocks.

4.6.2.5 Groundwater

Because field work was done during the drier summer months, initially seepage was not observed from many of the sites. Following rainfall periods, seepage was observed in seven of the sites and flow varied from non-continuous dripping to continuous reasonably-high pressure flow. These sites include Musick Point, Castor Bay, Mairangi Bay, Army Bay, Martins Bay, Matheson Bay and Leigh Marine Reserve. The majority of the sites however showed evidence of seepage through iron staining in the discontinuities and the observation of damp discontinuities. Darker, purple limonite staining showed where discontinuities had remained wet for a long period of time. Seepage was commonly seen to exit the cliff face at the base of sandstone beds or at the base of sandstone discontinuities rather than in the siltstone bed.

4.7 Summary

- Sixteen sites were selected on the basis of lithological and geographic spread, good cliff exposure and safety to best represent all Waitemata Group rock.
- Cliff heights ranged from 8 to 38 m; cliff angles range from 51 to 79^{o} and differ based on sandstone prominence; bed dips are both landward into the cliff face and seaward out of the cliff face; shore platforms are classified into four different morphologies based on horizontal and/or sloping profiles.
- Sandstone and siltstone beds were observed to be the result of turbidity currents; densite beds were noted where rip-up clasts were observed in the middle of sandstone beds; debrites were notably the Parnell Grit units.
- Cliff rock is slightly weathered with weak intact rock strength; siltstone surfaces are generally smoother than sandstone; apertures are less than 15 mm; infill types were soft clays and grit, and hard calcite and iron; spacing of discontinuities were smaller in siltstone beds with tertiary joints spaced as close as 5 mm, and primary joints in sandstone, densite and debrite beds were spaced up to 5 m; persistence of primary joints were tens of meters and minor joints persisted as little as 20 mm and were overall smaller in siltstone beds; siltstone has a very small block size and sandstone can have very small to large blocks; seepage was observed at many sites particularly at the base of sandstone beds.

CHAPTER FIVE

LABORATORY RESULTS, DERIVED PROPERTIES and GIS-SOURCED PARAMETERS

5.1 Introduction

This chapter firstly presents laboratory results measured from rock samples collected in the field, including intact rock strength, bulk density, porosity and slake durability (Section 5.2). Additional properties that have been derived from the both field and laboratory data are then presented in Sections 5.3 to 5.7, including: failure modes of the coastal cliffs determined from stereographic projection; rock mass classifications for five different classification systems; rock mass strength properties; a classification scheme for determining the proportion of sandstone to siltstone in a cliff section; and shore platform width measurements which long term erosion rates have been calculated from. Section 5.8 presents a range of GIS-sourced parameters for the selected cliff sites, and the methodology used to gain these.

5.2 Intact Rock Properties

5.2.1 Intact rock property results

Samples of sandstone and siltstone from each of the site locations were used to test the intact rock properties of Waitemata Group rock. Intact rock properties apply to individual blocks within the cliff face and give an indication of the behaviour of the rock material without the influence of discontinuities, which weaken rock strength. The intact rock strength parameters are also required for application in some of the rock mass classification systems. Intact rock strength was measured using an NCB Cone Indenter

and the Point Load Strength test for siltstone and sandstone respectively. Bulk density and porosity of the sandstone was determined using a saturation technique, and durability of the sandstones was tested using the modified jar slake test. A summary of the results for these parameters is presented in Table 5.1; original data are presented in Appendix Three.

Table 5.1: Intact rock properties of Waitemata Group rock including: siltstone and sandstone intact strength measurements; air dry bulk density, oven dry bulk density and porosity of sandstone; and the range of modified jar slake values recorded at each site. SST = sandstone. UCS = uniaxial compressive strength. BD = bulk density. Ij': 1 is durable, 8 is non-durable, full classification is in section 3.3.3. Error is 1 standard error.

SITE LOCATION	Siltstone UCS (MPa)	Sandstone UCS (MPa)	SST Air dry BD (kg m^{-3})	SST Oven dry BD (kg m^{-3})	SST Porosity (%)	Jar slake value range (Ij')
Cockle Bay	6.40 ± 0.28	19.86 ± 6.16	1875.1 ± 72.3	1762.4 ± 29.4	43.3 ± 4.1	2-8
Eastern Beach	5.46 ± 0.23	6.84 ± 0.51	1677.3 ± 12.2	1650.0 ± 22.5	41.5 ± 1.0	2-6
Musick Point	6.79 ± 0.21	12.87 ± 0.99	1757.8 ± 32.0	1679.6 ± 66.0	42.6 ± 4.7	2-6
Achilles Point	5.52 ± 0.20	23.87 ± 4.40	2108.8 ± 53.5	2061.2 ± 48.2	33.0 ± 3.4	1-7
Narrowneck Beach	5.09 ± 0.30	21.74 ± 0.51	1818.9 ± 18.2	1758.3 ± 19.6	39.2 ± 2.7	1-3
St Leonard's Beach	7.34 ± 0.21	24.99 ± 5.28	2014.7 ± 55.1	1962.3 ± 55.5	29.3 ± 2.1	1-3i
Castor Bay	8.13 ± 0.48	32.37 ± 2.86	2177.1 ± 101.7	2096.8 ± 102.8	37.9 ± 1.3	1-3
Mairangi Bay	7.03 ± 0.15	11.11 ± 1.32	1915.3 ± 15.5	1834.1 ± 52.2	31.4 ± 0.1	1-8
Waiake Bay	6.47 ± 0.25	11.44 ± 1.98	1841.1 ± 25.2	1782.6 ± 22.2	35.9 ± 0.7	2
Army Bay	10.29 ± 0.45	31.07 ± 3.52	2081.8 ± 18.3	2012.7 ± 19.4	29.7 ± 1.0	2-3
Waiwera Beach	10.25 ± 0.38	41.30 ± 5.28	2237.4 ± 22.6	2172.6 ± 21.4	16.1 ± 1.0	1-2
Opahi Bay	7.04 ± 0.54	38.28 ± 4.84	2190.2 ± 30.5	2131.4 ± 31.1	25.8 ± 0.9	1-3i
Martins Bay	10.69 ± 0.36	25.52 ± 2.20	2195.5 ± 28.5	2133.9 ± 28.0	28.4 ± 0.7	1-4
Buckleton Beach	9.50 ± 0.48	57.34 ± 5.50	2304.1 ± 95.9	2236.5 ± 89.8	17.9 ± 1.0	1
Matheson Bay	13.01 ± 1.14	98.94 ± 14.08	2445.1 ± 58.2	2375.4 ± 55.9	12.1 ± 0.6	1
Leigh Marine Reserve	12.64 ± 0.83	79.02 ± 14.08	2351.4 ± 18.5	2280.4 ± 18.8	13.5 ± 0.4	1

5.2.2 Intact rock strength

Siltstone intact rock strength is weak (NZGS, 2005) with a UCS of 5 ± 0.3 to 13 ± 1.1 MPa and sandstone intact rock strength is weak to strong (NZGS, 2005) with UCS values ranging from 7 ± 0.5 to 99 ± 14.1 MPa (Figure 5.1). Sandstone has a considerably larger strength range than siltstone material, but the data show a similar general trend to the siltstone of increasing intact strength northwards.

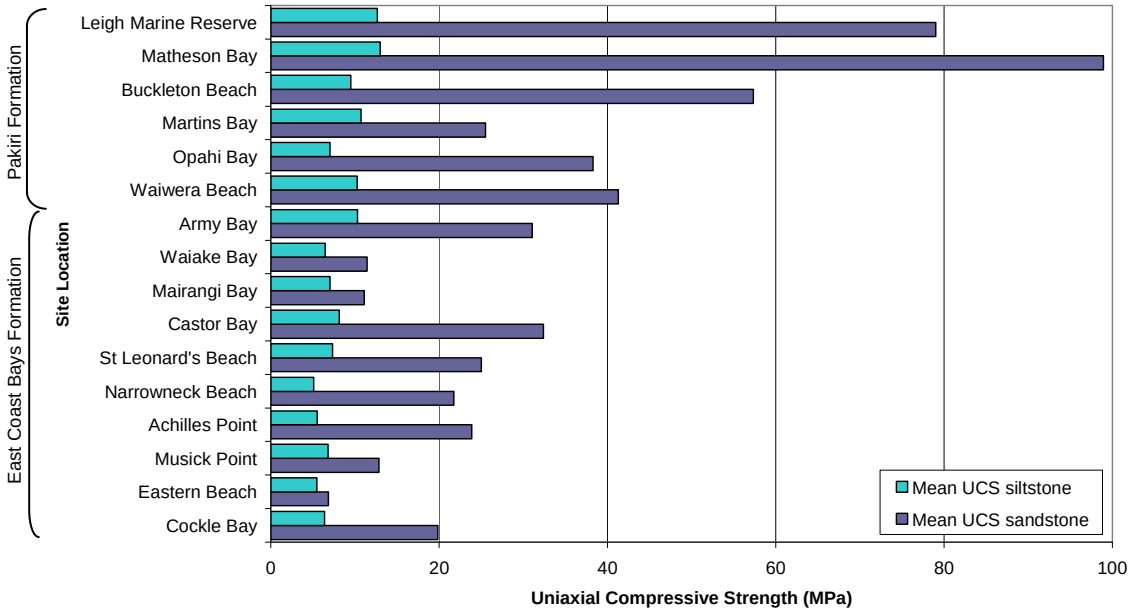

Figure 5.1: Mean siltstone and sandstone intact rock strength for Waitemata Group rock for southern (Cockle Bay) to northern (Leigh Marine Reserve) sites.

Schmidt Hammer strength results that were measured on *in situ* intact rock showed less variation between sandstone and siltstone intact strength measured in the laboratory, and moreover, produced higher strength values for siltstone than sandstone (refer to Figure 4.42).

5.2.3 Bulk density and porosity

Bulk density and porosity was tested for sandstone samples under both air-dried and oven-dried conditions. Siltstone bulk density and porosity values were sourced from New Zealand literature as the heavily frittered samples could not be measured efficiently following similar methods. Oven-dried bulk density ranged from 1650 ± 23 to 2375 ± 56 kg m^{-3}, and air-dried bulk density ranged from 1677 ± 12 to 2445 ± 58 kg m^{-3} due to the inability (under air-dry conditions) of the remaining moisture to be lost from the micropores of the rock (Figure 5.2). The oven-dried bulk density values for sandstone are all lower than the air-dried bulk densities by 27-114 kg m^{-3}. Siltstone bulk density is lower than sandstone, ranging from 1260 to 1850 kg m^{-3} according to typical soil and rock properties collated by Selby (1993).

The porosity of the sandstone ranges from 12 ± 1 % to 43 ± 5 % porosity. The published porosity values of siltstone rock is slightly greater than measured sandstone values, ranging from 29 to 52 % (Selby, 1993). Bulk density and porosity, of sandstone rock, both show a northwards trend whereby bulk density generally increased northwards and porosity generally decreased northwards (Figure 5.2). Porosity is on the whole the reciprocal of density and correlation is the highest when rocks have similar grain densities (ISRM, 1981). The intact rock strength of the sandstone followed a similar trend to the measured bulk density values, as is expected according to Selby (1993).

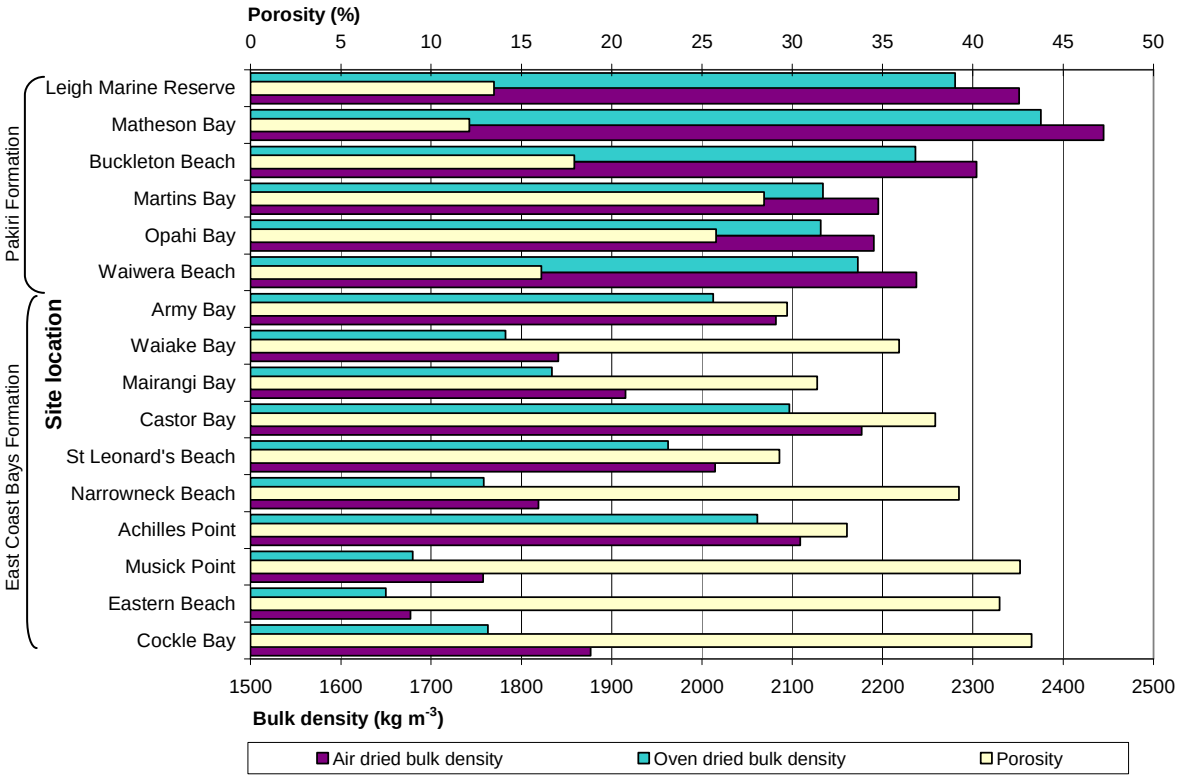

Figure 5.2: Graph of mean air-dried and oven-dried bulk density and porosity values for Waitemata Group sandstone. Note the decreasing porosity and increasing bulk density northwards.

5.2.4 Slake durability

Durability assesses the resistance of a rock to short-term weathering processes such as wetting and drying, and stress release (ISRM, 1981). During the saturation of sandstone samples for bulk density and porosity testing, slaking was observed in a number of

blocks from a range of sites. As a consequence of this, the durability of the sandstone at some of the sites were tested using the modified jar slake index test (Czerewko and Cripps, 2001) to see if there were any trends in the slaking behaviour and to quantify the rate of slaking. The sites tested were Cockle Bay, Eastern Beach, Musick Point, and Mairangi Bay. For the four tested sites, samples that showed no change in slaking behaviour at the 24 hour period were all tested for a further 24 hours from which no samples showed further slaking during this period. For the remaining sites, the final durability value was recorded (as an approximate measure) when the samples were removed from the saturation bath, which was after a period of approximately 24 hours.

Siltstone rock samples were too frittered to test durability but previous research by Simpson (1987) indicates that the smectite and illite clays found in Waitemata Group siltstone beds shrink and swell upon wetting and subsequent drying action and are therefore prone to low durability. In Tertiary Waikato Coal Measure mudstones measured by Beattie (1990) the durability was very low to medium high (from the slake durability test of Brown, 1981). Beattie (1990) observed three different mechanisms for disintegration of the mudrocks in a visual slake test of the same samples. The results of both tests show broadly that durability increases as the percentage of < 2 μm size particles decreases.

Figure 5.3 illustrates the final jar slake values recorded for all samples tested from each site. All of the Pakiri Formation sites displayed extreme durability (Ij' value of 1-3i) with the three most northern sites (Buckleton Beach, Matheson Bay, Leigh Marine Reserve) showing no visible sign of deterioration at all (Ij' value of 1). East Coast Bays Formation sites including Narrowneck Beach, St Leonard's Beach, Castor Bay, Waiake Bay and Army Bay also exhibit extremely durable sandstone. The sites which had samples that were non-durable included Cockle Bay, Eastern Beach, Musick Point, Achilles Point (the four most southern sites) and Mairangi Bay. All sites that had some samples which had durable properties (Ij' value of 4 to 5i) also had samples which were non-durable. Figure 5.4 illustrates all of the stages of durability for the modified jar slake index test.

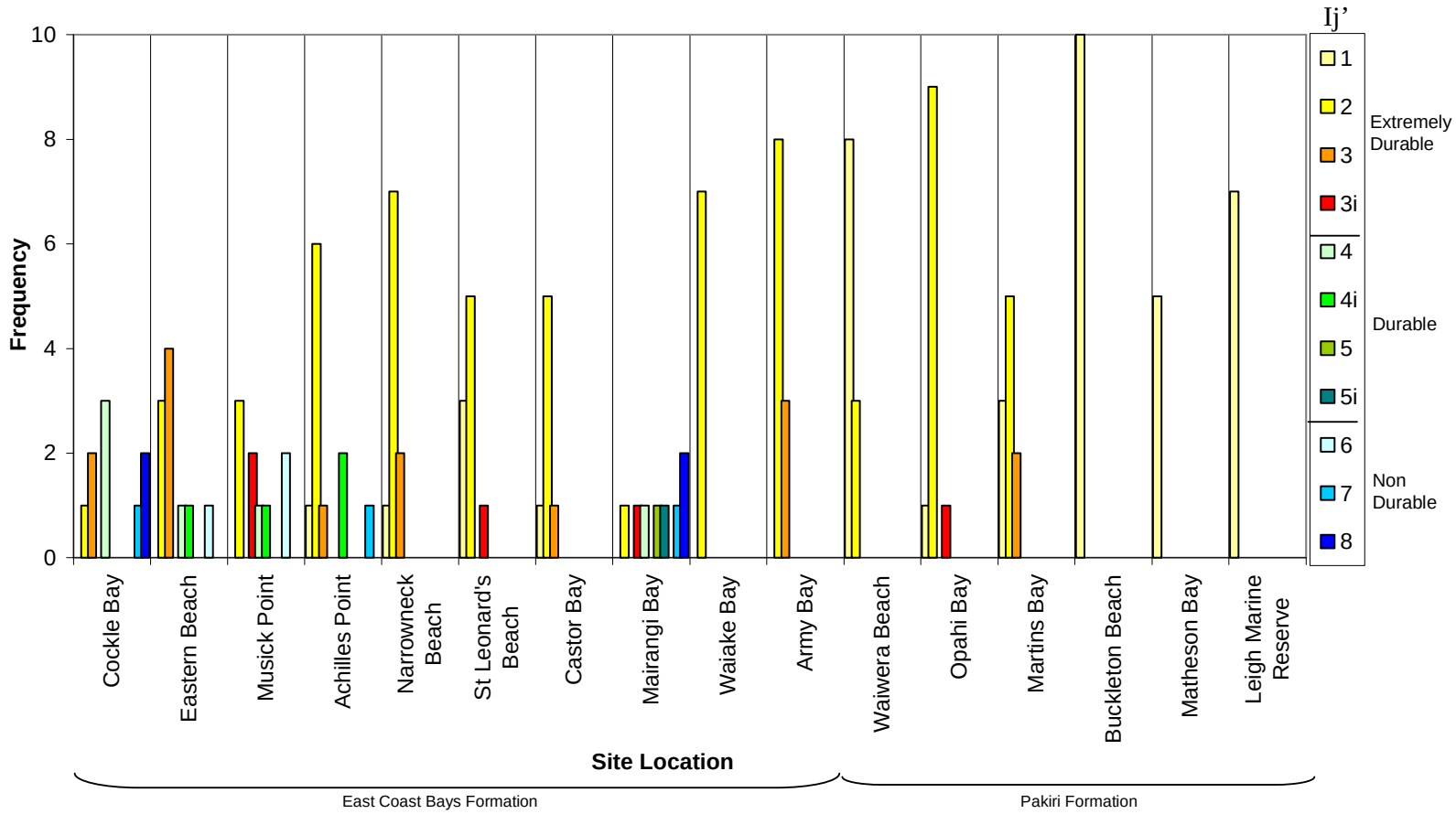

Figure 5.3: Modified Jar Slake test results for the described site locations. 1-3i are extremely durable (white through to red); 4-5i are durable (green); 6-8 are non durable (blue).

Interestingly, some samples in this study flaked, but others were durable at the same site. This is possibly because of the degree of weathering of individual samples or because the samples were chosen from different beds.

Slake durability of coarse-grained Waitemata Group rocks was found to range from low to very high by de la Mare (1992) and he recognised that the variation in durability can be due to the different mechanisms of wetting and drying or mechanical abrasion. A subsequent wetting and drying experiment, by de la Mare, of the samples revealed that sandstone sourced from Cape Rodney (within the vicinity of Leigh, north Auckland) disintegrates through mechanical abrasion as it did not fail at all when repeatedly wetted and dried. Comparatively, wetting and drying is sufficient to almost totally disintegrate sandstone from Waiake Bay, without any mechanical abrasion. The sandstone samples all had similar percentages of the < 2 μm grainsize fraction and so variation in durability was suggested to be from the type of material and the mineralogical fabric rather than proportions of grainsize. Simpson (1987) stated that it is the destruction of clay bridges that causes the general failure in sandstone. The modified jar slake test used in this study assessed the durability of sandstone when saturated, without mechanical abrasion or repeated wetting and drying; grainsize and microfabric analysis would contribute to understanding the variation in durability between the samples.

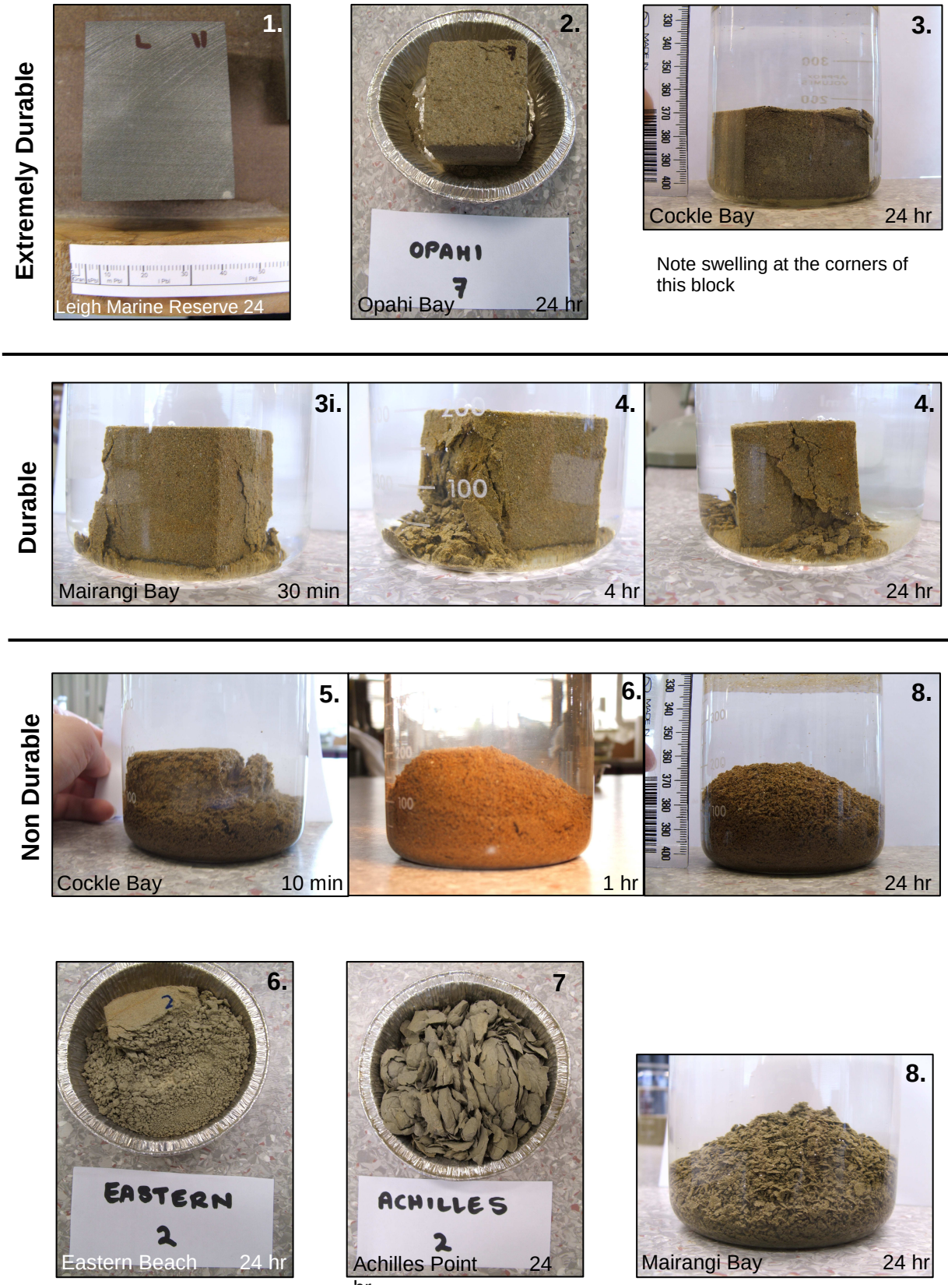

Figure 5.4: Various stages of the modified jar slake test. The Ij' value is written at the top right corner of each photograph.

5.3 Failure Mode

The results of kinematic analysis using stereonets constructed from scanline data are described on a site by site basis. The relation of this analysis to the mechanisms of failure in Waitemata Group rocks outlined by Moon and Healy (1994) and field observations is then discussed.

5.3.1 Kinematic analysis

Table 5.2 presents and interprets stereonets from each of the eight scanline sites. Stereographic projections can determine planar, wedge, toppling or circular failures with respect to the cliff face. However, they cannot be used to determine the susceptibility of the cliff face to rock fall (Wyllie and Mah, 2004) which is a prominent mechanism of failure in the bedded Waitemata Group rock. Refer to Appendix Four for complete stereonet graphics.

Table 5.2: Results of kinematic analysis using stereonets. The colour code of the various discontinuity orientations is: Green = cliff face orientation; blue = bedding plane; red = fault; black = joint set.

Site	Stereonet	Interpretation
Musick Point	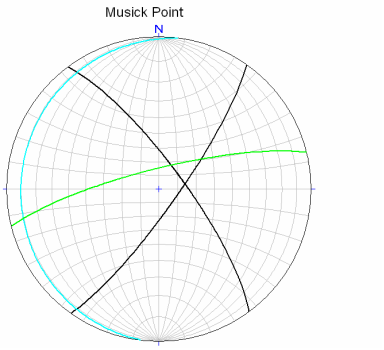	No notable mechanisms for failure
Narrowneck Beach	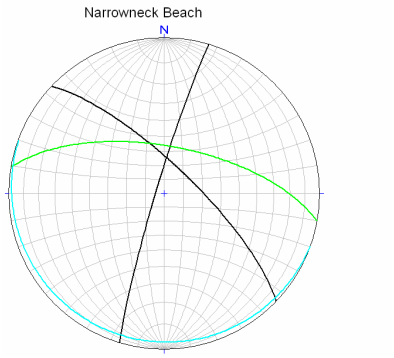	No notable mechanisms for failure

Castor Bay	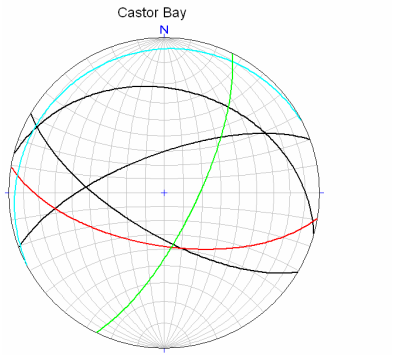	No dominant mechanisms for failure. Because of the number of intersecting discontinuities there is opportunity for wedge failure. However, there are no intersecting discontinuities with respect to the cliff face and there is only one intersection between the fault plane and joint 68/211 which have orientations close to within 20° of each other.
Waiake Bay	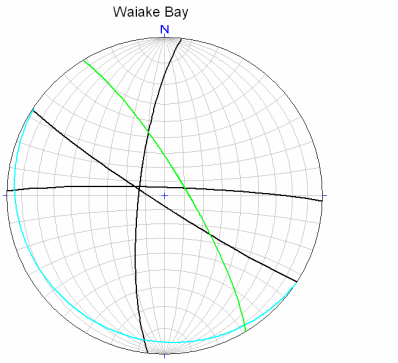	There are three intersecting joints but these do not follow kinematic guidelines for failure. Otherwise, no notable mechanisms for failure.
Army Bay	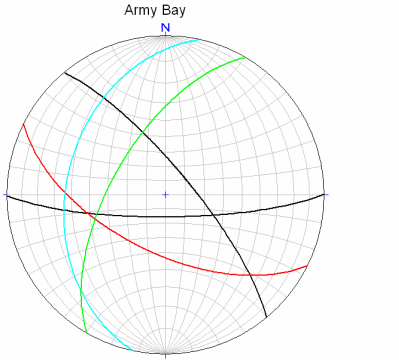	Evidence for planar failure along bedding plane 37/282. The number of intersecting discontinuities may contribute to wedge failure however there are no intersections which have the kinematic specifications required for failure.
Waiwera Beach	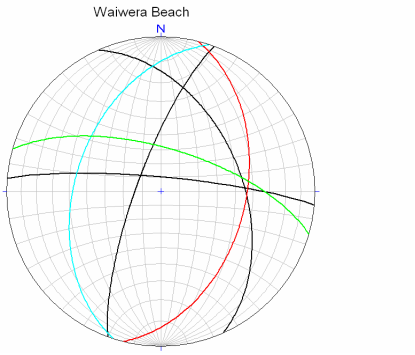	Evidence for planar failure along joint surface 82/005, except the dip angle of the planar discontinuity, 82°, is more than the dip angle of the slope face, 67°. The number if intersecting joints gives a propensity for wedge-type failure.

Martins Bay	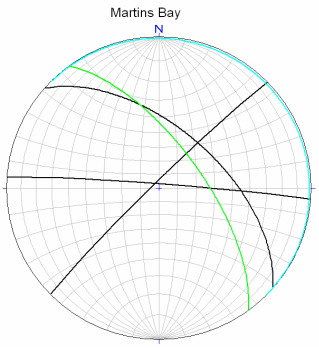	Evidence for planar failure along joint surface 58/041 and separately along the bedding plane. The bedding plane has a very low (01°) dip angle though so planar failure is unlikely. Potential for some wedge-type failures due to the number of intersecting discontinuities however no intersections follow the kinematic requirements for failure.
Leigh Marine Reserve	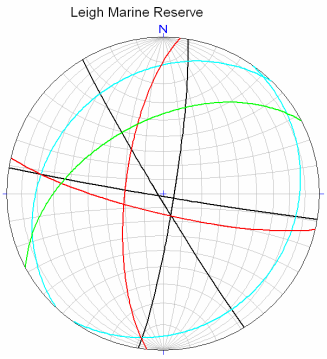	Evidence for planar failure along bedding plane 26/314, however the dip angle difference is >20°, at 25°, and numerous intersecting discontinuities gives a propensity for wedge-type failure, particularly the bedding intersection with joint 88/239.

The following paragraphs discuss the possible failure modes identified for each site.

Musick Point: The measured discontinuity surfaces did not reveal any obvious failure mechanisms at this site. Observation showed that when dry, the surface of the cliff becomes very dusty, which blows off in the wind. Slake durability tests found some of the sandstone samples were non-durable which may be an explanation for the dusty cliff surface. Heavy rainfall also acts to refresh the surface. Because of the lack of siltstone beds (there are only 2 thin beds in the cliff section) undercutting does not occur and so rock fall through undercutting of the sandstone beds is presumed not to occur. The lack of cross-cutting joint sets also discounts this failure mechanism. Erosion is believed to occur through retreat of the degraded surface rather than through mass wasting processes.

Narrowneck Beach: The measured discontinuity surfaces did not reveal any obvious failure mechanisms at this site. Observation showed that siltstone beds are frittered and heavily undercut the sandstone beds allowing sandstone blocks to fall. Small fragments

of siltstone are seen continually tumbling down the cliff face. Continuous faults may contribute to failure through rock fall. Beds are dipping landward so are effectively buttressed against planar failure.

Castor Bay: The scanline survey site, from which stereonets were constructed, is outside of the described cliff section because a thick sloping debrite bed (with lack of jointing) inhibited the access and efficacy of a scanline survey at the base of the described cliff section. The scanline survey was undertaken on an indented cove almost perpendicular to the strike of the described cliff section. Kinematic analysis of the rock mass structure at the scanline survey site, and field observations, suggest a possibility for wedge failure or rock fall with the presence of many lateral release surfaces. Beds are folded along the whole site such that they are dipping seaward at the described cliff section and hence planar failure is very likely. In the debrite units there is not a strong jointing pattern so erosion appears to be only through surface weathering such as occurs at Musick Point; turbidite beds exhibit some undercutting by siltstone so may experience rock fall.

Waiake Bay: Beds dip slightly landward so are effectively buttressed from planar failure joints show no likely wedge or planar failures. Rock fall will occur when siltstone beds sufficiently undercut the overlying sandstone beds, which is a common occurrence throughout the whole cliff section. Heavily frittered siltstone contributes to erosion and is seen continually tumbling down the cliff face. Faults (which exist regularly along the cliff but were not evident in the described section) and the three observed joint sets may act as surfaces along which wedge failure can occur. The debris from larger scale slides is evident along this section of coastline.

Army Bay: Planar failure is likely to occur along the steeply dipping bedding plane which is oriented parallel to the cliff face and dipping seaward. A number of other joint and fault surfaces appear to act as release surfaces for other small blocks to fall from. The weathered rock and heavily frittered siltstone appear to enhance erosion, with small fragments continually tumbling down the cliff face.

Waiwera Beach: At the cliff face studied beds dip seaward, but due to complex folding this regularly changes in the cliff face and on the shore platform. There is evidence for wedge-type failure to occur which will be accelerated by undercutting from siltstone beds and the overall steep dip of all the beds. The fold from which the scanline survey was taken is steeply dipping and results from a large thrust fault in the cliff section. Numerous faults offset a few beds at a time or cut through large sections of the cliff face. Calcite infill appears to weld some intact rock together.

Martins Bay: Planar failure could occur along one of the joint surfaces. The heavily frittered sandstone also contributes to accelerated erosion with small fragments continually tumbling down the cliff face and undercutting the overlying sandstone beds. Observation of the cliff face shows the propensity for rock fall to occur and there is evidence for it at the cliff base.

Leigh Marine Reserve: Planar failure will be the most likely mechanism for failure because beds are dipping strongly seaward. Intersecting faults provide surfaces along which other planar and wedge failure can occur, or simply provide release surfaces along which the small sandstone blocks can fail. The beds are heavily weathered and small fragments continually tumble from the entire cliff face.

5.4 Rock Mass Classifications

5.4.1 Classification systems

Data collected from field and laboratory work are used to classify rock masses as a whole; values for the RQD, RMR, SMR and RMS systems are displayed in Table 5.3. All data are presented in Appendix Six. The classifications were calculated for the entire heterogeneous rock mass rather than treating the sandstone and siltstone beds as separate rock masses as Brodnax (1991) does. Instead, the sites are classified based on a vertical section of the cliff, and a horizontal section. This is due to the majority of the parameters used for the classifications coming from separate sets of vertical and

horizontal scanline data. For each site, the horizontal and vertical components combined represent the range of the rock mass classification.

Table 5.3: Rock Mass Classification ratings for Waitemata Group coastal cliffs. H and V refer to the orientation of the scanline whereby: H = horizontal scanline results; and V = vertical scanline results. All classification systems have the same maximum value of 100 but have different grading schemes.

SITE & orientation		RQD		bRMR		aRMR		SMR		RMS	
Musick Point	H	93.1	excellent	57.2	fair	32.2	poor	71	good	57	moderate
	V	93.7	excellent	54.1	fair	29.1	poor	68	good	57	moderate
Narrowneck Beach	H	77. 9	good	59.4	fair	54.4	fair	73	good	64	moderate
	V	83.2	good	56.3	fair	51.3	fair	70	good	64	moderate
Castor Bay	H	46.1	poor	50.9	fair	0.9	very poor	62	good	55	moderate
	V	21.0	very poor	43.7	fair	-6.3	very poor	55	normal	48	weak
Waiake Bay	H	83.6	good	53.6	fair	48.6	fair	67	good	62	moderate
	V	65.3	fair	50.5	fair	45.5	fair	64	good	62	moderate
Army Bay	H	27.9	poor	51.6	fair	1.6	very poor	43	normal	46	weak
	V	2.6	very poor	47.4	fair	-2.6	very poor	38	bad	46	weak
Waiwera Beach	H	70.0	fair	60.9	fair	10.9	very poor	72	good	64	moderate
	V	55.9	fair	58.2	fair	8.2	very poor	70	good	48	weak
Martins Bay	H	89.3	good	60.9	fair	35.9	poor	70	good	56	moderate
	V	70.0	fair	54.2	fair	29.2	poor	63	good	57	moderate
Leigh Marine Reserve	H	24.0	very poor	47.9	fair	-2.1	very poor	59	normal	60	moderate
	V	0.9	very poor	39.1	poor	-10.9	very poor	51	normal	45	weak

5.4.2 Rock Quality Designation

RQD values in Waitemata Group rock cover almost the full spectrum of ratings. The horizontal scanline is 24.0 to 93.1, while the vertical scanline is 0.9 to 93.7. For sites such as Leigh Marine Reserve the RQD value is extremely low from vertical scanline data because siltstone beds are very thin and jointing is also very closely spaced. Castor Bay, Army Bay and Leigh Marine Reserve display the lowest RQD values (poor to very poor), representing closely spaced jointing in their respective cliff sections. In predominantly-thick, sandstone-bedded cliff sections such as Musick Point, horizontal scanline data result in a high RQD value that largely reflects the near-vertical joint spacing. Vertical scanlines could only be a few meters in length and thus at sites like

Musick Point, the scanline avoided nearly all the near-vertical joints and only passed through a few bedding planes, again resulting in a high RQD.

5.4.3 Rock Mass Rating

Basic RMR values have a small range from 39.1 to 60.9 across all the sites which classifies them as poor to fair rock masses. All of the sites have 'fair' ratings for both horizontal and vertical sections except for Leigh Marine Reserve (vertical) which has a 'poor' rock mass rating. Vertical scanlines give slightly lower ratings than horizontal scanlines for all the sites as well; values are lower than results from horizontal scanlines by 2.7 to 8.8 points. Adjusted RMR values are expectedly lower than basic RMR values, ranging from -10.9 to 54.4 (very poor to fair). The favourability of discontinuity orientations was determined using the classification by Selby (1993) as a specific qualitative assessment is not provided in Bieniawski (1989). The favourability classification was then given a rating based on the RMR table of Bieniawski (1989). The most unfavourable orientations can have 60 points deducted from the total bRMR which has a tendency to plunge RMR values too low (Romana, 1993). Musick Point, which, based on the thickness and predominance of the sandstone beds and high RQD and bRMR ratings appears to be one of the more stable rock masses, has a 'poor' aRMR rating purely because of the orientation of the bedding planes to the cliff face.

5.4.4 Slope Mass Rating

The SMR values range from 38 to 73 (bad to good). Five sites (Musick Point, Narrowneck Beach, Waiake Bay, Waiwera Beach and Martins Bay) have 'good' SMR values which imply that the orientation of the cliff face to the bedding planes does not have a detrimental effect on slope stability. Army Bay has a low ranking similar to other classification schemes and with a combination of closely jointed, weathered rock and beds dipping seaward, the cliff section appears to have the weakest overall rock mass. Leigh Marine Reserve and Castor Bay have 'normal' slope mass ratings which is a poorer grade than the 'good' SMR values and may be mostly due to the steeply seaward-dipping beds which aren't seen in other cliff sections apart from Army Bay. Waiwera does have similar steep beds but the orientation of these beds is not out of the cliff face so they are effectively buttressed.

5.4.5 Rock Mass Strength

RMS values ranged from 45 to 64 (weak to moderate), with the majority of sites (7 of 8) having moderate rock mass strengths. This classification scheme also uses discontinuity orientation to determine rock mass quality but this parameter only accounts for up to 20% of the total RMS and therefore does not dramatically lower the overall classification as the aRMR system does. Upon observation, the two sites (Army Bay and Leigh Marine Reserve) that have 'weak' rock mass strengths do have more highly jointed and disturbed rock masses, more so than the other sites that were classified.

Brodnax (1991) used the RMS system for Waitemata Group coastal cliffs and found Parnell Grit beds were strongest with an RMS of 68. Brodnax further treated sandstone and siltstone beds of the flysch as separate rock masses and found that sandstone beds had an RMS value of around 60, while the siltstones had an RMS value of around 50. He observed that although there was an explainable difference between the RMS values of the different lithologies, overall the values showed little variation within the Waitemata harbour coastal cliffs. Moon *et al.* (2001) also noted that the RMS system appears to be insensitive to soft rocks with a very narrow, peaked distribution within the Tertiary mudrocks studied. Moon *et al.* (2001) found that the RMR, SMR and RMS systems were often not satisfactory for determining the behaviour due to the transitional nature of the mudrock between hard rock and soil. When the sample rock behaves as hard rock then the classification systems work as they should and provide a fair assessment of their condition. However, if the conditions that lead to failure along discontinuities do not exist, then the soft rocks display behaviours of soil mechanics. The classification systems then appear to overestimate the contribution of intact strength to mass strength. With the heterogeneous rock of the Waitemata Group, sandstone and Parnell Grit beds will behave as rock while some siltstone beds which degrade into frittered soil-like material may behave as soil. By treating all beds as one rock mass, both of these situations are taken into account when determining the RMS.

5.4.6 Geological Strength Index

GSI values for Waitemata Group cliffs (Table 5.4) are highest for sandstone beds determined using the chart for jointed rock masses. The maximum value is 65 ± 5

recorded for 7 of 16 sites. Siltstone beds conversely record the lower GSI values ranging from 30 ± 5 to 45 ± 5 when using the chart for jointed rock masses because the structure has a decreased interlocking of rock pieces compared with the sandstone (that is, joints were more closely spaced and heavily fractured). Surface conditions are similar between the sandstone and siltstone beds. The chart for heterogeneous rock masses (which incorporates sandstone and siltstone beds as one rock mass) gives a range of values, from 20 ± 5 to 45 ± 5, that is overall lower than the separate sandstone and siltstone GSI values. Surface conditions are similar between all the sites and so variation in GSI values for the heterogeneous chart can be assumed to be due to the composition and structure of the rock mass.

Indeed, more sandstone dominant cliff sections such as Musick Point, Mairangi Bay, Opahi Bay and Buckleton Beach give the highest GSI values. If the cliff section is tectonically disturbed, as is Castor Bay, Army Bay, Waiwera Beach and Leigh Marine Reserve, GSI values are very low, despite any dominance of sandstone. Tonkin and Taylor (2005) estimated the GSI of East Coast Bays Formation as 35-65 and Pakiri Formation as 55-75. These ranges are overall slightly higher than the values determined in this study which were 30-65 and 37-65 for the East Coast Bays and Pakiri Formations respectively.

Table 5.4: Geological Strength Index values determined for the described cliff sites. Sst = sandstone rock mass; Zst = siltstone rock mass; Htg = Heterogeneous rock mass. All values have a range ± 5.

SITE LOCATION	Sst	Zst	Htg
Cockle Bay	60	37	45
Eastern Beach	50	37	42
Musick Point	65	45	45
Achilles Point	65	40	40
Narrowneck Beach	50	35	35
St Leonard's Beach	65	45	40
Castor Bay	42	42	24
Mairangi Bay	65	45	45
Waiake Bay	60-65	30	40
Army Bay	45	33	20
Waiwera Beach	37-40	41-45	20-24
Opahi Bay	55	40	45
Martins Bay	65	45	40
Buckleton Beach	65	45	48
Matheson Bay	45	37	25
Leigh Marine Reserve	45	45	20

Castor Bay, Leigh Marine Reserve and Army Bay appear to be the weakest overall rock masses across the range of different classification systems. This is seen to be mainly a result of the tectonically deformed nature of their rock mass as well as the orientation and seaward dipping angle of their bedding planes with respect to the cliff face.

5.5 Rock Mass Properties

5.5.1 Rock mass parameters

Because GSI is used as a variable in the estimation of rock mass strength parameters with RocLab 1.0 software, a separate calculation was done for both the sandstone and siltstone beds individually (from the jointed rock chart) and for the heterogeneous rock mass as a whole. Only the parameters derived for the heterogeneous rock mass are used for comparison here and are presented in Table 5.5. All results, including those for sandstone and siltstone individually are given in Appendix Six.

Table 5.5: Rock mass parameters for the cliff sites including the shear strength properties of cohesion and friction angle, and global rock mass strength.

SITE LOCATION	Cohesion (MPa)	Friction angle (°)	Rock Mass Strength (MPa)	Elastic modulus (MPa)
Cockle Bay	0.10	43	1.4	1542.0
Eastern Beach	0.066	37	0.6	1179.7
Musick Point	0.088	44	1.2	1542.0
Achilles Point	0.090	41	1.2	986.2
Narrowneck Beach	0.046	39	0.7	629.0
St Leonard's Beach	0.095	41	1.3	986.2
Castor Bay	0.033	32	0.5	232.6
Mairangi Bay	0.070	52	1.6	1542.0
Waiake Bay	0.072	38	0.8	986.2
Army Bay	0.045	25	0.5	161.9
Waiwera Beach	0.055	29	0.6	232.6
Opahi Bay	0.22	53	5.5	1542.0
Martins Bay	0.10	42	1.5	986.2
Buckleton Beach	0.29	57	9.0	2012.5
Matheson Bay	0.074	38	1.6	254.7
Leigh Marine Reserve	0.034	36	0.9	161.9

5.5.2 Cohesion and friction angle

Friction angle and cohesion are measures of the shear strength of rock material whereby 'friction angle' includes friction between plane surfaces as well as resistance due to the roughness of surfaces, and cohesion is produced in rock by the fusion of minerals or the cementing of grains. Shear strength was not directly measured in this study, but was rather derived through RocLab 1.0 software.

Cohesion values determined for heterogeneous rock masses range from 0.033 - 0.29 MPa. The sites with the lowest cohesion include Castor Bay (0.033 MPa) and Leigh Marine Reserve (0.034 MPa). Highest cohesion was determined for Opahi Bay (0.22 MPa) and Buckleton Beach (0.29 MPa). The estimated cohesion values for siltstone (ranging from 0.05 - 0.10 MPa) are predominantly an order of magnitude smaller than sandstone values (ranging from 0.10 - 0.66 MPa). Friction angle values calculated for the heterogeneous rock masses range from 25 - 57°. Friction angle values are highest for those sites with the highest cohesion (Opahi Bay and Buckleton Beach). The lowest friction angles were however determined for Army Bay (25°) and Waiwera Beach (29°). Friction angle values for siltstone rock masses range from 28 - 43° and are higher for sandstone rock masses, ranging from 44 - 61°. The sites that held the worst rock mass classification values for GSI, and also the other four classification systems, display the lowest shear strength (cohesion and friction angle) values. These sites are Castor Bay, Army Bay, Waiwera Beach and Leigh Marine Reserve.

5.5.3 Rock mass strength

Tensile, compressive and global rock mass strength values are also produced as part of the analysis in RocLab 1.0. For simple comparison between sites only the global rock mass strength values are presented in Table 5.5. Rock mass strength for heterogeneous rock masses ranged from 0.5 - 9.0 MPa. Strength was highest for Opahi Bay (5.5 MPa) and Buckleton Beach (9.0 MPa) and lowest for Castor Bay and Army Bay (0.5 MPa). Rock mass strength was lowest for siltstone beds and ranged from 0.4 - 1.0 MPa. Sandstone rock mass strength values were appreciably higher than for siltstone and ranged from 1.1 - 14.3 MPa.

The elastic modulus measures the elasticity of material by determining the relationship between applied load and deformation (the stiffness) and is thus equal to axial stress divided by axial strain (Selby, 1993). The elasticity modulus values determined for the cliff sites range from 162 to 2013 MPa which indicate that the rock mass is relatively deformable according to Selby (1993). The highest value was at Buckleton Beach, and the lowest value was both at Army Bay and Leigh Marine Reserve. Values for the siltstone rock masses ranges from 401 to 1542 MPa and for the sandstone rock masses are overall higher, ranging from 902 to 8588 MPa.

For sandstone and siltstone rock masses individually, shear strength values show a general increase northwards, which is probably due to the increasing uniaxial compressive strengths and unit weight of the Waitemata Group rocks northwards. Global rock mass strength however, follows a similar trend to the cohesion and friction angle values whereby lower values are associated with the low GSI values recorded for faulted and folded rock masses. This holds true for Castor Bay, Army Bay and Waiwera Beach which have the lowest global rock mass strengths values of 0.5 - 0.6 MPa. Leigh Marine Reserve, on the other hand, which is also a tectonically disturbed site, has a strength value of 0.9 MPa that is higher than other sites with "better quality" rock masses. This may be a result of the calculated combination of parameters at Leigh Marine Reserve, including a relatively low cliff height and considerably higher sandstone and siltstone intact rock strengths even after the adjusted weighting for the type of flysch based on Marinos and Hoek (2001).

5.6 A Classification Scheme for Sandstone : Siltstone Proportions in Cliff Sections

5.6.1 Development of the classification scheme

Following observation of the various thicknesses of Waitemata Group beds during field work some patterns of the proportion of sandstone to siltstone emerged. Various ratios appeared to repeat in all of the described sites and, from these observations, seven different classes (labelled A to G) were formed as part of a classification scheme based

on the relative thicknesses of sandstone and siltstone (Figure 5.5). While this classification scheme was originally developed for qualitative purposes as a comparison between sites, it was later realised that the proportion of sandstone to siltstone for the entire cliff section could be calculated by using the classification scheme with bed thickness data collected at each site. The visual appearance of each class is illustrated in Figure 5.6.

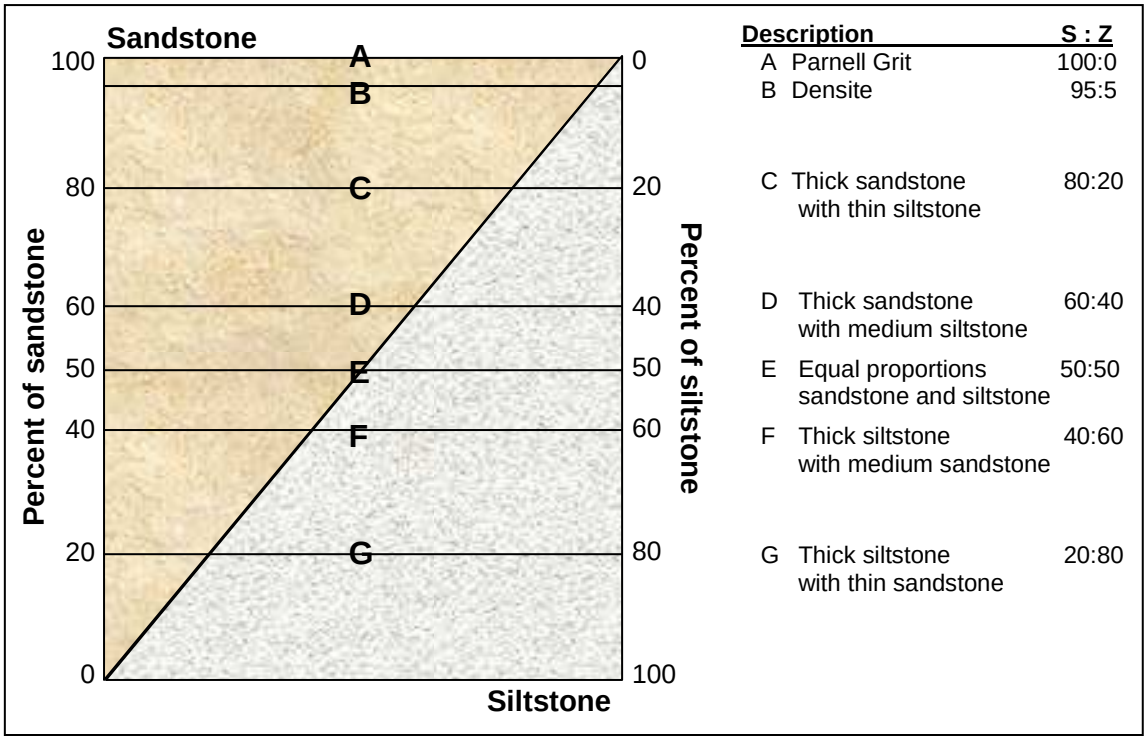

Figure 5.5: Schematic diagram of the classification scheme for Waitemata Group coastal cliffs with respect to the proportion of sandstone and siltstone.

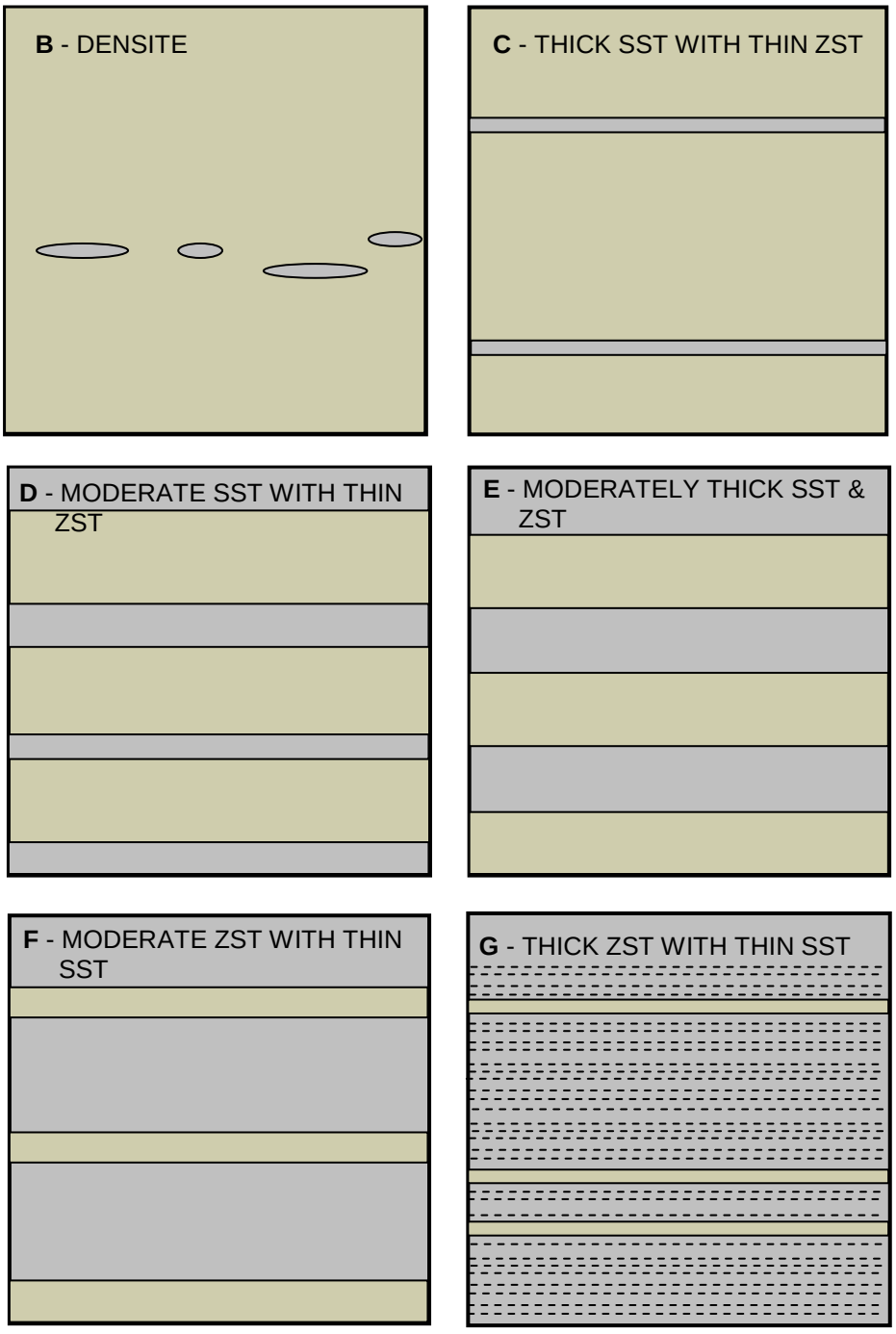

Figure 5.6: Relative thicknesses of sandstone and siltstone beds for each class (B-G). Class A is considered to be 100% sandstone. SST = sandstone (brown); ZST = siltstone (grey).

The majority of the described cliff sections exhibit a few different classes within the one cliff face. For instance, at one site the lower portion of the cliff could exhibit class F (40:60) beds followed by an upper portion of class C (80:20) beds. If the cliff section exhibited a 2.5 m thickness of Class F then the total thickness of sandstone would be 1 m (2.5 m x 40 %) and the total thickness of siltstone would be 1.5 m (2.5 m x 60 %). If the next portion of the cliff displayed 3.8 m of Class C then 2.56 m would be sandstone (3.8 m x 80 %) and 1.24 m would be siltstone (3.8 m x 20 %). The total proportion of sandstone to siltstone for the entire cliff section would be 57:43 sandstone to siltstone.

Note that the classification is not of sand and silt grain size but is based more broadly on the proportion of sandstone beds to siltstone beds. Parnell Grit beds which were only observed in the cliff sections at 2 sites (Waiwera and Army Bay) are classed as 100 % sandstone because the broad classification of siltstone includes no sand-sized grains.

5.6.2 Results

At each site the cliff section was divided into the different observed classes and the proportion of total sandstone to siltstone was calculated (Table 5.6). The sandstone proportion values, as a representative measure of the classification scheme, are added to the database of coastal cliff properties for later statistical analysis.

5.6.3 Verification of the classification scheme to the Geological Strength Index

This classification scheme was found to be related to the GSI rating for heterogeneous rock masses (Table 5.7). The composition and structure category determined as one half of the GSI classification (refer to Table 3.3) correlated well with the total sandstone/siltstone proportions calculated at each cliff site. This is justifiable because the GSI category is also based on the proportion of sandstone to siltstone; the GSI can thus act as verification of the calculations made from the classification scheme and vice versa. Only one overall value can be assigned to the cliff section from the GSI chart compared to the classification scheme which can assign numerous different classes within the one cliff section. In spite of this difference, both classifications correlate well and help to prove the worth of the GSI chart designed specifically for heterogeneous rock masses.

Classification scheme table

Table 5.7: Results of classification scheme for Waitemata Group coastal cliffs, shown as the total proportion of sandstone in the described cliff section. The GSI value is measured for the composition and structure of the rock mass whereby: **A** = Thick bedded sandstone; **B** = sandstone with thin siltstone interlayers; **C** = sandstone and siltstone in similar amounts; **D** = siltstone with sandstone layers; **E** = weak siltstone with sandstone interlayers; **F** = tectonically deformed variety of C, D or E; **G** = Silt with or without very thin sandstone; **H** = tectonically deformed variety of G.

Site Location	Proportion of sandstone	Proportion of siltstone	GSI
Cockle Bay	0.64	0.36	B-C
Eastern Beach	0.67	0.33	B-C
Musick Point	0.80	0.20	B
Achilles Point	0.61	0.39	C
Narrowneck Beach	0.51	0.49	D
St Leonard's Beach	0.53	0.47	C
Castor Bay	0.61	0.39	F
Mairangi Bay	0.80	0.20	B
Waiake Bay	0.45	0.55	C
Army Bay	0.71	0.29	F
Waiwera Beach	0.72	0.28	F
Opahi Bay	0.80	0.20	B
Martins Bay	0.52	0.48	C
Buckleton Beach	0.81	0.19	B
Matheson Bay	0.20	0.80	E-F
Leigh Marine Reserve	0.24	0.76	F

5.7 Shore Platform Widths and Coastal Cliff Erosion Rates

5.7.1 Calculation of Waitemata Group coastal cliff erosion rates

For each site, GPS data were used to calculate the width of the shore platform, from the cliff base to the shore platform edge. The platform widths were then used to calculate the long term erosion rate of the cliffs assuming an erosion period of 7120 ± 20 years. The mean shore platform widths and their associated long-term erosion rate are presented in Table 5.8.

Table 5.8: Shore platform widths measured at each site and the associated erosion rates based on a time period for erosion of 7120 ± 70 years. Error is 1 standard error.

Site Location	Mean Platform Width (m)	Rate (mm y^{1})
Cockle Bay	8.29 ± 0.51	1.16 ± 0.072
Eastern Beach	377.60 ± 0.37	53.03 ± 0.52
Musick Point	165.43 ± 7.57	23.23 ± 1.09
Achilles Point	28.35 ± 1.38	3.98 ± 0.20
Narrowneck Beach	18.67 ± 1.61	2.62 ± 0.23
St Leonard's Beach	33.79 ± 2.03	4.75 ± 0.29
Castor Bay	100.82 ± 0.77	14.16 ± 0.18
Mairangi Bay	58.58 ± 1.09	8.23 ± 0.17
Waiake Bay	53.08 ± 2.01	7.46 ± 0.29
Army Bay	140.74 ± 4.39	19.77 ± 0.65
Waiwera Beach	73.23 ± 3.41	10.29 ± 0.49
Opahi Bay	112.08 ± 1.01	15.74 ± 0.21
Martins Bay	137.84 ± 6.61	19.36 ± 0.95
Buckleton Beach	29.45 ± 0.71	4.14 ± 0.11
Matheson Bay	90.32 ± 0.47	12.69 ± 0.14
Leigh Marine Reserve	131.61 ± 0.90	18.48 ± 0.22

Erosion rates vary considerably across the entire eastern coastline of the Auckland region with no discernable trends based on location (Figure 5.7). However, erosion rates do tend to be similar where the shore platform morphologies are alike (refer to site sketches in Section 4.3). For instance, Achilles Point, Narrowneck Beach and St Leonard's Beach all exhibit stepped platforms with beds dipping landward and erosion rates range from 2.6 to 4.8 mm y^{-1}. Castor Bay has a horizontal platform with a steep drop-off at the seaward edge and beds dip seaward; the erosion is considerably larger than the aforementioned sites at 14.2 mm y^{-1}. The smallest erosion rate (1.2 mm y^{-1}) was recorded at Cockle Bay, which had a high, stepped platform. The largest recorded erosion rate (53.0 mm y^{-1}) was the next site north, Eastern Beach. This site had an extensive sloping platform, the seaward margin of which was not uncovered even at a spring low tide.

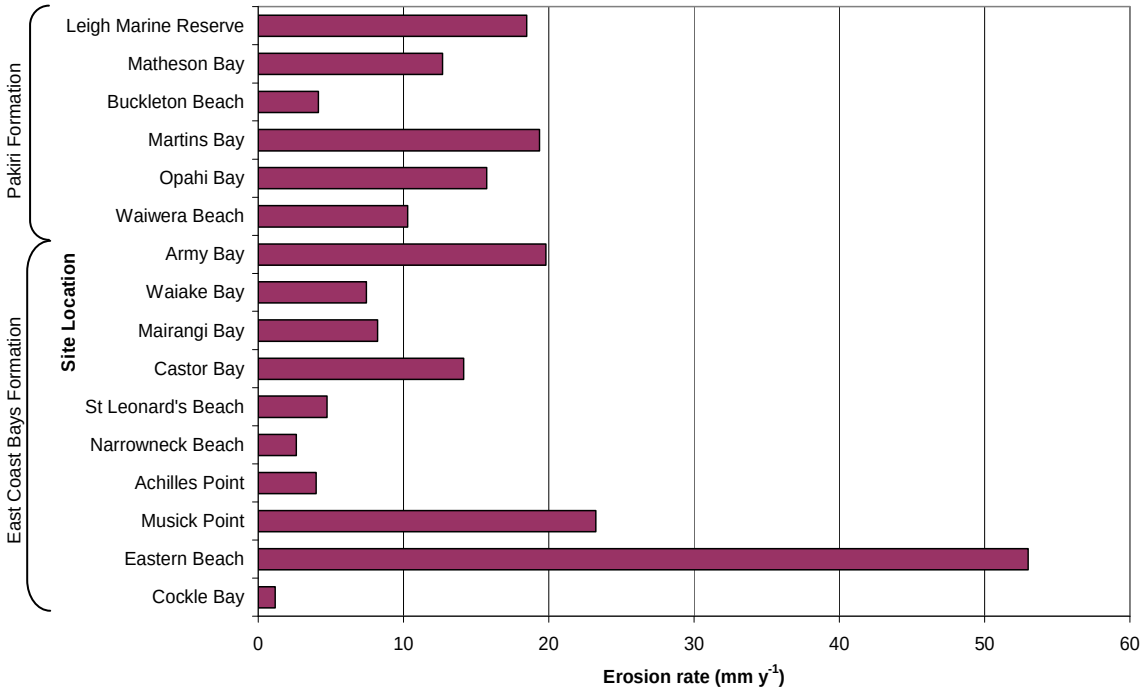

Figure 5.7: Erosion rates from southern to northern site locations.

The erosion rates calculated from this research are at the low end of values measured by other authors. 'Low' erosion rates include 3.5 mm y^{-1} measured in the North Shore using dated man-made structures by Gordon (1993) and 'high' erosion rates include 180 mm y^{-1} measured using aerial photography by Brodnax (1991) in Waitemata Harbour coastal cliffs.

While for this study erosion rates have been classified as long-term following the methods of de Lange and Moon (2005), the time period for work by Gordon (1993) was 60-70 years, and for work by Brodnax (1991) was 40 years, which were also classified as long-term measurements. Two previous studies have been published in which measured shore platform widths were used to determine long-term erosion rates synonymous with the time period for this study. Paterson and Prebble (2002) took spot measurements from North Shore locations and determined an average erosion rate of 31 mm y^{-1} while de Lange and Moon (2005) measured two relatively distant sites and determined lower erosion rates of 1.8 - 13.8 mm y^{-1} at the North Shore site and 1.4 - 14.3 mm y^{-1} at Tawharanui Peninsula. The sites measured across the eastern Auckland region coastline in this study fit well with the abovementioned published data. Compared to erosion rates

measured using shore platform widths for which the time period used was 6500 years or 7120 years, the other methods used for Waitemata Group cliff erosion studies (Table 2.3B) are seemingly measured on only a medium-term time scale.

Short-term erosion rates were measured using terrestrial laser scanning and terrestrial photogrammetry methods by Gulyaev and Buckeridge (2004) over a time period of 2 years and an erosion rate of 24 mm y^{-1} was calculated. As most geomorphic studies of processes are carried out over fewer than three years, the validity of short-term measurements is at best uncertain and at worst they are irrelevant (Conacher, 1988). With regards to measurement errors, the actual observed platform widths correlated extremely well with the calculated widths.

5.7.2 Configuration with sea-level trends and stillstands

During field work a number of observations were made with respect to varying platform heights and sea-level trends. A higher narrow platform was found at most of the southern sites in conjunction with a lower, much broader platform (section 4.5.4). These higher platforms are approximately 1 - 3 m above present sea-level.

The issue of which near-shoreline platform to measure to determine erosion rates became apparent during this research. A high, narrow platform was observed at Cockle Bay, Eastern Beach, Musick Point, Achilles Point, Castor Bay and Waiake Bay. At low tide, these platforms are completely exposed and are reached, but do not appear to be covered, at high tide. Platforms of the same horizontal morphology are found at other northern sites but are just exposed at low tide and are assumed to be part of the pre-existing cliff erosion/platform development system and are not higher benches from a different erosion phase. For this study the accepted causes of a higher bench (outlined in Section 2.8.3) include a stillstand of eustatic sea-level higher than the present sea-level and a high-tide bench. Because the cliff sites display these higher benches at both the low tide and high tide level, both explanations appear to be feasible. However, this has highlighted a need to better define the development of various platforms that are all part of the erosion system at one cliff site as it has potential to jeopardise the comparisons made between varying erosion rates within the same rock type.

5.8 Summary

- Intact rock strength for sandstone ranges from 7 to 100 MPa and for siltstone ranges from 5 to 13 MPa; bulk density for sandstone ranges from 1650 to 2450 kg m^{-3} and siltstone values have been sourced at 1260 to 1850 kg m^{-3}; porosity values for sandstone range from 12 to 43 % for sandstone and 29 to 52 % for siltstone; slake durability is high for Cockle Bay, Eastern Beach, Musick Point, Achilles Point and Mairangi Bay.
- Failure modes for the described cliff sections include planar failure and propensity for wedge failure due to many intersecting discontinuities. Weathering and frittered siltstone are observed as continual forms of cliff recession.
- Rock mass classification schemes show that Castor Bay, Army Bay, Waiwera Beach and Leigh Marine Reserve have the lowest rock mass quality. Good rock mass quality was determined for Musick Point, Narrowneck Beach and Waiake Bay.
- Cohesion values are relatively low ranging from 0.03 to 0.29 MPa; friction angles range from 25 to 57°; tensile, compressive and global rock mass strengths are overall low and the global rock mass strength ranged from 0.5 to 9.0 MPa; the elastic modulus ranged from 162 to 2013 MPa indicating rocks are relatively deformable. These values are for heterogeneous rock measured as one rock mass.
- A classification scheme has been developed for Waitemata Group coastal cliffs based on the proportion of sandstone beds to siltstone beds and shows a relation to the GSI classification for heterogeneous rock masses.
- Shore platform widths were used to determine long-term erosion rates and ranged from 8 to 378 m wide; erosion rates subsequently ranged from 1.2 to 53.0 mm y^{-1}. Higher platform benches are considered to be a result of a higher period of sea-level or are high-tide benche

CHAPTER 6

STATISTICAL ANALYSIS

6.1 Introduction

The set of data produced from field and laboratory tests, derived parameters, and GIS surfaces is collated into a database of 98 different parameters in preparation for statistical analysis. The aim of the statistical analysis is to examine the relationships of all the parameters with shore platform width (as a measure of erosion rate), cliff angle and cliff height as these are key determinants in any hazard assessment. Relationships are also sought for location based on northwards or southwards trends. The statistical analyses are based on the described sites only in relation to coastal cliff erosion and are not meant to deduce relationships for the extent of the whole eastern coastline.

The methodologies for three different forms of statistical analysis used in this study - correlation and regression, the student t-test, and multiple linear regression - are defined and the results of these analyses with respect to the determinants of hazard assessment and location are discussed.

6.2 Correlation and Regression

6.2.1 Methodology

A correlation matrix was used as the most efficient way to determine the regression values of all parameters against one another. Correlation and regression test whether there is any association between two particular parameters and how predictable one parameter is from another (Watts and Halliwell, 1996). Furthermore, correlation measures the strength of a linear relationship.

This was specifically important for seeing if there were any parameters that correlated well with shore platform width and erosion rate, cliff height, cliff angle and northing coordinates. Correlation coefficients (R) between +0.85 to +1.00 or, -0.85 to -1.00, were classified as having a very significant correlation; values from +0.70 to +0.84 or -0.70 to -0.84 were classified as having only a significant correlation. The arbitrary cut-off point of R= 0.70 is equal to R^2= 0.50 which has been commonly used by others (Moon, 1989; Beattie, 1990; Roy, 1997) for environmental and geomechanical analysis. The existence of a high correlation between two parameters does not necessarily mean that one parameter is caused by the other, particularly when the population size is small; therefore tests which showed a significant or very significant correlation were graphed as a scatterplot to better analyse the data. The scatterplots display any outliers or clusters of the data which will affect the correlation coefficient between the two parameters, and they also highlight whether the trendline is very flat or steep, which implies that there is no useful relationship between the two measured parameters.

6.2.2 Purpose of correlation and regression

The correlation matrix was used as a beginning stage for determining what parameters may be influencing (or be influenced by) erosion rates, cliff angle and height, and location. Secondly, it was important to determine any relationships between other parameters in order to develop a better understanding of how rock mass structure, geology and climate interrelate and whether any of these parameters specifically exhibit inter-dependence on another.

Regression coefficients are only determined linearly (compared to more complex logarithmic or exponential relationships) because the data are environmental parameters which exhibit natural scatter and for the purposes of this study a simple relationship is sought to determine the influence of environmental parameters on one another. Also it was thought that for the small population size of the dataset, more complex relationships would not be easily determined or be necessarily realistic.

6.2.3 Results of the correlation matrix

Significant relationships found from the correlation matrix are discussed for site location and geomorphology parameters, discontinuity parameters, bulk rock properties, rock mass classifications, rock mass parameters, and for the GIS-sourced parameters; scatterplot diagrams are presented for valid correlations found between these parameters. The full correlation matrix is presented in Appendix Seven and a summary of the significant relationships that are discussed in the text is given in Table 6.1. Results are not discussed where scatterplots show outliers or clusters which affect the validity of the results and where one parameter is determined from another (for instance, spacing versus RQD) even if the regression coefficient is 'significant'.

6.2.3.1 Site location and geomorphology parameters

The northing coordinates correlate well with a number of parameters and therefore highlight trends in the location of cliff sites. Sandstone and siltstone intact rock strength, and bulk density of sandstone have a positive correlation with northing coordinates (R = 0.85 - 0.88), and porosity has a negative correlation (R = -0.90), as illustrated in Figure 6.1A and B. This indicates the change in volcaniclastic content as sites move north into the Pakiri Formation and possibly the stratigraphic change in the Waitemata Group as well. Reflecting this change in intact rock strength, the global rock mass strength of both sandstone and siltstone also has a positive correlation with northing coordinates (R = 0.82 and 0.83 respectively) (Figure 6.1C). A number of climate parameters sourced from GIS surfaces have very significant, increasing trends northwards including various measures of solar radiation (R = 0.78 - 0.94), total rainfall (R = 0.78), and various measures of wind speed (R = 0.88 - 0.95) (Figure 6.1D is an example of this relationship). However, the values of these parameters have a small range which makes the reliability of the data questionable. Other studies have presented data for increasing climate conditions of wind and rainfall (such as Hurnard, 1979) as the eastern coastline of the Auckland region opens up to the north and so the general trends can therefore be considered to be true.

Table 6.1: Significant parameters discussed in the text. The following abbreviations represent the methodologies used to obtain results: S = sandstone rock mass; Z = siltstone rock mass; Htg = heterogeneous rock mass; V = measured from vertical scanline survey; H =measured from horizontal scanline survey.

Group	Parameter	Significant related parameters
Site location and geo-morphology	Northing	All bulk rock properties
		Global rock mass strength S and Z
		Solar radiation, rainfall, wind strength
	Cliff angle	Joint frequency V and H
		Proportion of sandstone
Discontinuity parameters	Persistence	Joint frequency
		Block size classification Z
		Aperture
		Elevation
		Plan curvature
	Aperture	Spacing, block area, joint frequency
	Spacing	GSI S and Htg
		Rock mass parameters for Htg
		Solar radiation
	Block size classification	Rock mass classifications
		Rock mass parameters for Htg
		Solar radiation
	Joint frequency	UCS S
		Rock mass classifications
		Rock mass parameters for Htg
	Bed dip	Persistence and Aperture
Bulk rock parameters	All parameters	RQD
		Cohesion, sigt, sigc Z
		sigcm S and Z
		Solar radiation, rainfall, temperature, wind strength
Rock mass classification parameters	GSI	RQD, RMS V, aRMR
		Rock mass parameters
	RQD	Rock mass classifications
		Rock mass parameters for Htg
		Profile curvature
	RMS	SMR, aRMR
		Friction angle & deformation modulus Htg
		Aspect, plan and profile curvature
		Bed dip

Group	Parameter	Significant related parameters
Rock mass classification parameters continued	bRMR	SMR V
		Temperature, solar radiation, wind strength
		Profile curvature
	aRMR	SMR V
		Deformation modulus Htg
		Plan and profile curvature
		Bed dip
Rock mass parameters	SMR	Aspect
		Profile curvature
	Cohesion	Annual water deficit
		Water balance ratio
		Rainfall, solar radiation
	sig t	Water balance ratio
		Solar radiation
	sig c	Annual water deficit
		Water balance ratio
		Rainfall, solar radiation
	sig cm	Solar radiation, rainfall, temperature, wind strength
	Deformation modulus S	Spacing, Block size classification, Joint Frequency, RQD
GIS-sourced parameters	Length slope factor	Stream power index
	Slope in percent	January solar radiation
		Compound topographic wetness index
		Annual water deficit
	Specific catchment area	Flow path length
		Area draining out of cells
	Water balance ratio	Rainfall, vapour pressure deficit
		Slope
	Annual water deficit	Solar radiation, temperature, rainfall, vapour pressure deficit
		Slope
	Solar radiation	Spacing, block size classification

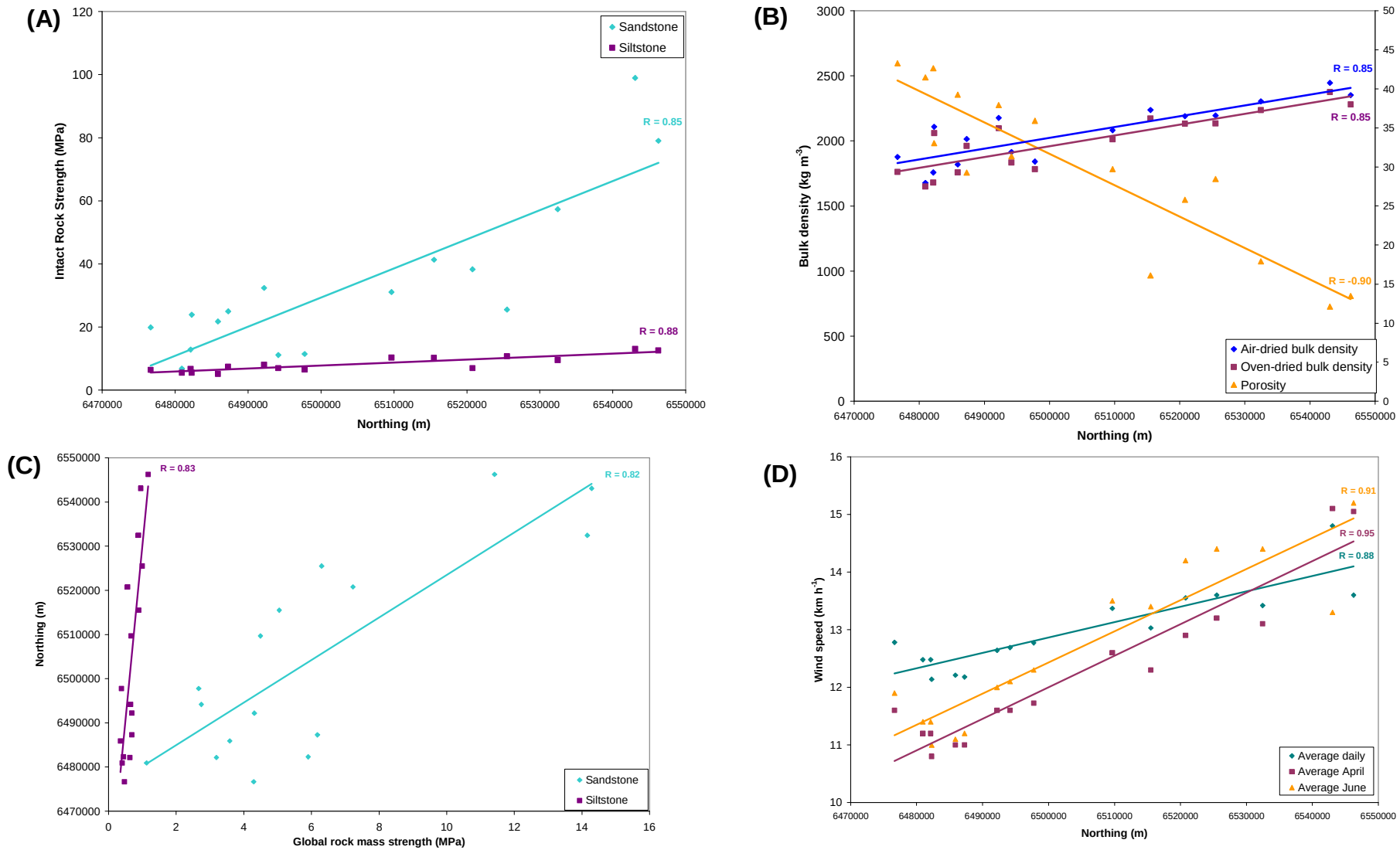

Figure 6.1: Scatterplot graphs showing the correlation between northings and intact rock strength (A), bulk density and porosity (B), global rock mass strength (C), and wind speed (D).

Cliff angle had a negative correlation with joint frequency measured horizontally across cliff sections (R = -0.73) and vertically down cliff sections (R = -0.78) (Figure 6.2A). Thus, as the number of joints per metre decreases, the cliff angle increases. This relationship is further exemplified by the significant correlation with RQD measured horizontally across the cliff section (R = 0.71) because RQD is a classification system based on joint frequency. Cliff angle has a positive correlation with RQD because higher RQD values are recorded for lower joint frequencies (Figure 6.2B). Cliff angles also correlate significantly with the proportion of sandstone (R = 0.71) whereby as the proportion of sandstone beds increases (siltstone decreases) overall cliff angles steepen (Figure 6.2C). The graph of joint frequency shows relatively large scatter and the graph of sandstone proportion shows clustering of the data which reduces their reliability. However, overall these appear to be justifiable findings because of physical observation of these relationships during field work. Thick to very thick sandstone beds have wide joint spacing, wide bedding planes and form steep cliff faces, as observed at Musick Point, Mairangi Bay, Opahi Bay and Buckleton Beach; the cliffs that are dominated by heavily jointed (very closely spaced) siltstone beds, including Matheson Bay and Leigh Marine Reserve, formed the lowest slope angles.

Shore platform width and erosion rate are directly proportional because erosion rate for all sites has been determined over the same time period. No parameters correlated significantly with erosion rate which is a key parameter of this study.

6.2.3.2 Discontinuity parameters

The spacing of discontinuities in a rock mass will determine the block area, block size and joint frequency within the rock mass and as such, these four properties (as measured parameters) all correlate with the same parameters; that is, rock mass classification parameters, rock mass parameters for heterogeneous rock masses and the deformation modulus for sandstone rock masses. The rock mass parameters (which quantify shear, tensile, compressive and global strength) measured for heterogeneous rock masses correlate further with aperture and block area. This is an appreciable relationship because more closely-spaced joints, wider apertures, and smaller block size leads to a decreased strength of the rock mass. However, the calculations used to determine the rock mass

parameters from the RocLab 1.0 software programme (Rocscience, 2006) do not require the input of any discontinuity parameters; thereby the correlation between rock mass and discontinuity parameters appears to be valid.

Persistence of discontinuities correlates well with joint frequency (R = -0.71 to -0.73) and block size (R = 0.75 respectively) of the rock mass (Figure 6.3A). In Waitemata Group coastal cliffs the majority of joints are non-continuous (low persistence), with only bedding planes displaying real continuity (high persistence). Fault planes also were generally continuous. When persistence from scanline surveys was averaged, values only ranged from 0.2 to 7.7 m which highlights the non-continuous nature of the majority of discontinuities in Waitemata Group rock. As discontinuities become more persistent, joint frequency tends to decrease and subsequently, block size tends to increase. Elevation (R = 0.77) and plan curvature (R = -0.80) of the land (Figure 6.3B and C) also correlate with persistence; plan curvature is the curvature of the contours of land. This relationship suggests that discontinuity persistence has some control on geomorphology and, as discontinuities become more persistent, elevation increases and the curvature of the land has a profile of negative radians.

Aperture measured from both vertical and horizontal scanline surveys has a positive correlation with persistence in sandstone (R = 0.81 and 0.77 respectively), and aperture measured horizontally correlated with spacing measured vertically (R = 0.89) and block area (R = 0.82). The classified aperture from sandstone beds correlated with spacing measured horizontally (R = 0.85), and joint frequency measured both horizontally and vertically (R = -0.79 and -0.70 respectively). These scatterplot graphs are all presented in Figure 6.4. All of these correlations may broadly imply that as the size of intact rock blocks increases, the aperture of discontinuities bounding the intact rock can also increase. Observationally, very small blocks would fall from the cliff face before apertures could get as wide as the apertures observed in thicker-bedded sandstone blocks. However, aperture of the described cliff rock masses did only vary over a relatively small range (0.1 to 15 mm) which adds some questionability to these calculated relationships.

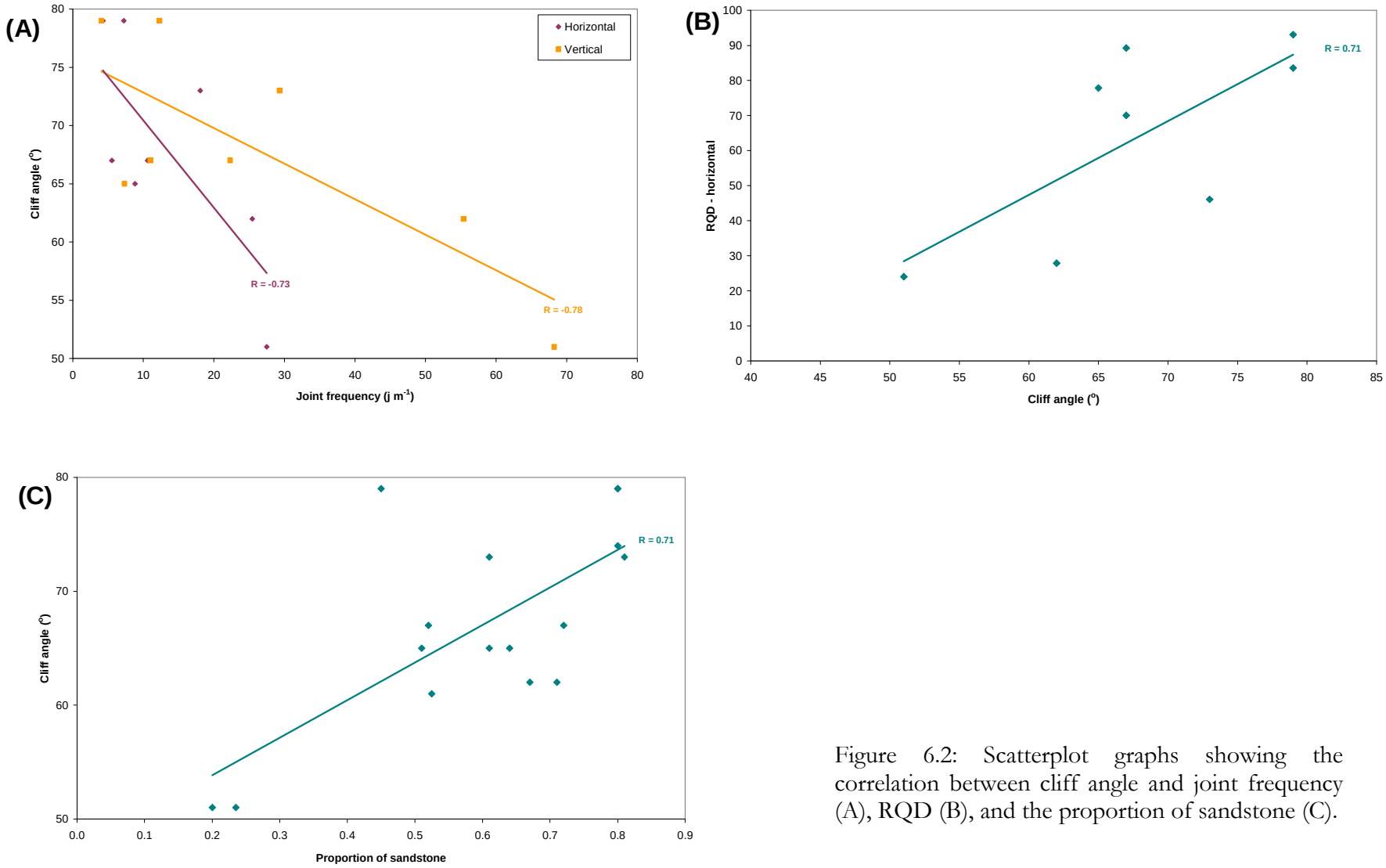

Figure 6.2: Scatterplot graphs showing the correlation between cliff angle and joint frequency (A), RQD (B), and the proportion of sandstone (C).

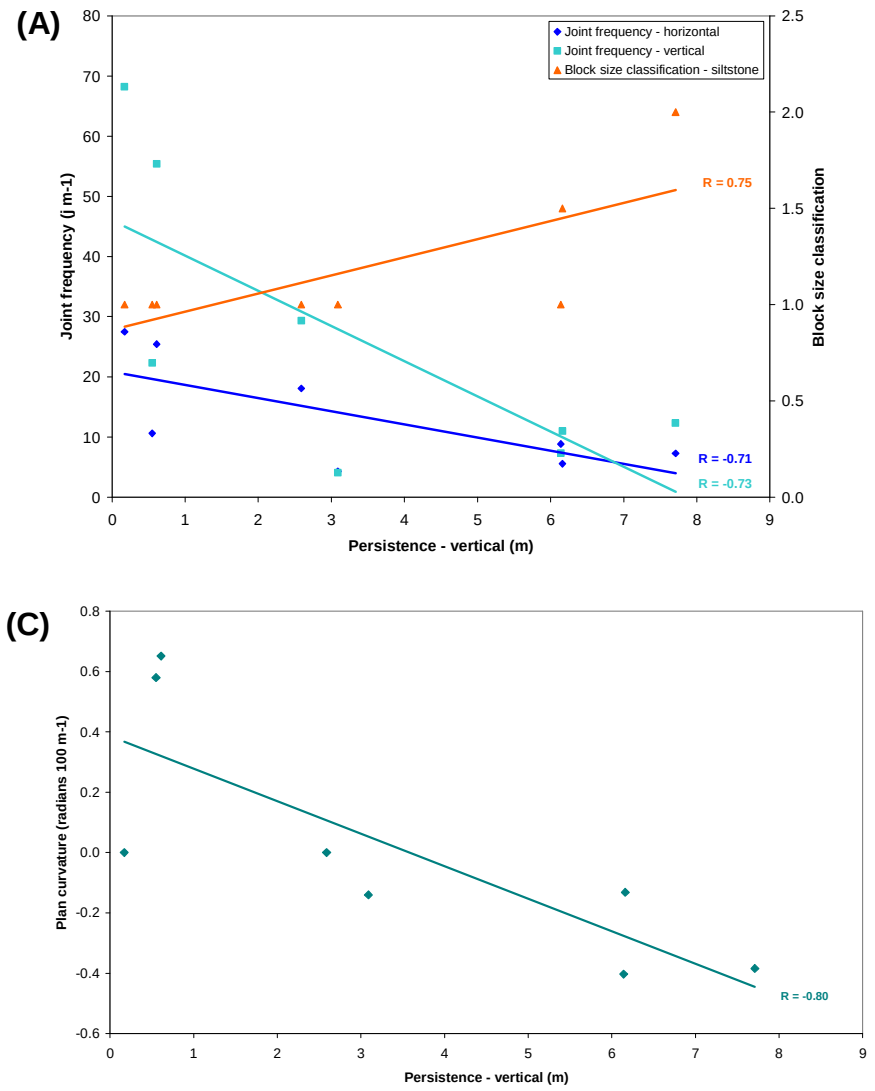

Figure 6.3: Scatterplot graphs showing the correlation between persistence, joint frequency, and block size classification (A), persistence and elevation (B), and persistence and plan curvature (C).

157

The dip of beds has a correlation with properties of the discontinuities including persistence and aperture, and the RMS and aRMR classification systems (Figure 6.5). For the database, beds dipping landward were recorded as negative values and beds dipping seaward were recorded as positive values. Vertically measured persistence ($R = -0.79$) and horizontally measured aperture ($R = -0.79$) decrease as beds dip further seaward (Figure 6.5A). This could imply that as beds dip steeper seaward, out of the cliff, discontinuities become less continuous and have tighter apertures or this may be a purely statistical error as a result of the small population size used. From observations at the cliff sites it appears that as stress is relieved from the beds exposed at the cliff face, particularly when beds dip steeply seaward, the intact rock loosens resulting in the production of low persistent joints and the breaking of previous persistence joints, as well as causing apertures to widen. The widening of apertures is converse to the results of the correlation analysis.

Rock Mass Strength measured from vertical scanlines has a very significant negative correlation with dip angle ($R = -0.88$) suggesting that as the beds dip further seaward the rock mass strength decreases (Figure 6.5B). The horizontally measured RMS does not have any significant correlation with bed dip so makes the correlation with vertical RMS difficult to justify. However, it holds true that RMS is reduced by unfavourable discontinuity parameters such as wider aperture. The adjusted Rock Mass Rating however shows a very significant negative correlation with bed dip both vertically ($R = -0.87$) and horizontally ($R = -0.89$). This suggests that for the entire cliff section the rock mass quality is reduced as bed dip increases. Because no correlation is shown between bed dip and the basic RMR, the orientation of the joints in combination with bed dip could be implied as a controlling factor of rock mass quality or simply a result of the methodology.

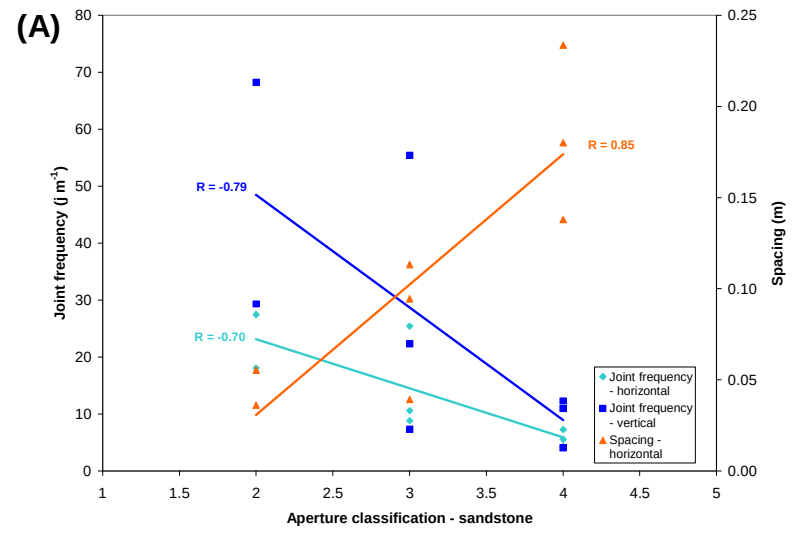

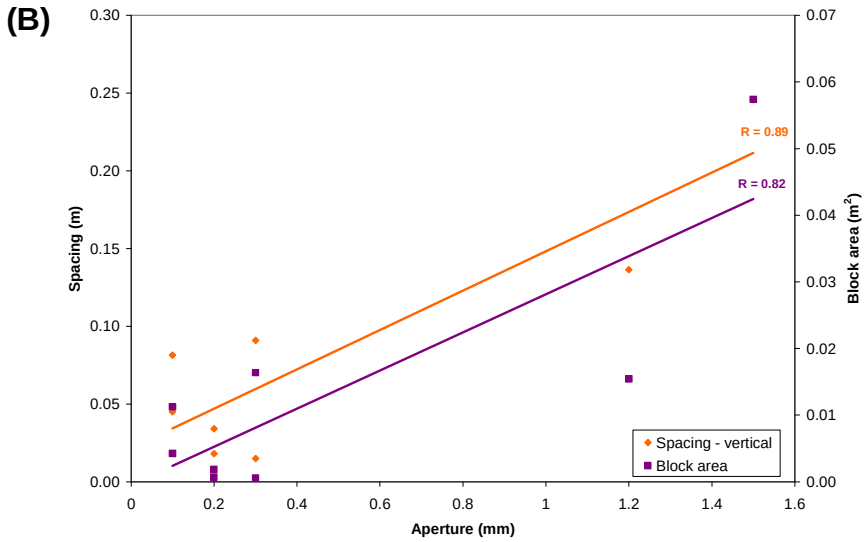

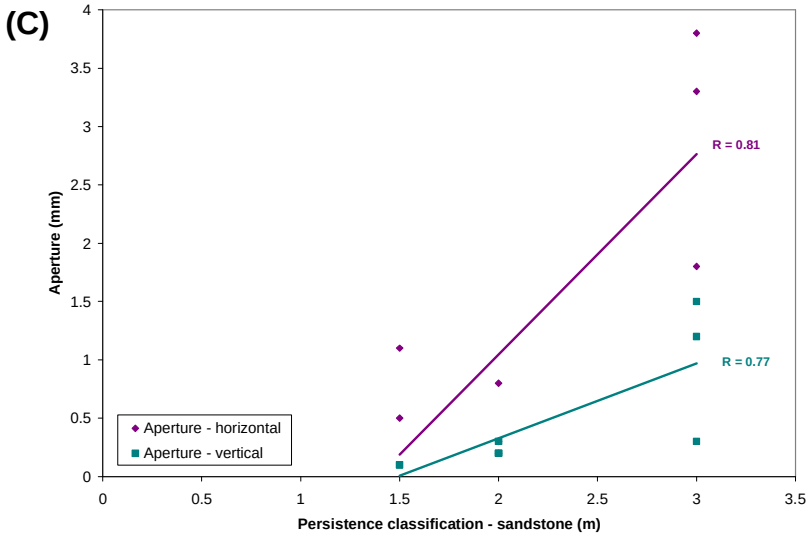

Figure 6.4: Scatterplot graphs showing the correlation between aperture, joint frequency and spacing (A), aperture, spacing and block area (B), and aperture and persistence (C).

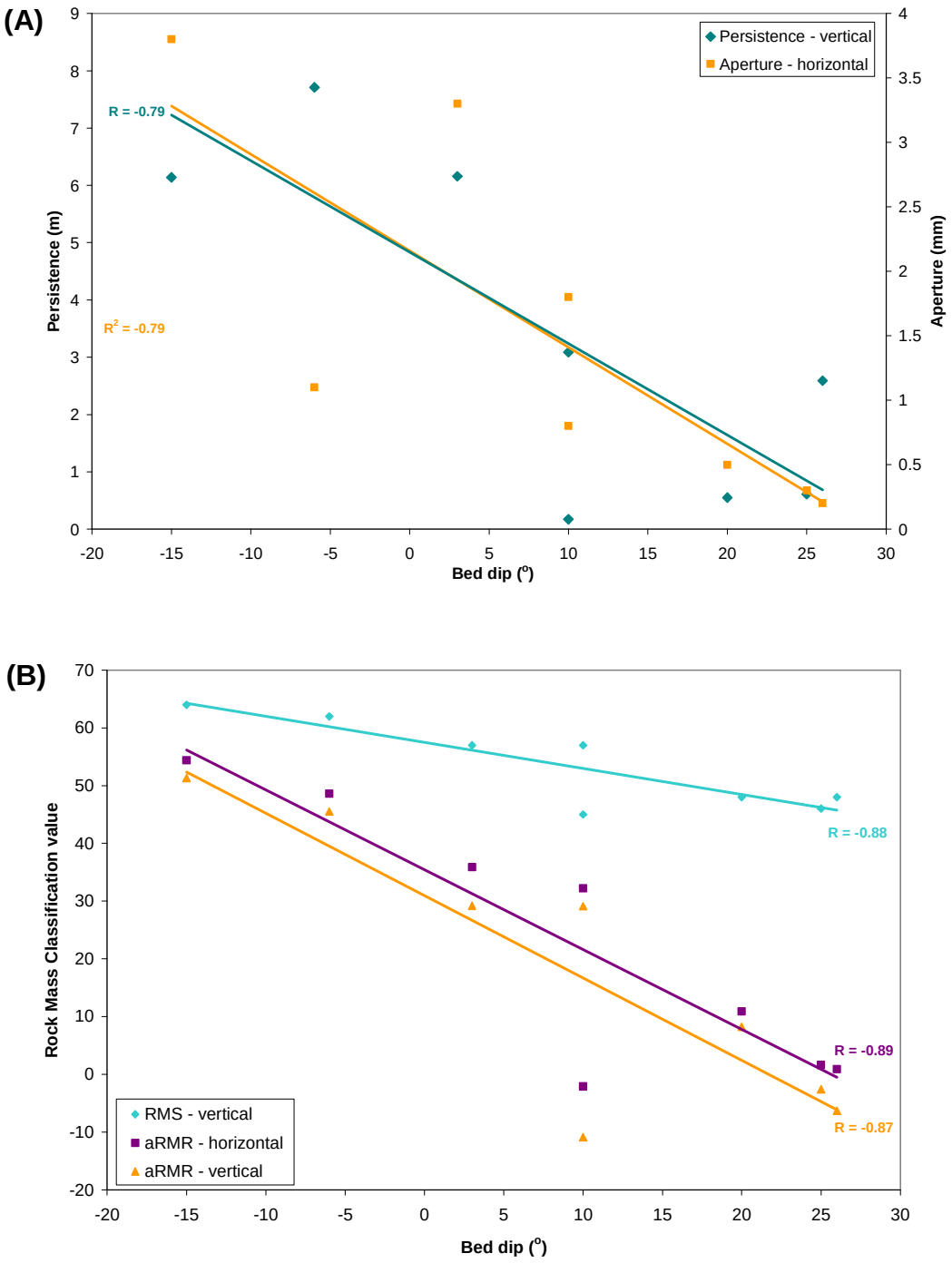

Figure 6.5: Scatterplot graphs showing the correlation between bed dip and persistence and aperture (A), and rock mass classification systems (B).

6.2.3.3 Bulk rock properties

Bulk density and intact rock strength show an increasing trend northwards (R = 0.85 to 0.88); porosity is inversely related (R = -0.90). There is also confirmation that as bulk density in the rock increases so too does the intact strength of the rock (R= 0.81 to R = 0.86). Siltstone strength correlates well with rock mass parameters calculated for siltstone beds (R = 0.80 to 0.93) and all of the bulk rock parameters correlate with the global rock mass strength measured for sandstone and siltstone rock masses (R = 0.71 to 0.92) (Figure 6.6). The bulk density and intact rock strength correlate very significantly with the aRMR, the RMS (vertical measurement only) and, to a less significant extent, with RQD. Certainly for the aRMR classification, intact rock strength was a property that was part of its calculation, and because bulk density correlates very significantly with intact rock strength, it has a similar relationship. The RMS classification used Schmidt Hammer measurements which also had an increasing trend northwards.

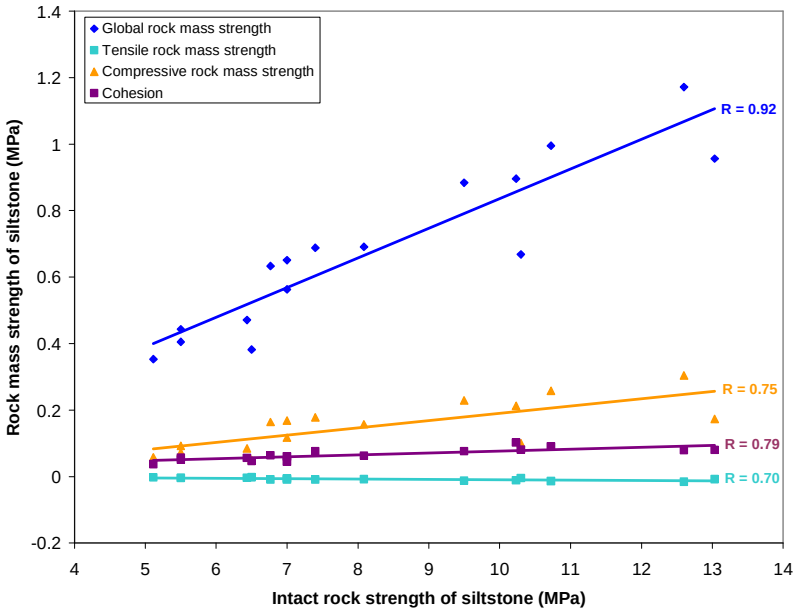

Figure 6.6: Scatterplot graph showing the correlation between intact rock strength and rock mass strength parameters.

A range of climate parameters including temperature, solar radiation, rainfall and wind speed, correlate with all the bulk rock parameters but this can be explained by the same climate parameters also having a northwards trend.

6.2.3.4 Rock mass classifications

Rock mass classification systems determine the overall quality of the rock mass with regards to slope stability and strength. Any correlations found with these parameters may imply what parameters are influencing rock mass quality and vice versa. Many rock mass classification systems correlate well with many of the discontinuity parameters including vertically-measured persistence, and horizontally-measured aperture and spacing. These correlations are not seen as being significant with respect to slope stability because the discontinuity parameters are themselves used in the calculation of the classification values.

All of the rock mass classification systems, with the exception of GSI, correlate well with geomorphology parameters sourced from GIS surfaces, including plan and profile curvature of the land, and aspect. These geomorphology parameters are negatively correlated to rock mass classification implying that as the rock mass quality improves, the slope curvature (profile) and the contour curvature (plan) of the land decreases, and the aspect of the slope decreases (moves to a more northerly aspect). The profile curvature correlated significantly with the most other parameters, as shown in Figure 6.7.

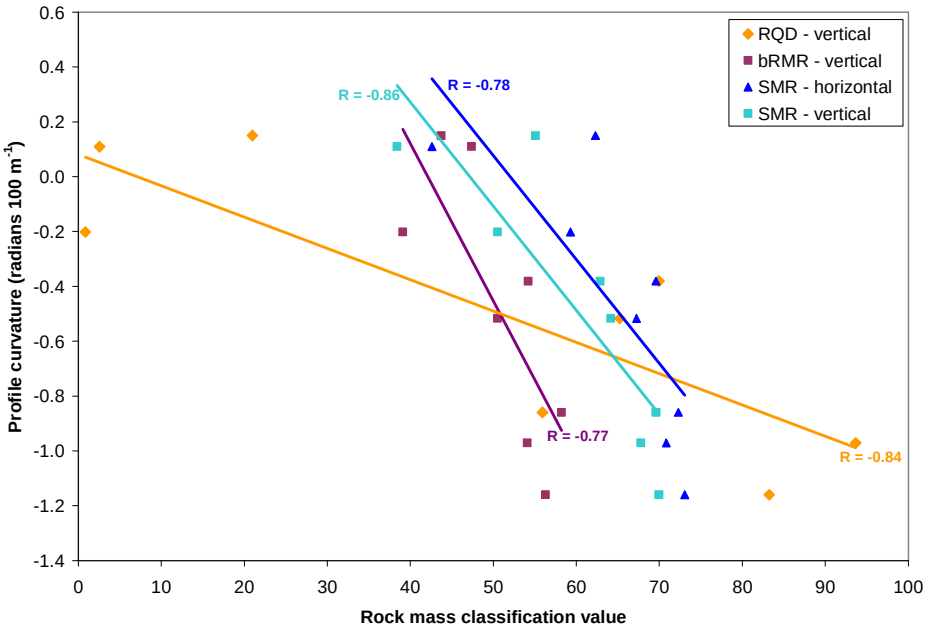

Figure 6.7: Scatterplot graph showing the correlation between various rock mass classification parameters and profile curvature of the land.

The bRMR classification system also shows a negative correlation with some climate parameters, namely average daily temperature (R= -0.71 and -0.81 for horizontal and vertical measures respectively), January solar radiation (R= -0.70), and average January and average October wind speed (R= -0.73 and -0.74 respectively) for horizontally-measured bRMR. The negative correlation implies that rock mass quality improves as climatic elements weaken; that is, less wind, less solar radiation, and lower temperatures. However due to the small dataset and the different methods for determining rock mass classification parameters (from site specific field measurements) and GIS-sourced climate and geomorphic parameters (cell-averaged), the physical reality of this relationship is questionable.

6.2.3.5 Rock mass parameters

Rock mass parameters include cohesion, friction angle, tensile strength, compressive strength, global rock mass strength, and the deformation modulus measured for sandstone beds, siltstone beds and heterogeneous rock masses. Overall, the strongest correlations are with the rock mass parameters measured from heterogeneous rock masses. These include: horizontal and vertical spacing, block area, horizontal and vertical joint frequency, and horizontal and vertical RQD. Tensile strength commonly shows a negative relationship with these parameters because it has a negative value itself. All of these parameters are to do with the size of individual blocks within the cliff rock mass which is part of the criteria for determining GSI for heterogeneous rock masses. Furthermore, the GSI value is used in part to determine the rock mass parameters. Global rock mass strength for sandstone (R = 0.90) and siltstone (R = 0.86) show an increasing trend northwards, as discussed previously.

The annual water deficit, water balance ratio, rainfall and solar radiation correlate repeatedly with the rock mass parameters measured for heterogeneous rock masses. That is, cohesion, compressive rock mass strength, and tensile rock mass strength increase as the abovementioned parameters decrease. This may broadly imply that an increase in water and/or solar radiation to the cliff rock mass, may act to reduce the rock mass strength.

However, as the global rock mass strength for sandstone and siltstone rock masses increase, the climate parameters of solar radiation, rainfall, temperature and wind speed also increase. These contradictions suggest that these relationships are unlikely to be realistic.

6.2.3.6 GIS-sourced parameters

There are numerous significant correlations between various climate, geomorphic and terrain parameters sourced from GIS surfaces. The specific GIS-sourced parameters that have an increasing trend northwards include: annual June solar radiation (R = 0.92); mean annual solar radiation (R = 0.78); average daily solar radiation (R = 0.94); minimum temperature of the coldest month (R = 0.71); total rainfall (R = 0.78); average daily wind speed (R = 0.88); average April wind speed (R = 0.95); average July wind speed (R = 0.91); and slope in degrees (R = 0.70). The climate relationships were illustrated in earlier in Figure 6.1. Slope shows a correlation with northing coordinates in that the gradient of the landmass (not the slope of the cliff face) gets steeper northwards (Figure 6.8). This may be a result of increasing intact strength (and therefore, potentially durability) and global rock mass strength in more northern volcanogenic rocks, as well as the orogenesis of the mountain ranges in the north Auckland region compared to the lowland harbour areas of the central Auckland isthmus.

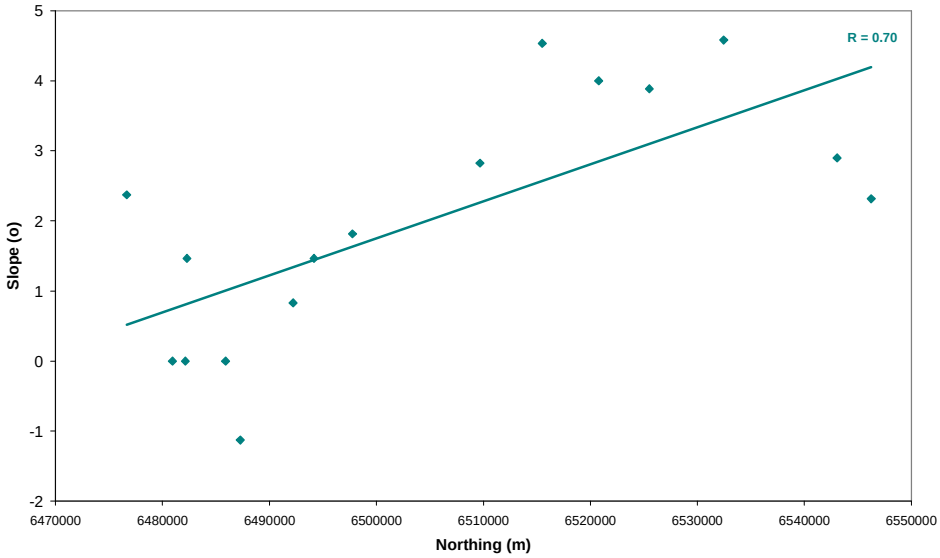

Figure 6.8: Scatterplot graph showing the correlation between northings versus slope of the land.

There are also a number of GIS-sourced parameters that inter-correlate, in particular terrain parameters, which contribute to the appreciation of the physical and hydrological structure of the landmass behind the coastal cliffs. These parameters include annual water deficit, water balance ratio, stream power index and the flow path length. Slope correlated significantly with annual water deficit (R = -0.77) and the water balance ratio (R = 0.74) (Figure 6.9). This highlights that as slope increases, the loss of water from the land decreases. No other parameters show any significant relationship to the key properties of coastal cliff geomorphology and erosion, thus do not need to be discussed any further.

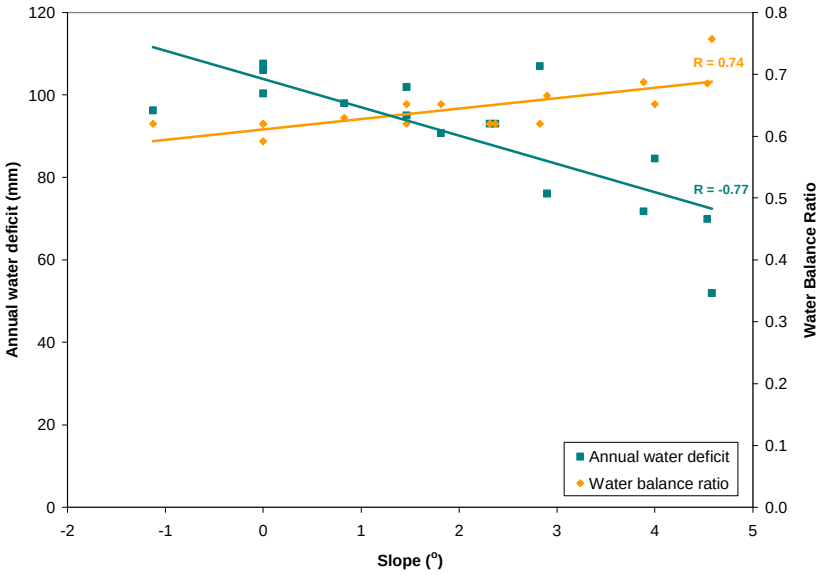

Figure 6.9: Scatterplot graph showing the correlation between slope and annual water deficit, and slope and the water balance ratio.

6.2.4 Summary of correlation and regression analysis

The only linear relationships found for the key hazard assessment parameters are with cliff angle, in that cliff angles are low where joint frequency is higher and the proportion of sandstone is lower. Parameters that show an increasing northward trend include intact and rock mass strength, bulk density and climate conditions. Discontinuity persistence and aperture held a number of relationships with other discontinuity parameters and geomorphic parameters. Rock mass classification systems correlated to geomorphic parameters, particularly profile curvature. Slope of the land increased northwards and was correlated to the water deficit on land.

6.3 Student T-tests (testing differences between means)

6.3.1 Methodology

The student t-test assesses the evidence provided by the data in favour of some claim about the population and by definition this is a test of significance (Moore and McCabe, 2003). Thus the student t-test can be used to determine the significance of the difference between the means of two samples; for the purposes of this study the parameter to be tested was separated into two sample means. The t-test is a broader method than correlation and regression analysis yet is still a statistically accurate one for estimating what parameters from the database may have an influence on others. The results of a test are expressed in terms of a probability value that measures how well the data and the null hypothesis agree (Moore and McCabe, 2003). The null hypothesis is that there is no difference between the two sample means. A smaller probability value implies that there is stronger evidence, provided by the data, against the null hypothesis; that is, there is a difference between the two sample means. Student t-tests assume a normally distributed data set (Moore and McCabe, 2003). In this study, probability values less than 0.12 (or 12 %) were chosen arbitrarily as the cut-off because of the small population size, and this means that 88 % of the population fits with the alternative hypothesis that the sample means are significantly different.

The student t-test was carried out on five of the parameters from the database. Three are key parameters of hazard assessments including erosion rate, cliff height and cliff angle. Bed dip was tested because observation of field data implied that it was an influence on erosion rates. Geology was tested based on variation between the volcanic-poor East Coast Bays Formation and the volcanic-rich Pakiri Formation, because a number of intact and rock mass parameters showed variation between these site locations. For each test the entire database was split (by site location) into the two samples arbitrarily determined for the tested parameter. For instance, in the first test, the parameter 'platform width' was split into site locations with platform widths < 100 m and site locations with platform widths > 100 m.

For this test, all of the other parameters in the database were split in the same way as the platform width parameter was (by site location), such that the t-test would determine what parameters from the database are associated with narrow (< 100 m) or wide (> 100 m) shore platform widths. Each test and their associated samples are listed in Table 6.2

Table 6.2: Student t-tests carried out on key parameters from the Waitemata Group coastal cliff database. ECB = East Coast Bays.

Parameter	Sample 1	Sample 2
1. Platform width	Width < 100 m	Width > 100 m
Erosion rate	Erosion < 13 mm y^{-1}	Erosion > 13 mm y^{-1}
2. Dip of beds	Beds dip landward	Beds dip seaward
Platform width	Width < 55 m	Width > 55 m
Erosion rate	Erosion < 8 mm y^{-1}	Erosion > 8 mm y^{-1}
3. Lithology version 1	ECB Formation	Pakiri Formation (Army Bay not incl.)
Lithology version 2	ECB Formation	Pakiri Formation (Army Bay included)
4. Cliff height	Height < 20 m	Height > 20 m
5. Cliff angle	Angle < 70°	Angle > 70°

In test 1, the platform width split equals a split at 13 mm y^{-1} for erosion rates; erosion rates are synonymous with platform width. In test 2, the split is based on beds dipping landward or seaward. A division of the sites into those with beds dipping landward and those with beds dipping seaward corresponded to a division of platform width of 55 m. This test can thus also be seen as a test of the significance between the means of platform widths less or more than 55 m and erosion rates less or more than 8 mm y^{-1}. In test 3, geology was split based on the northing coordinates of site locations. Two separate analyses were carried out to see if there was any difference between whether Army Bay was classified as belonging to the East Coast Bays Formation or belonging to the Pakiri Formation. This stems from the various placements of the boundary between the two Formations in the literature (refer to section 2.2.2). Tests 4 and 5 are split arbitrarily but are based on observations made during fieldwork on what defines 'low' and 'high' cliff heights and angles.

6.3.2 Results

The significant results from the five t-tests are presented separately with the level of significance displayed as the p-value and also as a percentage. The p-value of the parameter that a test is based on is also presented to prove the significance of the split of the data set. A lower p-value implies that the split resulted in two significantly different means; this is placed above the dashed line on the results table for each test.

6.3.2.1 Test 1 - Platform width and erosion rate

This test was to determine if there were any parameters whose mean was significantly different based on whether erosion rates were slower (less than 13 mm y^{-1}) or faster (greater than 13 mm y^{-1}). The parameters listed in Table 6.3 had significantly different means based on this split.

Table 6.3: Results of test 1

Platform width/Erosion rate	p value	p %
Erosion rate	0.002	0.2
Shore platform width	0.002	0.2
Bed dip	0.011	1.1
RMS H	0.036	3.6
Dip direction	0.094	9.4
Average daily maximum temperature	0.117	11.7
Soil drainage	0.120	12.0

The p-values for shore platform width and erosion rate are both 0.2 % which verifies that there is 99.8 % probability that the data for both parameters is from two separate means. Bed dip is the parameter with the lowest probability value (1.1 %) and this implies that it is the parameter that varies most significantly based on whether shore platforms are relatively narrow or wide. When beds dip landward into the cliff face, shore platform width and erosion rates are lower; the average erosion rate is 4.0 mm y^{-1}. When beds dip seaward, shore platform widths and erosion rates are greater and the average erosion rate is 19.5 mm y^{-1}. The correlation analysis results showed that as bed dip increased further seaward, rock mass quality measured from the aRMR and vertically-measured RMS decreased. T-test results show that horizontally-measured RMS also has a significant difference depending on whether shore platform widths are relatively narrow or wide (p = 3.6 %).

This may imply that wider platforms are broadly associated with weaker rock masses. The dip direction of the cliff face also varies significantly based on the shore platform width (p-value = 9.4 %)

The significance of daily temperature and soil drainage differing based on the shore platform width are questionable because temperature shows a general increasing trend northwards (based on correlation analysis) and soil drainage is quantified by a classification scheme rather than physically measured values.

6.3.2.2 Test 2 - Dip of beds

Because bed dip is the parameter which varied most significantly based on shore platform width and erosion rate, the entire data set was then split into the sites which had beds dipping landward, and the sites which had beds dipping seaward for test 2 (Table 6.4). Shore platform width and erosion rate as parameters were automatically then split based on the dip of beds seaward or landward as the initial split of 100 m platform width and 13 mm y^{-1} erosion rate in test 1 was only arbitrary. The split based on bed dip has resulted in the probability values of shore platform width and erosion rate, being from different populations, decreasing slightly as the probability percentage is now 1.1 %, compared to 0.2 % for the initial split.

Table 6.4: Results of test 2

Bed dip	p value	p %
Bed dip	0.001	0.1
Shore platform width	0.011	1.1
Erosion rate	0.011	1.1
RMS V	0.020	2.0
aRMR V	0.022	2.2
aRMR H	0.023	2.3
Persistence V	0.035	3.5
GSI S	0.051	5.1
Profile curvature	0.054	5.4
UCS Z	0.064	6.4
Global rock mass strength Z	0.071	7.1
Average daily wind speed	0.078	7.8
Deformation modulus S	0.079	7.9
Average April wind speed	0.103	10.3
GSI Htg	0.107	10.7
Compound topographic wetness index	0.112	11.2
Tensile rock mass strength S	0.115	11.5

This test identifies that bed dip is the strongest influence on coastal cliff erosion rates and shore platform development as it generates a very low probability value of 0.001. Thus, there is a 99.9 % probability that the shore platform width and erosion rate represent two different means when divided on the basis of seaward or landward dipping beds.

Some of the rock mass parameters vary significantly based on whether beds are dipping seaward or landward; these include global rock mass strength of siltstone (7.1 %), the deformation modulus of sandstone (7.9 %), and tensile rock mass strength of sandstone (11.5 %). The intact rock strength of siltstone was also significantly different depending on the dip of beds with a probability of 6.4 %. Strength plays an important role in rock mass quality and therefore as beds dip further seaward the strength of the rock mass could be reduced through stress release, leading to enhanced erosion. Rock mass classification values of the aRMR, RMS (vertically measured) and GSI (sandstone and heterogeneous rock masses) also have significantly different means when sites are split into seaward and landward dipping beds, meaning that relatively low rock mass quality for these schemes is associated with seaward dipping beds, and thus higher erosion rates.

The values for RMS measured from horizontal scanline surveys however do not have a significant relationship with bed dip and erosion rates. The components of the RMS system that have variation between vertical and horizontal scanline surveys at individual sites are discontinuity width (at Martins Bay and Waiake Bay), continuity and infill (Waiake Bay), intact rock strength (Waiwera Beach and Leigh Marine Reserve), and joint spacing (Castor Bay). Intact rock strength and joint spacing have the largest numerical difference between horizontal and vertical scanline surveys so are likely to be the statistical reason for the comparatively poor relationship between horizontal measured scanline surveys and bed dip. Also, as a purely observational note, horizontal scanline surveys did not often pass through siltstone beds where as vertical scanline surveys always passed through siltstone and sandstone beds, thereby including the closely spaced, weaker nature of the siltstone to the overall rock mass quality. A larger population size of the database would help to statistically confirm these observations.

Various measures of wind speed had significantly different means based on the split of the sites (p-values ranged from 7.8 % to 10.3 %). These results have to be deemed valuable and it is possible that wind strength does influence the rate of continual retreat through the clearing of loose debris (especially siltstone) from the cliff face, however the dominance of this parameter is questionable. Wind strengths recorded from the GIS database only ranged from 12.1-14.8 km h^{-1} for average daily wind speed, 10.8-15.1 km h^{-1} for average April wind speed, and 11.0-15.2 km h^{-1} for average July wind speed. This only varies from grade 2 to 3 (or from a light breeze to a gentle breeze) on the Beaufort Scale of wind strength so is difficult to justify the importance of wind strength as an erosion mechanism.

6.3.2.3 Test 3 - Geology

The correlation and regression analysis highlighted many parameters that vary depending on their location, with parameters such as intact and rock mass strength and bulk density showing positive relationships as site locations moved further north. As such the entire dataset was split firstly into southern sites from the East Coast Bays Formation (including Army Bay, from Edbrooke, 2001), and northern sites from the Pakiri Formation (excluding Army Bay) and then secondly into sites from the East Coast Bays Formation (excluding Army Bay, from Allen, 2004), and sites from the Pakiri Formation (including Army Bay). The results are presented in Table 6.5. Numerous parameters show a significant variation in their means when split based on geology. Of great significance are those parameters that have probability percentages less than 2 %, which are listed above the dot-and-dash line in the results table.

The results most interestingly highlight that the sample means do vary depending on whether Army Bay is classified as East Coast Bays Formation Rock or Pakiri Formation rock. The parameters that only show variation by a small fraction, such as the intact rock strength of siltstone which has a probability value of 0.1 % for version 1 and 0.0 % for version 2, are considered to be insignificant based on the classification of Army Bay. The results are considered to be significant where probability values for the same parameter differ by approximately > 2 %. Version 1 has more parameters that have significant difference of < 2 % in their sample means. The following parameters show

great variation between the two different test versions: cohesion of siltstone, average solar radiation, compound topographic wetness index, compressive rock mass strength of sandstone, and minimum temperature of the coldest month. The remaining parameters, > ~ 5 % probability of version 1, do not have any significance in version 2. The parameters of stream power index, RMS measured vertically, and length slope factor have a significant difference based on southern East Coast Bays Formation locations and northern Pakiri Formation locations which include Army Bay from version 2, but are not significant parameters in version 1.

Table 6.5: Results of test 3.

Geology version 1	p value	p %	**Geology version 2**	p value	p %
Northing	0.000	0.0	Northing	0.000	0.0
Air-dried bulk density	0.000	0.0	Air-dried bulk density	0.000	0.0
Oven-dried bulk density	0.000	0.0	Oven-dried bulk density	0.000	0.0
Porosity	0.000	0.0	Porosity	0.000	0.0
Annual water deficit	0.000	0.0	UCS Z	0.000	0.0
Average June solar radiation	0.000	0.0	Average June solar radiation	0.000	0.0
Slope	0.000	0.0	Slope	0.000	0.0
Total rainfall	0.000	0.0	Average daily solar radiation	0.000	0.0
Average daily wind speed	0.000	0.0	Average daily wind speed	0.000	0.0
Average April wind speed	0.000	0.0	Average April wind speed	0.000	0.0
Average July wind speed	0.000	0.0	Average July wind speed	0.000	0.0
Global rock mass strength ZST	0.001	0.06	Cohesion ZST	0.001	0.08
Global rock mass strength SST	0.001	0.09	Global rock mass strength Z	0.001	0.1
UCS S	0.001	0.1	UCS S	0.003	0.3
UCS Z	0.001	0.1	Total rainfall	0.003	0.3
Average daily solar radiation	0.001	0.1	Global rock mass strength S	0.004	0.4
Average daily maximum temperature	0.001	0.1	January solar radiation	0.006	0.6
January solar radiation	0.001	0.1	Annual water deficit	0.007	0.7
Compressive rock mass strength Z	0.003	0.3	Average daily max temp	0.010	1.0
Slope in percent	0.003	0.3	October vapour pressure deficit	0.011	1.1
Tensile rock mass strength Z	0.005	0.5	Slope in percent	0.011	1.1
Water balance ratio	0.005	0.5	Average daily vapour pressure deficit	0.012	1.2
October vapour pressure deficit	0.005	0.5	Soil drainage	0.016	1.6
Cohesion Z	0.006	0.6	Compressive rock mass strength Z	0.017	1.7
Solar radiation average	0.010	1.0	Mean annual solar radiation	0.020	2.0
Cohesion S	0.017	1.7	Water balance ratio	0.021	2.1
Mean annual solar radiation	0.025	2.5	Tensile rock mass strength Z	0.024	2.4
Average daily vapour pressure deficit	0.025	2.5	Cohesion S	0.026	2.6
Compound topographic wetness index	0.031	3.1	Solar radiation average	0.040	4.0
Compressive rock mass strength S	0.043	4.3	Compound topographic wetness index	0.066	6.6
Solar radiation July	0.045	4.5	Minimum temperature coldest month	0.085	8.5
Min temp coldest month	0.051	5.1	Stream power index	0.099	9.9
Global rock mass strength Htg	0.054	5.4	RMS V	0.100	10
Friction angle Z	0.090	9.0	Compressive rock mass strength S	0.119	11.9
Tensile rock mass strength Htg	0.093	9.3	Length slope factor	0.119	11.9
Persistence classification S	0.098	9.8			
Compressive rock mass strength Htg	0.103	10.3			
Cohesion Htg	0.104	10.4			
Tensile rock mass strength S	0.105	10.5			

6.3.2.4 Cliff height

Test 4 involved splitting the entire data set based on sites that had cliff heights < 20 m and sites that had cliff heights > 20 m and the significant results are presented in Table 6.6. The p-value for cliff height, based on the arbitrary split of 20 m, was 0.2 % which implies a valid segregation of the data.

Table 6.6: Results of test 4.

Cliff Height	p value	p %
Cliff height	0.002	0.2
Length slope factor	0.003	0.3
Stream power index	0.003	0.3
Friction angle Z	0.008	0.8
Aperture classification S	0.014	1.4
Slope in percent	0.042	4.2
Weathering	0.066	6.6
Deformation modulus Z	0.082	8.2
Friction angle S	0.103	10.3
Aperture V	0.105	10.5
GSI Z	0.105	10.5
Spacing classification S	0.115	11.5

There are several geomorphic, terrain and structural parameters of the coastal cliffs that have significant variation in their means based on whether cliff heights are relatively lower or higher. The geomorphic and terrain parameters include length slope factor, stream power index and slope in percent. The length slope factor estimates rill and sheet erosion by an equation for soil loss and thus implies that for relatively high cliffs (> 20 m) and associated cliff-top land, soil loss through rill and sheet erosion is higher; the probability for this is 0.3 %. The stream power index is another ratio that measures the strength of streams and can thereby indicate erosive abilities and again p = 0.3 %. Slope (in percent) determines the slope in the steepest downslope direction in the vicinity of the cliff site and slopes are relatively steeper where cliffs are relatively higher (p = 4.2 %). Note that the slope in percent has been averaged from the entire measured extent of the cliff-base to cliff-top of the site locations so is not directly linked to the cliff height measured from the described cliff section.

The structural parameters of aperture and spacing (both classifications for sandstone) are significantly lower for relatively lower cliff heights (p = 1.4 % and 11.5 % respectively).

Thus higher cliffs are associated with wider joint spacing and wider aperture. Aperture values (measured vertically) are conversely lower when cliff heights are relatively higher (p = 10.5 %). However, because the range of values for the classified parameters is small, no sound relationship can be concluded. The aperture values measured vertically are perhaps more reliable because they are sourced from detailed scanline survey data but the probability of the difference in the two means is higher than for classified aperture. The weathering grade of the cliff face shows significant variation, with weathering being more advanced where cliff heights are relatively higher. However, weathering only differed between a grade 2 for slightly weathered rock masses and a grade 3 for moderately weathered rock masses so the reliability of the probability value for this parameter is also questionable.

Friction angle for siltstone and sandstone rock masses individually are relatively higher for relatively lower cliff heights (p = 0.8 % and 10.3 % respectively). The deformation modulus of sandstone is also higher for relatively lower cliff heights (p = 8.2 %). The rock mass quality of siltstone, determined from GSI, is higher when cliff heights are lower (p = 10.5 %).

6.3.2.5 Cliff angle

The fifth test involved splitting the entire dataset based on cliff angles < 70^{o} and cliff angles > 70^{o} and results are presented in Table 6.7. Although this was an arbitrary split the p-value for cliff angle was at least less than 0.001 % which implies a valid segregation of the data. The friction angle of heterogeneous rock masses is higher when cliff angles are relatively steeper (p = 3.9 %). Other rock mass parameters from heterogeneous rock masses also show significant variation based on lower or higher cliff angles including the deformation modulus (p = 5.1 %), compressive rock mass strength (p = 6.8 %), global rock mass strength (p = 7.5 %), and cohesion (p = 10.4 %). Thus, flatter cliff angles have overall lower rock mass strength and deformability. This may also mean that stronger rock masses allow the development of relatively steeper cliff faces, which was highlighted in the correlation analyses of the described cliff sites.

Table 6.7: Results of test 5.

Cliff Angle	p value	p %
Cliff angle	0.000	0.0
Friction angle Htg	0.039	3.9
Deformation modulus Htg	0.051	5.1
Proportion of sandstone	0.065	6.5
Weathering	0.066	6.6
Compressive rock mass strength Htg	0.068	6.8
Land elevation	0.068	6.8
Global rock mass strength Htg	0.075	7.5
Cliff height	0.101	10.1
Cohesion Htg	0.104	10.4
GSI Htg	0.120	12.0

The proportion of sandstone (p = 6.5 %), weathering (p = 6.6 %), and land elevation (p = 6.8 %) all have similar probability values for their means differing based on low or high cliff angles. The proportion of sandstone was previously determined in Chapter Four to influence cliff angles as thick sandstone beds with thin siltstone beds produce steep cliffs, and siltstone dominated cliffs have the lowest angles; and this was further supported by correlation analysis. As for cliff heights, weathering also shows significant variation between flatter and steeper cliff angles and this is understandable because as rock material becomes more weathered, it degrades into smaller particles and falls from the cliff surface, resulting in lower angle as the cliff moves towards a stable equilibrium. Also, enhanced weathering results in reduced intact rock strength. However, removal of the debris by wave action in sites that have more weathered rock would hinder the development of flatter cliff angles, and as previously mentioned the weathering classification of the sites did only vary between grade 2 and grade 3. Elevation of cliff-top land, and also cliff height, showed significant variation between flatter and steeper cliff angles (6.8 % and 10.1 % respectively). The elevation measurements were sourced from a GIS database and are not direct measurements of the elevation at the cliff-top edge but are measurements of the land elevation within the 25 m x 25 m cell that the cliff base GPS points fitted in. This is the first time this relationship has been made during the study, as field observations and correlation analysis did not pick up the trend. However, the role of student t-tests to compare the significance of two means rather than find direct correlations may mean that lower cliff angles do develop where land elevations, and subsequently cliff heights, are lower.

6.3.3 Summary of student t-test analysis

Bed dip is the most probable parameter to differ depending on whether shore platform widths are relatively wide or relatively narrow. This means that erosion rates are higher where beds dip seaward and lower where beds dip landward. When data were split into sites that had seaward dipping beds and sites that had landward dipping beds, the aRMR and RMS classification schemes highlighted that rock mass quality is reduced when beds dip seaward. Intact and global rock mass strength of siltstone is also reduced when beds dip seaward. Numerous parameters show variation depending on whether sites are from the southern East Coast Bays Formation or the northern Pakiri Formation. This highlights that the change in volcanogenic content as sites move northward, and the more open coast in the north affects properties of the coastal cliffs. Lower cliff heights are associated with higher soil erosion, wider joint spacing and narrower joint aperture. Relationships with the slope parameter suggest that cliff height is mainly controlled by the surrounding geomorphology. Cliff angle is controlled by the proportion of sandstone to siltstone (whereby lower cliff angles are more siltstone-dominated), weathering, land elevation and cliff height, and rock mass strength as determined from the GSI classification chart for heterogeneous rock masses.

6.4 Multiple Linear Regression

Multiple linear regression is a statistical method used to predict a single response variable from two or more explanatory variables (Moore and McCabe, 2003). For this research the response variable would be cliff erosion rates or shore platform width and the explanatory variables would be all the other measured parameters that have a significant linear influence on cliff erosion rates. Because the general notion is held that erosion of coastal cliffs in Waitemata Group rock is a result of a number of processes acting separately or together (Brodnax, 1991) then this form of statistical analysis, initially, appears to be appropriate.

Brodnax (1991) developed a multiple linear regression model to determine erosion rates of Waitemata Group coastal cliffs and found the following seven explanatory parameters to have the strongest ability to predict the response variable, erosion rate:

1) width of shore platform (m);
2) the rock mass strength classification for groundwater from Selby (1993);
3) aspect of the cliff (if the bearing from the cliff is between 120^{o} and 200^{o} or not);
4) beach (if there is a beach at the base of the cliff or not);
5) strike (if geological strike is oriented the same direction as the coastline or not);
6) wave regime (if the regime is of a sheltered non-harbour or not);
7) rock type (if the rock type is Parnell Grit or not).

Five of these parameters were classified variables and in order for them to be able to be analysed linearly they had to be reconstructed as dummy variables (following Clark and Hosking, 1986). The classified values are given a score of either 1 or 0 (the dummy variable) based on the presence or absence of a given parameter, such as a beach at the base of a cliff. The reliability of analysing environmental properties that have been categorised as either a 1 or 0 is questionable seeing as in reality the properties tend to differ across a range of values rather than be distinctly one or the other (Clark and Hosking, 1986). Brodnax (1991) did however test a total of 25 variables first before choosing the most influential ones. For instance: one variable was 'No Beach', whereby a 1 was given to sites that had no beaches and a 0 was given for all other situations; a second variable was 'Beach' for which a 1 was given to sites that had a continuous beach and a 0 was given for all other situations. The testing of two versions of a similar parameter (in this case, a beach at the cliff base) helps to cover all situations that statistical analysis may find significant.

Student t-tests used in this research found a number of different parameters that differ based on whether they are from sites with beds dipping seaward or sites where beds are dipping landward. Initial aims of this research were to limit the amount of classified data and use true measured values to develop a multiple linear regression model for cliff erosion rates, thereby advancing on the work done by Brodnax (1991).

However, a number of limitations were found that prohibited the effective development of a model from the database compiled from this research. Firstly, the population size was found to be too small to develop statistically significant conclusions. The majority of the 96 different parameters were measured for all 16 sites, however for those parameters that were sourced from scanline data there were only values from 8 sites. To carry out multiple linear regression analysis the entire data set would have to be reduced to only those 8 sites; that is, the explanatory variables used in the analysis all have to be the same population size (McWhirter, pers. comm. 2006).

Secondly, the significant results that were determined from the student t-test analysis could not be incorporated further into multiple linear regression analysis because they analyse different population means. While student t-tests split one parameter into two different means (for instance, beds dipping landward and beds dipping seaward) multiple linear regression compares the total population mean of two different parameters (for instance, intact rock strength and cohesion) and looks for a correlation between their means plus the mean of the response variable, erosion rate. The correlation matrix of the database showed that no parameters correlate significantly with erosion rates which further confirms that a multiple linear regression analysis would prove to be unsuccessful. As environmental parameters rarely show perfect linear correlation, the comparison of two different means of one parameter, by the student t-test, is much more statistically robust.

6.5 Summary

- Statistical analysis of the collated database was aimed to establish which parameters were influencing the variation in cliff erosion rates.
- A correlation matrix was constructed to relate every parameter against one another. Significant correlation ($R > 0.70$) was determined for much geomorphic, rock mass classification, rock mass parameter, bulk rock property and discontinuity parameters. However, no correlations were found between shore platform widths or erosion rates with the 96 other parameters.

- Student t-tests were then carried out in order to compare the mean values for the cliff sites based on a two-way split of a particular parameter. When data was split into sites that had shore platform widths greater than 100 m and sites that had platform widths less than 100 m, the dip angle of the bedding planes was highlighted as the parameter which had the most significant variation based on this split. When a t-test was run for sites that had beds dipping landward and sites that had beds dipping seaward a range of appreciable parameters were highlighted as having significant variation based on this split.

CHAPTER SEVEN

CONCEPTUAL MODEL FOR COASTAL CLIFF EROSION

7.1 Introduction

The results of the statistical analysis on the properties of Waitemata Group coastal cliffs have allowed the development of a conceptual model for coastal cliff erosion. The model has two variants based on the primary factor for coastal cliff erosion which is the dip angle of bedding planes. The conceptual model is based predominantly on the statistical findings and field observations made during this research with additional contributions to the validity of the model from other authors.

7.2 Conceptual Model for Coastal Cliff Erosion in Waitemata Group Rock

The conceptual model for coastal cliff erosion in Waitemata Group rock states that erosion rates (E_r) are dependent upon the primary factor (1^oF) of the dip of the bedding planes, plus contributions from secondary factors (2^of) of different geological and structural properties:

$$E_r = 1^oF + 2^of$$

The model has two forms based on the primary factor for coastal cliff erosion: 1) where beds dip seaward and shear failure is enhanced; and 2) where beds dip landward which prohibits shear failure along bedding planes.

The combination of the primary factor for cliff erosion (bed dip) and secondary parameters allows the development of a conceptual model for coastal cliff erosion in Waitemata Group rock. The conceptual models are presented in Figure 7.1A (beds dip seaward) and Figure 7.1B (beds dip landward) and are annotated for the various secondary factors (summarised in Table 7.1).

7.2.1 Beds dip seaward

When beds dip seaward out of the cliff face (Figure 7.1A) shear stresses and rock fall processes are the important influences on cliff erosion rates.

Shear stresses affect bedding planes, siltstone beds and sandstone beds in different ways. Bedding planes tend to be continuous surfaces along which large-scale, localised planar failure can occur. These types of failures are infrequent but remove large volumes of material from the cliff face as the rock and soil material overlying the bed (which acted as a shearing surface) will also fail. On a smaller scale, individual blocks may also fail along a bedding surface if the block is large enough on a continuous discontinuity to slide.

Within siltstone beds, the ability of the rock to develop minor discontinuities from wetting and drying enhances its erodability and the resulting frittered rock readily gives way to shear stresses. Within sandstone beds failure occurs through tensile fracture between non-persistent joints. The sandstone blocks are bound by commonly three or four joint sets; tension in the seaward-dipping bed will weaken and widen the discontinuities, particularly the vertical joints that are parallel to the cliff face.

Fall processes are also a considerable erosion mechanism. Rock fall occurs most significantly in individual sandstone blocks (compared to siltstone) when they are loosened from the cliff face. Weathering contributes to weakening the block and shear stresses release the joints. Depending on the orientation of the discontinuities the blocks may topple out of the cliff face or sliding may occur. The fall processes will be enhanced by seaward-dipping surfaces, particularly at steeper angles than the shear strength of the rock material.

7.2.2 Beds dip landward

When beds dip landward into the cliff face (Figure 7.1B) shear stresses are not a feasible mechanism for failure and erosion rates are therefore strongly influenced by fall mechanisms. Rock fall occurs by the same mechanisms as in the model for beds dipping seaward except that there cannot be any assistance along bedding surfaces, and thus overall erosion rates are slowed.

Failure is largely through single block fall and is dependent upon the removal rate of underlying siltstone material and the size of the individual sandstone blocks. Where siltstone is heavily frittered, the individual fragments are readily removed from the cliff face, particularly from wind and rainfall. The rate of recession of this material contributes to how quickly overlying sandstone blocks can lose the underlying support. When the support is removed, the sandstone blocks are strongly influenced by the downward force of gravity and tension forces which weaken vertical discontinuities and loosen the block from the cliff face. The block size of the sandstone therefore also controls erosion rates because more time is required to weaken and loosen a larger block. That is, longer periods of time are required to remove enough siltstone material and degrade the cliff face through weathering before rock fall of a relatively large block could occur.

Table 7.1: Summary of the secondary factors that influence Waitemata Group cliff erosion rates.

Secondary Factor	Description
1) Strength	Cohesion and friction of the rock mass will determine how easily rock can give way to its strength and fail. Shear failure occurs along bedding planes.
2) Siltstone	Rock mass strength of siltstone rock is higher when beds dip landward and lower when beds dip seaward
3) Sandstone	Prevalence for rock fall is higher for smaller blocks; rock fall occurs more sporadically for larger blocks but results in a larger volume of eroded material from the cliff face
4) Orientation of joints and cliff face	If beds are not in similar orientation to the cliff face then shear failure cannot occur

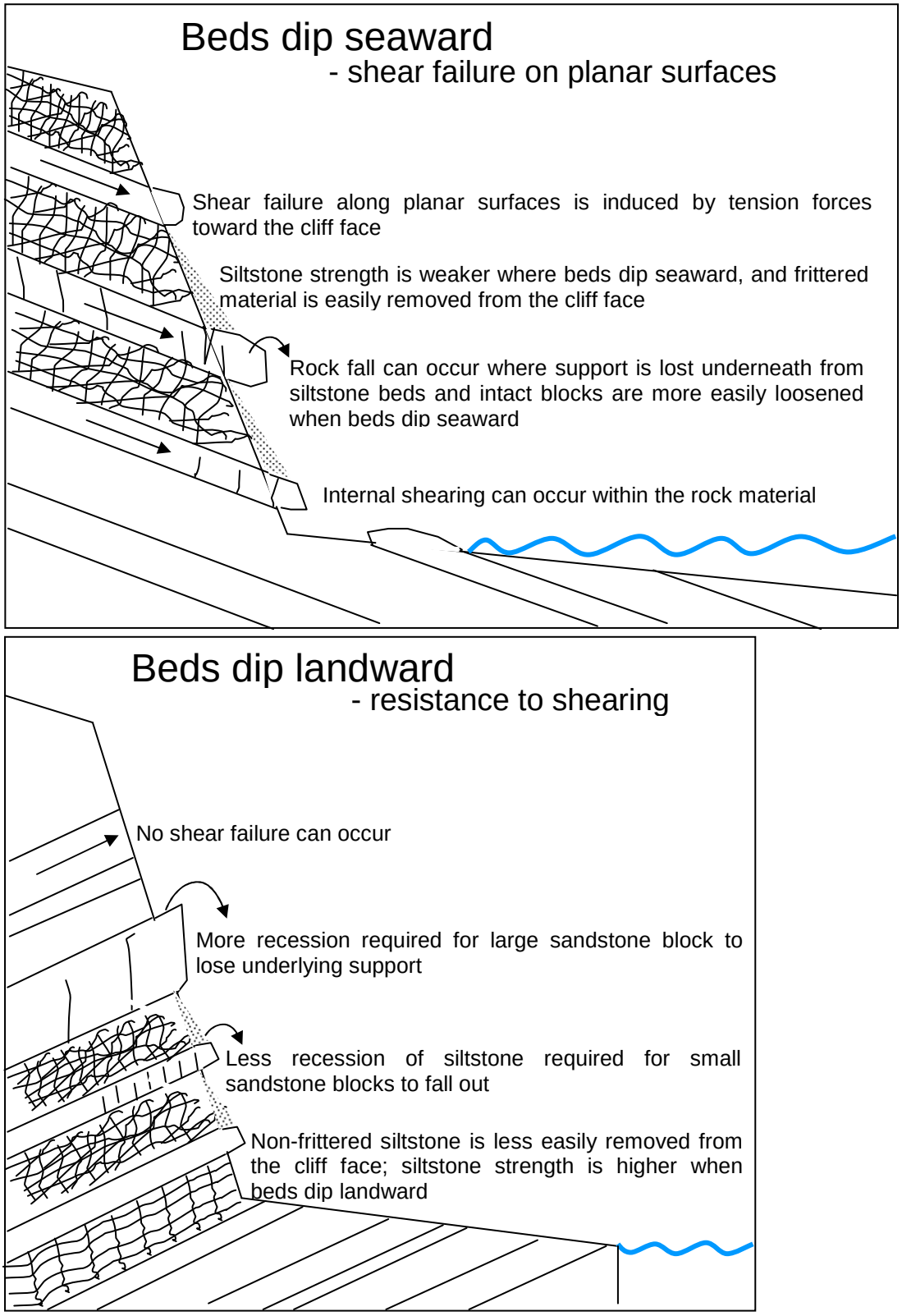

Figure 7.1: Conceptual model for coastal cliff erosion in Waitemata Group rock when: (A) beds are dipping landward and (B) beds are dipping landward. Note that the morphology of the shore platform, with a seaward edge, has no influence on erosion rates.

7.3 Discussion of the Model for Coastal Cliff Erosion With Respect To the Described Cliff Sites

7.3.1 Primary Control

Bed dip was determined, by the student t-test, to be the most influential parameter on cliff erosion rates, and thus shore platform development, in Waitemata Group rock. The dip angle of the bedding planes primarily controls erosion rates because seaward dipping beds allow shear failure to occur along the continuous discontinuity surface of the bed, whereas landward dipping beds are oriented such that shear failure cannot occur readily along the bedding planes. As a result of the dip angle of beds in a cliff section, various processes will then behave differently and therefore affect how the rock mass erodes. This variation allows for faster or slower rates of erosion to occur at different cliff sites constructed of the same geology. There is a strong variation in erosion rates between beds that dip landward and beds that dip seaward in the described cliff sections of this study. For the six cliff sites in which beds dip landward, the mean erosion rate is 4.0 ± 0.5 mm y^{-1} and for the ten sites in which beds dip seaward, the mean erosion rate is 19.5 ± 1.8 mm y^{-1}. For a 100 year planning period this works out to be a total of 0.4 ± 0.05 m when beds dip landward and 2.0 ± 0.18 m when beds dip seaward, which is a discernable difference.

Bed dip cannot be the exclusive control on erosion rates however because there is not a direct linear relationship between the degree of dip of the beds seaward and the erosion rate. For instance, the steepest dipping beds (26^{o}) recorded were at Castor Bay which had an erosion rate of 14.2 mm y^{-1}, and beds that dipped less (17^{o}) at Eastern Beach had the highest rate of erosion of 53.0 mm y^{-1}. This was the likewise situation for beds that dipped landward. Therefore, there must be other processes that act as secondary controls on cliff erosion rates.

7.3.2 Secondary controls

The secondary controls of cliff erosion in Waitemata Group rock are sourced from t-test results which show significant differences in the mean values of the parameters based on whether beds are dipping seaward or landward at that site. As further justification, the

parameters that correlated well with bed dip, and other significant relationships, sourced from the correlation matrix, are also considered as secondary controls on erosion rates. Field observations contribute to the visual interpretation of the conceptual model. Five properties have been determined as secondary factors that influence cliff erosion rates, including intact and rock mass strength, rock mass quality, sandstone properties, siltstone properties, and the orientation of discontinuities.

7.3.2.1 Intact and rock mass strength

In Waitemata Group coastal cliffs, the predominant surfaces on which shear failure could occur are bedding planes. Shear failure could also occur on fault planes but these are commonly sub-vertical and not at the necessary orientation for failure from the cliff face. For bedding plane surfaces, the conditions can be ripe for shear failure when the friction angle value of the rock is less than the dip angle of the bedding plane, and where cohesion values are relatively low. However, there must be other conditions that control whether shear failure can occur or not because there is no linear relationship between the angle of the bedding planes and erosion rates.

Intact rock strength (measured as uniaxial compressive strength) is affected by weathering as this increases its porosity and permeability and enhances the ease with which the rock is deformed (Selby, 1993). Therefore intact rock strength measurements can be used to indicate how easily the intact blocks may be broken down and eroded away from the cliff face. The global rock mass strength is defined as the average rock mass strength by Hoek (2005) and incorporates tensile and compressive strength of the overall rock mass. This measure can be used to indicate how well the intact rock will hold together as a rock mass. Intact and rock mass strength of siltstone increases northwards, synonymously with sandstone strength, but also has a relationship based on whether beds are dipping seaward or landward. Siltstone intact and rock mass strength is reduced where beds dip seaward and is stronger where beds dip landward. Cohesion is lost by fracturing (brittle failure) and thus the frittered nature of the siltstone, as a result of swelling clays, has great propensity for being eroded from the cliff face.

7.3.2.2 Siltstone properties

Siltstone beds are the weak, easily eroded material of Waitemata Group coastal cliffs, and therefore, their dominance in a cliff section will influence erosion rates and the mode of cliff recession. Physically, frittered siltstone rock can be easily removed by wind and rain from the cliff surface than more intact materials (Figure 7.2). In some locations, the siltstone does not fritter; erosion may still occur, albeit at a slower rate, through continual removal of the dusty surface but intact blocks do not appear to readily fall out (Figure 7.3).

Figure 7.2: Highly-frittered siltstone is readily blown away by wind and washed away by rain as at Martins Bay (left) and Army Bay (right).

Figure 7.3: Siltstone is more competent at Cockle Bay; the regular closely-spaced joints are still exhibited but loose, curved siltstone fragments that are easily removed from the cliff face are not apparent.

7.3.2.3 Sandstone beds

There are two properties of sandstone beds that have a secondary influence on cliff erosion rates. Firstly, the strength of sandstone rock determines resistance within the cliff rock mass, and secondly the joint frequency of the sandstone beds contributes to how readily loosened blocks can fall out of the cliff face.

Sandstone surfaces at the cliff face tend to be steep and prominent owing to their higher intact strength than siltstone. Also, discontinuity persistence, and the spacing and thickness of the beds affect the rock mass strength. Joint continuity (persistence) is an important aspect of the shear strength of discontinuity surfaces according to Orr (1974) whereby when the relative continuity of joints is less than 60 per cent then shear along their surfaces is very improbable. Where the discontinuity is non-continuous and shearing cannot occur, the sandstone blocks instead have to be loosened sufficiently through other processes so rock fall can occur. Smaller spacing between discontinuities and thinner beds result in smaller block sizes, while thicker beds (particularly from debrite and densite deposits) have wider joint spacing and subsequently larger block sizes.

Regular, small block fall may balance out to have the same rate of erosion as larger sporadic collapse (Figure 7.4). Where small block size is exhibited in sandstone beds, such as at Leigh Marine Reserve, relatively less weathering of the surrounding cliff face has to occur in order for the sandstone blocks to be loosened and tumble from the cliff face. Opahi Bay, which has thick-bedded sandstone beds in which large blocks develop, has a similar erosion rate to Matheson Bay which is siltstone-dominated and Castor Bay which has approximately medium bed thickness and a sandstone proportion of 0.61. Musick Point has 2 sets of sub-vertical joints which only sporadically intersect; therefore the rock mass does not develop blocks of sandstone bound by three joint sets and the resulting form of erosion appears to be just surface weathering. However, the erosion rate of Musick Point is higher than Opahi Bay, and one of the highest of all the described sites. Erosion rates are therefore not directly related to sandstone or siltstone prominence or sandstone block size.

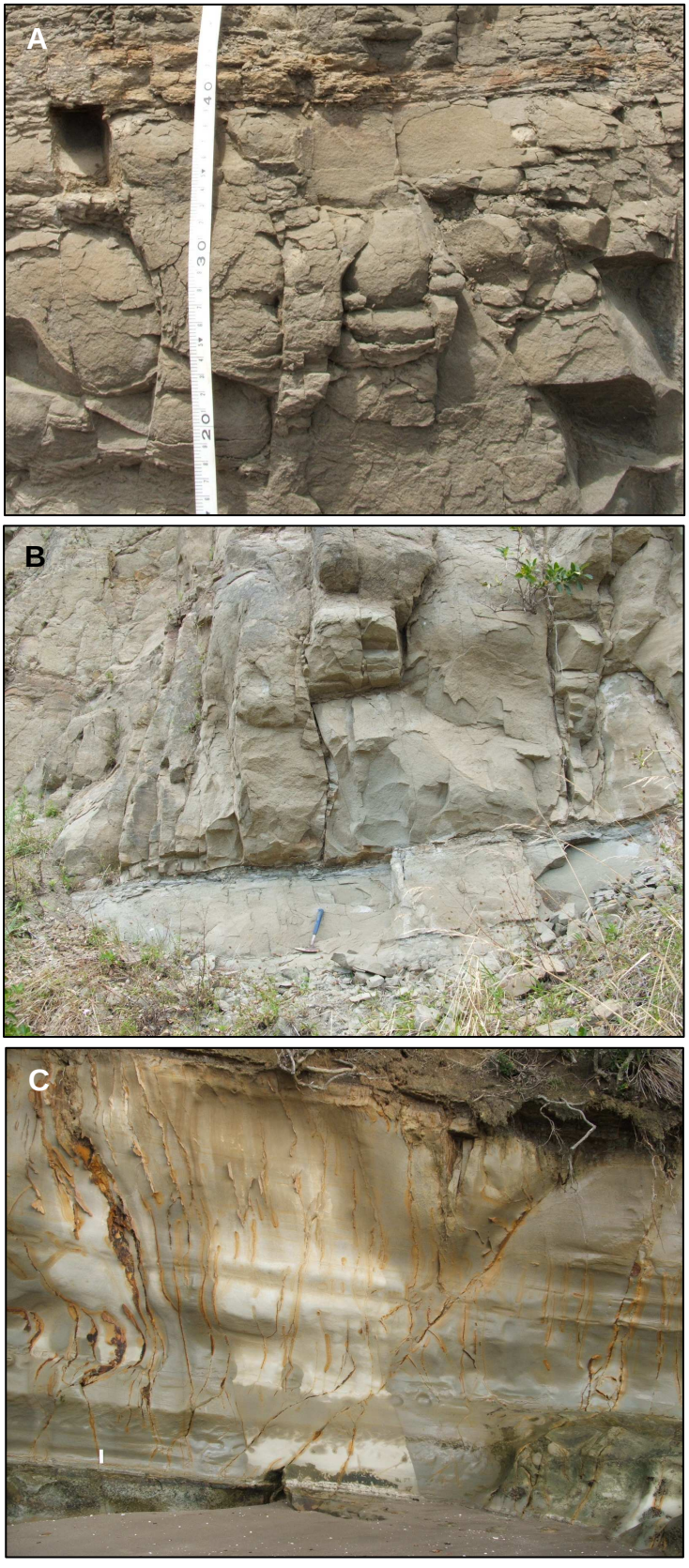

Figure 7.4: Prominence of rock fall for various sandstone beds. (A) Regular rock fall - small loose blocks at St Leonard's Beach. Tape measure marks 10 cm divisions. (B) Sporadic collapse - loosened, but still large, blocks in thick-bedded sandstone from Opahi Bay. Hammer for scale. (C) No block fall - competent Musick Point sandstone blocks. 15 cm white ruler for scale at bottom left of the figure.

7.3.2.4 Orientation of beds with respect to cliff face

The final secondary factor that can influence erosion rates, and may work in part with the primary factor of bed dip, is the orientation of primary joint sets including bedding planes (Figure 7.5). Beds that dip seaward at a similar orientation to the cliff face orientation have a stronger propensity for failure (Figure 7.5A) than when beds dip at a considerably different orientation to the cliff face such that they are effectively buttressed (Figure 7.5B). Furthermore beds need to be dipping seaward at a sufficient angle so to exceed the shear strength (cohesion and friction angle) of the rock mass. Discontinuity orientation is always studied in relation to the orientation of the cliff face and thus the ability for the cliff to experience shear failure is reliant on the cliff face orientation.

Figure 7.5: A: Beds dip (arrows) at an orientation (solid line) close to the orientation (dashed line) of the cliff face at Army Bay. B: Beds dip (arrow) seaward but are at an orientation (solid line) such that they are buttressed with respect to the cliff face (dashed line) at Waiwera Beach.

7.3.3 Confidence of the model

This conceptual model has been developed from real data but has also been constructed with the knowledge of previous work that has been done on the Waitemata Group coastal cliffs. Furthermore, it is a model of the dominant processes that act to erode these cliffs specifically and is not bound to a mathematical equation as other published models are.

De Lange and Moon (2005) have a simple means to finding the rate of cliff recession through measuring shore platform widths, but this is a site specific measurement which does not attempt to account for reasons why rates of recession vary along the eastern coastline of the Auckland region. The parameters required for some of the equation-based models which do take into account the whole cliff erosion process include: long-term rates of retreat; a safety factor that takes into account uncertainties; a hazard assessment period over which the amount of erosion needs to be determined; and the amount of sudden failure likely to occur with various mechanisms such as in the top-weathered soil layers and by landslip (viz. Glassey *et al.* 2003; Tonkin and Taylor, 2005a; Jongens *et al.* 2007). However, these properties ignore the specific contribution that individual processes have on the rates of erosion and rather broadly collate them into the type and estimated extent of failure mechanism that is likely to occur at the studied site.

Five of the seven parameters used by Brodnax (1991) in his regression equation for cliff erosion are given a value of 1 or 0 based only on whether the parameter is featured at the cliff site or not, so is a broad estimation of the dominance of that parameter on cliff recession. Furthermore, shore platform width was considered as only one of the response variables in the regression equation, and the dip of beds was not included at all.

Unlike the other models, Tonkin and Taylor (2005a) also use cliff angle and cliff height in their hazard zone delineation model as key determinants of a cliff erosion hazard assessment. In this study, cliff angle and cliff height have been determined, through statistical analysis, to have little impact and influence on cliff erosion rates, nor are they controlled by the rate of cliff erosion. Instead, it is other structural and geological

properties of the rock mass that cause the variation in erosion rates which the conceptual model has been developed from.

While there is a general consensus of the different parameters that influence erosion rates in Waitemata Group coastal cliffs, this study has highlighted a number of previously-unmentioned parameters that also influence cliff erosion rates. Thus, there is still the need to refine the dominant processes of cliff erosion and to further-develop models which explain the varying erosion rates across the eastern Auckland region based on real data sourced from individual sites.

7.3.4 Limitations of the model development

A notable limitation to the development of this model has been the small population size of the database; in total the population size was 16 cliff sections but for the parameters that were derived from scanline survey data the population size was halved to 8 cliff sections. A larger population size would allow better representation of randomly selected samples.

Irrespective of the time involved in collecting and deriving all the data required for one cliff section, a larger number of described cliff sites would allow more dependable relationships with erosion rates to be made. Furthermore, a detailed investigation undertaken along one entire cliff (from one headland to the next) similar to that undertaken for each individual, ~ 30 m wide cliff section, would allow relationships to be derived regarding the change in erosion rates along a continuous section of cliff coastline.

7.4 Cliff Height as a Key Determinant of a Hazard Assessment

Cliff height is commonly discussed as part of a hazard assessment of coastal cliff erosion (such as Tonkin and Taylor, 2005a) and, as such, was tested in detail for its relationship with cliff erosion in this study. No relationship was found between cliff erosion rates and cliff height in the described Waitemata Group coastal cliffs. Observations made in

the field suggest that cliff height is simply a result of geomorphology; the pre-existing landscape from past erosive processes. Student t-test analysis did highlight some parameters that have significantly different means when split into sites with relatively low cliff heights and sites with relatively high cliff heights (listed in Table 6.6). This analysis suggests that weathering and soil development, and the hydrology of the land behind the cliff face can contribute to reduction in cliff height through erosion and loss of soil or weathered rock material. Cliff height may also be in part controlled by some structural and strength properties of the cliff rock mass, as highlighted by the t-test results. Moon and Healy (1994) note that the size of the bevelled zone of a cliff face is an important aspect of hazard zone delineation because if the bevelled zone is deeper, the angle of repose of soil will result in greater recession at the cliff-top. Assuming that the top of the cliff is measured at the top of the cliff scarp and the base of the bevelled zone, then a larger bevelled zone will result in a reduced cliff height (Figure 7.6).

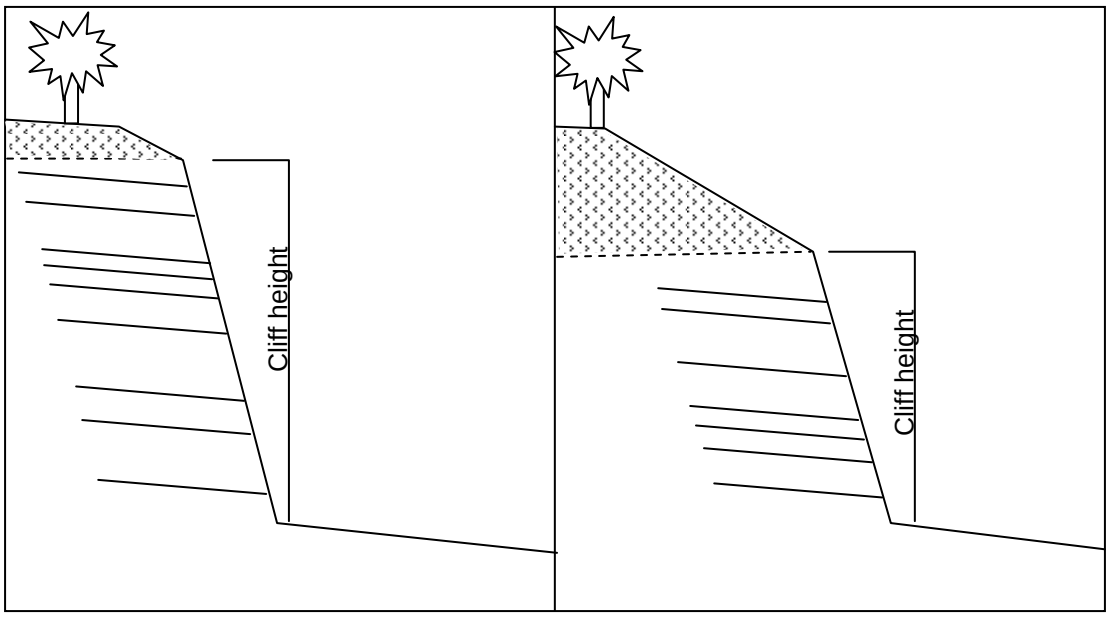

Figure 7.6: Model for the relationship between cliff height, soil depth and the size of the bevelled zone in Waitemata Group rock.

7.5 Cliff Angle as a Key Determinant of a Hazard Assessment

Correlation analysis and field observations highlighted that cliff angles were related to joint frequency (synonymously with spacing and block size) and the proportion of sandstone to siltstone in the cliff section. While cliff angle is not directly related to erosion rates at the cliff base (through increasing shore platform width), a lower cliff angle will mean that the cliff-top will recede further back. Where siltstone dominates the rock mass, the overall joint frequency will be high as the siltstone beds have much closer-spaced joints than sandstone beds, and cliff angles in these rock masses tend to be lower (Figure 7.7).

T-test results show that cliff angle is also influenced by the proportion of sandstone. Sandstone beds naturally form steep faces and so cliffs comprising mostly sandstone will have overall steeper cliff faces. The results also show a relationship between lower cliff angles and lower rock mass parameters for heterogeneous rock masses, rather than sandstone and siltstone rock masses measured separately. Rock mass parameters determine the various strength characteristics of the rock mass; where the rock mass strength is relatively low, the rock can thus degrade and erode more readily, resulting in lower cliff angles.

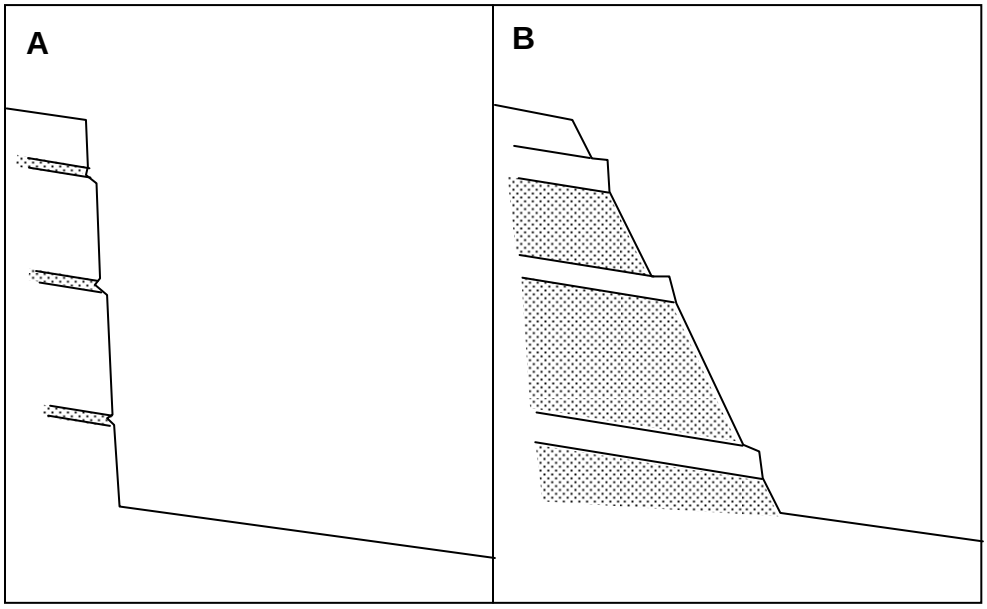

Figure 7.7: Model for the relationship between cliff angle and block size, rock mass strength and sandstone proportion in Waitemata Group rock. (A): higher cliff angle. (B): lower cliff angle. The dotted pattern represents siltstone.

7.6 Summary

- A conceptual model for coastal cliff erosion has been developed for Waitemata Group coastal cliffs, based on the dominant processes that act on the cliffs determined from statistical analysis and field observations and contributes to the explanation of why cliff erosion rates vary so considerably within the relatively uniform geology of the Waitemata Group.
- The primary factor for cliff erosion is bed dip, whereby seaward dipping beds have much wider shore platforms than landward dipping beds. The secondary factors for cliff erosion include: the intact and rock mass strength of the rock; the rock mass quality determined from rock mass classification systems; strength of the siltstone beds; strength and block size of the sandstone beds; and orientation of the bedding planes with respect to the cliff face.
- Cliff height and cliff angle do not have a direct relationship to erosion rates but models have been developed to explain which parameters influence their variability along the eastern Auckland region coastline.

CHAPTER EIGHT

CONCLUSIONS

8.1 Summary of Research Findings

A database of 98 parameters were collated to determine the relationships with coastal cliff erosion in Waitemata Group rock and to particularly appreciate why erosion rates vary within the Waitemata Group.

8.1.1 Properties of the Waitemata Group coastal cliffs

The 16 cliff sites described in this study have a range of geological, structural, geomorphic and climatic properties which influence the way in which cliffs erode and their erosion rate. Overall, the Waitemata Group rock has weak strength and is slightly weathered; sandstone rock is considerably stronger than siltstone rock but both increase in intact and rock mass strength northwards. Joint spacing is variable and is dependent on the lithological type. There are four classified lithological units within the Waitemata Group: sandstone beds of turbidites with variable joint spacing dependent on bed thickness; sandstone beds of densites with wide joint spacing and limited block formation; siltstone beds which readily fritter to very small blocks; and debrite beds of the Parnell Grit Member which are coarser-grained and have limited joint development. The cliff rock masses have generally non-persistent discontinuities except for persistent bedding and fault planes. A classification scheme has been developed for Waitemata Group coastal cliffs based on the proportion of sandstone beds to siltstone beds for which sandstone dominated cliffs have steeper cliff angles and a higher GSI value.

Long-term cliff erosion rates are derived from shore platform widths and the time period for platform development of 7120 ± 70 years. Erosion rates range from 1.2 to 53.0 mm y^{-1}. The four different platform morphologies at the described cliff sites

include: horizontal platforms that have a seaward edge; gently sloping platforms that have no seaward edge; narrow horizontal platforms with lower sloping platforms that have a seaward edge; and narrow horizontal platforms with lower sloping platforms that do not have a seaward edge. The higher platform benches are considered to be a result of a stillstand at a higher sea-level or are high-tide platforms. The combination of higher horizontal platforms and lower sloping platforms in one cliff site provides a challenge to ensuring the measured platform width (for determining cliff erosion rates) is from only one continuous period of sea-level oscillation.

Failure modes for the described cliff sections that occur sporadically include planar and wedge failure. Rock fall is a more frequent, but smaller scale, form of failure observed in most, but not all, sites. The small siltstone fragments that are readily removed by wind and rain allow a continual form of cliff recession. Rock mass classification schemes show that Castor Bay, Army Bay, Waiwera Beach and Leigh Marine Reserve have the lowest rock mass quality. Good rock mass quality was determined for Musick Point, Narrowneck Beach and Waiake Bay.

8.1.2 Conceptual models for cliff erosion, cliff height and cliff angle

A conceptual model for coastal cliff erosion has been developed for Waitemata Group coastal cliffs, based on the dominant processes that act on the cliffs determined from statistical analysis and field observations. Cliff height and cliff angle have no relationship with cliff erosion rates but are influenced by other properties.

The primary factor for cliff erosion is the dip angle of bedding planes, whereby cliffs with seaward dipping beds have higher cliff erosion rates than cliffs with landward dipping beds. The secondary factors for cliff erosion include: the intact and rock mass strength of the rock; the rock mass quality; the low durability of siltstone beds; strength and structure of the sandstone beds; and orientation of the bedding planes with respect to the cliff face.

When beds dip seaward out of the cliff face, shear stresses and rock fall processes are the important influences on cliff erosion rates. Shear failure can occur along continuous

surfaces, particularly bedding planes. Shear failure may also occur in sandstone blocks that have a failure surface that is persistent enough to allow sliding. Rock fall occurs most significantly in individual sandstone blocks (compared to siltstone) when they are loosened from the cliff face. The blocks are loosened by tensile fracture between non-persistent joints, whereby tension in the seaward-dipping bed will weaken and widen the discontinuities, and also the loss of support from underlying frittered siltstone beds. The fall processes will be enhanced by seaward-dipping surfaces, particularly at steeper angles than the shear strength of the rock material.

When beds dip landward into the cliff face shear stresses are not a feasible mechanism for failure and erosion rates are therefore strongly influenced by fall mechanisms. Rock fall occurs by the same mechanisms as in the model for beds dipping seaward except that there cannot be any assistance along bedding surfaces, and thus overall erosion rates are slowed. Failure is largely through single block fall and is dependent upon the removal rate of underlying siltstone material and the size of the individual sandstone blocks; larger sandstone blocks require more weathering and loss of support to fall from the cliff face.

Cliff heights range from 8 to 38 m and have no relationship to site location. Instead, cliff height is mainly controlled by the surrounding geomorphology of the pre-existing landscape. Cliff heights may also be associated with soil erosion of the land surface, and joint spacing of the cliff rock mass.

Cliff angles range from 51 to 79°. Cliff angles are low when the proportion of siltstone and joint frequency (synonymously) are higher. Cliff angle may also be controlled by weathering and rock mass strength of the cliff as a single heterogeneous rock mass.

8.1.3 Summary

This study has highlighted that coastal cliff erosion in Waitemata Group rock is largely dependent on the geology and structure of the rock mass. Cliff erosion rates do vary along the eastern coastline, primarily as a result of the dip of the bedding planes seaward or landward. The results of this study also show that erosion rates at individual cliff sites

can vary due to a number of different properties, some of which may not be present at every cliff site.

With regards to hazard assessment of the cliff erosion risk and hazard zone delineation of cliff-top land, it seems that the most accurate means for determining the rate of erosion and failure mechanisms are by individual site evaluations. Some published hazard assessment methodologies which classify a range of cliff sites into the same defined set of properties may miscalculate the true erosion risk for individual sites. Furthermore, some of the properties used in these methodologies may have no influence on erosion rates, such as cliff height and cliff angle, as was highlighted in this study.

There is a continual debate on the most accurate and efficient ways of evaluating the environment, particularly when it comes to risk analysis of hazards and planning for the future. Broader-scale analysis (such as the aforementioned methodologies) allows larger-scale evaluation to occur in a smaller time-frame however, the accuracy can be reduced. Conversely, site specific analysis allows more accurate evaluation of the environment but is less efficient with respect to time, money and labour. It appears that more site specific work is required in Waitemata Group coastal cliffs as there are still discrepancies in the hazard assessment of the cliff erosion. Therefore, this study has highlighted overall that current hazard assessment methodologies for predicting future cliff erosion should continue to be used with caution.

8.2 Recommendations for Future Work on Waitemata Group Coastal Cliffs

The limitations found during this research process, have highlighted where future work on cliff erosion in Waitemata Group rock is required to follow on from the findings of this study.

Firstly, it would be interesting to carry out similar research to this study along one continuous section of cliff, compared to the spot locations used here. This would allow the dominant processes acting to erode the cliff to be associated with the change in

erosion rate along the coastline; the advantage to this is that the change in the structure and geology of the cliff can be better observed and recorded.

Secondly, computer modelling of cliff erosion may contribute to understanding why cliff erosion rates vary. Computer modelling allows the simulation of countless scenarios for a given environment, such as a coastal cliff in heterogeneous rock. It can be difficult and inefficient to gather sufficient amounts of real data to not only understand processes occurring at one site but also to compare and understand variation across a range of sites. Although the accuracy of computer modelling is sometimes questioned, it would be advantageous to be able to use real data (which is available for Waitemata Group coastal cliffs) to model various scenarios based on the influential properties of the cliff rock mass.

Lastly, hazard zonation methods should aim to better quantify zones on cliff-top land that are susceptible to erosion. Recent publications of hazard zonation on cliff-top land in Waitemata Group rock only qualitatively define the zones, such as likely, possible, unlikely and rare. Quantitative zonation would mean that certain setback distances at the cliff-top would have an associated time-period for erosion, for instance a high-risk zone may be calculated to erode 2 m in 20 years. Such quantitative zonation may be best applied to small areas of coastline individually, such as the East Coast Bays in Auckland, rather than the entire region, particularly because site specific work seems to most accurately determine cliff erosion processes and rate of retreat.

References

Allaby, M. and Allaby, A. 1991: Concise dictionary of Earth Sciences. Oxford University Press, Oxford. 410 p.

Allen, S. 2004: The Parnell Grit beds revisited: Are they the products of sector collapse of western sub-aerial volcanoes of the Northland Volcanic Arc? *New Zealand Journal of Geology and Geophysics 4*: 509–524.

ArcInfo, 2006: Wind strength values for New Zealand land surfaces.

Arnould, M. 2006: Discontinuity networks in mudstones: a geological approach. Implications for radioactive wastes isolation in deep geological formations in Belgium, France, Switzerland. *Bulletin of Engineering geology and the Environment 65(4)*: 413-422.

Auckland Regional Council (ARC), 2007: Auckland Region Locality Map. August 2005. URL: http://www.arc.govt.nz/arc/auckland-region/maps-of-auckland-region/

Ballance, P. F. 1968: The physiography of the Auckland district. *New Zealand Geographer 24*: 23–49.

Ballance, P. F. 1974: An inter-arc flysch basin in northern New Zealand; Waitemata Group (upper Oligocene to lower Miocene). *Journal of Geology 82*: 439–471.

Ballance, P. F.; Williams, P. 1992: The geomorphology of Auckland and Northland. *In.* Soons J. M.; Selby, M. J. *eds.* Landforms of New Zealand. Longman Paul, Auckland. Pp 210–232.

Ballance, P. F. 1993: Geological history and structure of the Auckland district. *In*: Morton, J. *ed.* A natural history of Auckland. David Bateman Ltd, Auckland. Pp 4-11.

Beattie, A. G. 1990: Petrological controls on the geomechanical behaviour of coal measure soft rocks, Waikato, New Zealand. Unpublished MSc(Tech) Thesis. University of Waikato, Hamilton, New Zealand. 121 p.

BECA Consultants Ltd, 2003: Kohimarama Beach seawall protection project – coastal engineering report. Report for Auckland City Council. BECA Consultants Ltd, Auckland.

Benumof, B. T.; Griggs, G. B. 1999: The dependence of seacliff erosion rates on cliff material properties and physical processes: San Diego County, California. *Shore and Beach 67(3)*: 29–41.

Benumof, B. T.; Storlazzi, C. T.; Seymour, R. J.; Griggs, G. B. 2000: The relationship between incident wave energy and seacliff erosion rates: San Diego County, California. *Journal of Coastal Research 16(4)*: 1162–1178.

Bieniawski Z. T. 1979: The geomechanics classification in rock engineering applications. *Proceedings of the 4th International Congress on Rock Mechanics 2*: 51-58.

Bieniawski, Z. T. 1989: Engineering Rock Mass Classifications. Wiley, New York. 248 p.

Bird, E. C. F. 1974: Pitted rocks at Jubilee Point, Victoria. *Victorian Naturalist* 91: 60-65.

Bird, E. C. F. 1976: Coasts. 2nd Ed. Australian National University Press, Canberra. 282 p.

Bouma, A. H. 1962: Sedimentology of Some Flysch Deposits-A Graphic Approach to Facies Interpretation: Elsevier, Amsterdam. 168 p.

Brady, B. H.; Brown, E. T. 2004: Rock mechanics: for underground mining. Kluwer Academic Publishers, Boston. 626 p.

Brodnax, R. C. 1991: Cliff erosion in the Waitemata Harbour and Hauraki Gulf. Unpublished MSc Thesis, University of Auckland, Auckland, New Zealand. 145 p.

Brook, N. 1985: The equivalent core diameter method of size and shape correction in Point Load testing. *International Journal of Rock Mechanics and Mining Sciences 22(2)*: 61–70.

Buckeridge, J. S. 1995: Land stability in urban sites of the North Shore, Auckland, NZ. *In:* Bell, D.H. *ed. Proceedings of the Sixth International Symposium on Landslides 3*: 2129-2136. Balkema, Rotterdam.

Budetta, P.; Galietta, G.; Santo, A. 2000: A methodology for the study of the relation between coastal cliff erosion and the mechanical strength of soils and rock masses. *Engineering Geology 56*: 243–256.

City Design, 1996: Eastern Bays Coastal Management Strategy. Report prepared for Environmental and Coastal Planning. City Design, Auckland.

Clark, W. A. V.; Hosking, P. L. 1986: Statistical Methods for Geographers. John Wiley and Sons, Inc., New York. 581 p.

Conacher, A. J. 1988: The geomorphic significance of process measurements in an ancient landscape. *Catena Supplement 13*: 147-164.

Czerewko, M. A.; Cripps, J. C. 2001: Assessing the durability of mudrocks using the modified jar slake index test. *Quarterly Journal of Engineering Geology and Hydrogeology 34*: 153–163.

de la Mare, G. N. 1992: Microstructural controls on the geomechanics of coarse grained soft rocks; Waitemata Group, Auckland. Unpublished MSc Thesis, University of Waikato, Hamilton, New Zealand. 126 p.

de Lange, W. P.; Moon, V. G. 2005: Estimating long-term cliff recession rates from shore platform widths. *Engineering Geology 80*: 292–301.

Deere, D. U. 1964: Technical description of rock cores for engineering purposes. *International Society for Rock Mechanics 1*: 17-22.

Edbrooke, S. W. 2001: GNS geology map of the Auckland Region. Geological and Nuclear Sciences Ltd, Wellington.

Edbrooke, S. W.; Mazengarb, C.; Stephenson, W. 2003: Geology and geological hazards of the Auckland urban area, New Zealand. *Quaternary International 103*: 3–21.

Emery, K.; Kuhn, G. 1982: Sea cliffs: their processes, profiles, and classification. *Geological Society of America Bulletin 93 (7)*: 644–654.

Giani, G. P. 1992: Rock slope stability analysis. AA Balkema Publishers, Brookfield. 361 p.

Gani, M. R. 2004: From turbid to lucid: a straightforward approach to sediment gravity flows and their deposits. *The Sedimentary Record 2(3)*: 4–8.

Gelinas, P. J.; Quigley, R. M. 1973: The influence of geology on erosion rates along the north shore of Lake Erie. *Proceedings of the 16th conference on Great Lakes Research.* Pp 412-430.

Gibb, J. G. 1994: Defining coastal hazard areas and zones to control subdivision, use and development. Natural Hazards Management Workshop Proceedings. GNS, Wellington. Pp 43–46.

Gibb, J. G. 1986: A New Zealand regional Holocene eustatic sea-level curve and its application to determination of vertical tectonic movements. *Royal Society of New Zealand Bulletin 24*: 377–395.

Glassey, P.; Gibb, J.; Hoverd, J.; Jongens, R.; Alloway, B.; Coombes, K.; Benson, A. 2003: Establishing a methodology for coastal cliff hazard mapping: an East Coast Bays, Auckland pilot study. *In*: Kench, P.; Hume, T. *eds. Coasts and Ports Australasian Conference, Auckland 49*: 1–12.

Gordon, D. A. 1993: A Holocene sediment budget for the Waitemata Harbour. Unpublished MSc(Tech) Thesis. University of Waikato, Hamilton, New Zealand. 192 p.

Gulyaev, S. A.; Buckeridge, J. S.; 2004: Terrestrial methods for monitoring cliff erosion in an urban environment. *Journal of Coastal Research 20 (3)*: 871–878.

Hayward, B. W. 1979: Eruptive history of the early to mid Miocene Waitakere Volcanic arc and paleogeography of the Waitemata Basin, northern New Zealand. *Journal of the Royal Society of New Zealand 9:* 297-320.

Healy, T. R. 1967: Shore platform morphology on the Whangaparaoa Peninsula, Auckland. *In:* NZ Geographical Society, Proceedings of the fifth New Zealand geography conference. Pp 163–167.

Healy, T. R. 1968: Bioerosion on shore platforms developed in the Waitemata formation, Auckland. *Earth Science Journal. 2*: 26–37.

Healy, T. R.; Kirk, R. M. 1992: Coasts. *In:* Soons, J.M.; Selby, M.J. *eds*. Landforms of New Zealand. Longman Paul, Auckland. Pp 163–183.

Hoek, E. 2005: Uniaxial compressive strength versus global strength in the Hoek-Brown criterion. *In:* Rocscience Inc. 2007.
URL: http://rocscience.com/library/rocnews/Spring2005/CompressiveStrength.pdf

Hoek, E.; Bray, J. W. 1977: Rock Slope Engineering, revised 2nd edition. Institution of Mining and Metallurgy, London. Pp 226-257.

Hoek, E.; Brown, E. T. 1980: Empirical strength criterion for rock masses. *Journal of Geotechnical Engineering Division, proceedings of the American Society of Civil Engineers, 106(GT9)*: 1013-1035.

Hoek, E.; Brown, E. T. 1997: Practical estimates of rock mass strength. *International Journal of Rock Mechanics, Mining Sciences, and Geomechanics Abstracts 34(8)*: 1165-1186.

Hoek, E.; Carranza-Torres, C. T.; Corkum, B. 2002: Hoek-Brown failure criterion. *In*: *Proceedings of the fifth North American rock mechanics symposium,* Toronto, Canada, vol. 1. Pp. 267–273.

Hoek, E.; Marinos, P. G.; Marinos, V. P. 2005: Characterisation and engineering properties of tectonically undisturbed but lithologically varied sedimentary rock masses. *International Journal of Rock Mechanics and Mining Sciences. 42*: 227–285.

Horikawa, K.; Sunamura, T. 1967: A study on erosion of coastal cliffs by using aerial photographs. *Coastal Engineering in Japan 10*: 67-83.

Hurnard, S. M. 1979: Auckland's climate. *In*: Brook, P. J. *ed*. Natural History of Auckland: an Introduction. An Auckland War Memorial Museum Handbook, Auckland. 80 p.

International Society of Rock Mechanics (ISRM), 1981: *Rock Characterization, Testing and Monitoring: ISRM Suggested Method*. Pergamon Press, Oxford.

International Society of Rock Mechanics (ISRM), 1985: Suggested method for determining point load strength. *International Journal of Rock Mechanics and Mining Sciences and Geomechanics Abstracts*, *22 (2)*: 53–60.

Jones, D. G.; Williams, A. T. 1991: Statistical analysis of factors influencing cliff erosion along a section of the west Wales coast, U.K. *Earth Surface Processes and Landforms*. 16: 95–111.

Jones J. R.; Comerson, B.; Fisher, J. J. 1993: Analysis of cliff retreat and shoreline erosion: Thompson Island, Massachusetts, U.S.A. *Journal of Coastal research 9(1)*: 87-96.

Jongens, R.; Gibb, J.; Alloway, B. V. 2007: A new hazard zonation methodology applied to residentially developed seacliff with very low erosion rates, East Coast Bays, Auckland, New Zealand. *Natural Hazards 40*: 223–244.

Kamphuis, J. W. 1987: Recession rate of glacial till bluffs. *Journal of Waterway, Port, Coastal and Ocean Engineering 113(1):* 60-73.

Lahousse, P.; Pierre, G. 2003: The retreat of chalk cliffs at Cape Blanc-Nez (France): Autopsy of an erosional crisis. *Journal of Coastal Research 19(2)*: 431–440.

Leathwick, J.R.; Stephens, R.T.T.; Wilson, G.W. 2002. New Zealand Climate Surfaces. Landcare Research Contract Report 9798/126, Hamilton, New Zealand.

Lutton, R. J. 1977: Design and construction of compacted shale embankments. Vol. 3. Slaking Indexes for Design. U.S. Army Engineer Waterways Experiment Station, Vicksburg, Report No. FHWA-RD-77-1 (National Technical Information Service, Springfield, Virginia 22161), 88.

Mano, A.; Suzuki, S. 1999: Erosion characteristic of sea cliff on the Fukusima coast. *Coastal Engineering Journal 41(1)*: 43–63.

Marinos, P.; Hoek, E. 2001: Estimating the geotechnical properties of heterogeneous rock masses such as flysch. *Bulletin of Engineering Geology and the Environment 60*: 85–92.

Masselink, G.; Hughes, M. G. 2003: Introduction to Coastal processes and Geomorphology. Oxford University Press, New York. 345 p.

McLeod, M. 1988: Soil stability analysis of East Coast Bays City, Auckland. Unpublished MSc thesis, University of Waikato, Hamilton. 158 p.

McWhirter, J. 2006: Personal Communication. School of Applied Statistics, University of Waikato, Hamilton.

Mining Research and Development Establishment (MRDE). 1977: NCB Cone Indenter, MRDE Handbook No. 5.

Moon, V. G. 1984: Report on coastal cliff geology, East Coast Bays. City Council, East Coast Bays.

Moon, V. G.; Healy, T. R. 1994: Mechanisms for coastal cliff retreat and hazard zone delineation in soft flysch deposits. *Journal of Coastal Research 10 (3)*: 663-680.

Moon, V.; Russell, G.; Stewart, M. 2001: The value of rock mass classification systems for weak rock masses: a case example from Huntly, New Zealand. *Engineering Geology 61*: 53–67.

Moore, D. S.; McCabe, G. P.; 2003: Introduction to the practice of statistics, 4th Edition. Freeman, New York. 828 p.

Nichol, R. 1992: The eruption history of Rangitoto: reappraisal of a small New Zealand myth. *Journal of the Royal Society of New Zealand 22*: 159–180.

NZ Geotechnical Society Inc (NZGS). 2005: Field Description of Soil and Rock. New Zealand Geotechnical Society.

Ollier, C. D. 1984: Weathering. 2nd Ed. Longman, London. 270 p.

Orr, C. M. 1974: The geological description of *in situ* rock masses as input data for engineering design. *C.S.I.R. South Africa Report,* serial MEG/344, number ME1274.

Patterson, R. D.; Prebble, W. M. 2004: Engineering geology and coastal cliff erosion at Takapuna, Auckland, New Zealand. *In*: Farquhar, G.; Kelsey, P.; Marsh, J.; Fellows, D. *eds*. 9th Australia New Zealand Conference on Geomechanics. NZ Geotechnical Society and Australian Geomechanics Society, Auckland. Pp 775–781.

Pethick, J. 1984: An introduction to coastal geomorphology. Edward Arnold, London. 260 p.

Pickrell, R. A.; Mitchell, J. S. 1979: Ocean wave characteristics around New Zealand. *New Zealand Journal of Marine and Freshwater Research 13(4)*: 501–520.

Pierre, G. 2006: Processes and rate of retreat of the clay and sandstone sea cliffs of the northern Boulonnais (France). *Geomorphology 73(1-2)*: 64-77.

Pierre, G.; Lahousse, P. 2006: The role of groundwater in cliff instability: an example at Cape Blanc-Nez (Pas-de-Calais, France). *Earth Surface Processes and Landforms 31(1)*: 31-45.

Pillans, B. 1986: A late Quaternary uplift map for the North Island, New Zealand. *Royal Society of New Zealand Bulletin 24*: 409-417.

Playfair, J. 1802: *Illustrations of the Huttonian Theory of Earth*. Dover, New York. p 528.

Priest S. D.; Hudson, J. A. 1976: Discontinuity spacings in rocks. *International Journal of Rock Mechanics and Mining Sciences 13*: 135–148.

Prothero, D. R.; Schwab, F. L. 1996: Sedimentary Geology: an introduction to sedimentary rocks and stratigraphy. Freeman, New York. 575 p.

Riley Consultants Ltd, 2001: Erosion of seacliffs between Murrays Bay and Campbells Bay. Report prepared for Auckland Regional Council. Riley Consultants Ltd, Auckland.

Robinson, M. 1985: Morphodynamics of Orewa Beach July 1984 – July 1985. Unpublished MA (Geography) Thesis. University of Auckland. 107 p.

RockWare Inc. 2002: RockWorks 2002, Colorado.

Rocscience Inc. 2006: Roclab, version 1.021. Toronto.

Romana, M. R. 1985: New adjustment ratings for application of Bieniawski's Classification to slopes. *Proceedings of the International Symposium on the Role of Rock Mechanics.* Zacatecas. Pp 49-53.

Romana, M. R. 1993: A geomechanical classification for slopes: slope mass rating. *In*: Hudson, J. A. *ed.* Comprehensive Rock Engineering. Pergamon, Oxford. Pp 576–599.

Runyan, K.; Griggs, G. B. 2003: The effects of armoring seacliffs on the natural sand supply to the beaches of California. *Journal of Coastal Research 19(2)*: 336–347.

Searle, E. J. 1981: City of volcanoes: A Geology of Auckland. 2nd Ed. Longman Paul, Auckland. 195 p.

Selby, M. J. 1980: A rock mass strength classification for geomorphic purposes: with tests from Antarctica and New Zealand. *Zietschrift für Geomorphologie 24*: 31-51.

Selby M. J. 1993: Hillslope Materials and Processes, 2nd Edition. Oxford University Press, Oxford. 445 p.

Shepard, F. P. 1954: Nomenclature based on sand-silt-clay ratios. *Journal of Sedimentary Petrology 24*: 151–158.

Simpson, K. A. 1987: Rock properties and slope processes of the Waitemata group soft rock, along sections of the east coast of Auckland, New Zealand. Unpublished MSc (in applied geology) Thesis. University of Auckland, Auckland, New Zealand.

Sporli, K. B.; Browne, G. H. 1981: Structure in a Miocene interarc basin: Waitemata Group at White Bluff, Auckland, New Zealand. *Journal of the Royal Society of New Zealand. 11*: 87–92.

Statistics New Zealand website (Statistics NZ), 2006: 2006 Census data.
URL: http://www.stats.govt.nz/census/2006-census-data/default.htm

Stephenson, W. J.; Kirk, R. M. 1996. Measuring erosion rates using the micro-erosion meter: 20 years of data from shore platforms, Kaikoura Peninsula, South Island, New Zealand. *Marine Geology 131(3/4)*: 209-218.

Sunamura, T. 1976: Feedback relationship in wave erosion of laboratory rocky coast. *Journal of Geology 84*: 427-437.

Sunamura, T. 1977: A relationship between wave-induced cliff erosion and erosive force of waves. *Journal of Geology 85*: 613-618.

Sunamura, T. 1983: Processes of sea cliff and platform erosion. *In:* P.D Komar, CRC Handbook of Coastal Processes and Erosion. CRC Press, Boca Raton, Florida. Pp 233-265.

Sunamura, T. 1992: Geomorphology of Rocky Coasts. John Wiley and Sons, Chichester. 302 p.

Thompson, B. N. 1961: Sheet 2A Whangarei (1st Ed) New Zealand geological map 1:250,000. Department of Scientific and Industrial Research, Wellington, New Zealand.

Tonkin and Taylor. 2005a: Regional Coastal Erosion Hazard Assessment. Report to: Auckland Regional Council. Report No: 19891.100.

Tonkin and Taylor. 2005b: Regional Coastal Erosion Hazard Assessment. Vol. I. Report to: Auckland Regional Council. Report No: 19891.100.

Toyoshima, O.; Okuda, M.; Muto, T. 1973: On the erosion and characteristics of the Fukushima Coast. *Japanese Conference on Coastal Engineering 20*: 507-511.

Trenhaile, A. S. 1973: The geometry of shore platforms in England and Wales. *Institutes of British Geographers, Transactions. 62*: 120–141.

Trenhaile, A. S. 1987: The Geomorphology of Rock Coasts. Clarendon Press, Oxford. 379 p.

Trenhaile, A. S. 2002: Rocky coasts, with particular emphasis on shore platforms. *Geomorphology 48*: 7-22.

Varnes, D. J. 1958: Landslide types and processes. *Highway Research Board, Special Report* (Washington, DC) *29*: 20-47.

Walkden, M. J. and Hall, J. W. 2005: A Predictive Mesoscale Model of the Erosion and Profile Development of Soft Rock Shores. *Coastal Engineering 52*: 535- 563.

Walker, R. G. 1979: Facies models. Ainsworth Press Limited, Ontario. 211 p.

Watts, S.; Halliwell, L. 1996: Essential Environmental Science. Methods and Techniques. Routledge, London. 512 p.

Wells-Green, P. S. 1975: Current, wave and sediment transport – Upper Waitemata Harbour. *New Zealand Engineering 30(10).*

Williams, P. W. 2006: Personal communication. Department of Geology, University of Auckland.

Woodroffe, C. D. 2002: Coasts, Form processes and evolution. Cambridge University Press, Cambridge. 623 p.

Wyllie, D. C.; Mah, C. W. 2004: Rock Slope Engineering, Civil and Mining. Spon Press, Suffolk. 431 p.

Yamanouchi, H. 1964: On the retreat of the sea cliffs along the Pacific Coast at Haranomachi, Japan. *Geographical Review of Japan 37*: 138-145.

Zviely, D.; Klein, M. 2004: Coastal cliff retreat rates at Beit-Yannay, Israel, in the 20th century. *Earth Surfaces Processes and Landforms* 29: 175–184.

APPENDIX 1

BULK DENSITY, POROSITY AND MODIFIED JAR SLAKE TESTS

Terms for bulk density and porosity data

Term	Description	Units	Calculation
V	Volume of block	m^3	= length x width x depth
M_{cont}	Mass of aluminium container	kg	
$M_{sat+cont}$	Saturated-surface-dry mass + mass of container	kg	
M_{sat}	Saturated-surface-dry mass	kg	= $M_{sat+cont}$ - M_{cont}
M_{s+cont}	Grain mass of oven-dried sample + mass of container	kg	
M_s	Grain mass of oven-dried sample	kg	= M_{s+cont} - M_{cont}
M_a	Air dry mass of the block	kg	
ρ_w	Density of water = 1000 kg m^{-3}	kg m^{-3}	
V_v	Pore volume	m^3	= (M_{sat} - M_s) / ρ_w
n	Porosity	%	= 100V_v / V
ρ_d	Bulk density of oven-dried sample	kg m^{-3}	= M_s / V
ρ_a	Bulk density of 48 hr air-dried sample	kg m^{-3}	= M_a / V
na	Not applicable		

Block Volume (mm^3)

SITE	1	2	3	4	5	6	7	8	9	10	11
Cockle Bay	74025.59	95541.85	34686.36	94730.41	72551.76	64102.04	95105.14	69202.13	62207.18		
Std. Error	812.23	1006.65	543.28	1755.99	458.25	697.19	786.01	763.64	439.86		
Eastern Beach	181930.55	168327.91	67935.07	119016.34	75524.07	122051.16	106870.76	48306.77	127694.60		
Std. Error	2556.61	2096.15	986.23	1562.82	1014.80	3108.80	2010.83	743.03	2565.62		
Musick Point	87010.80	101404.60	85460.46	118806.95	145066.52	137142.22	274957.04	109294.75	144923.75	137659.85	
Std. Error	2089.26	2862.52	1623.55	3431.05	2330.58	2751.68	4963.90	1624.31	2432.87	3672.83	
Achilles Point	59041.13	74077.92	70237.93	70398.61	64112.76	51703.74	63708.46	56443.04	69011.33	51471.06	30207.62
Std. Error	1357.79	828.71	534.84	1421.22	1616.14	1109.27	1173.89	1547.45	824.17	1071.24	646.86
Narrowneck Beach	74015.37	93522.65	32735.27	34829.67	42897.13	49696.98	75116.77	72619.05	78805.72	61886.32	
Std. Error	1072.58	2175.44	771.07	573.47	558.42	594.72	994.80	780.33	625.92	518.50	
St Leonard's Beach	60042.74	70217.06	100238.67	63172.27	54763.62	35001.76	31256.20	45947.57	61823.98	129762.01	
Std. Error	629.98	1266.28	853.88	997.99	491.96	601.87	540.71	605.03	1122.83	710.27	
Castor Bay	73501.07	70525.05	59161.46	62423.58	38498.33	56302.79	64748.32				
Std. Error	434.02	870.84	837.11	720.07	275.68	665.50	772.70				
Mairangi Bay	89472.24	67684.03	122110.37	62031.24	149253.76	95345.63	54558.23	40639.33			
Std. Error	1682.45	1824.16	2155.26	777.08	2446.97	1648.25	437.68	360.23			
Waiake Bay	86829.34	143312.34	103769.66	76385.06	108820.25	75817.17	118893.99				
Std. Error	564.16	1412.86	709.50	406.18	1020.74	1334.18	574.94				
Army Bay	79516.22	126137.87	112472.14	79582.67	104083.04	61559.99	57461.23	72006.69	103739.28	94129.50	
Std. Error	1389.62	1226.54	2567.27	688.49	1243.78	446.60	2163.57	619.77	2498.97	1729.56	
Waiwera Beach	121212.36	49343.87	33758.39	65370.66	74235.24	102754.10	102689.42	117004.10	104381.70	99355.53	103018.88
Std. Error	1759.55	723.30	1547.99	809.72	1567.77	1800.73	1101.21	2490.16	629.36	768.75	1292.28
Opahi Bay	75113.49	67737.13	54897.36	52633.97	118562.28	109231.30	97877.15	67150.86	114636.57	94486.89	82327.88
Std. Error	2898.79	2487.52	851.24	671.76	1864.02	2688.71	2998.34	2635.43	1727.25	836.36	1917.76
Martins Bay	102617.32	92418.29	130403.77	113259.09	48357.55	53886.54	60018.82	85795.46	96126.61	155565.75	
Std. Error	2263.39	1335.19	1071.69	2045.72	1010.73	2368.48	1026.91	1293.71	2694.98	3106.39	
Buckleton Beach	100805.83	54807.03	86679.76	48212.74	43891.70	86058.21	77094.95	200186.53	124192.25	233831.10	
Std. Error	1901.05	5367.98	1942.50	1862.92	737.54	5217.54	1783.05	3220.16	2072.64	3991.30	
Matheson Bay	108209.04	67738.92	89427.38	114047.54	90926.23						
Std. Error	1892.29	1467.00	1432.22	1845.71	875.91						
Leigh Marine Reserve	134602.65	115775.48	108557.44	148704.96	74224.98	90842.04	79941.79				
Std. Error	1472.62	1802.82	2488.78	3107.74	1458.60	1208.17	1754.45				

Bulk density and Porosity

Cockle Bay

Sample	V (m^3)	M_{cont} (kg)	$M_{sat+cont}$ (kg)	M_{sat} (kg)	M_{S+cont} (kg)	M_s (kg)	M_a (kg)	V_v (m^3)	N (%)	ρ_d (kg m^{-3})	ρ_a (kg m^{-3})
1	0.0000740						0.131				1768.784
2	0.0000955	0.00208	0.214	0.212	0.165	0.163	0.168	0.0000492	51.485	1707.733	1758.496
3	0.0000347	0.00207	slaked				0.059				1696.830
4	0.0000947	0.00208	slaked				0.163				1719.535
5	0.0000726						0.127				1752.680
6	0.0000641	0.00296	0.144	0.141	0.119	0.116	0.119	0.0000248	38.735	1808.367	1858.911
7	0.0000951	0.00209	0.208	0.206	0.171	0.168	0.173	0.0000376	39.558	1771.083	1820.715
8	0.0000692						0.156				2257.878
9	0.0000622						0.139				2241.864
								Mean	43.260	1762.394	1875.077
								Std. dev.	7.128	50.995	216.913
								Std. error	4.115	29.442	72.304

Eastern Beach

Sample	V (m^3)	M_{cont} (kg)	$M_{sat+cont}$ (kg)	M_{sat} (kg)	M_{S+cont} (kg)	M_s (kg)	M_a (kg)	V_v (m^3)	N (%)	ρ_d (kg m^{-3})	ρ_a (kg m^{-3})
1	0.000182						0.308				1693.668
2	0.000168						0.287				1703.681
3	0.0000678						0.115				1688.586
4	0.000119	0.00207	0.249	0.247	0.201	0.199	0.204	0.0000485	40.865	1671.474	1714.081
5	0.0000755						0.122				1617.233
6	0.000122	0.00208	0.255	0.253	0.206	0.204	0.210	0.0000490	40.147	1673.397	1722.474
7	0.000107						0.175				1636.631
8	0.0000483						0.0808				1672.643
9	0.000128	0.00209	0.262	0.260	0.207	0.205	0.210	0.0000554	43.441	1604.985	1646.514
								Mean	41.484	1649.952	1677.279
								Std. dev.	1.732	38.954	36.600
								Std. Error	1.000	22.490	12.200

Musick Point

Sample	V (m^3)	M_{cont} (kg)	$M_{sat+cont}$ (kg)	M_{sat} (kg)	M_{S+cont} (kg)	M_s (kg)	M_a (kg)	V_v (m^3)	N (%)	ρ_d (kg m^{-3})	ρ_a (kg m^{-3})
1	0.0000870						0.158				1811.844
2	0.000101	0.00208	0.214	0.212	0.164	0.162	0.169	0.0000506	49.919	1592.729	1666.197
3	0.0000855						0.144				1690.021
4	0.000119	0.00208	0.249	0.247	0.197	0.195	0.202	0.0000525	44.215	1637.110	1703.688
5	0.000145	0.00207	slaked				0.268				1849.722
6	0.000137						0.259				1891.030
7	0.000275						0.440				1598.468
8	0.000109						0.183				1676.842
9	0.000145	0.00208	0.313	0.311	0.264	0.262	0.269	0.0000489	33.735	1809.020	1856.148
10	0.000138						0.252				1833.795
								Mean	42.623	1679.619	1757.776
								Std. dev.	8.209	114.24	101.337
								Std. Error	4.739	65.957	32.046

Achilles Point

Sample	V (m^3)	M_{cont} (kg)	$M_{sat+cont}$ (kg)	M_{sat} (kg)	M_{S+cont} (kg)	M_s (kg)	M_a (kg)	V_v (m^3)	N (%)	ρ_d (kg m^{-3})	ρ_a (kg m^{-3})
1	0.0000588	0.00209	0.169	0.167	0.140	0.138	0.142	0.0000289	49.191	2340.706	2415.521
2	0.0000736	0.00205	slake test				0.150				2037.301
3	0.0000702	0.00208	0.157	0.155	0.134	0.132	0.136	0.0000228	32.404	1883.455	1929.727
4	0.0000704	0.00207	0.172	0.170	0.139	0.137	0.142	0.0000330	46.904	1945.777	2019.642
5	0.0000641	0.00208	0.151	0.149	0.126	0.124	0.128	0.0000254	39.555	1930.973	2000.226
6	0.0000517	0.00208	0.125	0.123	0.116	0.114	0.116	0.00000942	18.219	2203.322	2238.716
7	0.0000637	0.00207	0.155	0.153	0.139	0.137	0.140	0.0000153	24.047	2153.560	2197.824
8	0.0000563	0.00209	0.129	0.127	0.111	0.109	0.111	0.0000186	33.065	1926.919	1973.775
9	0.0000690	0.00209	0.159	0.157	0.131	0.129	0.134	0.0000276	39.993	1872.736	1941.710
10	0.0000515	0.00207	0.124	0.122	0.111	0.109	0.111	0.0000129	25.140	2114.392	2158.300
11	0.0000298	0.00208	0.0753	0.073	0.0688	0.0668	0.068	0.00000649	21.780	2240.398	2284.025
								mean	33.030	2061.224	2108.797
								Std. dev.	10.719	159.720	169.056
								Std. Error	3.390	48.157	53.460

Narrowneck Beach

Sample	V (m^3)	M_{cont} (kg)	$M_{sat+cont}$ (kg)	M_{sat} (kg)	M_{S+cont} (kg)	M_s (kg)	M_a (kg)	V_v (m^3)	N (%)	ρ_d (kg m^{-3})	ρ_a (kg m^{-3})
1	0.0000740	0.00298	0.164	0.161	0.134	0.131	0.136	0.0000304	41.046	1763.958	1831.376
2	0.0000935	0.00207	0.204	0.202	0.166	0.164	0.170	0.0000384	41.092	1749.737	1814.748
3	0.0000327	0.00181	0.0715	0.0697	0.0594	0.0576	0.0597	0.0000121	36.963	1759.265	1822.194
4	0.0000348	0.00296	0.0805	0.0775	0.0650	0.0621	0.0646	0.0000154	44.330	1781.814	1853.592
5	0.0000428	0.00174	0.0990	0.0973	0.0735	0.0717	0.0746	0.0000255	59.597	1674.824	1742.527
6	0.0000494	0.00174	0.107	0.105	0.0888	0.0871	0.0901	0.0000181	36.640	1762.003	1822.901
7	0.0000751	0.00207	0.165	0.163	0.142	0.140	0.143	0.0000236	31.431	1858.440	1908.895
8	0.0000726	0.00206	0.158	0.156	0.135	0.133	0.137	0.0000223	30.722	1834.505	1883.115
9	0.0000787	0.00207	0.164	0.162	0.139	0.137	0.141	0.0000247	31.405	1743.512	1788.230
10	0.0000619	0.00209	0.129	0.127	0.105	0.102	0.107	0.0000242	39.120	1654.808	1721.544
								mean	39.235	1758.287	1818.912
								Std. dev.	8.524	61.829	57.617
								Std. Error	2.695	19.552	18.220

St Leonard's Beach

Sample	V (m^3)	M_{cont} (kg)	$M_{sat+cont}$ (kg)	M_{sat} (kg)	M_{S+cont} (kg)	M_s (kg)	M_a (kg)	V_v (m^3)	N (%)	ρ_d (kg m^{-3})	ρ_a (kg m^{-3})
1	0.0000600	0.00208	0.126	0.124	0.106	0.103	0.106	0.0000208	34.709	1722.773	1767.574
2	0.0000702	0.00209	0.160	0.158	0.145	0.143	0.146	0.0000154	21.932	2031.558	2074.852
3	0.000100	0.00208	0.242	0.240	0.219	0.217	0.222	0.0000229	22.865	2166.030	2213.218
4	0.0000632	0.00209	0.144	0.142	0.123	0.121	0.125	0.0000211	33.401	1912.865	1981.249
5	0.0000548	0.00208	0.120	0.117	0.103	0.100	0.103	0.0000170	31.116	1834.064	1886.837
6	0.0000346	0.00297	0.079	0.076	0.066	0.063	0.064	0.0000130	37.521	1814.807	1861.889
7	0.0000313	0.00208	0.074	0.072	0.063	0.061	0.063	0.0000116	37.049	1940.735	2014.960
8	0.0000459	0.00205	0.113	0.111	0.104	0.102	0.104	0.00000924	20.110	2222.098	2271.502
9	0.0000618	0.00208	0.150	0.148	0.136	0.134	0.137	0.0000139	22.548	2167.444	2213.057
10	0.0000965	0.00207	0.207	0.205	0.177	0.175	0.180	0.0000305	31.599	1810.952	1861.544
								mean	29.285	1962.333	2014.668
								Std. dev.	6.733	175.521	174.378
								Std. Error	2.129	55.505	55.143

Castor Bay

Sample	V (m^3)	M_{cont} (kg)	$M_{sat+cont}$ (kg)	M_{sat} (kg)	M_{S+cont} (kg)	M_s (kg)	M_a (kg)	V_v (m^3)	N (%)	ρ_d (kg m^{-3})	ρ_a (kg m^{-3})
1	0.0000735	0.00209	0.202	0.200	0.172	0.170	0.176	0.0000297	40.353	2317.109	2397.108
2	0.0000705	0.00293	0.163	0.160	0.136	0.133	0.138	0.0000268	38.001	1883.870	1961.005
3	0.0000592	0.00177	0.137	0.135	0.117	0.115	0.119	0.0000202	34.076	1940.621	2006.712
4	0.0000622	0.00299	0.150	0.147	0.129	0.126	0.130	0.0000204	32.839	2027.547	2095.024
5	0.0000410	0.00181	0.101	0.099	0.084	0.082	0.086	0.0000167	40.687	2000.021	2104.298
6	0.0000562	0.00175	0.129	0.127	0.108	0.106	0.112	0.0000210	37.434	1892.719	1986.838
7	0.0000647	0.00209	0.199	0.197	0.171	0.169	0.174	0.0000273	42.132	2615.821	2688.873
								mean	37.932	2096.815	2177.123
								Std. dev.	3.468	271.864	269.035
								Std. Error	1.311	102.755	101.686

Mairangi Bay

Sample	V (m^3)	M_{cont} (kg)	$M_{sat+cont}$ (kg)	M_{sat} (kg)	M_{S+cont} (kg)	M_s (kg)	M_a (kg)	V_v (m^3)	N (%)	ρ_d (kg m^{-3})	ρ_a (kg m^{-3})
1	0.0000895						0.176				1970.779
2	0.0000675						0.132				1959.602
3	0.000122	0.00208	0.264	0.262	0.226	0.224	0.229	0.0000383	31.373	1834.078	1874.616
4	0.0000620						0.122				1966.106
5	0.000149						0.281				1883.571
6	0.0000953	0.00210	slaked				0.179				1872.556
7	0.0000546	0.00206	slaked				0.103				1879.643
8	0.0000406						0.078				1915.878
								mean	31.373	1834.078	1915.344
								Std. dev.	~	~	43.724
								Std. Error	0.061	52.191	15.459

Waiake Bay

Sample	V (m^3)	M_{cont} (kg)	$M_{sat+cont}$ (kg)	M_{sat} (kg)	M_{S+cont} (kg)	M_s (kg)	M_a (kg)	V_v (m^3)	N (%)	ρ_d (kg m^{-3})	ρ_a (kg m^{-3})
1	0.0000868	0.00209	0.190	0.188	0.161	0.159	0.164	0.0000291	33.491	1829.105	1884.041
2	0.000143	0.00208	0.300	0.298	0.248	0.246	0.254	0.0000518	36.110	1717.926	1773.818
3	0.000104	0.00208	0.224	0.222	0.184	0.182	0.188	0.0000401	38.734	1751.814	1810.292
4	0.0000764	0.00207	0.170	0.168	0.144	0.141	0.146	0.0000270	35.282	1851.802	1908.750
5	0.000109	0.00207	0.240	0.238	0.203	0.201	0.211	0.0000369	33.946	1847.634	1934.475
6	0.0000758	0.00206	0.161	0.158	0.133	0.131	0.134	0.0000279	36.812	1721.905	1772.422
7	0.000119	0.00297	0.256	0.253	0.212	0.209	0.215	0.0000440	36.999	1757.700	1804.128
								mean	35.911	1782.555	1841.132
								Std. dev.	1.831	58.617	66.707
								Std. Error	0.692	22.155	25.213

Army Bay

Sample	V (m^3)	M_{cont} (kg)	$M_{sat+cont}$ (kg)	M_{sat} (kg)	M_{S+cont} (kg)	M_s (kg)	M_a (kg)	V_v (m^3)	N (%)	ρ_d (kg m^{-3})	ρ_a (kg m^{-3})
1	0.0000795	0.00297	0.184	0.181	0.159	0.156	0.164	0.0000247	31.101	1963.715	2062.353
2	0.000126	0.00300	0.288	0.285	0.250	0.247	0.258	0.0000375	29.744	1961.000	2047.319
3	0.000112	0.00209	0.249	0.247	0.219	0.217	0.223	0.0000305	27.286	1937.375	1996.254
4	0.0000793	0.00207	0.187	0.185	0.166	0.164	0.168	0.0000203	25.590	2074.057	2119.609
5	0.000103	0.00209	0.243	0.241	0.211	0.209	0.216	0.0000318	30.748	2021.445	2089.872
6	0.0000616	0.00207	0.144	0.142	0.123	0.121	0.126	0.0000211	34.292	1968.324	2040.611
7	0.0000575	0.00209	0.137	0.135	0.118	0.115	0.119	0.0000200	34.719	2008.833	2078.097
8	0.0000720	0.00209	0.175	0.173	0.156	0.154	0.159	0.0000196	27.247	2132.441	2204.795
9	0.000104	0.00209	0.245	0.243	0.216	0.214	0.221	0.0000290	27.974	2065.177	2126.292
10	0.0000930	0.00209	0.214	0.212	0.188	0.186	0.191	0.0000265	28.477	1994.915	2053.289
								mean	29.718	2012.728	2081.849
								Std. dev.	3.029	61.445	57.745
								Std. Error	0.958	19.431	18.261

Waiwera Beach

Sample	V (m^3)	M_{cont} (kg)	$M_{sat+cont}$ (kg)	M_{sat} (kg)	M_{S+cont} (kg)	M_s (kg)	M_a (kg)	V_v (m^3)	N (%)	ρ_d (kg m^{-3})	ρ_a (kg m^{-3})
1	0.000121	0.00208	0.280	0.278	0.255	0.253	0.261	0.0000253	20.897	2085.183	2149.203
2	0.0000491	0.00206	0.118	0.116	0.113	0.111	0.115	0.00000578	11.778	2252.656	2333.349
3	0.0000338	0.00209	0.081	0.078	0.075	0.073	0.075	0.00000527	15.611	2166.573	2220.189
4	0.0000654	0.00207	0.156	0.153	0.145	0.143	0.147	0.0000103	15.787	2189.361	2255.293
5	0.0000742	0.00299	0.179	0.176	0.172	0.169	0.175	0.0000070	9.443	2278.971	2353.060
6	0.000103	0.00299	0.249	0.246	0.231	0.228	0.236	0.0000179	17.459	2219.571	2296.648
7	0.000103	0.00299	0.242	0.239	0.225	0.222	0.227	0.0000171	16.681	2160.982	2214.347
8	0.000117	0.00298	0.280	0.277	0.259	0.256	0.263	0.0000207	17.700	2187.616	2246.246
9	0.000104	0.00297	0.238	0.235	0.220	0.217	0.225	0.0000183	17.551	2076.992	2159.957
10	0.0000994	0.00298	0.227	0.224	0.208	0.205	0.210	0.0000184	18.519	2066.417	2117.748
11	0.000103	0.00208	0.246	0.244	0.230	0.228	0.233	0.0000162	15.754	2214.060	2265.701
								mean	16.107	2172.580	2237.431
								Std. dev.	3.149	70.982	74.976
								Std. Error	0.950	21.402	22.606

Opahi Bay

Sample	V (m^3)	M_{cont} (kg)	$M_{sat+cont}$ (kg)	M_{sat} (kg)	M_{S+cont} (kg)	M_s (kg)	M_a (kg)	V_v (m^3)	N (%)	ρ_d (kg m^{-3})	ρ_a (kg m^{-3})
1	0.0000751	0.00208	0.186	0.184	0.169	0.167	0.171	0.0000174	23.125	2221.305	2274.957
2	0.0000677	0.00209	0.169	0.167	0.151	0.148	0.153	0.0000190	27.976	2190.970	2254.746
3	0.0000541	0.00294	0.136	0.133	0.123	0.120	0.123	0.0000134	24.807	2217.692	2272.737
4	0.0000526	0.00297	0.128	0.125	0.114	0.111	0.114	0.0000148	28.138	2100.355	2160.202
5	0.000119	0.00210	0.282	0.280	0.257	0.254	0.260	0.0000253	21.356	2145.708	2196.145
6	0.000109	0.00209	0.266	0.264	0.237	0.235	0.242	0.0000285	26.272	2166.392	2227.260
7	0.0000979	0.00208	0.217	0.215	0.185	0.183	0.190	0.0000321	32.827	1871.836	1937.429
8	0.0000685	0.00207	0.168	0.165	0.150	0.148	0.152	0.0000176	25.632	2158.549	2217.957
9	0.000115	0.00209	0.271	0.269	0.242	0.240	0.246	0.0000293	25.533	2089.822	2149.663
10	0.0000945	0.00210	0.219	0.217	0.196	0.194	0.200	0.0000227	24.056	2055.312	2113.627
11	0.0000822	0.00207	0.205	0.203	0.185	0.183	0.188	0.0000197	24.016	2226.977	2287.320
								mean	25.794	2131.356	2190.186
								Std. dev.	3.066	103.070	101.032
								Std. Error	0.924	31.077	30.462

Martins Bay

Sample	V (m^3)	M_{cont} (kg)	$M_{sat+cont}$ (kg)	M_{sat} (kg)	M_{S+cont} (kg)	M_s (kg)	M_a (kg)	V_v (m^3)	N (%)	ρ_d (kg m^{-3})	ρ_a (kg m^{-3})
1	0.000103	0.00298	0.248	0.245	0.215	0.212	0.219	0.0000331	32.303	2062.884	2136.304
2	0.0000924	0.00302	0.214	0.211	0.186	0.183	0.188	0.0000273	29.583	1981.859	2034.121
3	0.000130	0.00207	0.319	0.317	0.280	0.278	0.286	0.0000388	29.821	2138.446	2202.194
4	0.000113	0.00295	0.282	0.279	0.251	0.248	0.255	0.0000305	26.956	2192.672	2248.914
5	0.0000484	0.00207	0.126	0.124	0.112	0.110	0.113	0.0000143	29.654	2273.895	2342.344
6	0.0000539	0.00207	0.132	0.130	0.118	0.116	0.119	0.0000137	25.331	2151.743	2207.787
7	0.0000600	0.00299	0.154	0.151	0.138	0.135	0.138	0.0000164	27.241	2243.130	2304.444
8	0.0000855	0.00298	0.210	0.207	0.184	0.181	0.187	0.0000258	30.227	2121.506	2188.326
9	0.0000961	0.00208	0.231	0.229	0.206	0.204	0.209	0.0000253	26.351	2120.121	2176.401
10	0.000156	0.00298	0.364	0.361	0.322	0.319	0.329	0.0000419	26.928	2053.151	2114.026
								mean	28.439	2133.941	2195.486
								Std. dev.	2.180	88.410	90.113
								Std. Error	0.689	27.958	28.496

Buckleton Beach

Sample	V (m^3)	M_{cont} (kg)	$M_{sat+cont}$ (kg)	M_{sat} (kg)	M_{S+cont} (kg)	M_s (kg)	M_a (kg)	V_v (m^3)	N (%)	ρ_d (kg m^{-3})	ρ_a (kg m^{-3})
1	0.000101	na	na	0.234	na	0.219	0.227	0.0000151	15.017	2170.530	2248.645
2	0.0000429	na	na	0.139	na	0.129	0.133	0.0000100	23.427	3000.490	3111.092
3	0.0000865	na	na	0.213	na	0.197	0.204	0.0000160	18.544	2273.596	2357.876
4	0.0000467	na	na	0.113	na	0.105	0.109	0.00000797	17.074	2247.874	2328.209
5	0.0000439	na	na	0.100	na	0.094	0.097	0.0000063	14.240	2138.445	2203.606
6	0.0000812	na	na	0.193	na	0.182	0.188	0.0000111	13.659	2246.202	2314.310
7	0.0000770	na	na	0.181	na	0.168	0.173	0.0000130	16.894	2175.940	2243.333
8	0.000200	na	na	0.452	na	0.416	0.424	0.0000361	18.039	2080.337	2121.296
9	0.000124	na	na	0.279	na	0.252	0.257	0.0000277	22.303	2027.979	2070.105
10	0.000234	na	na	0.515	na	0.468	0.477	0.0000470	20.093	2003.383	2042.490
								mean	17.929	2236.478	2304.096
								Std. dev.	3.276	283.848	303.368
								Std. Error	1.036	89.761	95.933

Matheson Bay

Sample	V (m^3)	M_{cont} (kg)	$M_{sat+cont}$ (kg)	M_{sat} (kg)	M_{S+cont} (kg)	M_s (kg)	M_a (kg)	V_v (m^3)	N (%)	ρ_d (kg m^{-3})	ρ_a (kg m^{-3})
1	0.000108	0.00206	na	0.258	0.248	0.245	0.252	0.0000121	11.206	2280.620	2345.106
2	0.0000675	0.00296	na	0.164	0.159	0.156	0.161	0.00000727	10.767	2316.715	2382.026
3	0.0000894	0.00208	na	0.217	0.208	0.206	0.212	0.0000110	12.256	2302.427	2372.987
4	0.0000996	0.00296	na	0.272	0.261	0.258	0.265	0.0000139	13.953	2586.149	2664.949
5	0.0000889	0.00297	na	0.224	0.216	0.213	0.219	0.0000111	12.442	2391.227	2460.522
								mean	12.125	2375.427	2445.118
								Std. dev.	1.240	124.918	130.143
								Std. Error	0.554	55.865	58.202

Leigh Marine Reserve

Sample	V (m^3)	M_{cont} (kg)	$M_{sat+cont}$ (kg)	M_{sat} (kg)	M_{S+cont} (kg)	M_s (kg)	M_a (kg)	V_v (m^3)	N (%)	ρ_d (kg m^{-3})	ρ_a (kg m^{-3})
1	0.000135	0.00206	na	0.317	0.303	0.301	0.311	0.0000167	12.372	2234.000	2309.123
2	0.000116	0.00205	na	0.270	0.258	0.256	0.265	0.0000138	11.887	2216.361	2287.767
3	0.000109	0.00202	na	0.269	0.256	0.254	0.261	0.0000152	14.020	2335.169	2405.363
4	0.000149	0.00205	na	0.356	0.337	0.335	0.345	0.0000211	14.209	2249.488	2321.644
5	0.0000740	0.00204	na	0.185	0.176	0.174	0.179	0.0000110	14.929	2346.443	2418.518
6	0.0000859	0.00203	na	0.208	0.198	0.196	0.202	0.0000115	13.345	2283.056	2349.314
7	0.0000799	0.00206	na	0.195	0.186	0.184	0.189	0.0000109	13.622	2298.047	2368.098
								mean	13.483	2280.366	2351.404
								Std. dev.	1.059	49.815	49.027
								Std. Error	0.400	18.828	18.531

Modified Jar Slake Test

Ij'	Sample Behaviour	Classification
1	No visible sign of specimen deterioration - air bubbles may be emitted from the sample.	Extremely Durable
2	No notable specimen deterioration, development of occasional hairline fractures, (usually bedding fractures, or parallel to bedding) air bubbles generally emitted from these fractures.	
3	Slight specimen deterioration, consisting of closely spaced (10-20 mm), up to 1 mm open fractures, usually parallel to bedding. Sample may exhibit up to 5% slaking, usually from the sample corners.	
3i	Same as 3, but fractures tend to be randomly orientated.	
4	Moderate specimen deterioration, generally consisting of many very closely spaced (5-10 mm) fractures which are open up to 2 mm. Sample may exhibit up to 15% slaking producing gravel sized fragments and shards.	Durable
4i	Same as 4, but fractures tend to be randomly orientated.	
5	Moderate to high specimen deterioration, consisting of many extremely closely spaced (2-5 mm) fractures which are open up to 4 mm and generally parallel to bedding. Sample block integrity is maintained, although the block may have split into a few free standing columns. Sample block/s have a heavily desiccated appearance. Sample may exhibit up to 25% slaking producing gravel sized fragments and shards.	
5i	Same as 5, but fractures tend to be randomly orientated.	
6	High degree of sample deterioration. The specimen block shape is only partially retained, either in the form of multiple free-standing columns, or as a column supported within a pile of slaked debris. Sample block/s have a heavily desiccated and unstable appearance. Horizontal fractures are extremely closely spaced (2-6 mm) and generally open 2-4 mm with many crossing fractures. Sample may exhibit up to 75% mass slaking.	Non Durable
7	The sample block shape is largely or completely destroyed. The slaked debris (75-100% of the block) generally consists of a pile of angular gravel sized shards or blocky fragments occasionally supported with free-standing fragments of the original sample block.	
8	Total sample disintegration consisting of a pile of soil like debris i.e. high proportion of sub-gravel sized debris and some fine to medium gravel sized fragments	

Site	Ij'	1 min	10 min	30 min	1 hr	2 hr	3 hr	4 hr	6 hr	8 hr	24 hr
Cockle Bay	1	1 8 9	8 9	8 9	8 9	9					
	2	5	1			8	8 9	8 9	8 9	8 9	9
	3			1	1	1	1				8 7
	3i										
	4							1	1	1	1 2 6
	4i										
	5		5								
	5i										
	6			5	5						
	7					5					3
	8						5	5	5	5	4 5
Eastern Beach	1										
	2	2 3 5 7 8	2 3 5 7	2 3 5 7	2 3 5 7	2 3 5 7	2 3 5 7	2 3 5 7	2 3 5 7	2 3 5 7	2 6 7
	3		8	8	8	8	8	8	8	8	3 4 5 8
	3i										
	4										9
	4i										1a
	5										
	5i										
	6										2a
	7										
	8										
Musick Point	1	3 6 8	3 6	3 6	3	3					
	2	10	8	8	6 8	6 8	3 6 8	3 6 8	6	6	2, 6, 9
	3	1	10	10							
	3i		1	1	1 10	10	10	10	3 8 10	3 8 10	3 8
	4					1	1	1			10
	4i										4
	5								1	1	
	5i										
	6										1 5
	7										
	8										
Achilles Point	1										7
	2										1 3 5 6 10 11
	3										8
	3i										
	4										
	4i										4 9
	5										
	5i										
	6										
	7										2
	8										
Narrow-neck Beach	1										6
	2										1 2 3 5 7 9 10
	3										4 8
	3i										
	4										
	4i										
	5										
	5i										
	6										
	7										
	8										

Site	Ij'	1 min	10 min	30 min	1 hr	2 hr	3 hr	4 hr	6 hr	8 hr	24 hr
St Leonard's Beach	1										2 8 9
	2										1 3 4 7 10
	3										
	3i										6
	4										
	4i										
	5										
	5i										
	6										
	7										
	8										
Castor Bay	1										4
	2										2 3 5 6 7
	3										1
	3i										
	4										
	4i										
	5										
	5i										
	6										
	7										
	8										
Mairangi Bay	1	1	1								
	2	4 5		1							3
	3	2 8	2 8		1	1	1	1	1		
	3i			2 8	8	8	8			1	1
	4		4 5					8	8	8	8
	4i				2	2	2	2	2	2	
	5			5							7
	5i			4							2
	6				4						
	7				5	4 5					6
	8						4 5	4 5	4 5	4 5	4 5
Waiake Beach	1										
	2										1 2 3 4 5 6 7
	3										
	3i										
	4										
	4i										
	5										
	5i										
	6										
	7										
	8										
Army Bay	1										
	2										1 2 3 4 5 6 8 9
	3										1a 7 10
	3i										
	4										
	4i										
	5										
	5i										
	6										
	7										
	8										

Site	Ij'	1 min	10 min	30 min	1 hr	2 hr	3 hr	4 hr	6 hr	8 hr	24 hr
Waiwera Beach	1										1 2 3 4 5 6 9 11
	2										7 8 10
	3										
	3i										
	4										
	4i										
	5										
	5i										
	6										
	7										
	8										
Opahi Bay	1										5
	2										1 2 3 4 7 8 9 10 11
	3										
	3i										6
	4										
	4i										
	5										
	5i										
	6										
	7										
	8										
Martins Bay	1										6 7
	2										2 4 5 8 10
	3										1 3
	3i										
	4										9
	4i										
	5										
	5i										
	6										
	7										
	8										
Buckleton Beach	1										1 2 3 4 5 6 7 8 9 10
	2										
	3										
	3i										
	4										
	4i										
	5										
	5i										
	6										
	7										
	8										
Matheson Bay	1										1 2 3 4 5 6 7
	2										
	3										
	3i										
	4										
	4i										
	5										
	5i										
	6										
	7										
	8										
Leigh Marine Reserve	1										1 2 3 4 5
	2										
	3										
	3i										
	4										
	4i										
	5										
	5i										
	6										
	7										
	8										

APPENDIX TWO

INTACT ROCK STRENGTH

Schmidt Hammer Rebound Value

The lowest 50% of the Schmidt Hammer Rebound values for each site have been deleted and the mean Rebound value (R) is calculated from the remaining values.

H = test done at a horizontal orientation
V = test done at a vertical orientation
S = sandstone
Z = siltstone
PG = Parnell Grit

Site	Test	Lithology	Orientation	1	2	3	4	5	6	7	8	9	10	Mean
Cockle Bay	1	S	H	14.5	14.5	14.5	15	16	16	16	16	16	16	15 ±1
	2	S	H	18	18	18	18	18.5	19	19	20	20	22	19 ±1
	3	S	H	10.5	10.5	10.5	10.5	11	11	11	11.5	11.5	13.5	11 ±1
Eastern Beach	1	S	H	11.5	11.5	11.5	12	12	12.5	12.5	13	13.5	15	13 ±1
	2	S	V	12.5	12.5	13	13	13	14	14	14	14	14	13 ±1
	3	S	H	12	13	13	13.5	14	14	14	14.5	15	16.5	14 ±1
	4	S	H	13	13	13	13	13	13.5	14	14	14	14	13 ±1
	5	Z	H	15.5	16	16	16	17	17.5	17.5	18	18	18.5	17 ±1
Musick Point	1	S	H	15	15.5	15.5	16	16	16	16	16.5	17.5	17.5	16 ±1
	2	S	H	13.5	13.5	13.5	13.5	13.5	14	14	14	14	15	14 ±1
	3	S	V	16.5	17	17	17	17.5	18	18	18	18	18	18 ±1
Achilles Point	1	S	H	18	18	19	19	19.5	20	20	21.5	22	22	20 ±1
	2	S	H	16	17	18	18	19.5	21.5	23				19 ±1
	3	S	V	18	18	19	19	19	19.5	21	22	23	25.5	20 ±1
Narrowneck Beach	1	S	H	16.5	16.5	17	18	18	18	19	19.5	20	21	18 ±1
	2	S	H	13.5	14	14.5	16	16	16	16	16	16	18	16 ±1
	3	S	H	14.5	14.5	14.5	15	16	16	16	17.5	18.5	18.5	16 ±1
	4	S	H	17.5	17.5	18	18	18	18	18.5	19	20	20.5	19 ±1
	5	S	H	18	18	18	19	19	19.5	19.5	20	20	20	19 ±1
	6	Z	V	19.5	19.5	20	21	21.5	22	22	22.5	23	23	21 ±1
St Leonard's Beach	1	S	H	18.5	19.5	20.5	20.5	22	22	22	22	25.5	26	22 ±1
	2	S	H	18	19.5	20	20	20	20	20.5	21	22	22	20 ±1
	3	S	H	19.5	20	20.5	21	21	21.5	22	22	22	22	21 ±1
	4	Z	H	18.5	20	20	22	23	24	24.5				22 ±1
	5	S	H	21.5	21.5	22	22	22	22.5	24	25.5	32	32	25 ±1
	6	S	H	20	20	20	21	21	21.5	22	22	22	24.5	21 ±1
Castor Bay	1	S	V	17.5	18	18	18	18	18	18	20	21	21	19 ±1
	2	S	H	17.5	18	18	18	18	18	18.5	19	19.5	20	18 ±1
	3	S	H	18	18	18.5	18.5	19	19.5	19.5	20.5	22	22.5	20 ±1

Mairangi Bay	1	S	H	16	16.5	18	18	19	19	20.5	21.5	22	22.5	19 ±1
	2	S	H	16	17	17.5	18	18.5	19	19.5	20	20	22	19 ±1
	3	S	H	14	14	14.5	15	16	16	16	16	17	17	16 ±1
	4	S	V	18	18	18	18	18.5	19.5	20	20	20.5	21	19 ±1
Waiake Bay	1	S	H	12.5	13.5	13.5	14	14	16					14 ±1
	2	S	H	12.5	13	14	18	18						15 ±1
	3	Z	H	17	17.5	18	18	19.5	20	21	21.5	22		19 ±1
	4	Z	H	19	19.5	19.5	20	20	20	20.5	21	21.5	22.5	20 ±1
Army Bay	1	S	H	17	17.5	17.5	17.5	18	18	18	18.5	18.5	20	18 ±1
	2	S	H	23	24	24.5	25	25	25.5	29.5	30	30.5	34	27 ±1
	3	S	H	25	25.5	25.5	25.5	25.5	26	26	26	26	28	26 ±1
	4	S	V	18.5	19	19	19.5	20	20	20	20.5	21	22	20 ±1
Waiwera Beach	1	S	H	24	24.5	26	26	27	28	28.5	28.5	30	30	27 ±1
	2	S	V	22	22	22	22.5	23	24	24	24.5	26.5	27.5	24 ±1
	3	Z	H	27.5	28.5	28.5	29	30	30	30	30	30.5	32	30 ±1
Opahi Bay	1	S	H	18	18	18	18.5	19	20	20	20.5	22	23	20 ±1
	2	S	H	24	24	24	24	24.5	25.5	25.5	26	27	28	25 ±1
	3	S	V	21	22	22	22	23.5	23.5	24	24	24	26	23 ±1
Martins Bay	1	S	H	24	24	24	25	25	25.5	26	27.5	28	30	26 ±1
	2	S	V	22.5	23.5	24	24	24	25	25	26.5	28	28.5	25 ±1
	3	Z	H	26	26	28	28	28	29	30	32	34	34	30 ±1
Buckleton Beach	1	S	H	22.5	25	25.5	26	26.5	27	27	27.5	30	30	27 ±1
	2	S	V	24	24	24	24.5	25	26	26	26.5	27	27	25 ±1
	3	S	V	31.5	31.5	31.5	31.5	32	32	32.5	33	34	34.5	32 ±1
	4	S	H	21.5	21.5	21.5	21.5	22	22	22	22	24.5	25	22 ±1
	5	PG	H	16.5	17	17	18	18.5	19	19.5	21	21.5	22	19 ±1
Matheson Bay	1	S	V	39.5	40	40	40	40.5	41	42	42	42	42.5	41 ±1
	2	S	H	37	37.5	37.5	38	38	38.5	38.5	39.5	41	41.5	39 ±1
Leigh Marine Reserve	1	S	H	17.5	17.5	17.5	18	19.5	19.5	20	22	22.5	23.5	20 ±1
	2	S	H	22.5	22.5	23	24	24	24.5	24.5	25	25.5	25.5	24 ±1
	3	Z	H	39	40	40	40	40	41	41	42	42.5	43	41 ±1

Point Load Strength

The lowest and highest values have been deleted from each site's set of data and the mean Point Load Strength Index is calculated from the remaining values. The mean value for each site is converted to a uniaxial compressive strength by multiplying by 22 MPa.

Uncorrected Point Load Strength (I_S)

$$I_S = P / D_e^2$$

Where: P = Load required to break the block sample (dimensionless)

And, $D_e^2 = 4A / \pi$

Where: D_e = the "equivalent core diameter" is calculated from D_e^2, the "failure plane area" for block and lump tests.

The "failure plane area" = $A = WD$ = *W*idth of block x *D*epth of block

Point Load Strength Index ($I_{S(50)}$)

$$I_{s(50)} = F \times I_s$$

Where: F = Size Correction Factor $= (D_e / 50)^{0.45}$

Conversion of the Point Load Strength Index into uniaxial compressive strength (MPa)
$= I_{s(50)} \times 22$ MPa

Cockle Bay

Sample	Length (mm)	Width (mm)	Depth (mm)	Area (mm^3)	P (units)	P (N)	D_e^2 (mm^2)	D_e (mm)	I_s	F	$I_{s(50)}$
11	44.85	35.32	30.92	1091.87	0.31	353.11	1390.22	37.29	0.25	0.88	0.22
12	41.20	36.53	32.10	1172.72	0.35	398.70	1493.15	38.64	0.27	0.89	0.24
13	58.90	46.38	32.95	1528.33	0.82	934.31	1945.93	44.11	0.48	0.95	0.45
14	54.50	36.05	33.80	1218.49	0.49	558.24	1551.43	39.39	0.36	0.90	0.32
15	46.00	39.05	30.05	1173.45	3.21	3657.96	1494.09	38.65	2.45	0.89	2.18
16	56.65	48.58	32.72	1589.48	3.71	4227.76	2023.79	44.99	2.09	0.95	1.99
19	56.00	47.82	36.44	1742.28	1.55	1766.22	2218.34	47.10	0.80	0.97	0.78
20	65.60	46.65	36.50	1702.73	2.04	2324.62	2167.98	46.56	1.07	0.97	1.04
										Mean	0.90
										Std. dev.	0.78
										Std. Error	0.28
										UCS (MPa)	19.86

Eastern Beach

Sample	Length (mm)	Width (mm)	Depth (mm)	Area (mm^3)	P (units)	P (N)	D_e^2 (mm^2)	D_e (mm)	I_s	F	$I_{s(50)}$
10	69.40	53.10	39.27	2085.06	0.95	1082.46	2654.78	51.52	0.41	1.01	0.41
11	53.30	45.03	42.88	1931.18	0.67	763.37	2458.85	49.59	0.31	1.00	0.31
12	60.00	54.52	47.05	2565.01	0.80	911.52	3265.87	57.15	0.28	1.06	0.30
13	72.30	62.47	49.92	3118.13	1.06	1207.81	3970.12	63.01	0.30	1.11	0.34
14	56.00	57.33	31.57	1809.82	0.74	843.14	2304.34	48.00	0.37	0.98	0.36
15	70.40	58.40	53.88	3146.79	0.74	843.14	4006.61	63.30	0.21	1.11	0.23
16	52.40	40.98	31.12	1275.26	0.52	592.43	1623.72	40.30	0.36	0.91	0.33
17	59.80	50.10	36.85	1846.19	0.42	478.47	2350.64	48.48	0.20	0.99	0.20
18	42.20	41.98	40.27	1690.53	0.79	900.12	2152.45	46.39	0.42	0.97	0.40
20	64.40	55.32	50.82	2811.01	0.64	729.18	3579.09	59.83	0.20	1.08	0.22
										Mean	0.31
										Std. dev.	0.07
										Std. Error	0.02
										UCS (MPa)	6.84

Musick Point

Sample	Length (mm)	Width (mm)	Depth (mm)	Area (mm^3)	P (units)	P (N)	D_e^2 (mm^2)	D_e (mm)	I_s	F	$I_{s(50)}$
11	64.20	53.22	51.12	2720.26	1.86	2119.50	3463.54	58.85	0.61	1.08	0.66
12	58.80	50.35	40.75	2051.76	1.59	1811.80	2612.39	51.11	0.69	1.01	0.70
13	46.65	40.83	31.97	1305.31	0.96	1093.85	1661.97	40.77	0.66	0.91	0.60
14	63.55	64.20	36.90	2368.98	1.01	1150.83	3016.28	54.92	0.38	1.04	0.40
15	66.75	63.92	35.43	2264.78	1.13	1287.59	2883.61	53.70	0.45	1.03	0.46
16	50.90	44.53	41.00	1825.87	1.17	1333.17	2324.77	48.22	0.57	0.98	0.56
17	62.30	42.80	42.22	1806.87	1.21	1378.75	2300.58	47.96	0.60	0.98	0.59
18	61.00	51.38	42.15	2165.81	1.98	2256.25	2757.59	52.51	0.82	1.02	0.84
19	51.95	46.42	40.38	1874.46	0.97	1105.25	2386.64	48.85	0.46	0.99	0.46
										Mean	0.59
										Std. dev.	0.14
										Std. Error	0.05
										UCS (MPa)	12.87

Achilles Point

Sample	Length (mm)	Width (mm)	Depth (mm)	Area (mm^3)	P (units)	P (N)	D_e^2 (mm^2)	D_e (mm)	I_s	F	$I_{s(50)}$
12	39.00	39.93	51.12	2041.26	5.81	6620.92	2599.01	50.98	2.55	1.01	2.57
13	41.40	34.70	40.75	1414.03	1.25	1424.34	1800.39	42.43	0.79	0.93	0.73
15	75.30	51.05	36.90	1883.75	3.17	3612.37	2398.46	48.97	1.51	0.99	1.49
16	36.30	35.18	35.43	1246.66	1.23	1401.55	1587.30	39.84	0.88	0.90	0.80
17	44.30	37.60	41.00	1541.60	1.62	1845.99	1962.83	44.30	0.94	0.95	0.89
18	46.85	34.57	42.22	1459.29	0.98	1116.65	1858.03	43.10	0.60	0.94	0.56
19	45.25	39.68	42.15	1672.65	1.66	1891.58	2129.69	46.15	0.89	0.96	0.86
21	56.65	37.75	42.70	1611.93	1.04	1185.02	2052.37	45.30	0.58	0.96	0.55
22	59.70	42.49	44.23	1879.47	1.55	1766.22	2393.02	48.92	0.74	0.99	0.73
23	39.80	36.88	30.52	1125.58	2.37	2700.69	1433.13	37.86	1.88	0.88	1.66
										Mean	1.08
										Std. dev.	0.64
										Std. Error	0.20
										UCS (MPa)	23.87

Narrowneck Beach

Sample	Length (mm)	Width (mm)	Depth (mm)	Area (mm^3)	P (units)	P (N)	D_e^2 (mm^2)	D_e (mm)	I_s	F	$I_{s(50)}$
11	51.35	47.60	36.80	1751.68	2.05	2336.02	2230.31	47.23	1.05	0.97	1.02
14	40.70	36.00	30.43	1095.60	1.32	1504.11	1394.96	37.35	1.08	0.88	0.95
15	53.10	46.12	44.58	2056.03	2.16	2461.38	2617.82	51.16	0.94	1.01	0.95
16	39.25	38.30	32.17	1231.98	1.47	1675.05	1568.61	39.61	1.07	0.90	0.96
17	50.20	39.08	32.05	1252.62	1.44	1640.86	1594.89	39.94	1.03	0.90	0.93
18	43.40	43.63	40.88	1783.88	2.24	2552.54	2271.30	47.66	1.12	0.98	1.10
19	41.00	42.28	33.02	1396.05	1.70	1937.16	1777.51	42.16	1.09	0.93	1.01
										Mean	0.99
										Std. dev.	0.06
										Std. Error	0.023
										UCS (MPa)	21.74

St Leonard's Beach

Sample	Length (mm)	Width (mm)	Depth (mm)	Area (mm^3)	P (units)	P (N)	D_e^2 (mm^2)	D_e (mm)	I_s	F	$I_{s(50)}$
12	58.80	44.35	38.07	1688.26	2.14	2438.58	2149.56	46.36	1.13	0.97	1.10
13	46.65	46.03	42.38	1951.05	1.27	1447.13	2484.15	49.84	0.58	1.00	0.58
14	63.55	43.82	30.08	1318.15	1.35	1538.30	1678.32	40.97	0.92	0.91	0.84
16	50.90	50.65	32.63	1652.88	1.09	1242.00	2104.51	45.87	0.59	0.96	0.57
18	61.00	33.65	33.00	1110.45	0.84	957.10	1413.87	37.60	0.68	0.88	0.60
19	51.95	54.32	38.58	2095.72	3.44	3920.07	2668.35	51.66	1.47	1.01	1.49
20	68.50	54.98	36.88	2027.97	5.74	6541.15	2582.09	50.81	2.53	1.01	2.55
21	69.60	37.05	29.07	1076.92	1.88	2142.29	1371.18	37.03	1.56	0.87	1.36
										Mean	1.14
										Std. dev.	0.68
										Std. Error	0.24
										UCS (MPa)	24.99

Castor Bay

Sample	Length (mm)	Width (mm)	Depth (mm)	Area (mm^3)	P (units)	P (N)	D_e^2 (mm^2)	D_e (mm)	I_s	F	$I_{s(50)}$
11	50.00	43.52	34.77	1512.93	2.62	2985.59	1926.32	43.89	1.55	0.94	1.46
12	37.75	38.15	34.40	1312.36	3.01	3430.04	1670.95	40.88	2.05	0.91	1.87
13	49.00	44.12	36.67	1617.61	2.09	2381.60	2059.61	45.38	1.16	0.96	1.11
15	43.60	33.43	32.93	1101.07	1.22	1390.15	1401.93	37.44	0.99	0.88	0.87
16	51.90	38.07	35.00	1332.33	2.56	2917.22	1696.38	41.19	1.72	0.92	1.58
17	51.00	43.07	40.72	1753.53	3.82	4353.11	2232.67	47.25	1.95	0.97	1.90
18	46.30	33.13	31.07	1029.34	2.31	2632.32	1310.60	36.20	2.01	0.86	1.74
19	46.50	33.17	30.20	1001.63	1.62	1845.99	1275.32	35.71	1.45	0.86	1.24
										Mean	1.47
										Std. dev.	0.37
										Std. Error	0.13
										UCS (MPa)	32.37

Mairangi Bay

Sample	Length (mm)	Width (mm)	Depth (mm)	Area (mm^3)	P (units)	P (N)	D_e^2 (mm^2)	D_e (mm)	I_s	F	$I_{s(50)}$
11	50.65	41.68	33.87	1411.68	0.58	660.81	1797.40	42.40	0.37	0.93	0.34
12	63.60	52.68	37.00	1949.28	0.85	968.50	2481.90	49.82	0.39	1.00	0.39
15	46.50	38.27	34.75	1329.77	0.87	991.29	1693.11	41.15	0.59	0.92	0.54
16	42.80	35.42	34.68	1228.37	0.57	649.41	1564.01	39.55	0.42	0.90	0.37
17	45.80	41.62	30.30	1260.99	0.60	683.60	1605.54	40.07	0.43	0.91	0.39
18	45.00	39.45	31.60	1246.62	0.95	1082.46	1587.25	39.84	0.68	0.90	0.62
19	49.65	47.65	38.07	1813.88	1.75	1994.14	2309.50	48.06	0.86	0.98	0.85
20	38.70	37.52	34.70	1301.83	0.88	1002.69	1657.54	40.71	0.60	0.91	0.55
										Mean	0.51
										Std. dev.	0.17
										Std. Error	0.06
										UCS (MPa)	11.11

Waiake Bay

Sample	Length (mm)	Width (mm)	Depth (mm)	Area (mm^3)	P (units)	P (N)	D_e^2 (mm^2)	D_e (mm)	I_s	F	$I_{s(50)}$
11	75.25	51.83	40.60	2104.43	0.78	888.73	2679.45	51.76	0.33	1.02	0.34
12	58.15	50.55	39.58	2000.94	0.94	1071.06	2547.67	50.47	0.42	1.00	0.42
13	55.10	42.20	35.95	1517.09	0.93	1059.67	1931.62	43.95	0.55	0.94	0.52
14	38.40	30.87	29.70	916.74	0.49	558.24	1167.23	34.16	0.48	0.84	0.40
16	56.45	47.27	46.20	2183.72	2.69	3065.36	2780.40	52.73	1.10	1.02	1.13
17	51.45	45.85	38.07	1745.36	0.73	831.75	2222.26	47.14	0.37	0.97	0.36
18	46.70	42.90	44.10	1891.89	0.98	1116.65	2408.83	49.08	0.46	0.99	0.46
20	41.00	41.45	33.47	1387.19	0.95	1082.46	1766.23	42.03	0.61	0.92	0.57
										Mean	0.52
										Std. dev.	0.26
										Std. Error	0.09
										UCS (MPa)	11.44

Army Bay

Sample	Length (mm)	Width (mm)	Depth (mm)	Area (mm^3)	P (units)	P (N)	D_e^2 (mm^2)	D_e (mm)	I_s	F	$I_{s(50)}$
11	45.55	44.75	39.92	1786.27	2.37	2700.69	2274.35	47.69	1.19	0.98	1.16
12	50.25	45.13	39.53	1784.27	2.89	3293.28	2271.80	47.66	1.45	0.98	1.42
13	48.75	44.62	28.43	1268.60	1.59	1811.80	1615.23	40.19	1.12	0.91	1.02
14	42.25	41.68	34.33	1431.13	3.61	4113.80	1822.17	42.69	2.26	0.93	2.10
15	51.30	37.43	34.35	1285.84	1.50	1709.24	1637.18	40.46	1.04	0.91	0.95
16	52.20	51.73	43.45	2247.81	5.07	5777.62	2862.00	53.50	2.02	1.03	2.08
18	57.45	49.68	47.95	2382.32	3.87	4410.09	3033.26	55.08	1.45	1.04	1.52
20	54.90	41.83	40.37	1688.67	2.05	2336.02	2150.08	46.37	1.09	0.97	1.05
										Mean	1.41
										Std. dev.	0.46
										Std. Error	0.16
										UCS (MPa)	31.07

Waiwera Beach

Sample	Length (mm)	Width (mm)	Depth (mm)	Area (mm^3)	P (units)	P (N)	D_e^2 (mm^2)	D_e (mm)	I_s	F	$I_{s(50)}$
12	36.85	32.25	29.15	940.09	3.22	3669.35	1196.96	34.60	3.07	0.85	2.60
13	46.60	45.03	45.18	2034.76	5.98	6814.65	2590.73	50.90	2.63	1.01	2.65
14	44.10	44.80	40.48	1813.65	5.37	6119.50	2309.22	48.05	2.65	0.98	2.60
16	39.30	37.17	35.55	1321.28	1.95	2222.06	1682.30	41.02	1.32	0.91	1.21
17	41.90	43.97	38.03	1672.20	4.14	4717.79	2129.11	46.14	2.22	0.96	2.14
19	40.50	41.47	40.55	1681.47	2.59	2951.40	2140.92	46.27	1.38	0.97	1.33
20	50.60	45.75	40.85	1868.89	2.90	3304.68	2379.54	48.78	1.39	0.99	1.37
21	39.70	37.32	33.07	1233.94	1.71	1948.56	1571.10	39.64	1.24	0.90	1.12
										Mean	1.88
										Std. dev.	0.69
										Std. Error	0.24
										UCS (MPa)	41.30

Opahi Bay

Sample	Length (mm)	Width (mm)	Depth (mm)	Area (mm^3)	P (units)	P (N)	D_e^2 (mm^2)	D_e (mm)	I_s	F	$I_{s(50)}$
12	62.70	47.97	37.72	1809.14	3.22	3669.35	2303.47	47.99	1.59	0.98	1.56
13	62.60	44.38	39.23	1741.31	5.98	6814.65	2217.10	47.09	3.07	0.97	2.99
15	42.80	42.30	39.80	1683.54	4.07	4638.01	2143.55	46.30	2.16	0.97	2.09
16	46.15	45.48	40.23	1829.95	1.95	2222.06	2329.96	48.27	0.95	0.98	0.94
17	43.65	39.95	30.72	1227.13	4.14	4717.79	1562.43	39.53	3.02	0.90	2.72
19	77.30	51.17	41.37	2116.59	2.59	2951.40	2694.93	51.91	1.10	1.02	1.11
20	46.15	42.35	37.37	1582.48	2.90	3304.68	2014.87	44.89	1.64	0.95	1.56
21	64.80	41.25	38.33	1581.25	1.71	1948.56	2013.31	44.87	0.97	0.95	0.92
										Mean	1.74
										Std. dev.	0.70
										Std. Error	0.22
										UCS (MPa)	38.28

Martins Bay

Sample	Length (mm)	Width (mm)	Depth (mm)	Area (mm^3)	P (units)	P (N)	D_e^2 (mm^2)	D_e (mm)	I_s	F	$I_{s(50)}$
11	64.90	38.28	35.62	1363.52	1.56	1777.62	1736.09	41.67	1.02	0.92	0.94
12	66.05	38.53	37.10	1429.59	2.41	2746.28	1820.21	42.66	1.51	0.93	1.40
13	50.40	39.52	36.43	1439.72	1.60	1823.20	1833.11	42.81	0.99	0.93	0.93
14	51.75	48.18	36.43	1755.48	2.25	2563.94	2235.15	47.28	1.15	0.98	1.12
15	62.90	59.08	37.08	2191.01	1.91	2176.48	2789.68	52.82	0.78	1.02	0.80
17	57.30	58.45	40.93	2392.55	3.35	3817.50	3046.29	55.19	1.25	1.05	1.31
18	62.45	44.97	38.98	1752.95	3.39	3863.09	2231.93	47.24	1.73	0.97	1.69
19	50.75	50.67	48.77	2470.84	2.95	3361.66	3145.98	56.09	1.07	1.05	1.13
										Mean	1.16
										Std. dev.	0.29
										Std. Error	0.10
										UCS (MPa)	25.52

Buckleton Beach

Sample	Length (mm)	Width (mm)	Depth (mm)	Area (mm^3)	P (units)	P (N)	D_e^2 (mm^2)	D_e (mm)	I_s	F	$I_{s(50)}$
11	49.15	48.00	29.75	1428.00	4.54	5173.63	1818.19	42.64	2.85	0.93	2.65
12	44.45	43.55	32.42	1411.75	3.34	3806.11	1797.49	42.40	2.12	0.93	1.97
13	67.90	49.92	29.68	1481.69	4.24	4831.75	1886.55	43.43	2.56	0.94	2.40
15	51.50	42.10	36.93	1554.89	6.80	7749.13	1979.75	44.49	3.91	0.95	3.71
16	45.30	37.70	33.28	1254.78	5.43	6187.87	1597.64	39.97	3.87	0.90	3.50
17	53.90	55.52	43.20	2398.32	6.37	7259.10	3053.64	55.26	2.38	1.05	2.49
18	63.05	54.30	47.63	2586.49	6.81	7760.52	3293.22	57.39	2.36	1.06	2.51
20	64.30	55.35	53.48	2960.30	4.89	5572.49	3769.17	61.39	1.48	1.10	1.62
										Mean	2.61
										Std. dev.	0.70
										Std. Error	0.25
										UCS (MPa)	57.34

Matheson Bay

Sample	Length (mm)	Width (mm)	Depth (mm)	Area (mm^3)	P (units)	P (N)	D_e^2 (mm^2)	D_e (mm)	I_s	F	$I_{s(50)}$
11	47.20	37.82	35.68	1349.42	8.63	9834.60	1718.14	41.45	5.72	0.92	5.26
12	45.80	46.05	38.65	1779.83	1.67	1902.97	2266.15	47.60	0.84	0.98	0.82
13	53.65	40.20	45.87	1843.84	8.27	9424.34	2347.65	48.45	4.01	0.99	3.96
14	65.65	47.43	45.87	2175.61	12.17	13868.78	2770.07	52.63	5.01	1.02	5.12
15	56.55	47.48	40.95	1944.44	11.66	13287.59	2475.74	49.76	5.37	1.00	5.36
16	60.30	49.87	48.38	2412.72	10.12	11532.60	3071.96	55.43	3.75	1.05	3.93
17	55.10	54.22	39.45	2138.85	7.86	8957.10	2723.27	52.18	3.29	1.02	3.35
										Mean	4.50
										Std. dev.	1.69
										Std. Error	0.64
										UCS (MPa)	98.94

Leigh Marine Reserve

Sample	Length (mm)	Width (mm)	Depth (mm)	Area (mm^3)	P (units)	P (N)	D_e^2 (mm^2)	D_e (mm)	I_s	F	$I_{s(50)}$
11	51.50	41.60	33.02	1373.49	4.24	4831.75	1748.79	41.82	2.76	0.92	2.55
12	56.20	36.32	28.70	1042.29	6.92	7885.88	1327.08	36.43	5.94	0.87	5.15
13	57.60	53.08	36.47	1935.77	8.99	10244.85	2464.70	49.65	4.16	1.00	4.14
14	52.65	51.20	34.98	1791.15	5.15	5868.78	2280.56	47.76	2.57	0.98	2.52
										Mean	3.59
										Std. dev.	1.29
										Std. Error	0.64
										UCS (MPa)	79.02

NCB Cone Indenter Strength

The lowest and highest values have been deleted from each site's set of data and the mean intact rock strength is calculated from the remaining values.

Penetration of weak rock (P_w)

$$P_w = (M_3 - M_0) - D_3$$

Where: P_w = Penetration of the cone into the specimen of weak rock
M_0 = Initial micrometer reading
M_3 = Final micrometer reading when load equivalent to 12N is applied
D_3 = Spring deflection as indicated by dial gauge (for applied load of 12N this deflection is 0.23 mm)

Cone indenter number for weak rock (I_w)

$$I_w = \frac{0.23}{P_w}$$

Conversion of cone indenter number for weak rock into uniaxial compressive strength (MPa)

$$= I_w \times 16.5 \text{ MPa}$$

Cockle Bay

Sample	M_0	M_1	D_1	P_W	I_W
1	7.425	8.175	0.23	0.52	0.44
2	6.725	7.550	0.23	0.60	0.39
3	7.750	8.675	0.23	0.70	0.33
4	7.775	8.500	0.23	0.50	0.46
5	7.675	8.425	0.23	0.52	0.44
6	7.700	8.625	0.23	0.70	0.33
7	7.350	8.150	0.23	0.57	0.40
8	7.325	8.100	0.23	0.55	0.42
9	6.700	7.675	0.23	0.75	0.31
10	6.075	7.100	0.23	0.79	0.29
11	6.250	7.025	0.23	0.55	0.42
12	7.050	7.775	0.23	0.50	0.46
13	7.675	8.600	0.23	0.70	0.33
				Mean	0.39
				Std. dev.	0.06
				Std Error	0.02
				UCS (MPa)	6.40

Eastern Beach

Sample	M_0	M_1	D_1	P_W	I_W
1	5.900	6.950	0.23	0.82	0.28
2	6.950	7.750	0.23	0.57	0.40
3	6.975	7.800	0.23	0.60	0.39
4	6.675	7.700	0.23	0.80	0.29
5	6.675	7.525	0.23	0.62	0.37
6	7.350	8.200	0.23	0.62	0.37
7	7.200	8.275	0.23	0.85	0.27
8	6.700	7.600	0.23	0.67	0.34
9	8.850	9.725	0.23	0.65	0.36
10	6.075	6.975	0.23	0.67	0.34
12	7.875	8.750	0.23	0.65	0.36
13	6.525	7.625	0.23	0.87	0.26
14	6.975	8.075	0.23	0.87	0.26
				Mean	0.33
				Std. dev.	0.05
				Std Error	0.01
				UCS (MPa)	5.46

Musick Point

Sample	M_0	M_1	D_1	P_W	I_W
1	6.625	7.325	0.23	0.47	0.49
2	7.675	8.475	0.23	0.57	0.40
3	7.575	8.425	0.23	0.62	0.37
4	8.275	9.050	0.23	0.55	0.42
5	7.325	8.225	0.23	0.67	0.34
6	7.625	8.375	0.23	0.52	0.44
8	6.475	7.325	0.23	0.62	0.37
9	7.250	8.000	0.23	0.52	0.44
10	7.800	8.500	0.23	0.47	0.49
11	7.175	7.975	0.23	0.57	0.40
13	7.200	8.050	0.23	0.62	0.37
14	6.200	7.075	0.23	0.65	0.36
15	7.450	8.200	0.23	0.52	0.44
				Mean	0.41
				Std. dev.	0.05
				Std Error	0.01
				UCS (MPa)	6.79

Achilles Point

Sample	M_0	M_1	D_1	P_W	I_W
2	7.075	7.900	0.23	0.60	0.39
3	8.625	9.425	0.23	0.57	0.40
4	7.400	8.300	0.23	0.67	0.34
5	8.050	8.950	0.23	0.67	0.34
6	7.450	8.450	0.23	0.77	0.30
7	8.100	8.950	0.23	0.62	0.37
8	6.025	7.050	0.23	0.79	0.29
9	6.725	7.600	0.23	0.65	0.36
10	6.150	7.200	0.23	0.82	0.28
11	6.125	7.275	0.23	0.92	0.25
12	7.150	8.050	0.23	0.67	0.34
13	7.475	8.375	0.23	0.67	0.34
14	8.400	9.300	0.23	0.67	0.34
				Mean	0.33
				Std. dev.	0.04
				Std Error	0.01
				UCS (MPa)	5.52

Narrowneck Beach

Sample	M_0	M_1	D_1	P_W	I_W
1	6.900	8.250	0.23	1.12	0.21
2	7.125	7.975	0.23	0.62	0.37
3	6.200	7.050	0.23	0.62	0.37
4	6.775	7.625	0.23	0.62	0.37
5	5.350	6.625	0.23	1.05	0.22
7	5.925	7.000	0.23	0.85	0.27
8	6.650	7.575	0.23	0.70	0.33
10	6.800	7.950	0.23	0.92	0.25
11	6.900	8.000	0.23	0.87	0.26
12	7.625	8.750	0.23	0.90	0.26
13	6.850	7.650	0.23	0.57	0.40
14	7.575	8.450	0.23	0.64	0.36
15	7.025	7.950	0.23	0.70	0.33
				Mean	0.31
				Std. dev.	0.07
				Std Error	0.02
				UCS (MPa)	5.09

St Leonard's Beach

Sample	M_0	M_1	D_1	P_W	I_W
1	4.525	5.275	0.23	0.52	0.44
2	5.650	6.450	0.23	0.57	0.40
3	6.825	7.475	0.23	0.42	0.55
4	6.000	6.725	0.23	0.50	0.46
5	5.525	6.225	0.23	0.47	0.49
6	6.475	7.225	0.23	0.52	0.44
8	7.000	7.700	0.23	0.47	0.49
9	5.775	6.550	0.23	0.55	0.42
10	7.125	7.950	0.23	0.60	0.39
11	6.650	7.400	0.23	0.52	0.44
12	6.400	7.225	0.23	0.59	0.39
13	5.600	6.375	0.23	0.55	0.42
15	7.400	8.150	0.23	0.52	0.44
				Mean	0.44
				Std. dev.	0.05
				Std Error	0.01
				UCS (MPa)	7.34

Castor Bay

Sample	M_0	M_1	D_1	P_W	I_W
1	7.550	8.200	0.23	0.42	0.55
2	7.450	8.200	0.23	0.52	0.44
3	7.000	7.625	0.23	0.40	0.58
4	7.050	7.700	0.23	0.42	0.55
5	8.025	8.600	0.23	0.34	0.67
7	8.625	9.275	0.23	0.42	0.55
8	6.675	7.400	0.23	0.50	0.46
9	7.625	8.350	0.23	0.50	0.46
10	5.950	6.900	0.23	0.72	0.32
11	8.900	9.500	0.23	0.37	0.62
12	8.150	8.900	0.23	0.52	0.44
14	7.475	8.350	0.23	0.65	0.36
15	7.175	7.975	0.23	0.57	0.40
				Mean	0.49
				Std. dev.	0.10
				Std Error	0.03
				UCS (MPa)	8.13

Mairangi Bay

Sample	M_0	M_1	D_1	P_W	I_W
1	7.075	7.875	0.23	0.57	0.40
2	4.150	4.925	0.23	0.55	0.42
3	5.575	6.350	0.23	0.55	0.42
4	6.450	7.225	0.23	0.55	0.42
5	5.850	6.575	0.23	0.50	0.46
6	5.725	6.525	0.23	0.57	0.40
8	7.175	8.050	0.23	0.65	0.36
10	5.900	6.600	0.23	0.47	0.49
11	8.300	9.100	0.23	0.57	0.40
12	6.775	7.550	0.23	0.55	0.42
13	7.625	8.375	0.23	0.52	0.44
14	6.875	7.625	0.23	0.52	0.44
15	5.625	6.375	0.23	0.52	0.44
				Mean	0.43
				Std. dev.	0.03
				Std Error	0.01
				UCS (MPa)	7.03

Waiake Beach

Sample	M_0	M_1	D_1	P_W	I_W
1	7.125	8.125	0.23	0.77	0.30
2	6.575	7.450	0.23	0.65	0.36
3	7.550	8.425	0.23	0.65	0.36
4	7.150	7.900	0.23	0.52	0.44
5	7.175	8.025	0.23	0.62	0.37
6	7.075	7.775	0.23	0.47	0.49
7	6.350	7.225	0.23	0.65	0.36
8	7.000	7.850	0.23	0.62	0.37
9	7.500	8.275	0.23	0.55	0.42
10	5.825	6.650	0.23	0.60	0.39
11	7.175	7.900	0.23	0.50	0.46
12	7.825	8.575	0.23	0.52	0.44
15	6.725	7.625	0.23	0.67	0.34
				Mean	0.39
				Std. dev.	0.06
				Std Error	0.02
				UCS (MPa)	6.47

Army Bay

Sample	M_0	M_1	D_1	P_W	I_W
1	7.750	8.350	0.23	0.37	0.62
2	5.325	5.925	0.23	0.37	0.62
3	6.475	7.000	0.23	0.30	0.78
4	7.900	8.450	0.23	0.32	0.72
5	6.825	7.550	0.23	0.50	0.46
7	8.600	9.150	0.23	0.32	0.72
8	7.200	7.850	0.23	0.42	0.55
9	7.125	7.700	0.23	0.35	0.67
10	8.225	8.825	0.23	0.37	0.62
11	7.050	7.675	0.23	0.40	0.58
13	7.125	7.750	0.23	0.40	0.58
14	7.925	8.650	0.23	0.50	0.46
15	7.650	8.200	0.23	0.32	0.72
				Mean	0.62
				Std. dev.	0.10
				Std Error	0.03
				UCS (MPa)	10.29

Waiwera Beach

Sample	M_0	M_1	D_1	P_W	I_W
1	6.850	7.425	0.23	0.35	0.67
2	7.100	7.650	0.23	0.32	0.72
3	6.950	7.525	0.23	0.35	0.67
4	7.000	7.625	0.23	0.40	0.58
5	6.375	6.975	0.23	0.37	0.62
6	7.300	8.000	0.23	0.47	0.49
7	8.175	8.775	0.23	0.37	0.62
8	5.525	6.100	0.23	0.34	0.67
9	6.875	7.625	0.23	0.52	0.44
11	5.700	6.250	0.23	0.32	0.72
12	7.375	8.025	0.23	0.42	0.55
13	8.375	8.950	0.23	0.34	0.67
15	7.400	7.975	0.23	0.34	0.67
				Mean	0.62
				Std. dev.	0.08
				Std Error	0.02
				UCS (MPa)	10.25

Opahi Bay

Sample	M_0	M_1	D_1	P_W	I_W
1	5.500	6.300	0.23	0.57	0.40
2	4.175	4.850	0.23	0.45	0.52
3	4.900	5.925	0.23	0.79	0.29
4	7.575	8.200	0.23	0.39	0.58
5	5.050	5.700	0.23	0.42	0.55
6	8.275	9.475	0.23	0.97	0.24
7	5.100	5.875	0.23	0.55	0.42
8	5.925	6.675	0.23	0.52	0.44
9	6.325	7.375	0.23	0.82	0.28
11	5.600	6.250	0.23	0.42	0.55
12	6.975	7.625	0.23	0.42	0.55
13	7.525	8.550	0.23	0.80	0.29
14	7.600	8.350	0.23	0.52	0.44
				Mean	0.43
				Std. dev.	0.12
				Std Error	0.03
				UCS (MPa)	7.04

Martins Bay

Sample	M_0	M_1	D_1	P_W	I_W
1	6.975	7.525	0.23	0.32	0.72
2	7.050	7.625	0.23	0.35	0.67
3	6.125	6.825	0.23	0.47	0.49
4	6.500	7.125	0.23	0.40	0.58
5	7.925	8.450	0.23	0.30	0.78
6	8.050	8.675	0.23	0.40	0.58
8	7.375	7.975	0.23	0.37	0.62
9	7.750	8.400	0.23	0.42	0.55
10	6.475	7.050	0.23	0.35	0.67
11	7.525	8.100	0.23	0.34	0.67
12	7.100	7.650	0.23	0.32	0.72
14	7.175	7.725	0.23	0.32	0.72
15	8.500	9.075	0.23	0.34	0.67
				Mean	0.65
				Std. dev.	0.08
				Std Error	0.02
				UCS (MPa)	10.69

Buckleton Beach

Sample	M_0	M_1	D_1	P_W	I_W
1	5.350	6.075	0.23	0.50	0.46
2	6.050	6.675	0.23	0.40	0.58
3	7.650	8.225	0.23	0.34	0.67
4	6.675	7.250	0.23	0.35	0.67
6	7.625	8.150	0.23	0.30	0.78
7	6.925	7.725	0.23	0.57	0.40
9	6.250	6.825	0.23	0.35	0.67
10	7.475	8.075	0.23	0.37	0.62
11	7.300	8.000	0.23	0.47	0.49
12	6.100	6.750	0.23	0.42	0.55
13	7.625	8.250	0.23	0.40	0.58
14	5.900	6.550	0.23	0.42	0.55
15	5.175	5.900	0.23	0.50	0.46
				Mean	0.58
				Std. dev.	0.10
				Std Error	0.03
				UCS (MPa)	9.50

Matheson Bay

Sample	M_0	M_1	D_1	P_W	I_W
1	7.450	7.975	0.23	0.30	0.78
2	8.325	8.800	0.23	0.25	0.94
3	6.250	6.800	0.23	0.32	0.72
4	6.225	6.850	0.23	0.40	0.58
5	7.325	7.950	0.23	0.40	0.58
7	7.150	7.575	0.23	0.20	1.18
8	4.600	5.075	0.23	0.25	0.94
10	7.350	7.900	0.23	0.32	0.72
11	6.975	7.775	0.23	0.57	0.40
12	6.675	7.125	0.23	0.22	1.05
13	6.700	7.125	0.23	0.20	1.18
14	6.550	7.225	0.23	0.45	0.52
15	6.050	6.625	0.23	0.35	0.67
				Mean	0.79
				Std. dev.	0.25
				Std Error	0.07
				UCS (MPa)	13.01

Leigh Marine Reserve

Sample	M_0	M_1	D_1	P_W	I_W
1	6.825	7.325	0.23	0.27	0.85
2	7.700	8.225	0.23	0.30	0.78
3	7.125	7.650	0.23	0.30	0.78
4	7.400	7.925	0.23	0.30	0.78
5	6.850	7.550	0.23	0.47	0.49
6	8.050	8.550	0.23	0.27	0.85
7	7.925	8.475	0.23	0.32	0.72
8	7.350	8.000	0.23	0.42	0.55
9	7.050	7.600	0.23	0.32	0.72
10	8.500	8.975	0.23	0.25	0.94
12	6.150	6.800	0.23	0.42	0.55
14	6.125	6.650	0.23	0.30	0.78
15	7.650	8.075	0.23	0.19	1.18
				Mean	0.77
				Std. dev.	0.18
				Std Error	0.05
				UCS (MPa)	12.64

APPENDIX THREE

SCANLINE DATA

J1 = joint number
F1 = fault number
? = a value that could not be measured **or** was estimated rather than measured

Type of discontinuity:

J = joint	F = fault
Jf = joint face	sF = splay fault
B = bedding plane	

Persistence greater than 20 m was assumed for any discontinuities that persisted past the site description area as this is the largest classification of discontinuity persistence given in NZGS (2005).

The **adjusted persistence** has all discontinuities less than 0.1 m discarded in order to calculate the rock mass properties required for the RQD and RMS rock mass classification systems.

Termination classification:

O = obscured
B = beyond described cliff section
D = terminates in another discontinuity
R = terminates in rock material

Apertures that was measured as tight or hairline (t) were given a value of 0.1 mm in order to calculate an average aperture value.

Infill classification:

cl = clean	c = soft clay
g = soft fault gouge	fe = breakable iron crust
calc = hard calcite vein	
grit = loose sediment fallen or blown into discontinuity	

Roughness:

sl = slightly	stp = stepped
v = very	und = undulating
R = rough	pln = planar
Sm = smooth	

Water flow observed at time of scanline survey:

n = no
y = yes

Musick Point **Horizontal** Easting: 2679917 Northing: 6482339

Joint No.	Distance	Type	Dip	Dip Direction	Persistence (m)	Termination Upper	Termination Lower	Aperture (mm)	Infill	Surface Roughness	Water flow	Remarks
1	0.36	J	78	053	1.70	D	R	6	fe	slR-R	n	Fe lined
2	0.42	J	80	131	1.43	R	R	2.5	-	slR-R	n	Fe lined without fill, J1 intersects J2
3	0.54	J	82	132	2.30	D (J2)	R	1	-	slR-R	n	Fe lined without fill, J3 intersects J2
4	0.68	J	86	145	1.24	R	R	1	-	slR-R	n	Fe lined without fill, joint spacing 8 cm
5	1.04	J	55	322	0.57	D (J4)	D (J6)	t	-	-	n	Fe lining, little fe filling
6	1.28	J	85	123	1.88	R	R	1	-	slR-R	n	Fe lined without fill, joint spacing 57 cm
7	1.50	J	60	070	0.37	D	D	1	-	-	n	Fe lined without fill
8	1.68	J	75	120	1.60	R	R	2.5	-	slR-R	n	Fe lined without fill
9	2.11	J	82	120	0.44	R	R	2.5	-	slR	n	Fe lined without fill, joint spacing 63 cm, J8-J9
10	3.00	J	85	035	0.30	R	R	t	-	-	n	Fe lined
11	2.65	J	80	125	>3.00	D	D (J12)	2.5	fe	R	n	Fe lined with a little fe infill, joint spacing 18 cm, J11-J12
12	2.85	J	85	124	1.00	R	D (J11)	t	fe	slR-R	n	Fe lined with a little fe infill, joint spacing 28 cm, J12-J13
13	3.04	J	87	138	1.10	R	R	1	grit/c	slR	n	Fe lined, joint spacing 25 cm, J13-J14
14	3.30	J	80	130	>3.00	D or soil	D (J13)	2.5	-	R	n	Fe lined with no infill, joint spacing 13 cm, J14-J15
15	3.65	J	85	110	>3.00	D*	R	5	fe/grit	R	n	Fe lined with some infill, joint spacing 11 cm, J15-J16,
16	3.96	J	85	120	0.55	D (J15)	R	2.5	grit/c	slR-R	n	Fe lined with some infill
17	4.28	J	86	264	2.50	D	D	1	c	slR-R	n	Fe lined
18	4.58	J	82	124	2.80	D (3xjts)	D (J19)	0.2	-	-	n	Fe lined
19	5.78	J	74	252	2.00	D	R	0.2	-	-	n	Fe lined
20	5.51	*[1]	-	-	0.26	-	-	1			n	*[1] little fracture, * part of joint complex of ~6-7 joints
21	5.91	J	82	121	0.75	R	D (J24)	0.2	grit	-	n	Small % pale grit
22	4.78	J	83	133	>3.00	R	R	2.5	c	slR	n	Fe lined, a lot of clay infill
23	5.20	J	73	132	3.00	D	R	0.2	c	-	n	Fe lined
24	6.04	J	62	132	0.80	R	R	t	-	-	n	Fe lined
25	6.24	J	63	122	0.50	R	D (J26)	t	-	-	n	Fe lined
26	6.12	J	54	151	2.22	D	R	2	cl/fe	slR	n	Fe stained clay infill
27	6.43	J	83	103	1.37	R	D	0.5	cl/c	-	n	Fe lined
28	6.59	J	80	122	>0.86	R	D	0.25	cl/fe	-	n	Mostly tight aperture
29	6.64	J	52	132	>4.00	R	R	15	cl/c	R	n	A lot had clay/fe skin that filled part of the aperture
30	7.16	J	65	272	0.60	D (J29)	D (J31)	0.25	cl	-	n	Fe lined
31	7.24	J	75	302	0.60	R	D	0.25	cl/c	slR	n	Fe lined
32	7.69	J	86	280	0.22	R	R	t	fe	-	n	Fe lined
33	7.71	J	82	130	2.20	D (J29)	R	1	c	slR -R	n	Fe lined
34	7.81	J	68	287	0.32	D (J33)	D (J35)	t	fe	-	n	Fe lined
35	7.81	J	81	113	0.47	D	R	0.5	cl	5	n	Fe lined
36	8.03	J	78	124	>1.70	D (J29)	R	0.5	cl/c	5	n	Fe lined
37	9.57	J	88	141	>0.70	R	R/O	15	cl	5	n	Larger aperture filled with sediment brought in at high tide
38	9.52	J	58	172	0.77	R	R	2	cl/c	slR -R	n	Fe lined, joints 37-39 cross over one another plus few small
39	9.71	J	70	141	>3.00	R	R/O	6	c	R	n	fractures in a complex
40	9.80	Jf	64	214	?	R	R/O	0.25	cl	R	n	Fe lined, joint spacing 0.17 m
41	10.02	J	70	131	>1.00	D	R/O	1	c	slR?	n	Fe lined
42	10.17	Jf	65	214	?	R	R/O	0.5	cl/c	-	n	Fe lined
43	9.67	J	52	149	0.18	R	D	0.5	cl	-	n	Fe lined
44	10.04	J	87	104	0.15	D	D	8	cl/c	-	n	Fe lined, thick

45	10.00	J	69	129	>1.00	D	D	9	cl/c	slR	n	Fe lined, terminates in upper sst joint complex
46	10.10	J	88	277	?	D	D	0.5	cl	-	n	Fe lined & skins, joint spacing ~0.04 m
47	10.49	J	74	131	>0.90	D	R/O	0.25	cl	slR	n	Fe lined
48	10.80	J	88	316	>1.40	R	R/O	1	cl	R	n	Fe lined
49	10.92	J	75	128	0.62	D	D	0.25	cl	-	n	Fe lined
50	11.97	Jf	88	235	?	D (J49)	D (J51)	0.5	c	-	n	Fe lined, joint spacing 0.085 m
51	10.98	J	80	148	>1.40	R	R/O	0.5	cl	-	n	Fe lined
52	11.60	Jf	80	035	?	D	D (J51)	t	-	-	n	Fe lined, joint spacing ~7.00 cm
53	11.31	J	79	122	0.41	R	D	0.5	cl	-	n	Splits into 2 joints in upper sst
54	11.49	J	65	104	0.56	R	R/O	0.5	cl	R	n	Fe lined
55	11.52	J	72	172	>1.50	R	R/O	1	c	-	n	Ends in splay of fractures in upper sst
56	11.73	J	75	068	>0.30	D (J55)	R/O	1	cl/c	R	n	Fe lined
57	11.60	J	79	329	~0.10	R	D (J55)	0.25	cl	slR	n	Fe lined
58	11.85	J	83	124	>0.70	D (J55)	R/O	t	cl	-	n	Fe lined, thick
59	12.74	J	72	076	~1.10	R	R	0.25	cl	slR	n	Fe lined

Musick Point Vertical Easting: 2679917 Northing: 6482339

Joint No.	Distance	Type	Dip	Dip Direction	Persistence (m)	Termination Upper	Termination Lower	Aperture (mm)	Infill	Surface Roughness	Water flow	Remarks	
1	0.30	J	50	133	>5.0	R/O	B	2	c	R	n	Max aperture of 10 mm	
2	1-2.10	J	65	132	0.87	R	R	1	cl/c	Sm	n	Upper ends in splay of ~4 fractures	ALL
3	1.86-2.0	J	66	118	0.16	R	R	0.5	cl	-	n	-	
4	1.90	J	10	336	0.14	D (J2)	D (J6)	t	fe	-	n	Horizontal joint	FE
5	1.92	J	10	336	0.15	R	D (J6)	t	fe	-	n	Horizontal joint	
6	2.28	J	71	124	1.18	R	R	1	cl	Sm?	n	-	LINED
7	2.48	J	71	124	1.18	R	R		cl	Sm?	n	-	
8	3.17	B	10	277	>20.0	-	-	t		-	n	Boundary between 2 different sandstone units, flame structures	
9	3.25	J	56	133	~4.0	R	D	t	c	-	n	Further up aperture is ~5mm, Fe lined	
10	3.26	J	85	122	0.75	R	R/O	5.0	c	R	n	-	
11	3.30	J	70	136	>6.0	R	R	10	cl/c	R?	n	Aperture up to 20mm on platform, small rock pool (evaporate or drain?)	
12	3.38	J	70	136	1.23	R	D	t	-	-	n	-	
13	3.43	J	70	136	0.63	R	D	t	-	-	n	-	
14	3.54	J	70	136	>1.2	R	R	0.5	cl/c	-	n	Max aperture of 2 mm	
15	3.74	J	70	136	>2.0	R	R	1.5	cl/c	-	n	-	

Narrowneck Beach Horizontal Easting: 2671536 Northing: 6486096

Joint No.	Distance (m)	Type	Dip	Dip Direction	Persistence (m)	Termination Upper	Termination Lower	Aperture (mm)	Infill	Surface Roughness	Water flow	Remarks
1	0.09	J	82	320	1.20	R	D	8	cl/c	R	n	Fe lined
2	0.34	J	85	301	2.00	R	R	8	c	R	n	Fe lined
3	0.09-0.34	Jf	82	030	0.25	-	-	-	cl	Sm/stp	n	-

4	0.50	Jf	76	042	?	-	-	-	fe	R	n	-
5	0.62	J	74	046	0.65	D (J2)	R	2	cl/c	R	n	Fe lined
6	0.97	J	81	286	>0.40	R	R	1	c	-	n	Fe lined
7	0.99	J	88	281	>1.00	R	R	6-7	c	-	n	Fe lined
8	0.99	J	85	310	0.15	R	D	t	-	-	n	Fe stained
9	1-1.13	J	30	018	?	O	O	0.5	cl/c	-	n	0.13 cm joint spacing
10	1.13	J	86	335	0.65	R	D (J11)	10	cl/grit	Sm/stp	n	-
11	0.96	J	81	356	0.55	D (J10)	R	15	cl	-	n	Aperture very wide at cliff face but tightens ~10cm in
12	1.13-1.32	Jf	56	047	?	O	R	0.1-0.25	cl/fe	slR	n	0.19 cm spacing, persistence unknown
13	1.35	J	78	131	>1.30	R	R	8	cl/c	slR	n	Fe lined
14	1.44	J	84	088	>0.60	R	R	0.1-0.25	c	slR	n	Fe lined
15	1.84	J	86	300	1.00	R/O	R	2.5	cl/c	R	n	Fe lined, clay 1-2 cm in from cliff face
16	1.47-1.7	Jf	56	009	>1.00	R	R	?	?	slR	n	Fe lined
17	1.98	J	87	296	>0.50	R	D (J18)	2.5	c	Sm/stp	n	Fe lined
18	2.30	J	87	286	>1.00	R	R	2.5	c	-	n	Fe lined
19	1.86	J	78	354	0.80	D (J17)	R	1	c	-	n	Fe lined
20	1.86-2.03	Jf	70	034	0.85	O	O	?	?	slR	n	0.08 cm joint spacing
21	2.38	J	88	270	>0.80	R	R	1	cl/c	Sm/stp	n	-
22	2.14	Jf	83	339	>0.10	R/O	R	?	-	R/und-stp	n	-
23	2.53	J	87	259	1.00	D	R	5	c	-	n	Fe lined
24	2.38-2.53	Jf	89	215	>1.05	R	R/O	?	c	R	n	Fe lined, 0.15 cm joint spacing
25	2.56	J	81	309	0.60	R	R	0.1-0.25	cl	R?	n	Fe lined
26	2.73	Jf	69	052	?	R/O	R	-	-	slR	n	Frittery grey, little Fe
27	2.86	Jf	86	132	~0.10	R	R	-	-	R	n	No Fe, spacing ~0.12 m
28	2.73-2.86	Jf	73	348	>0.60	R	R	-	-	slR	n	Frittery grey, little Fe
29	5.20	J	88	024	>1.00	R	O	15	cl/c/grit	slR	n	Fe, grit about 15 cm in
30	3.70	J	73	054	0.90	D (J25)	R	9	cl	slR	n	Patches of Fe
31	3.00	J	86	319	>1.00	R	R	5	c	slR	n	Fe lined
32	3.00-3.30	Jf	68	032	>1.00	R	R	?	?	slR	n	No Fe
33	3.40	J	88	098	>1.00	R	R	2	c	slR?	n	Fe lined
34	3.70	J	65	069	0.20	D(J32) or R	D (J32)	1	cl	R	n	Little Fe
35	3.90	Jf	75	046	?	O	R	-	-	slR	n	No Fe
36	2.80	Jf	83	358	?	R/O	R	-	-	slR	n	No Fe
37	3.20-3.70	Jf	61	019	>0.50?	R	R	-	-	R	n	Frittery grey, little Fe
38	3.85	J	75	080	>1.00	R	R	3	c	slR?	n	Fe
39	3.63	J	81	313	>1.00	R	R	5	cl/c	-	n	Fe
40	3.70-3.78	Jf	69	022	?	R	R/O	-	-	slR	n	Roughness 4 but frittery, spacing <0.10 m, patch of Fe
41	3.63-3.96	Jf	63	044	0.18	D	D	-	-	Sm/stp	n	Spacing = 0.18 m
42	4.10	J	79	092	0.12	D	D	t	-	?	n	Fe lined
43	3.70-3.98	J	64	215	?	R	O	0.1-0.25	c	slR	n	Fe lined
44	3.98	J	64	288	>0.60	R	R	0.25	cl/c	-	n	Fe lined
45	4.19	J	89	097	>0.30	R	D	0.25	c	stp	n	Fe lined
46	4.50	J	80	045	0.20	R	R	0.25	c	-	n	Fe lined
47	4.17	J	75	320	0.36	R	R	t	-	-	n	Fe lined
48	4.22	J	82	300	0.95	D	R	15	c	-	n	Fe lined
49	4.46	Jf	50	009	?	O	R	0.5	cl	-	n	Little Fe
50	4.62	J	82	288	1.10	R	R	2	c	R	n	Fe lined

Narrowneck Beach Vertical

Easting: 2671536 Northing: 6486096

Joint No.	Distance (m)	Type	Dip	Dip Direction	Persistence (m)	Termination Upper	Termination Lower	Aperture (mm)	Infill	Surface Roughness	Water flow	Remarks
1	3.00	Jf	69	015	al 0.90	O	O	10	cl	R	n	Loosened block, joint at back of block
2	3.00	Jf	77	038	al 0.80	O	O	-	-	R/und	n	Joint at front of block
3	2.80	J	80	318	>1.00	R	R/O	6	cl/c	-	n	Right side of block, splays into a number of fractures
4	2.80	Jf	88	290	al 0.80	O	O	-	-	R	n	Left side of block, butts against J1
5	2.16	B	25	198	>20.00	-	-	t	fe	-	n	>20m visible before dips below ground, Fe crust
6	2.12	B	25	198	~0.40	D	D	t	fe	-	n	-
7	1.99	B	25	198	~0.30	D	D	t	fe	-	n	-
8	1.90	J	83	288	>2.00	D/O	B	0.5	fe/cl	Sm	n	Probably part of J3 and J11
9	1.68	B	10	212	>20.00	-	-	t	-	R	n	Bed dips below ground, >20m persist, grades into z/platform
10	1.68-1.20	Jf	72	030	al 0.45	D/O	D/O	-	-	Sm	n	Fe stained lightly
11	1.50	J	85	115	>2.00	D/O	D/O	4	cl	R?	n	Probably part of major vertical joint, tightens at top
12	1.18	J	26	019	0.60 w	D (J9)	D (J11)	0.5	cl/fe	-	n	Fe skin, horizontal joint
13	1.70	Jf	65	211	0.06	R/O	D (J12)	-	-	R/stp	n	Fe lined
14	1.28	B	24	197	>20.0	-	-	t	-	-	n	Grades
15	1.10	J	74	142	>2.00	D/O	R	0.1	-	-	n	Vertical joint part of J3 and J11
16	0.90	B	15	197	>20.0	-	-	t	-	R	n	Zst bed above with a sharp contact
17	0.72	J	86	282	0.09	R	R	t	fe	-	n	Fe lined, terminates lower thin convoluted sst
18	0.40	J	84	096	>0.50	R/O	B	0.2	fe	-	n	Fe lined
19	0.24	B	06	198	>20.0	-	-	t	-	R	n	Grades, sst bed is Fe stained
20	0.22	B	06	198	>20.0	-	-	0.5	cl	-	n	-
21	0.61	B	15	202	1.36	-	-	t	cl	-	n	Lense of massive sst, apert ≤ 5mm where lower zst eroded out
22	0.70	B	10	200	>20.00	-	-	t	fe	-	n	Fe lined
23	0.40	Jf	47	353	>0.17	R/O	R/O	-	-	R	n	-
24	0.25	Jf	56	018	>0.11	O	R/O	0.2	fe/cl	Sm	n	Fe lined
25	0.00	Jf	40	016	>0.05	O	O	0.1	fe	Sm	n	Fe lined

Castor Bay Horizontal

Easting: 2668355 Northing: 6492207

Joint No.	Distance	Type	Dip	Dip Direction	Persistence (m)	Termination Upper	Termination Lower	Aperture (mm)	Infill	Surface Roughness	Water flow	Remarks
1	0.00	F	64	190	al 5.00	R	B	0.4	c/g	-	n	Throw 2 cm No Fe Sandstone
2	0.14	Jf	73	118	0.19	R	O	-	-	Sm/und	n	-
3	0.15	Jf	89	234	0.18	R	O	-	-	Sm/und	n	-
4	0.17	J	80	184	~0.34	R	R	t	-	-	n	-
5	0.50	J	71	124	al 0.14	R	O	0.8	cl	-	n	-
6	0.36	J	80	184	al 0.10	R	R	t	-	-	n	-
7	0.45	J	80	184	al 0.15	R	R	t	-	-	n	-
8	0.55	J	80	184	al 0.20	R	R	t	-	-	n	-
9	0.35	Jf	71	092	0.30	R	O	-	-	Sm/und	n	-
10	0.76	J	86	157	al 0.23	R	R	t	cl	-	n	-
11	0.52	Jf	69	082	0.12	R	O	-	-	Sm/und	n	-

12	0.90	J	62	126	al 0.14	R	D	t	cl	-	n	-
13	0.66	Jf	67	056	al 0.14	R	D	-	-	Sm/und	n	-
14	0.85	J	71	086	al 0.20	R	R	1	cl	-	n	-
15	0.85	B	07	344	-	-	-	t	-	-	n	-
16	0.90	B	07	344	-	-	-	t	-	-	n	No Fe
17	0.87	J	63	336	0.26	R	R	t	cl	Sm/stp	n	No Fe
18	0.93	J	66	352	0.25	R	R	t	cl	Sm/stp	n	No Fe
19	1.00	J	70	338	0.22	R	R	t	cl	Sm/stp	n	No Fe
20	1.07	J	68	341	0.22	R	R	t	cl	Sm/stp	n	No Fe
21	1.24	J	65	336	0.28	R	R	t	cl	Sm/stp	n	No Fe
22	0.77	Jf	60	083	0.42	R	R	-	-	slR/stp	n	No Fe
23	1.00	Jf	54	074	0.93	R	R	-	-	slR/stp	n	No Fe
24	1.29	J	79	012	0.21	R	R	t	cl	-	n	No Fe
25	1.40	J	84	353	0.21	R	R	t	cl	-	n	No Fe
26	1.45	J	74	353	0.22	R	R	t	cl	Sm/pln	n	Sub-horizontal joints in siltstone were all very closely spaced
27	1.48	J	71	348	0.21	D	R	t	cl	Sm/pln	n	(persist <0.05 m) approximately 65/200
28	1.59	J	71	340	0.27	R	R	t	cl	Sm/pln	n	-
29	1.65	J	70	350	0.25	R	R	t	cl	Sm/pln	n	-
30	1.76	J	69	329	0.20	D	R	t	cl	Sm/pln	n	-
31	1.82	J	68	335	0.25	R	R	t	cl	Sm/pln	n	-
32	1.85	J	77	341	0.25	R	D	t	cl	Sm/pln	n	-
33	1.86	J	84	004	0.17	R	D	t	cl	Sm/pln	y	Water seepage from upper base of sst bed
34	1.97	J	64	010	0.13	R	D	t	cl	Sm/pln	y	Low pressure, continuous flow
35	1.79	F	60	189	>9.00	B	B	1.5	c/g	slR/und	n	slR to R and und to stp. Throw = 0.15 m
36	2.01	J	60	174	al 0.10	D (F35)	R	t	cl	R	n	Fe
37	2.00	J	60	174	al 0.10	D (F35)	R	t	cl	R	n	Fe
38	0.96	Jf	75	082	0.08	R	R	-	-	R	n	Sst – convoluted bed/cross-bedded, 0.06m thick
39	2.01	Jf	57	077	0.16	R	R	-	-	R	n	-
40	2.03	J	60	174	0.12	R	R	t	-	-	n	Fe
41	2.16	J	51	134	al 0.17	R	R	t	-	-	n	Fe
42	2.11	J	80	069	0.13	R	R	t	-	-	n	Fe
43	2.18	J	72	071	0.23	R	R	-	-	R	n	No Fe
44	2.19	J	85	354	0.16	R	R	t	cl	slR/und	n	No Fe
45	2.26	J	76	003	0.16	R	R	t	cl	slR/und	n	No Fe
46	2.26	J	76	198	0.11	R	R	t	cl	slR/und	n	No Fe
47	2.31	J	65	217	0.18	R	R	t	cl	slR/und	n	No Fe
48	1.88	Jf	89	110	1.20	-	-	-	-	Stp	n	No Fe
49	2.33	J	30	009	0.29	R	D	t	cl	-	n	-
50	2.44	J	40	025	0.31	R	D	t	cl	-	n	-
51	2.55	J	31	013	0.25	R	D	t	cl	Sm/und	n	No Fe
52	2.63	J	43	023	0.20	R	D	t	cl	Sm/und	n	No Fe
53	2.70	J	36	005	0.36	R	R	t	cl	Sm/und	n	No Fe
54	2.91	J	45	034	0.30	R	D	t	cl	Sm/und	n	No Fe
55	3.01	J	30	350	0.40	R	R	t	cl	Sm/und	n	No Fe
56	2.80	J	28	018	0.31	R	R	t	cl	Sm/und	n	No Fe
57	2.30	J	55	205	0.17	R	R	t	cl	Sm/und	n	No Fe
58	2.43	J	87	014	0.05	D	R	t	cl	Sm/und	n	No Fe
59	2.47	J	89	018	0.04	D	R	t	cl	Sm/und	n	No Fe
60	2.49	J	61	188	0.06	D	R	t	cl	Sm/und	n	No Fe

61	2.54	J	65	209	0.07	D	R	t	cl	Sm/und	n	No Fe
62	2.58	J	65	212	0.05	D	R	t	cl	Sm/und	n	No Fe
63	2.73	J	89	343	0.06	D	R	t	cl	Sm/und	n	No Fe
64	2.77	J	69	210	0.05	D	D	t	cl	Sm/und	n	No Fe
65	2.95	J	75	354	0.03	D	D	t	cl	Sm/und	n	No Fe
66	2.91	J	16	214	0.11	D	D	t	cl	Sm/und	n	No Fe
67	2.92	J	66	202	0.14	R	R	t	cl	Sm/und	n	No Fe
68	2.98	J	85	204	0.08	D	R	t	cl	Sm/und	n	No Fe
69	3.30	J	55	176	al 0.30	R	R	t	cl	Sm/und	n	No Fe
70	3.21	J	58	042	0.23	R	R	t	cl	Sm/und	n	No Fe

Castor Bay Vertical Easting: 2668355 Northing: 6492207

Joint No.	Distance	Type	Dip	Dip Direction	Persistence (m)	Termination Upper	Termination Lower	Aperture (mm)	Infill	Surface Roughness	Water flow	Remarks
1	0.14	J	73	223	0.02	R	R	t	-	-	n	0.02 thick zst bed
2	0.13	B	09	323	>7.00	-	-	t	-	w/c	n	-
3	0.135	B	09	323	>7.00	-	-	t	-	w/c	n	-
4	0.14	B	09	323	>7.00	-	-	t	-	w/c	n	-
5	0.16	B	09	323	>7.00	-	-	t	-	w/c	n	-
6	0.175	B	09	323	>7.00	-	-	t	-	w/c	n	-
7	0.18	B	09	323	>7.00	-	-	t	-	w/c	n	-
8	0.185	B	09	323	>7.00	-	-	t	-	w/c	n	-
9	0.21	J	86	219	0.045	R	R	t	-	-	n	-
10	0.245	B	09	323	0.50	-	-	t	-	R/und	n	0.8cm thick laminated thin sst bed
11	0.26	J	72	212	0.04	R	R	t	-	-	n	-
12	0.28	B	09	323	0.60	-	-	0.7	cl	R/und	n	-
13	0.10	Jf	67	291	0.05	R	R	-	-	slR/und	n	-
14	0.19	Jf	62	299	0.09	R	R	-	-	slR/stp	n	-
15	0.29	J	53	200	0.04	R	D	t	-	-	n	-
16	0.21	Jf	49	298	0.10	R	R	-	-	R	n	-
17	0.28	Jf	27	314	al 0.17	R	D	-	-	R	y	Seepage along this joint
18	0.25	Jf	60	294	0.30	D	D	-	-	R	n	-
19	0.54	J	50	093	>0.10	-	-	t	-	-	y	-
20	0.51	J	50	093	>0.10	-	-	t	-	-	y	-
21	0.48	J	72	190	0.05	R	R	t	-	-	y	This 5cm thick zst is saturated
22	0.40	B	09	323	>7.00	-	-	0.2	cl	w/c	y	-
23	0.45	B	25	323	0.50	-	-	0.5	cl	w/c	y	Bed base
24	0.58	J	34	021	0.20	D	D	t	cl	-	n	-
25	0.57	J	63	200	0.05	D	R	t	-	-	n	-
26	0.62	J	45	025	al 0.40	R	R	t	cl	-	n	-
27	0.60	B	25	323	>7.00	-	-	t	-	-	n	-
28	0.70	B	25	350	>7.00	-	-	0.2	cl	w/c	n	-
29	0.745	B	25	350	>7.00	-	-	t	-	w/c	n	-
30	0.63	J	84	218	0.09	D	R	t	-	-	n	-
31	0.64	J	70	219	0.08	D	R	t	-	-	n	-

32	0.61	J	75	206	0.05	R	D	t	-	-	n	-
33	0.72	B	25	350	>7.00	-	-	0.5	cl/c	w/c	n	-
34	0.75	J	85	023	0.05	R	R	t	cl	-	n	-
35	0.80	B	25	350	>7.00	-	-	t	-	w/c	n	-
36	0.85	B	25	350	>7.00	-	-	grades	-	w/c	n	-
37	0.86	J	58	082	0.11	R	D	t	cl	slR/und	n	-
38	0.87	J	38	189	0.05	R	D	t	cl	slR/und	n	-
39	0.89	J	69	210	0.05	D	D	t	cl	slR/und	n	-
40	0.99	B	11	015	>7.00	-	-	grades	-	w/c	n	-
41	1.02	B	11	015	>7.00	-	-	t	-	w/c	n	-
42	1.23	B	14	360	>7.00	-	-	grades	-	w/c	n	-
43	1.22	J	60	010	0.30	D	R	t	cl	Sm/pln	n	-
44	1.19	J	60	010	0.30	R	R	t	cl	Sm/pln	n	-
45	1.20	J	73	021	0.21	D	R	t	cl	Sm/pln	n	-
46	1.19	J	20	178	0.03	D	D	t	cl	Sm/pln	n	-
47	1.23	J	20	178	0.02	D	D	t	cl	Sm/pln	n	-
48	1.22	J	20	178	0.02	D	D	t	cl	Sm/pln	n	-
49	1.235	B	14	360	>7.00	-	-	1	cl	w/c	n	-
50	1.26	J	85	003	al 0.70	R	R	t	fe	-	n	Basal Sst
51	0.50	Jf	76	109	0.70	D	D	-	-	R/stp	n	-

Waiake Bay **Horizontal** Easting: Northing:

Joint No.	Distance	Type	Dip	Dip Direction	Persistence (m)	Termination Upper	Termination Lower	Aperture (mm)	Infill	Surface Roughness	Water flow	Remarks
1	0.00	J	78	274	0.60	R	D	1	cl/c	R	n	Fe skin
2	0.10	Jf	76	188	0.14	R	D	0.5	c	R	n	Fe stained
3	0.15	Jf	89	092	>0.42	D	D	0.4	c	R	n	Terminates in sst & zst joints, salt, Fe
4	0.20	J	65	350	0.11	D	R	t	c?	-	n	Fe skin
5	0.24	J	85	012	0.40	R	R	0.4	c	-	n	Fe skin
6	0.55	J	75	022	0.38	D	R	3	cl	R	n	Very large asperities, clean to ~10cm in from cliff face
7	0.62	J	65	000	0.58	D	D	2	cl	R	n	Very large asperities, clean to ~10cm in from cliff face
8	0.69	J	85	188	al 1.36	D	D	0.8	cl	-	n	Fe skin
9	0.70	Jf	80	215	0.72	D	D	-	-	Sm/und	n	No Fe skin
10	0.74	J	75	341	0.36	D	D	t	c	R	n	Fe skin
11	0.80	Jf	76	002	~0.27	D	D	-	-	R	n	Fe skin on parts
12	0.57	J	70	077	al 0.27	D	D	t	c	-	n	Fe skin
13	0.20	J	75	260	al 0.40	R	D/O	6	cl	R	n	Fe skin
14	1.12	Jf	84	212	0.75	R	R/O	-	-	Sm/und	n	No Fe skin
15	1.06	J	81	296	0.30	R	R	t	-	-	n	Fe lined
16	1.21	Jf	84	278	~0.55	R/O	R	5	cl	R	n	Fe lined
17	1.42	Jf	85	218	0.24	R	R/O	-	-	Sm/und	n	No Fe
18	1.49	J	89	000	~0.68	R	R	t/6	cl?	R	n	Fe skin
19	1.25	Jf	79	075	al 0.28	R/O	R/O	-	-	Sm/und	n	No Fe
20	1.25	Jf	60	072	0.21	D	R	-	-	Sm/und	n	No Fe
21	1.37	Jf	86	263	~0.34	D	D	-	-	R	n	Fe Skin

22	2.01	J	89	174	al 0.39	R	R	3	cl	R	n	Fe Skin
23	2.15	Jf	82	204	0.40	D	R	-	-	R	n	Fe Skin
24	1.44	Jf	62	068	0.24	D	R	-	-	R	n	Fe Skin
25	2.12	J	72	126	al 1.10	D	R	1	cl	R	n	Fe Skin
26	2.34	Jf	56	044	0.25	D	R	-	-	R	n	No Fe
27	2.38	J	87	212	0.30	R	R/O	1	cl/c	R	n	Fe skin
28	2.38	J	87	288	~0.70	D	R	1.5	c	R	n	Fe skin
29	2.40	J	83	171	0.09	D	D	0.8	cl	R	n	Fe skin
30	2.38	J	83	171	0.06	D	D	t	c	R	n	Fe skin
31	2.38	Jf	65	083	0.58	D	R	-	-	Sm/und	n	No Fe skin but is stained
32	2.88	Jf	66	046	~0.50	D	R	-	-	R	n	Some Fe patches
33	2.88	J	88	156	0.39	D	D	1	cl/c	R	n	Fe skin
34	2.98	J	83	000	al 0.13	D	R	t	-	R	n	Thick Fe skin
35	3.30	Jf	69	062	0.34	R	R/O	-	-	Sm/und	n	No Fe skin just staining
36	3.25	Jf	65	108	0.25	R	R/O	-	-	Sm/und	n	No Fe skin just staining
37	3.63	J	83	023	0.47	D	D	0.5	c	R (?)	n	Fe skin
38	3.28	Jf	71	099	~0.21	R	R	-	-	Sm/und	n	No Fe skin
39	4.10	J	89	204	~0.80	R/O	D	1.5	c	R	n	Fe skin
40	3.48	Jf	85	100	0.68	R	R	1.2	cl	R/und	n	Dark Fe skin and halite
41	4.25	J	80	183	al 0.32	D	R/O	0.5	c	-	n	Fe skin
42	4.24	J	81	358	al 0.85	D	R/O	1	c	-	n	Fe skin
43	4.66	Jf	87	357	0.70	R	R	0.8	cl	R	n	Fe skin
44	3.75	J	75	089	0.74	D	R/O	2	cl	-	n	Fe skin
45	4.44	Jf	74	273	al 0.60	R	R/O	1	cl	R/und	n	Fe skin
46	5.10	Jf	89	006	al 0.70	R	R	-	-	R	n	Fe skin
47	5.10	Jf	79	251	al 0.23	R	R/O	-	-	Sm/und	n	No Fe
48	5.25	Jf	80	264	0.50	R	D	1	c	SlR	n	No Fe
49	6.35	Jf	86	030	0.41	R	R	1	c	SlR	n	No Fe
50	6.25	J	88	042	0.95	R	R	0.6	cl	SlR	n	Fe skin
51	6.15	Jf	72	274	0.57	R	D	-	-	SlR	n	Patches Fe
52	6.59	J	86	182	al 1.10	D	R	0.7	cl/c	-	n	Fe skin
53	6.95	Jf	82	212	0.14	D	R	-	-	R	n	Fe Skin
54	7.00	Jf	78	222	~0.32	R	R	-	-	Sm/und	n	No Fe
55	7.00	J	69	195	al 0.70	R	R	0.8	c	R	n	Fe Skin
56	6.36	Jf	76	252	0.58	R	R	0.5	c	SlR	n	Fe patches, Fe lined jt
57	6.54	Jf	71	280	>0.50	R	R/O	0.5	c	R	n	Fe Skin and halite
58	7.21	J	89	196	al 0.55	R	R/O	0.5	c	-	n	Fe skin
59	7.03	J	89	007	~1.10	D	R	0.5	c	SlR	n	Fe skin
60	6.75	J	65	280	0.56	R	R	0.8	cl/c	R (?)	n	Fe skin and halite
61	7.91	Jf	82	032	al 0.70	R	R	-	-	R	n	Fe patches
62	7.66	J	80	278	al 0.82	R	R	0.5	c	-	n	Fe skin
63	7.92	J	80	194	0.12	R	?	0.5	c	-	n	Fe skin
64	7.81	Jf	79	280	~0.59	D	R/O	0.4	c	SlR	n	Fe skin
65	8.30	Jf	75	028	~0.52	D	R	-	-	Sm/und	n	No Fe
66	8.23	Jf	64	070	al 0.53	D	R	-	-	Sm/und	n	Some Fe patches
67	8.80	J	74	330	0.46	D	R	0.8	cl	Sm	n	Fe skin
68	9.03	Jf	58	044	0.20	D	R	0.8	cl	SlR	n	Fe skin, damp
69	9.38	J	68	228	>0.18	R	O	t	c	SlR	n	No Fe skin, gritty weathering
70	9.15	Jf	89	091	>0.20	R	O	0.4	c	SlR	n	Fe skin

Waiake Bay **Vertical** Easting: Northing:

Joint No.	Distance	Type	Dip	Dip Direction	Persistence (m)	Termination Upper	Termination Lower	Aperture (mm)	Infill	Surface Roughness	Water flow	Remarks
1	1.85	Jf	82	047	>0.30	O	O	-	-	R	n	Fe lined, roughness profile drawn
2	1.59	B	09	226	>20.0	-	-	t	-	R	n	Fe lined, roughness profile drawn
3	1.54	J	66	347	>0.04	R/O	R/O	0.2	cl	Sm	n	Fe lined
4	1.55	B	15	198	>0.04	O	D	-	-	Sm/und	n	No Fe lining, faint staining
5	1.52	J	86	149	>0.04	O	D	t	-	-	n	Fe? Vertical joint between J4 and J6
6	1.50	B	01	226	al 0.10	O	D	-	-	Sm/und	n	Fe lined
7	1.47-1.50	J	81	004	0.15	D	D	0.2	cl	Sm/und	n	Fe lined
8	1.43	B	09	193	>20.0	-	-	t	-	R	n	Fe lined
9	1.43	J	50	317	0.22	D (J8)	D	t	-	-	n	Fe lined. Lower sst bed grades into zst
10	1.28-1.39	J	65	142	0.11	D (J9)	D	t	-	-	n	Fe stained, faint
11	1.19	B	11	218	>3.00	-	-	t-0.1	-	und	n	Fe lined. At least 3m persistence then dust covers it. Wavy for 20cm
12	1.18	B	11	218	>3.00	-	-	t	-	und	n	Fe lined. Wavy boundary
13	1.00	J	64	304	0.18	D	D	0.2	cl	R/pln	n	Fe lined. Zst grades into lower sst
14	0.79	B	11	218	>20.0	-	-	t	-	R/und	n	Fe lined
15	0.75	J	86	326	0.08	D (J14)	D (J16)	t	-	-	n	Fe?
16	0.71	B	11	218	>20.0	-	-	t	-	R	n	Fe? Sporadic/discontinuous zst grading into upper sst
17	0.65	B	11	218	>20.0	-	-	t	-	-	n	Fe stained
18	0.63	B	11	218	>20.0	-	-	t	-	-	n	Fe stained
19	0.61	B	10	034	>20.0	-	-	t-0.2	cl	und	n	Fe lined
20	0.52-0.71	J	75	358	0.19	D (J16)	D	0.2	cl	-	n	Fe lined
21	0.48	B	04	041	>20.0	-	-	t	-	und	n	2-5cm thick sst bed grades into upper zst, total Fe staining
22	0.79	Jf	84	039	~0.20	R	O	-	-	R	n	No Fe
23	0.71-0.48	Jf	54	041	~0.20	D (J16)	D (J21)	-	-	R	n	Some Fe staining
24	1.05-1.39	Jf	69	045	~0.30	D (J8)	O	-	-	R	n	1-4 cm thick sst beds
25	0.44	B	04	041	>20.0	-	-	t	-	und	n	-
26	1.24	B	04	041	>20.0	-	-	t	-	und	n	1-4cm thick Fe stained sst
27	0.14	J	88	110	>0.06	D (J26)	B	0.2	cl	-	n	-

Many laminations/beds of same orientation as 04/041
Series of thin sst beds grading into medium zst beds.
Similar vertical fractures in zst but immeasurable
0.89-1.10 zst bed, 3 major joint sets (cliff face, 2 x vertical)
Plus random fractures of few cm persistence

Army Bay **Horizontal** Easting: 2672866 Northing: 6509643

Joint No.	Distance	Type	Dip	Dip Direction	Persistence (m)	Termination Upper	Termination Lower	Aperture (mm)	Infill	Surface Roughness	Water flow	Remarks
1	0.40	J	56	030	0.29	D	R	0.5	c	slR/pln	n	Fe lined
2	0.40	Jf	54	099	0.12	D	D	-	c	slR/und	n	Fe lined
3	0.50	J	87	043	>0.41	R	R	0.2	c	-	n	Fe lined

4	0.55	Jf	84	169	0.08	R	R	t	c	-	n	Fe lined
5	0.54	J	88	052	Al 0.05	D	R/O	-	-	slR/pln	n	No Fe
6	0.58	J	82	138	Al 0.10	D	D	t	-	R	n	Fe lined
7	0.57	J	88	052	0.38	R	R	1	c	slR/pln	n	Fe lined
8	0.73	Jf	78	138	0.08	D	D	-	c	slR/pln	n	Fe lined
9	0.68	Jf	75	186	0.14	D	D	-	c	slR/pln	n	Fe lined
10	0.73	J	85	199	Al 0.05	D	R/O	0.2	c	R	n	Fe lined
11	0.69	Jf	80	055	Al 0.05	D (J10)	R/O	-	-	R/stp	n	Fe lined
12	0.81	J	87	143	0.12	D	R	-	c	slR/und	n	Fe lined
13	0.80	J	88	040	0.12	D	D	t	-	-	n	Fe lined
14	0.85	J	74	198	0.35	R	R	t	-	-	n	Fe lined
15	0.92	Jf	80	120	0.11	R	R	-	c	slR/pln	n	Fe lined
16	0.93	J	79	194	0.52	R	R	0.5	c	und	n	Fe lined
17	0.92	J	80	198	0.16	R	R	t	c	-	n	Fe lined
18	0.85	Jf	75	115	0.12	R	D	-	-	slR/pln	n	Fe lined
19	1.05	F	56	192	>5.00	B	B	1.5	g	slR/stp	n	Fe lined
20	1.18	J	82	001	~1.40	D	D	1	cl/c	slR/pln	n	Fe lined
21	1.10	J	88	033	0.14	R	R	t	cl	Sm/pln	n	Fe lined
22	1.07	J	88	033	0.12	R	R	t	cl	Sm/pln	n	Fe lined
23	1.14	J	88	033	0.12	R	R	1	cl	Sm/pln	n	Fe lined
24	1.06	J	72	070	0.11	R	R	t	cl	Sm/pln	n	Fe lined
25	1.11	J	72	070	0.10	R	R	t	cl	Sm/pln	n	Fe lined
26	1.19	J	72	070	0.16	R	R	1	cl/c	Sm/und	n	Fe lined
27	1.16	J	72	070	0.12	R	R	t	cl	Sm/und	n	Fe lined
28	1.15	J	79	179	0.15	D	D	0.5	cl/c	slR/pln	n	Fe lined
29	1.07	J	79	179	0.16	R	R	t	cl	-	n	Fe lined
30	1.21	J	79	177	~0.20	R	R	t	cl	-	n	Fe lined
31	1.23	J	79	177	0.18	D	R	t	cl	-	n	Fe lined
32	1.28	J	79	177	0.26	R	R	0.5	cl/c	-	n	Fe lined
33	1.33	J	79	177	Al 0.36	D	D	t	cl	-	n	Fe lined
34	1.40	J	79	177	0.18	R	R	0.8	c	slR/pln	n	Fe lined
35	1.69	J	79	177	al 0.85	R	R	1	c	slR/pln	n	Fe lined
36	1.58	J	79	177	~0.15	R	R	t	cl	-	n	Fe lined
37	1.67	J	79	177	~0.15	R	R	t	cl	-	n	Fe lined
38	1.28	J	71	043	0.74	R	R	0.5	c	-	n	Fe lined
39	1.25	B	31	284	>1.00	-	-	0.2	cl	slR/pln	n	Fe lined
40	1.45	B	31	284	>1.00	-	-	0.2	cl	slR/pln	n	Fe lined
41	1.10	B	31	284	>1.00	-	-	0.2	cl	slR/pln	n	Fe lined
42	0.60	B	31	284	>1.00	-	-	0.2	cl	slR/pln	n	Fe lined
43	1.39	J	70	083	0.36	R	R	t	cl/c	slR/pln	n	Fe lined
44	1.86	sF	76	184	al 3.00	D (F46)	B	t	g	slR/stp	n	Fe lined
45	1.77	J	62	093	0.16	D	D	0.8	cl/c	-	n	Fe lined
46	2.41	F	61	195	>5.00	B	B	0.8	g	R?/pln	n	Fe lined
47	1.84	J	76	050	0.23	R	R	t	cl	slR/pln	n	Fe lined
48	1.82	J	76	050	al 0.31	R	R	0.8	c	-	n	Fe lined
49	2.00	J	76	050	0.16	R	R	t	-	-	n	Fe lined
50	2.14	J	76	050	~0.28	R	R	t	-	-	n	Fe lined
51	2.20	J	76	050	>0.10	R	R	t	cl/c	slR/pln	n	Fe lined
52	2.18	J	76	050	>0.10	R	R	t	cl/c	slR/pln	n	Fe lined

53	2.17	J	76	050	>0.10	R	R	t	cl/c	slR/pln	n	Fe lined
54	2.16	J	76	050	>0.10	R	R	t	cl/c	slR/pln	n	Fe lined
55	2.10	J	76	050	>0.10	R	R	t	cl/c	slR/pln	n	Fe lined
56	1.97	J	76	050	>0.10	R	R	t	cl/c	slR/pln	n	Fe lined
57	1.94	J	76	050	al 0.2	R	R	t	cl/c	slR/pln	n	Fe lined
58	1.75	J	76	050	0.20	R	R	t	cl/c	slR/pln	n	Fe lined
59	1.98	J	78	182	>0.20	R	R	t	c	slR/pln	n	Fe lined
60	1.96	J	78	182	0.12	R	R	t	cl	slR/pln	n	Fe lined
61	1.93	J	78	182	0.12	R	R	t	cl	slR/pln	n	Fe lined
62	2.06	J	78	182	0.16	R	R	t	cl	slR/pln	n	Fe lined
63	2.13	J	78	182	0.16	R	R	t	cl	-	n	Fe lined
64	2.20	J	78	182	0.32	R	R	t	cl	-	n	Fe lined
65	2.24	J	78	182	0.18	R	R	t	cl	-	n	Fe lined
66	2.22	J	78	182	0.18	R	R	t	cl	-	n	Fe lined
67	2.32	J	78	182	0.20	R	R	t	cl	-	n	Fe lined
68	2.33	J	78	182	0.22	R	R	t	cl	-	n	Fe lined
69	2.35	J	78	182	0.24	R	R	t	cl	-	n	Fe lined
70	2.37	J	78	182	0.26	R	R	t	cl	-	n	Fe lined
71	2.10	B	49	301	>1.00	-	-	t	-	pln	n	Fe lined
72	2.55	J	69	194	>1.50	D	B	0.5	c	slR/pln	n	Fe lined
73	2.46	J	69	194	0.32	R	R	t	c	slR/pln	n	Fe lined
74	2.48	J	69	194	0.45	D	R	1	c	slR/pln	n	Fe lined
75	2.45	Jf	79	298	~0.40	R	R	-	-	R/stp	n	Fe lined
76	2.75	F	58	228	>5.00	B	B	t	g	R/pln	n	Fe lined, planar to stepped roughness for J76 & J77
77	3.27	F	64	226	>5.00	B	B	t	g	R/pln	n	Fe lined, zone of fractures sub-parallel to fault

Army Bay **Vertical** Easting: 2672866 Northing: 6509643

Joint No.	Distance	Type	Dip	Dip Direction	Persistence (m)	Termination Upper	Termination Lower	Aperture (mm)	Infill	Surface Roughness	Water flow	Remarks	
1	0.33	Jf	66	115	0.10	R	R	-	-	slR/und	n	Fe lined	
2	0.34	Jf	74	184	0.15	R	R	t	c	slR/und	n	Fe lined	
3	0.35	J	88	047	~0.30	R	R	t	cl/c	slR/und	n	Fe lined	
4	0.36	J	88	047	~0.30	R	R	t	cl/c	slR/und	n	Fe lined	Fractured fragments which have a very small
5	0.335	B	34	322	>3.00	-	-	grades	-	R/stp	n	Fe lined	persistence (1-2 cm) are between the siltstone
6	0.325	B	34	322	>3.00	-	-	t	-	R/stp	n	Fe lined	main joint sets and have aperture of 0.5-1 mm
7	0.41	B	34	322	>3.00	-	-	0.5	cl	R/stp	n	Fe lined	plus seaward slope i.e. very loose and crumble
8	0.42	J	66	115	>0.10	R	R	t	cl	-	n	Fe lined	out continuously
9	0.48	J	75	111	>0.10	R	R	t	cl	-	n	Fe lined	
10	0.53	Jf	75	111	>0.10	R	R	t	cl	slR/und	n	Fe lined	
11	0.51	J	75	111	0.13	R	R	t	cl	slR/und	n	Fe lined	
12	0.55	J	85	007	0.12	R	R	0.5	cl/c	slR/und	n	Fe lined	
13	0.48	J	75	220	0.21	R	R	t	cl	slR/und	n	Fe lined	
14	0.61	Jf	70	020	~0.10	R	R	-	-	slR/und	n	Fe lined	
15	0.68	B	42	296	>3.00	-	-	t	cl	R/stp	n	Fe lined	
16	0.66	B	42	296	>0.10	-	-	t	cl	R/stp	n	Fe lined	

17	0.65	B	42	296	>0.10	-	-	t	cl	R/stp	n	Fe lined
18	0.56	B	40	288	>0.10	-	-	t	cl	R/stp	n	Fe lined
19	0.67	J	85	186	0.18	R	D	1	cl/c	-	n	Fe lined
20	0.61	J	75	111	0.04	R	R	t	cl	-	n	Fe lined
21	0.71	J	64	174	>1.00	D	D	0.5	cl/c	slR/und	n	Fe lined
22	0.67	Jf	50	086	~0.06	R	R	-	-	R/stp	n	Fe lined
23	0.77	B	38	281	0.10?	-	-	t	-	R/stp	n	Fe lined
24	0.79	B	38	281	0.10?	-	-	t	-	R/stp	n	Fe lined
25	0.82	B	38	281	0.10?	-	-	t	-	R/stp	n	Fe lined
26	0.86	B	38	281	~0.17	D	-	t	cl	slR/stp	n	Fe lined
27	0.89	B	38	281	~0.17	D	-	t	cl	slR/stp	n	Fe lined
28	0.90	B	38	281	~0.17	D	-	t	cl	slR/stp	n	Fe lined
29	0.92	B	38	281	~0.17	D	-	t	cl	slR/stp	n	Fe lined
30	0.94	B	38	281	~0.17	D	-	t	cl	slR/stp	n	Fe lined
31	0.95	B	38	281	~0.17	D	-	t	cl	slR/stp	n	Fe lined
32	0.97	B	38	281	~0.17	D	-	t	cl	slR/stp	n	Fe lined
33	0.98	B	38	281	~0.17	D	-	t	cl	slR/stp	n	Fe lined
34	1.00	B	38	281	~0.17	D	-	t	cl	slR/stp	n	Fe lined
35	0.82	J	80	174	>1.00	D	D	0.4	cl/c	slR/stp	n	Fe lined
36	0.86	J	80	174	al 0.30	R	R	0.5	c	slR/und	n	Fe lined
37	0.72	J	50	086	0.27	R	R	1	cl/c	slR/und	n	Fe lined
38	0.81	J	50	086	al 0.57	R	R	1	c	slR/und	n	Fe lined
39	0.93	sF	68	062	~0.53	D	R	0.4	g	slR/und	n	Fe lined
40	1.00	Jf	78	356	al 0.19	R	R	t	cl	slR/und	n	Fe lined
41	1.05	F	62	191	>6.00	D	B	t	g	slR/pln	n	Fe lined
42	1.02	J	78	356	al 0.20	D	R	t	cl/c	-	n	Fe lined
43	1.07	J	55	090	0.21	R	R	t	-	R/stp	n	Fe lined

Waiwera Beach **Horizontal** Easting: 2663501 Northing: 6515497

Joint No.	Distance	Type	Dip	Dip Direction	Persistence (m)	Termination Upper	Termination Lower	Aperture (mm)	Infill	Surface Roughness	Water flow	Remarks
1	1.00	B	55	275	~3.00	D	B	t	-	R	n	Convoluted base, base of bed
2	1.05	J	10	299	0.66	D	D/O	1	c	-	n	-
3	1.02	Jf	73	318	1.5	D	O	-	-	R	n	-
4	1.69	J	76	058	2.30	D	O	0.5-2	cl/c	-	n	-
5	1.76	F	12	132	1.74	D	D	2	g	-	n	-
6	2.15	J	35	066	1.20	D	D	1	c	-	n	-
7	2.49	J	35	066	0.90	D (J11)	D	0.5	c	-	n	-
8	2.35	J	35	066	1.00	D (J11)	D	0.5	c	-	n	-
9	1.32	J	12	132	0.58	D (J4)	D	1	c	-	n	-
10	1.44	F	52	038	~1.50	D	O	1	g	-	n	-
11	2.14	J	56	059	1.49	D	R	1	calc	-	n	-
12	2.54	F	73	052	1.05	D	D (J11)	1	g	-	n	-
13	2.36	F	80	215	>1.00	D	D (J11)	0.5	g	-	n	-
14	2.36	B	44	283	0.27	D	D	t	-	-	n	J14 to J21 are beds within 2 bounding faults

15	2.46	B	44	283	0.30	D	D	t	-	-	n	J22 and J23 bound in next fault set
16	2.52	B	44	283	0.31	D	D	t	-	-	n	-
17	2.53	B	44	283	0.31	D	D	t	-	-	n	-
18	2.55	B	44	283	0.32	D	D	t	-	-	n	-
19	2.58	B	44	283	0.34	D	D	t	-	-	n	-
20	2.60	B	44	283	0.35	D	D	t	-	-	n	-
21	2.63	B	44	283	0.37	D	D	t	-	-	n	-
22	2.76	B	44	283	0.33	D	D	t	-	-	n	-
23	2.89	B	44	283	0.45	D	D	t	-	-	n	-
24	1.80-3.00	Jf	75	007	2.00	D	B	-	-	-	n	-
25	2.71	F	76	288	1.80	R	R	1.5	g/calc	-	n	-
26	3.28	B	44	296	0.98	-	-	1	fe	w/c	n	-
27	3.43	B	44	296	0.68	-	-	1	fe	w/c	n	-
28	3.48	B	44	296	0.61	-	-	t	-	w/c	n	-
29	3.53	B	44	296	0.54	-	-	t	-	w/c	n	-
30	3.83	B	44	296	0.37	-	-	t	-	w/c	n	-
31	3.94	B	44	296	0.23	-	-	t	-	w/c	n	-
32	4.15	B	44	296	1.43	-	-	1	grit/c	w/c	n	-
33	3.44	J	68	302	0.45	D	D	0.8	calc	-	n	-
34	3.27	J	76	301	0.45	D	D	1	calc	-	n	-
35	3.30	J	63	086	1.57	D	B	1	calc	-	n	-
36	3.49	J	83	350	1.70	D	B	1	calc	-	n	Infill clean where reopened
37	3.68	J	59	143	>1.90	R	B	1	calc	-	n	Infill clean where reopened
38	4.05	Jf	75	233	~2.50	D	B	-	-	-	n	-
39	4.26	Jf	72	048	~2.50	D/O	B/O	-	-	-	n	-
40	4.27	J	81	273	0.69	D	D (J41)	1	c/calc	-	n	-
41	4.27	J	86	281	>1.10	D	B/O	2	c/calc	R	n	-
42	4.20	Jf	81	026	al 0.97	O	O	-	-	-	n	-
43	4.26	Jf	80	003	~0.70	D	D (J44)	-	-	-	n	-
44	4.65	F	31	119	2.00	R	D (J41)	1	g	-	n	-
45	4.63	J	56	071	~0.85	R	D (J41)	1	c	-	n	-
46	6.39	B	56	246	0.40	D (J44)	D (J53)	t	-	w/c	n	-
47	6.50	B	56	246	0.42	D (J44)	D (J53)	t	-	w/c	n	Slumped bed with basal “black”
48	6.60	B	56	246	0.51	D (J44)	D (J53)	t	-	w/c	n	-
49	6.66	B	56	246	0.68	D (J44)	D (J53)	t	-	w/c	n	-
50	6.70	B	56	246	0.76	D (J44)	D (J53)	t	-	w/c	n	-
51	6.74	B	56	246	0.53	D (J44)	D (J53)	t	-	w/c	n	-
52	6.77	B	56	246	0.49	D (J44)	D (J53)	t	-	w/c	n	-
53	6.36	F	87	096	>5.00	D	B	1	g	w/c	n	-
54	6.00	Jf	87	192	~2.00	D	D	-	-	-	n	-
55	6.55	Jf	87	002	1.00	D	D	-	-	-	n	-
56	6.80	J	56	260	0.40	D	D	0.8	c	-	n	
57	6.82	J	72	278	0.40	D	D	t	-	-	n	NO
58	6.92	B	46	284	0.73	D (F53)	D (F63)	t	-	-	n	
59	6.97	B	46	284	0.56	D (F53)	D (F63)	t	-	-	n	FE
60	7.14	B	46	284	0.56	D (F53)	D (F63)	t	-	-	n	
61	7.16	B	46	284	0.56	D (F53)	D (F63)	t	-	-	n	STAINING/
62	7.28	B	46	284	0.70	D (F53)	D (F63)	t	-	-	n	
63	6.83	F	85	124	>5.00	D	D	1	g	-	n	LINING

64	7.14	B	36	296	1.19	D (F63)	D (F69)	t	-	-	n
65	7.17	B	36	296	1.19	D (F63)	D (F69)	t	-	-	n
66	7.21	B	36	296	1.19	D (F63)	D (F69)	t	-	-	n
67	7.32	B	36	296	1.25	D (F63)	D (F69)	t	-	-	n
68	7.38	B	36	296	1.15	D (F63)	D (F69)	t	-	-	n
69	7.73	F	66	161	>5.00	D	B	1	g	-	n
70	7.32	J	87	310	0.23	R	D (J71)	t	-	-	n
71	7.77	Jf	58	061	>0.06	O	O	0.5?	calc	R	n
72	7.77	Jf	83	228	>0.31	D (J71)	O	-	-	R/pln	n
73	7.99	Jf	88	233	>0.40	D (F63)	D (F74)	-	-	R	n
74	7.65	F	86	339	~1.60	R	B	0.5	g	-	n
75	7.75	F	75	328	~1.50	R	B	0.5	g	-	n

Waiwera Beach Vertical

Easting: 2663501 Northing: 6515497

Joint No.	Distance (m)	Type	Dip	Dip Direction	Persistence (m)	Termination Upper	Termination Lower	Aperture (mm)	Infill	Surface Roughness	Water flow	Remarks
1	0.20	Jf	84	007	0.42	D	D	-	-	slR/und	n	-
2	0.00	B	35	261	0.25	-	-	t	-	R	n	-
3	0.04	B	35	261	0.27	-	-	t	-	slR/stp	n	Plus numerous laminations in-between beds ~2 mm
4	0.07	B	35	261	0.28	-	-	t	-	slR/stp	n	thick
5	0.30	B	35	261	0.30	-	-	t	-	w/c	n	-
6	0.29	J	88	154	al 0.56	R/O	R/O	t	calc	-	n	-
7	0.44	B	36	268	0.30	-	-	t	-	R/stp	n	Laminations in-between
8	0.40	B	36	268	0.28	-	-	t	-	w/c	n	-
9	0.41	Jf	85	170	0.05	D	R/O	t	-	-	n	-
10	1.00	B	46	324	0.91	-	-	t	-	w/c	n	Medium thick sandstone bed
11	0.44	B	43	290	0.37	-	-	t	-	-	-	-
12	0.47	B	43	290	0.37	-	-	t	-	-	-	-
13	0.51	B	43	290	0.37	-	-	t	-	-	-	-
14	0.54	B	43	290	0.37	-	-	t	-	-	-	-
15	0.58	B	43	290	0.37	-	-	t	-	-	-	-
16	0.61	B	43	290	0.37	-	-	t	-	-	-	-
17	0.65	B	43	290	0.37	-	-	t	-	-	-	-
18	0.68	B	43	290	1.03	-	-	t	-	-	-	-
19	0.72	B	43	290	1.03	-	-	t	-	-	-	-
20	0.75	B	43	290	1.03	-	-	t	-	-	-	-
21	0.79	B	43	290	1.03	-	-	t	-	-	-	-
22	0.84	B	43	290	1.03	-	-	t	-	-	-	-
23	0.89	B	43	290	1.03	-	-	t	-	-	-	-
24	0.05	Jf	74	178	0.13	D	D	-	-	SlR	n	-
25	1.21	B	62	280	al 1.30	-	-	t	-	R/stp	n	-
26	1.25	B	62	280	~1.30	-	-	0.2	cl	R/stp	n	Near vertical joints intersect bedding and stop
27	1.28	B	62	280	~0.50	-	-	t	-	R/und	n	persistence

28	1.30	B	62	280	~0.50	-	-	t	-	R/stp	n	-
29	1.01	Jf	79	038	~0.12	O	O	-	-	slR	n	-
30	1.27	Jf	77	030	al 0.16	D	O	-	-	R	n	-

Martins Bay **Horizontal** Easting: Northing:

Joint No.	Distance	Type	Dip	Dip Direction	Persistence (m)	Termination Upper	Termination Lower	Aperture (mm)	Infill	Surface Roughness	Water flow	Remarks
1	0.00	J	89	152	0.34	R	R	1.5	cl	R	n	Dark Fe surface
2	0.38	J	77	351	>0.98	R	D (J7)	10	cl	R	n	No Fe stain
3	0.00	Jf	74	035	0.50	D	D (J1)	-	-	R	n	Faint Fe stain
4	0.25	Jf	63	020	0.23	D	D (J2)	-	-	R	n	No Fe
5	0.58	J	80	131	0.09	R	R	-	-	R	n	No Fe
6	0.00	Jf	55	045	>0.17	R/O	R/O	-	-	R	n	No Fe
7	0.43	J	86	186	>1.50	R	R	2	cl/grit	R	n	No Fe
8	0.69	J	54	271	0.23	R	R	-	-	R	n	No Fe
9	0.60	Jf	65	016	0.14	R	-	-	-	R	n	No Fe
10	0.69	Jf	88	170	0.14	R	R	-	-	R	n	No Fe
11	0.95	J	78	154	0.14	R	R	3	cl	-	n	No Fe
12	1.59	Jf	74	060	0.09	D (J11)	R/O	-	-	R	n	No Fe
13	1.03	Jf	86	331	0.10	O	D (J14)	-	-	R	n	No Fe
14	0.45	J	55	080	>0.33	R	R	9	cl	R	n	No Fe
15	1.06	Jf	85	006	>0.40	R	R	-	calc	R	n	White vein skin left on parts of joint face
16	2.25	Jf	58	074	>0.40	R	R	-	-	R	n	No Fe
17	2.33	J	77	082	>1.30	R	R	4	cl	R	n	Fe stain on parts of surface
18	2.12	J	80	259	~0.12	R/O	R	1	cl	R	n	Salt and Fe skin
19	2.49	J	86	262	~1.20	R	R	11	cl	R	n	Small amount of salt and Fe
20	1.51	Jf	60	356	0.40	R	R	-	-	R	n	Fe lined
21	1.16	Jf	85	350	>0.12	R/O	R	-	c	R	n	Clay and Fe skin, old infill
22	1.35	Jf	45	342	>0.40	R	R	-	-	R	n	No Fe
23	1.93	Jf	47	358	>0.19	R/O	R/O	-	-	R	n	No Fe
24	2.05-2.25	B	05	261	0.07	D	D	?	cl	R	n	No Fe
25	2.77	Jf	74	074	>0.27	R	D	-	-	R	n	No Fe
26	1.94	J	79	003	>0.37	R	R/O	1	cl	R	n	No Fe stain
27	2.39-2.71	J	29	030	?	R/O	D	0.7	cl	R	n	No Fe stain
28	1.88	J	84	008	0.26	R	R	5	grit	-	n	-
29	2.28	Jf	80	160	>0.13	R	R	-	-	-	n	No Fe stain
30	2.82	J	83	082	>0.26	R	R	0.5	cl	R	n	Fe lined
31	2.30	J	84	184	1.00	R	R	26	cl	R	n	No Fe
32	3.00	Jf	74	072	0.48	R	R	-	-	R	n	Faint Fe
33	3.07	Jf	83	000	>0.18	R/O	R	-	-	R	n	No Fe
34	3.35	Jf	76	122	>0.45	R/O	R	-	-	R	n	-
35	3.67	J	85	077	>4.00	D	R	2	calc/cl	R	n	Major joint
36	3.38	Jf	60	334	0.16	R	R	-	-	R	n	No Fe
37	3.46-3.60	Jf	77	042	>0.15	R	R	-	-	R	n	No Fe
38	3.87	J	84	071	0.66	R	R	1	grit	R	n	-

39	3.70	J	80	324	0.38	R	D	4	cl	-	n	-
40	4.71	Jf	76	066	>1.00	R	R	-	-	R	n	Dark purple staining on parts
41	4.25	J	77	128	1.63	R	R	0.5	calc/cl	Sm	n	No Fe but white vein
42	4.20	Jf	76	000	>0.70	R/O	R	-	-	R	n	Faint Fe
43	5.00	J	79	065	>0.90	D (J42)	R	2	cl	R	n	-
44	4.92	Jf	85	305	0.23	R	R	-	-	R	n	No Fe
45	4.45	J	89	189	0.87	R	R	t	calc	R	n	Fe stained + white vein
46	7.00	Jf	54	040	1.05	R	R	0.8	cl	R	n	No Fe, less flaky
47	6.02	J	88	252	>0.25	R	R	t	-	R	n	No Fe
48	4.88	J	89	176	>0.27	R	R	t	-	R	n	Rusted object above joint has washed down into joint
49	4.70-4.92	Jf	60	040	0.20	R	R	-	-	R	n	No Fe
50	5.50	J	86	008	>0.95	R	R	t	calc	R	n	Dark purple staining
51	8.20	Jf	53	033	>1.00	R	R	-	-	R	n	Slightly Fe/purple stain
52	7.70	Jf	72	050	0.55	R	R	t	-	R	n	Slightly Fe/purple stain
53	7.40	J	89	180	>0.74	R	R	0.5	calc	-	n	White vein
54	7.50 on	Jf	66	045	>1.00	R	R	-	-	R	n	Fe and purple stain,
55	9.02	J	83	129	>0.65	R	R	t	calc	-	n	White vein

Martins Bay **Vertical** Easting: Northing:

Joint No.	Distance	Type	Dip	Dip Direction	Persistence	Termination Upper	Termination Lower	Aperture/ Width	Infill	Surface Roughness	Water flow	Remarks
1	0.07	J	48	032	>0.30	D	R	0.8	cl	R	n	-
2	0.16	J	45	028	>0.24	D	R	1.5	cl	R	n	-
3	0.23	J	45	033	>0.19	D	R	0.8	cl	R	n	-
4	0.45	Jf	59	043	al 0.36	O	O	-	-	R	n	-
5	0.07	J	80	254	0.05	D (J1)	D (J2)	-	-	R	n	-
6	0.14	J	80	254	0.06	D (J2)	D (J3)	-	-	R	n	-
7	0.80	B	01	042	>20.0	-	-	t	-	-	n	-
8	0.91	B	01	042	>20.0	-	-	t	-	-	n	-
9	0.975	B	01	042	>20.0	-	-	t	-	-	n	-
10	1.09	B	01	042	>20.0	-	-	t	-	-	n	-
11	1.105	B	01	042	>20.0	-	-	t	-	-	n	-
12	0.49	J	80	322	0.10	R	R	0.3	cl	-	n	-
13	1.05	J	89	316	0.12	D	R	t	-	-	n	-
14	1.06	Jf	50	034	0.09	D	R	-	-	-	n	-
15	1.12	B	25	290	0.07	-	-	0.5	cl	-	n	Base of sst hole (looks like ray feeding structure)
16	1.15	J	85	304	0.10	D	D	0.5	cl	-	n	-
17	1.14	J	15	225	0.16	D	D	0.5	cl	-	n	-
18	1.22	Jf	64	020	0.04	D	D	-	-	-	n	-
19	1.22	J	66	076	0.015	D (J18)	D	t	-	-	n	-
20	1.30	B	05	040	>20.0	-	-	t	-	-	n	-
21	1.30	Jf	76	043	0.19	D	D	-	-	-	n	-
22	1.33	B	05	040	>20.0	-	-	t	-	-	n	-
23	1.48	B	18	340	>20.0	-	-	0.2	-	-	n	-
24	1.49	B	18	340	>20.0	-	-	0.2	cl	-	n	-

25	1.47	Jf	64	086	0.10	D	D (J23)	-	-	-	n	-
26	1.51	J	85	283	0.07	D	R	t	-	-	n	-
27	1.53	Jf	42	041	~0.30	D (J24)	R/O	-	-	R	n	-
28	1.68	Jf	79	054	0.17	D (J27)/O	R/O	-	-	R	n	-
29	1.89	J	86	183	>1.20	R	B	0.5	calc	R/stp	n	Dark purple staining, major joint
30	1.89	Jf	49	041	>0.82	R	R/O	-	-	R	n	-

Leigh Marine Reserve Horizontal

Easting: 2671748 Northing: 6546264

Joint No.	Distance	Type	Dip	Dip Direction	Persistence (m)	Termination Upper	Termination Lower	Aperture (mm)	Infill	Surface Roughness	Water flow	Remarks
1	0.06	F	84	192	al 2.00	D	B	1	calc	Sm	n	Throw 2cm
2	0.00	Jf	83	094	~0.60	O	O	-	-	slR	n	-
3	0.23	J	70	180	0.10	D	D	0.5	cl/grit	Sm	n	-
4	0.34	J	70	180	0.25	D	D	0.2	cl/grit	-	n	-
5	0.15	B	31	301	>20.0	-	-	t	-	slR	n	Bedding orientation
6	0.52	J	88	160	0.34	R	D	0.8	c	-	n	-
7	0.32	J	71	227	0.24	R	D	0.5	cl	slR	n	CRUSH
8	0.39	J	86	011	al 0.67	R	D	0.8	c	-	n	ZONE
9	1.00	J	79	342	al 1.10	D	R	0.5	calc	-	n	-
10	0.40	J	65	226	>0.90	D	D (J11)	0.5	calc	-	n	Frittering results in cracking of
11	0.35	J	70	254	>0.90	D	R	1	calc	-	n	sandstone surface which means
12	0.43	J	64	247	0.48	D	D (J10)	0.8	calc	-	n	smaller block size able to fall out
13	0.45	J	81	248	0.67	D	D (J10)	0.8	calc	-	n	-
14	0.46	J	79	261	>1.70	D	B	3	calc	-	n	-
15	0.61	J	69	256	0.79	D	R	0.5	cl	-	n	-
16	0.60	J	69	256	0.18	D	D	0.2	cl	-	n	-
17	0.67	J	69	242	0.82	D (J14)	R	t	-	-	n	-
18	0.80	Jf	85	220	0.89	D	R	t	-		n	-
19	0.83	J	89	234	0.11	D	D	0.2	cl	slR	n	-
20	0.79	J	89	234	0.07	D	D	1	cl	-	n	-
21	0.89	J	89	234	0.08	D	D	0.5	cl	-	n	-
22	0.92	J	84	019	0.42	R	D	t	-	-	n	-
23	0.97	J	84	019	0.42	R	D	t	-	-	n	-
24	1.02	J	84	019	1.04	R	R	t	-	Sm	n	-
25	0.85	J	74	269	0.12	R	D	-	-	Sm/und	n	-
26	0.80	J	74	269	0.16	D	R	1	cl/c	-	n	-
27	0.98	J	88	240	0.46	D	R	t	-	Sm	n	-
28	1.02	J	88	240	0.37	D	D (J29)	1.5	cl/grit	Sm	n	-
29	1.00	J	86	266	>3.00	D	B	3	calc	slR	n	Major joint slR/pln, butts against J 29
30	1.15	J	86	218	>0.62	D	R	2	cl	slR	n	-
31	1.12	J	79	269	0.69	D	R	t	-	-	n	-
32	1.13	J	79	269	0.84	D	R	0.5	c	-	n	-
33	1.19	J	58	249	0.33	R	R	0.2	cl	-	n	-
34	1.18	J	88	090	0.14	R	D	t	-	-	n	-
35	1.25	J	81	238	al 0.55	R	R	t	-	-	n	-

36	1.28	J	81	238	al 0.55	R	R	0.5	calc	-	n	-
37	1.31	J	81	238	al 0.55	R	R	t	-	-	n	-
38	1.31	J	38	248	0.20	D	D	t	-	-	n	-
39	1.39	J	65	070	0.20	R	D	0.2	-	-	n	-
40	1.39	J	85	040	al 0.72	R	R	t	cl	-	n	-
41	1.38	J	64	284	0.22	D	R	0.5	cl	slR	n	-
42	1.50	J	86	246	0.81	R	R	1.5	calc	slR	n	Partly open 1-2 mm in places too
43	1.50	J	86	360	al 0.14	R	R	-	-	R	n	-
44	1.54	J	88	190	al 0.14	R	R	0.2	cl	slR	n	-
45	1.58	J	88	190	al 0.14	R	R	0.5	cl	slR	n	-
46	1.54	J	73	258	al 0.14	R	R	-	-	slR	n	-
47	1.46	J	88	001	0.17	D	D	0.8	calc	-	n	Curved
48	1.62	J	88	190	0.09	D	D	-	-	R	n	-
49	1.66	J	80	042	0.19	D	D	0.5	cl/c	-	n	-
50	1.70	J	80	042	0.20	R	R	t	-	-	n	-
51	1.75	J	80	042	0.07	D	D	t	-	-	n	Many fe stained surfaces but no
52	1.65	Jf	70	291	al 0.20	D	R	-	-	R	n	Fe-skin. Clay is often limonitised
53	1.78	J	83	210	al 0.80	D	R	1.5	c	R	n	-
54	1.70	J	25	213	0.48	R	D	t-0.8	cl	-	n	-
55	1.83	J	88	148	0.72	D	R	t-0.8	cl/c	-	n	-
56	2.00	J	87	029	0.88	D	R	2	c/calc	slR	n	Major joint
57	1.84	J	72	255	0.38	D	R	1	calc	slR	n	-
58	1.86	J	72	255	0.18	D	R	t-1.5	cl	slR	n	-
59	1.83	Jf	82	190	0.11	D	D	-	c	slR	n	-
60	1.92	Jf	82	190	0.15	D	D	-	-	slR	n	-
61	2.19	J	81	333	0.10	D	D	-	-	R	n	-
62	1.63	Jf	69	294	al 0.39	D	D	-	-	R	n	-
63	2.04	J	84	056	0.53	D	D	t	-	Sm	n	-
64	1.90	Jf	89	300	~0.30	R	R	-	-	-	n	-
65	2.28	F	75	194	>3.00	D	B	9	cl/c	-	n	Throw 3cm
66	2.25	J	88	240	0.46	D	D (J65)	t	-	-	n	-
67	2.55	Jf	79	339	al 0.82	D	D	0.5	c	-	n	-
68	2.19	J	89	082	0.32	R	R	t	-	-	n	-
69	2.28	J	89	082	0.24	R	R	t	-	-	n	-
70	2.32	J	89	082	>1.42	R	B	0.7	calc	-	n	-
71	2.46	F	84	268	>3.00	D	B	3	calc	-	n	Throw 2cm
72	2.48	Jf	80	052	0.36	D (J71)	R	-	-	slR	n	-
73	2.62	J	88	026	al 0.66	D	D	t	-	R	n	-
74	2.48	J	75	290	0.32	R	D	t	-	-	n	-
75	2.44	J	75	290	0.36	R	D	t	-	-	n	-

Leigh Marine Reserve **Vertical** Easting: 2671748 Northing: 6546264

Joint No.	Distance (m)	Type	Dip	Dip Direction	Persistence (m)	Termination Upper	Termination Lower	Aperture (mm)	Infill	Surface Roughness	Water flow	Remarks
1	1.50	J	88	186	>0.30	D	R	0.8	cl/grit	R	n	Rough because of frittering
2	1.63	J	65	018	0.20	D	R	2	cl	R	n	
3	1.70	B	10	302	0.02	-	-	t-0.5	cl	Sm	n	**1** Bedding persistence controlled
4	1.61	B	10	302	0.02	-	-	t-0.5	cl	Sm	n	by vertical joints
5	1.59	B	10	302	0.02	-	-	t-0.5	cl	Sm	n	
6	1.57	B	10	302	0.02	-	-	t-0.5	cl	Sm	n	
7	1.55	B	10	302	0.02	-	-	t-0.5	cl	Sm	n	
8	1.53	B	10	302	0.02	-	-	t-0.5	cl	Sm	n	
9	1.50	B	10	302	0.02	-	-	t-0.5	cl	Sm	n	
10	1.49	B	10	302	0.02	-	-	t-0.5	cl	Sm	n	
11	1.48	B	10	302	0.02	-	-	t-0.5	cl	Sm	n	
12	1.47	B	10	302	0.02	-	-	t-0.5	cl	Sm	n	
13	1.46	B	10	302	0.02	-	-	t-0.5	cl	Sm	n	
14	1.45	B	10	302	0.02	-	-	t-0.5	cl	Sm	n	
15	1.44	B	10	302	0.06	-	-	t	-	R	n	**2** very strong laminations in order of 1-2mm.
16	1.42	B	10	302	0.06	-	-	t	-	R	n	Bedding persistence controlled by vertical joints
17	1.39	B	10	302	0.06	-	-	t	-	R	n	**3** 3-4 no beds but a few fractures of 10/302
18	1.33	B	10	302	0.13	D	D	t-0.5	cl	-	n	
19	1.27	B	10	302	0.08	D	D	t-0.5	cl	-	n	
20	1.23	B	10	302	0.08	D	D	t-0.5	cl	-	n	3/4 and 4/5 bed has 0.59m persistence between
21	1.19	B	10	302	0.08	D	D	t-0.5	cl	-	n	2 faults.
22	1.07	B	10	302	0.11	D	D	t-0.5	cl	-	n	
23	1.02	B	10	302	0.10	D	D	t-0.5	cl	-	n	
24	0.97	B	10	302	0.09	D	D	t-0.5	cl	-	n	
25	0.95	B	10	302	0.07	D	D	t-0.5	cl	-	n	
26	0.94	B	10	302	0.07	D	D	t-0.5	cl	-	n	
27	0.91	B	10	302	0.07	D	D	t-0.5	cl	-	n	
28	0.85	B	17	122	0.59	-	-	t	-	slR/stp	n	**4** 4-5 lamination about every 1 cm of 17/122
29	0.84	B	17	122	0.10	-	-	t	-	slR/stp	n	
30	0.83	B	17	122	0.10	-	-	t	-	slR/stp	n	
31	0.82	B	17	122	0.10	-	-	t	-	slR/stp	n	
32	0.81	B	17	122	0.10	-	-	t	-	slR/stp	n	
33	0.80	B	17	122	0.10	-	-	t	-	slR/stp	n	
34	0.79	B	17	122	0.10	-	-	t	-	slR/stp	n	
35	0.78	B	17	122	0.10	-	-	t	-	slR/stp	n	
36	0.77	B	17	122	0.10	-	-	t	-	slR/stp	n	
37	0.76	B	17	122	0.10	-	-	t	-	slR/stp	n	
38	0.75	B	17	122	0.10	-	-	t	-	slR/stp	n	
39	0.74	B	17	122	0.10	-	-	t	-	slR/stp	n	
40	0.73	B	17	122	0.10	-	-	t	-	slR/stp	n	
41	0.72	B	17	122	0.10	-	-	t	-	slR/stp	n	
42	0.71	B	17	122	0.10	-	-	t	-	slR/stp	n	
43	0.70	B	17	122	0.10	-	-	t	-	slR/stp	n	
44	0.69	B	17	122	0.10	-	-	t	-	slR/stp	n	

45	0.68	B	17	122	0.10	-	-	t	-	slR/stp	n	
46	0.67	B	17	122	0.10	-	-	t	-	slR/stp	n	
47	0.66	B	17	122	0.10	-	-	t	-	slR/stp	n	
48	0.65	B	17	122	0.10	-	-	t	-	slR/stp	n	
49	0.64	B	17	122	0.10	-	-	t	-	slR/stp	n	
50	0.63	B	17	122	0.10	-	-	t	-	slR/stp	n	
51	0.62	B	17	122	0.10	-	-	t	-	slR/stp	n	
52	0.61	B	17	122	0.10	-	-	t	-	slR/stp	n	
53	0.60	B	17	122	0.10	-	-	t	-	slR/stp	n	
54	0.59	B	17	122	0.10	-	-	t	-	slR/stp	n	
55	0.58	B	17	122	0.10	-	-	t	-	slR/stp	n	
56	0.57	B	17	122	0.10	-	-	t	-	slR/stp	n	
57	0.56	B	17	122	0.10	-	-	t	-	slR/stp	n	
58	0.55	B	17	122	0.10	-	-	t	-	slR/stp	n	
59	0.54	B	17	122	0.10	-	-	t	-	slR/stp	n	
60	0.53	B	17	122	0.10	-	-	t	-	slR/stp	n	
61	0.52	B	17	122	0.10	-	-	t	-	slR/stp	n	
62	0.51	B	17	122	0.10	-	-	t	-	slR/stp	n	
63	0.50	B	17	122	0.10	-	-	t	-	slR/stp	n	
64	0.49	B	17	122	0.10	-	-	t	-	slR/stp	n	
65	0.48	B	17	122	0.10	-	-	t	-	slR/stp	n	
66	0.47	B	17	122	0.10	-	-	t	-	slR/stp	n	
67	0.46	B	09	134	0.59	-	-	t-0.2	cl	Sm	n	**5** 5-6 lamination about every 0.5cm of 09/134
68	0.45	B	09	134	0.10	-	-	t-0.2	cl	Sm	n	
69	0.43	B	09	134	0.10	-	-	t-0.2	cl	Sm	n	
70	0.42	B	09	134	0.10	-	-	t-0.2	cl	Sm	n	
71	0.41	B	09	134	0.10	-	-	t-0.2	cl	Sm	n	
72	0.40	B	09	134	0.10	-	-	t-0.2	cl	Sm	n	
73	0.39	B	09	134	0.10	-	-	t-0.2	cl	Sm	n	
74	0.38	B	09	134	0.10	-	-	t-0.2	cl	Sm	n	
75	0.37	B	09	134	0.10	-	-	t-0.2	cl	Sm	n	
76	0.36	B	09	134	0.10	-	-	t-0.2	cl	Sm	n	
77	0.35	B	09	134	0.10	-	-	t-0.2	cl	Sm	n	
78	0.34	B	09	134	0.10	-	-	t-0.2	cl	Sm	n	
79	0.33	B	42	326	0.10	-	-	t-0.5	cl	Sm/stp	n	**6** lamination about every 0.5cm of 42/326
80	0.32	B	42	326	0.10	-	-	t-0.5	cl	Sm/stp	n	
81	0.31	B	42	326	0.10	-	-	t-0.5	cl	Sm/stp	n	
82	0.30	B	42	326	0.10	-	-	t-0.5	cl	Sm/stp	n	
83	0.29	B	42	326	0.10	-	-	t-0.5	cl	Sm/stp	n	
84	0.28	B	42	326	0.10	-	-	t-0.5	cl	Sm/stp	n	
85	0.27	B	42	326	0.10	-	-	t-0.5	cl	Sm/stp	n	
86	0.26	B	42	326	0.10	-	-	t-0.5	cl	Sm/stp	n	
87	0.25	B	42	326	0.10	-	-	t-0.5	cl	Sm/stp	n	
88	0.24	B	42	326	0.10	-	-	t-0.5	cl	Sm/stp	n	
89	0.23	B	42	326	0.10	-	-	t-0.5	cl	Sm/stp	n	
90	0.22	B	42	326	0.10	-	-	t-0.5	cl	Sm/stp	n	
91	0.21	B	42	326	0.10	-	-	t-0.5	cl	Sm/stp	n	
92	0.20	B	42	326	0.10	-	-	t-0.5	cl	Sm/stp	n	
93	0.19	B	42	326	0.10	-	-	t-0.5	cl	Sm/stp	n	

94	0.18	B	42	326	0.10	-	-	t-0.5	cl	Sm/stp	n	
95	0.17	B	42	326	0.10	-	-	t-0.5	cl	Sm/stp	n	
96	0.16	B	42	326	0.10	-	-	t-0.5	cl	Sm/stp	n	
97	0.15	B	42	326	0.10	-	-	t-0.5	cl	Sm/stp	n	
98	0.14	B	42	326	0.10	-	-	t-0.5	cl	Sm/stp	n	
99	0.13	B	42	326	0.10	-	-	t-0.5	cl	Sm/stp	n	
100	0.12	B	42	326	0.10	-	-	t-0.5	cl	Sm/stp	n	
101	0.11	B	42	326	0.10	-	-	t-0.5	cl	Sm/stp	n	
102	0.10	B	42	326	0.10	-	-	t-0.5	cl	Sm/stp	n	
103	0.09	B	42	326	0.10	-	-	t-0.5	cl	Sm/stp	n	
104	0.08	B	42	326	0.10	-	-	t-0.5	cl	Sm/stp	n	
105	0.07	B	42	326	0.10	-	-	t-0.5	cl	Sm/stp	n	
106	0.06	B	42	326	0.10	-	-	t-0.5	cl	Sm/stp	n	
107	0.05	B	42	326	0.10	-	-	t-0.5	cl	Sm/stp	n	
108	0.04	B	42	326	0.10	-	-	t-0.5	cl	Sm/stp	n	
109	0.03	B	42	326	0.10	-	-	t-0.5	cl	Sm/stp	n	
110	0.02	B	42	326	0.10	-	-	t-0.5	cl	Sm/stp	n	
111	0.01	B	42	326	0.10	-	-	t-0.5	cl	Sm/stp	n	
112	0.00	B	42	326	0.10	-	-	t-0.5	cl	Sm/stp	n	
113	1.47	J	75	285	0.05	D	R	1	cl/c	slR	n	
114	1.38	J	84	220	0.55	D	D	t	-	Sm	n	Joints through sandstone are in regular sets but
115	1.25	J	84	220	0.55	D	D	t	-	Sm	n	curve like siltstone does when weathered
116	0.90	J	84	220	0.55	D	D	t	-	Sm	n	
117	1.00	J	78	254	0.33	R	D	t	calc	Sm	n	
118	1.60	J	88	080	0.25	D	D	0.5	cl	slR	n	
119	1.37	J	84	220	0.10	R	D	t	-	-	n	
120	1.30	Jf	82	334	0.16	R	D	-	-	R	n	
121	0.90	Jf	83	337	0.34	D	D	-	-	R	n	
122	1.40	Jf	77	346	0.30	R	R	-	-	R	n	
123	0.79	J	58	293	al 0.60	R	B	t	-	-	n	
124	0.77	J	58	293	al 0.60	R	B	t	-	-	n	
125	0.82	J	58	293	al 0.60	R	B	t	-	-	n	
126	0.63	J	58	293	al 0.60	R	B	t	-	-	n	
127	0.58	J	58	293	al 0.60	R	B	t	-	-	n	
128	0.62	J	58	293	al 0.60	R	B	t	-	-	n	
129	0.48	Jf	77	032	al 0.13	R	R	-	-	slR	n	
130	0.20	J	84	100	al 0.39	D	B	0.5	c	slR	n	
131	0.26	J	84	100	al 0.39	D	B	0.5	c	slR	n	
132	0.15	J	84	100	al 0.39	D	B	0.5	c	slR	n	
133	0.38	J	84	100	al 0.39	D	B	0.5	c	slR	n	
134	0.06	J	84	100	al 0.39	D	B	0.5	c	slR	n	
135	0.04	J	84	100	al 0.39	D	B	0.5	c	slR	n	
136	0.45	F	54	284	>3.00	D	B	2	g	R	n	Throw 0.11 m
137	0.24	J	55	206	0.12	D	D	t	-	-	n	
138	1.45	Jf	75	334	al 0.10	R	R	-	-	R	n	

Summary of scanline results (H = horizontal scanline survey; V = vertical scanline survey)

SITE		Scanline length (m)	No. of discontinuities	No. of discontinuities >0.1 m	Discontinuity spacing (m jt^{-1})	Discontinuity frequency ($jt\ m^{-1}$)	Mean Persistence (m)	Mean Persistence >0.1 m (m)	Mean Aperture (mm)
Musick Point	H	12.38	59	53	0.23	4.28	1.29 ± 0.13	1.31 ± 0.13	1.80 ± 0.41
	V	3.44	15	14	0.25	4.07	3.09 ± 1.39	3.09 ± 1.39	1.54 ± 0.69
Narrowneck Beach	H	4.53	50	40	0.11	8.83	0.71 ± 0.063	0.74 ± 0.062	3.78 ± 0.77
	V	3.00	25	22	0.14	7.33	6.14 ± 1.77	6.97 ± 2.00	1.16 ± 0.58
Castor Bay	H	3.21	70	58	0.055	18.07	0.41 ± 0.15	0.48 ± 0.17	0.16 ± 0.03
	V	1.16	51	34	0.034	29.31	2.59 ± 0.46	3.86 ± 0.58	0.16 ± 0.03
Waiake Bay	H	9.38	70	68	0.14	7.25	0.48 ± 0.033	0.49 ± 0.032	1.05 ± 0.17
	V	1.71	27	21	0.081	12.28	7.71 ± 1.85	9.90 ± 2.27	0.13 ± 0.0095
Army Bay	H	2.87	77	73	0.039	25.44	0.58 ± 0.13	0.61 ± 0.13	0.29 ± 0.04
	V	0.74	43	41	0.018	55.41	0.61 ± 0.18	0.64 ± 0.19	0.23 ± 0.04
Waiwera Beach	H	6.99	75	74	0.094	10.59	1.11 ± 0.12	1.12 ± 0.12	0.52 ± 0.06
	V	1.30	30	29	0.045	22.31	0.55 ± 0.069	0.56 ± 0.069	0.10 ± 0.004
Martins Bay	H	9.02	55	50	0.18	5.54	0.56 ± 0.084	0.60 ± 0.089	3.31 ± 1.09
	V	1.82	30	20	0.091	10.99	6.16 ± 1.68	9.20 ± 2.24	0.34 ± 0.081
Leigh Marine Reserve	H	2.62	75	72	0.036	27.48	0.84 ± 0.27	0.87 ± 0.28	0.75 ± 0.16
	V	1.70	138	116	0.015	68.24	0.17 ± 0.024	0.20 ± 0.028	0.25 ± 0.022

SITE		Roughness (average)	Infill (average)	Groundwater (general conditions)	Groundwater (maximum flow observed)
Musick Point	H	sIR – R	soft -none <5mm	Damp	Slight
	V	sIR	soft-none <5mm		
Narrowneck Beach	H	sIR	soft-none <5mm	Dry	None
	V	sIR – R	soft-none <5mm		
Castor Bay	H	sm – sIR	soft-none <5mm	Damp	Slight
	V	sIR	soft-none <5mm		
Waiake Bay	H	sIR	soft-none <5mm	Damp to wet	Slight
	V	sIR – R	none <5mm		
Army Bay	H	sIR	soft-none <5mm	Dry	Trace
	V	sIR – R	soft-none <5mm		
Waiwera Beach	H	R	soft-hard <5mm	Dry	None
	V	sIR – R	none-hard <5mm		
Martins Bay	H	R	none-hard <5mm	Damp	Moderate
	V	R	none <5mm		
Leigh Marine Reserve	H	sIR	soft-none <5mm	Damp to wet	Slight
	V	sm – sIR	soft-none <5mm		

APPENDIX FOUR

STEREOGRAPHIC PROJECTION

For each site, stereonets are presented with pole concentrations (top diagram) and without pole concentrations (bottom diagram)

Summary of the orientations determined from stereonet pole concentrations

SITE	JOINTS		CLIFF FACE		FAULTS		BEDDING PLANES	
	Dip	Dip Direction	Dip	Dip Direction	Dip	Dip Direction	Dip	Dip Direction
Musick Point	80	125	79	346			10	277
	77	054						
Narrowneck Beach	86	287	65	010			05	200
	75	044						
Castor Bay	69	340	73	116	62	190	09	332
	33	015						
	68	211						
Waiake Bay	86	002	79	059			10	214
	86	213						
	77	276						
Army Bay	79	180	62	300	60	206	37	282
	77	050						
Waiwera Beach	77	290	67	016	44	104	44	288
	82	005						
	47	066						
Martins Bay	58	041	67	054			01	045
	87	316						
	88	004						
Leigh Marine Reserve	84	099	51	332	70	276	26	314
	89	190			80	193	16	125
	88	239						

Number of discontinuities for each parameter

SITE	Cliff face	Faults	Bedding	Joints	Total (Faults+Beds+Joints)
Musick Point	1	0	1	72	73
Narrowneck Beach	1	0	10	65	75
Castor Bay	1	2	23	96	121
Waiake Bay	1	0	14	83	97
Army Bay	1	5	24	89	118
Waiwera Beach	1	4	59	35	98
Martins Bay	1	0	11	74	85
Leigh Marine Reserve	1	4	111	98	213

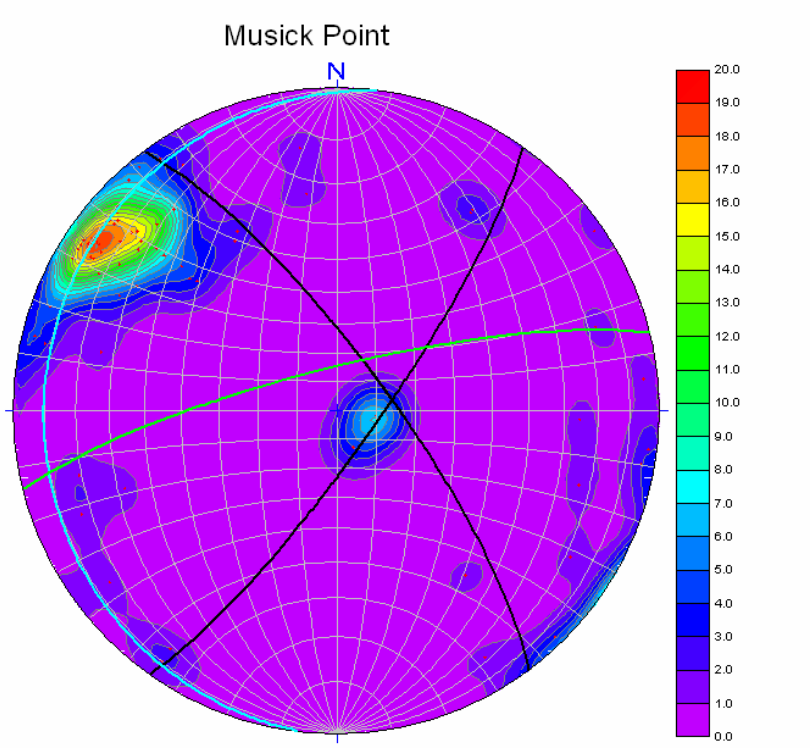
Musick Point
N
20.0
19.0
18.0
17.0
16.0
15.0
14.0
13.0
12.0
11.0
10.0
9.0
8.0
7.0
6.0
5.0
4.0
3.0
2.0
1.0
0.0

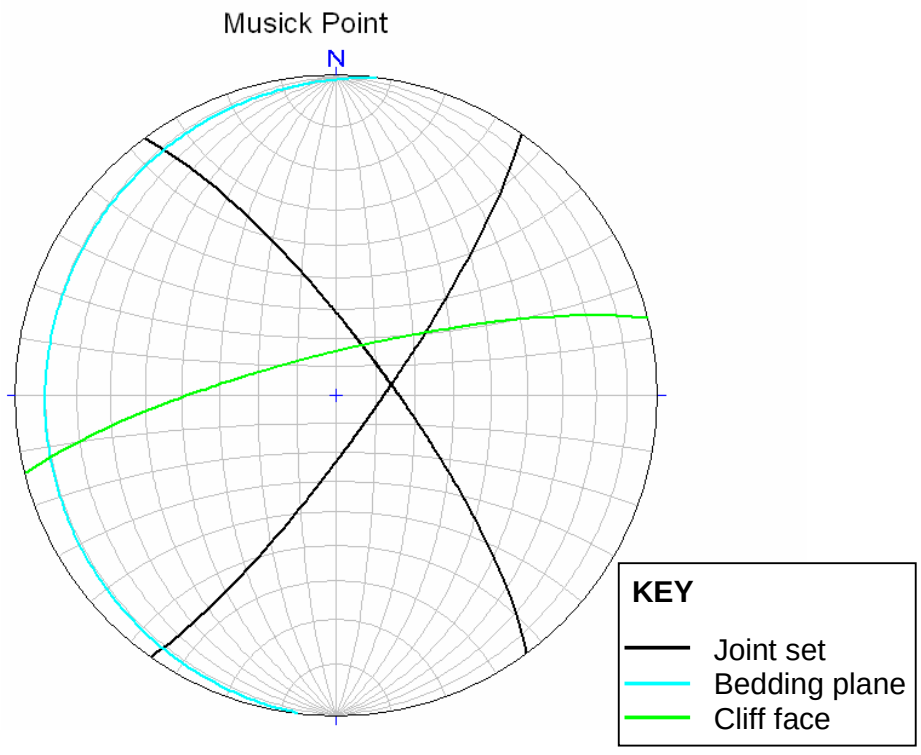
Musick Point
N
KEY
Joint set
Bedding plane
Cliff face

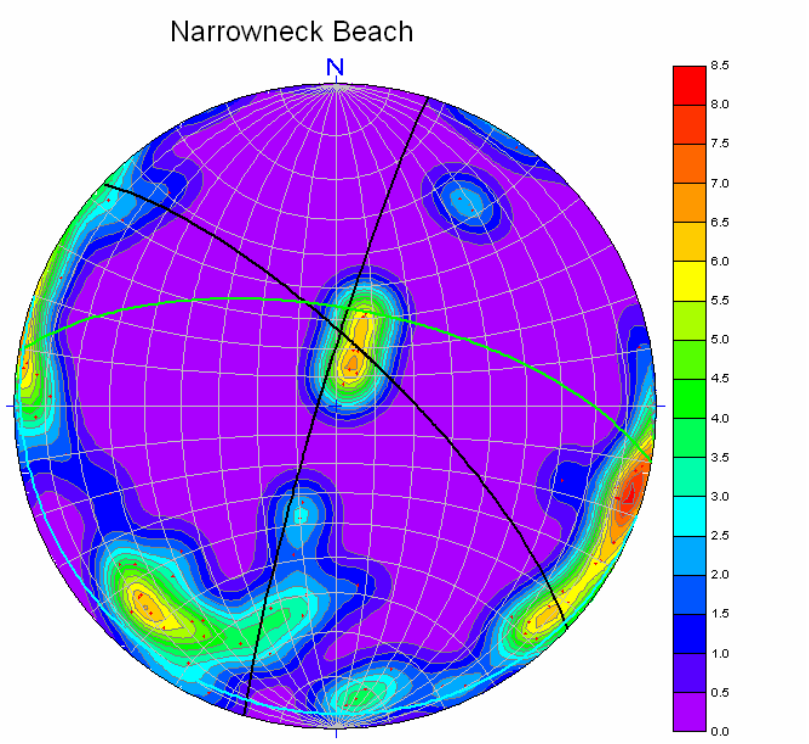
Narrowneck Beach
N
8.5
8.0
7.5
7.0
6.5
6.0
5.5
5.0
4.5
4.0
3.5
3.0
2.5
2.0
1.5
1.0
0.5
0.0

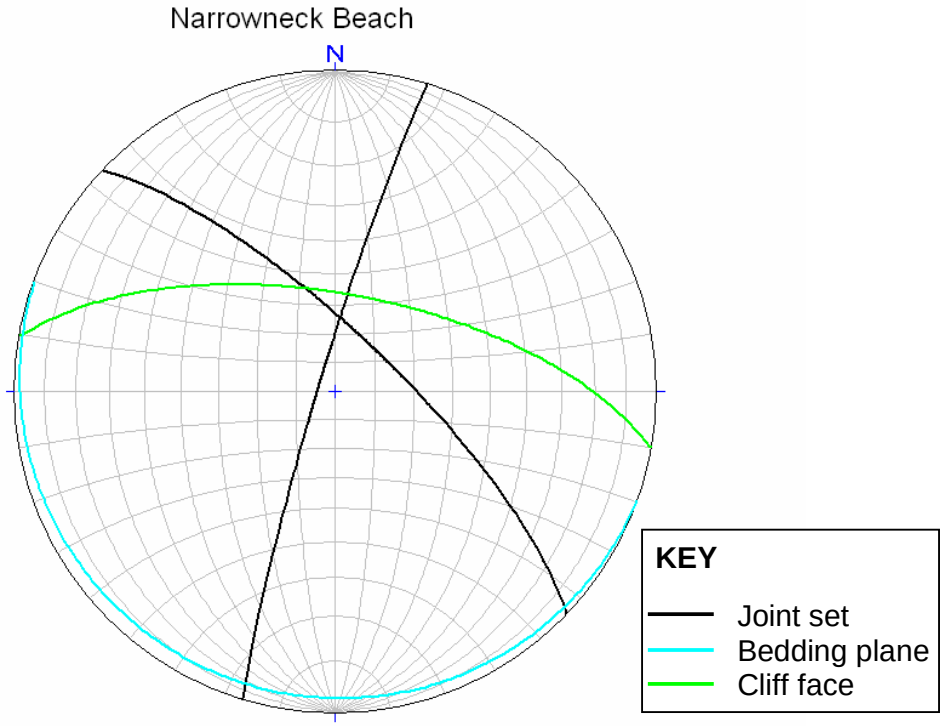
Narrowneck Beach
N
KEY
Joint set
Bedding plane
Cliff face

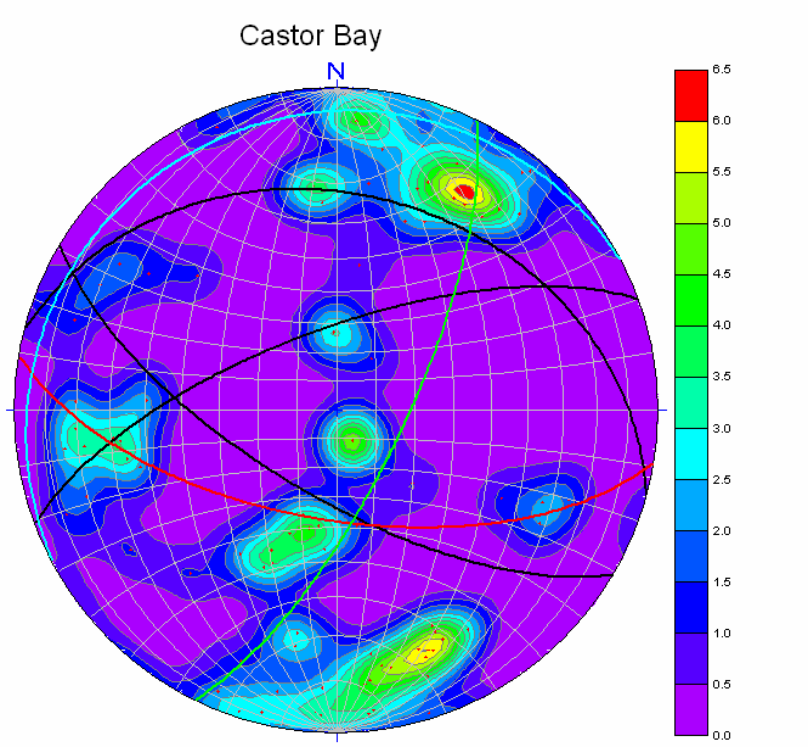
Castor Bay
N
6.5
6.0
5.5
5.0
4.5
4.0
3.5
3.0
2.5
2.0
1.5
1.0
0.5
0.0

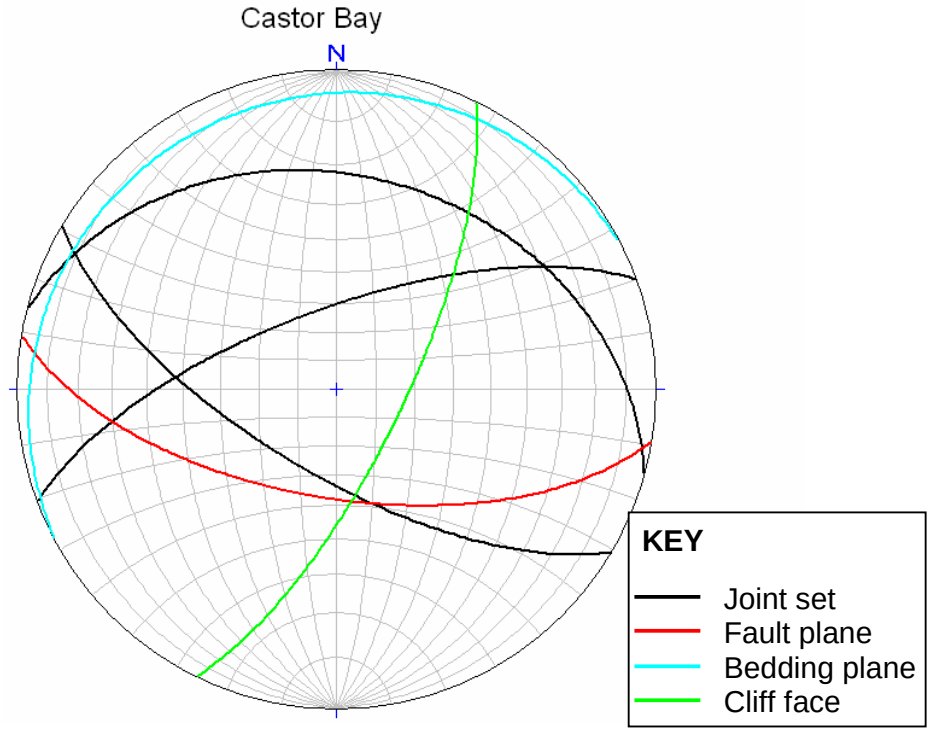
Castor Bay
N
KEY
Joint set
Fault plane
Bedding plane
Cliff face

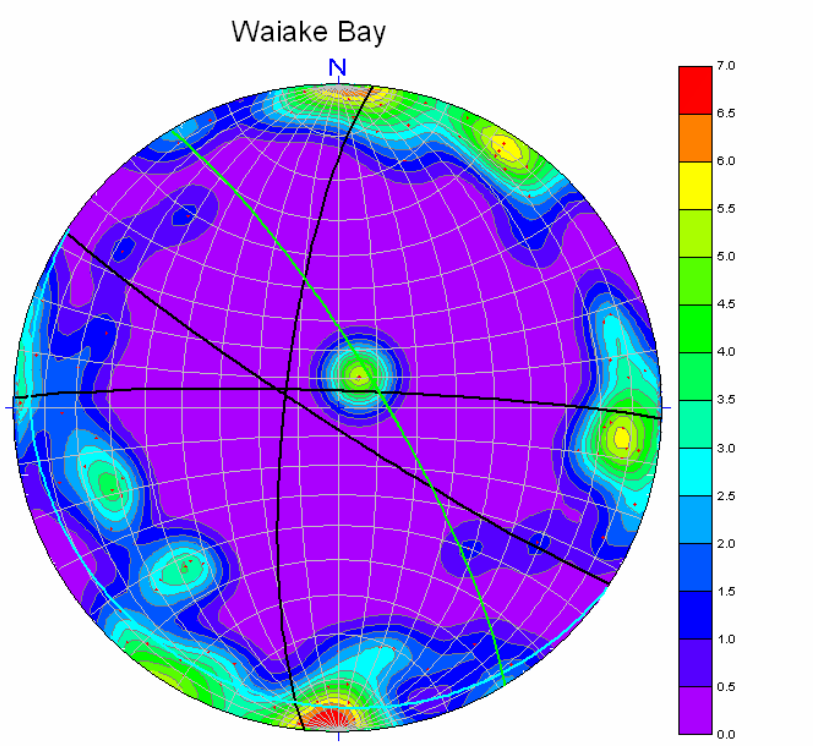
Waiake Bay
N
7.0
6.5
6.0
5.5
5.0
4.5
4.0
3.5
3.0
2.5
2.0
1.5
1.0
0.5
0.0

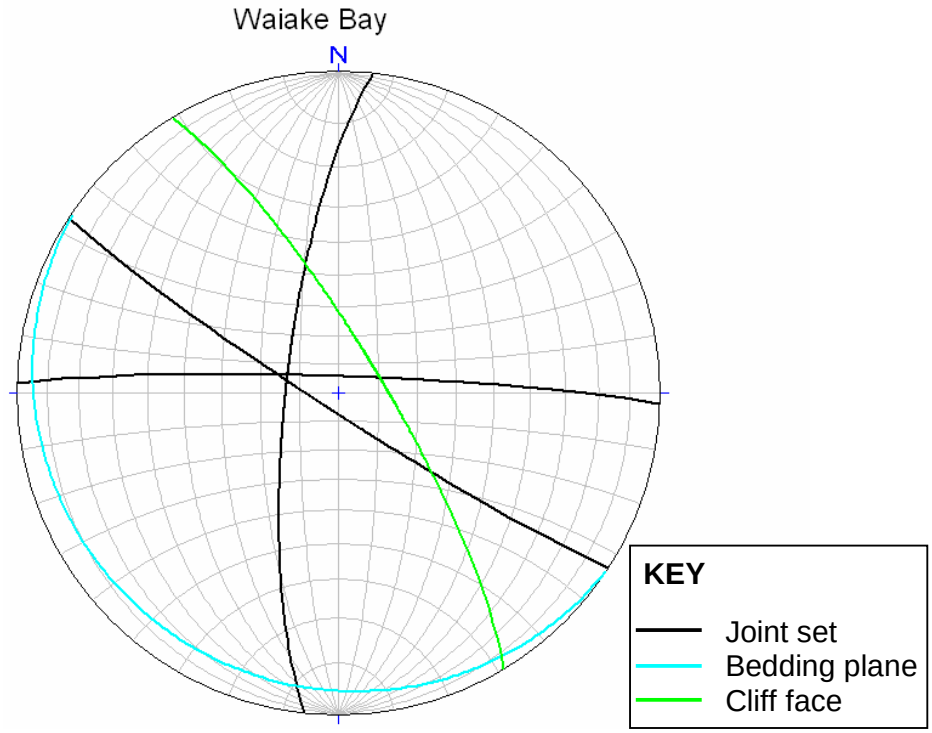
Waiake Bay
N
KEY
Joint set
Bedding plane
Cliff face

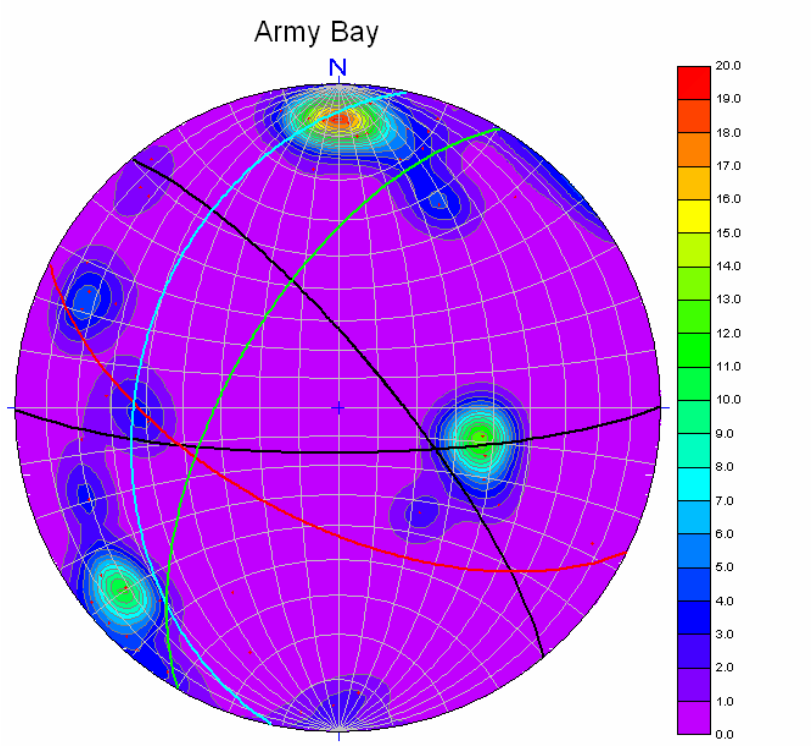
Army Bay
N
20.0
19.0
18.0
17.0
16.0
15.0
14.0
13.0
12.0
11.0
10.0
9.0
8.0
7.0
6.0
5.0
4.0
3.0
2.0
1.0
0.0

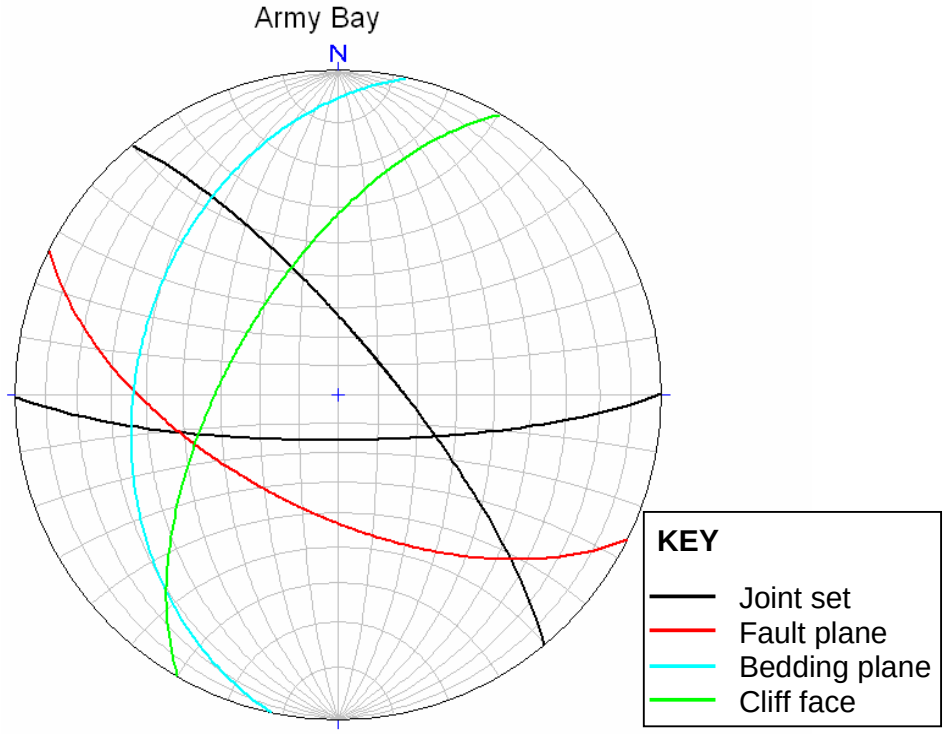
Army Bay
N
KEY
Joint set
Fault plane
Bedding plane
Cliff face

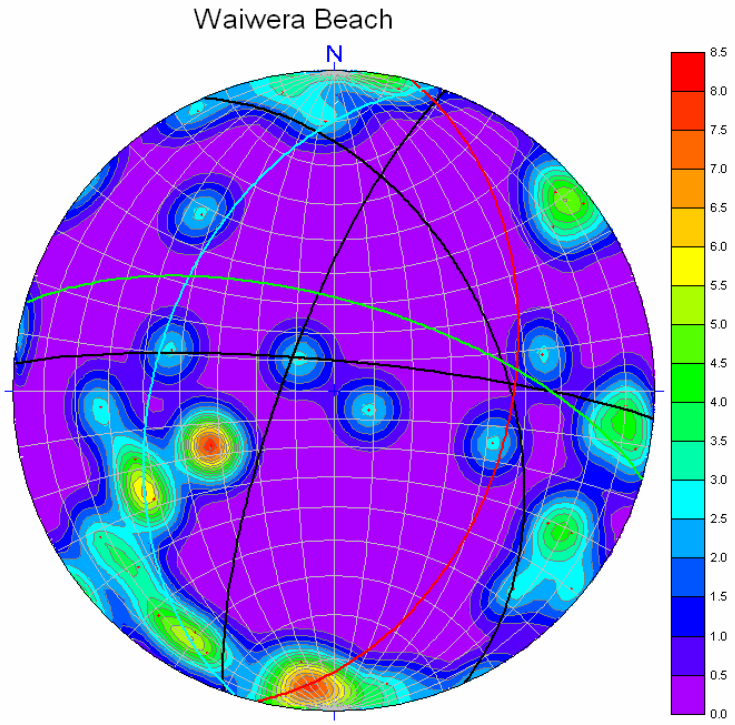
Waiwera Beach
N
8.5
8.0
7.5
7.0
6.5
6.0
5.5
5.0
4.5
4.0
3.5
3.0
2.5
2.0
1.5
1.0
0.5
0.0

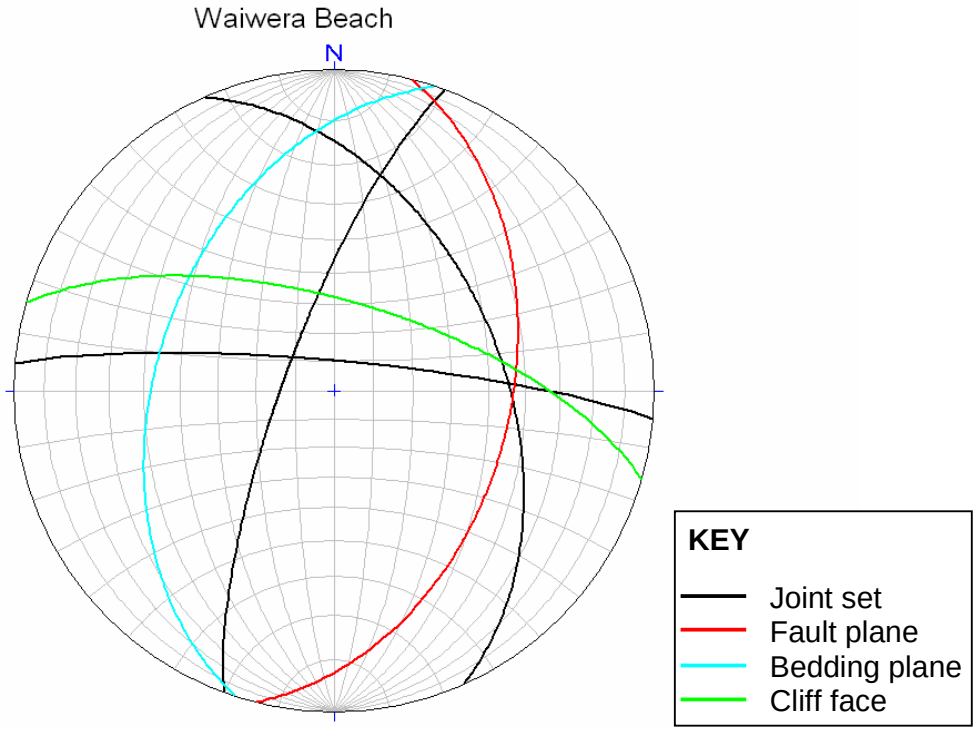
Waiwera Beach
N
KEY
Joint set
Fault plane
Bedding plane
Cliff face

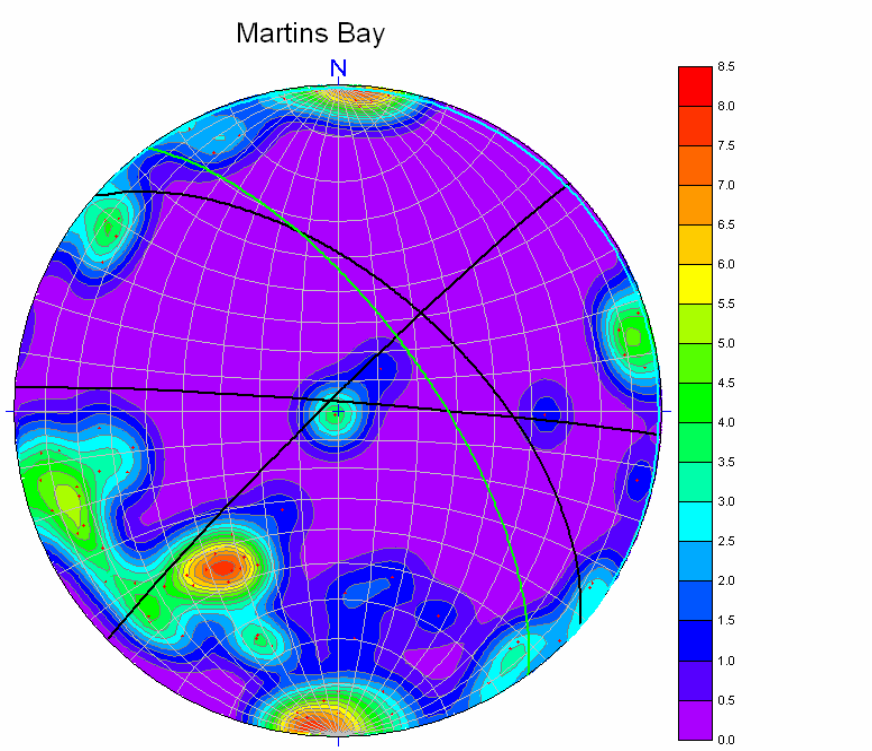
Martins Bay
N
8.5
8.0
7.5
7.0
6.5
6.0
5.5
5.0
4.5
4.0
3.5
3.0
2.5
2.0
1.5
1.0
0.5
0.0

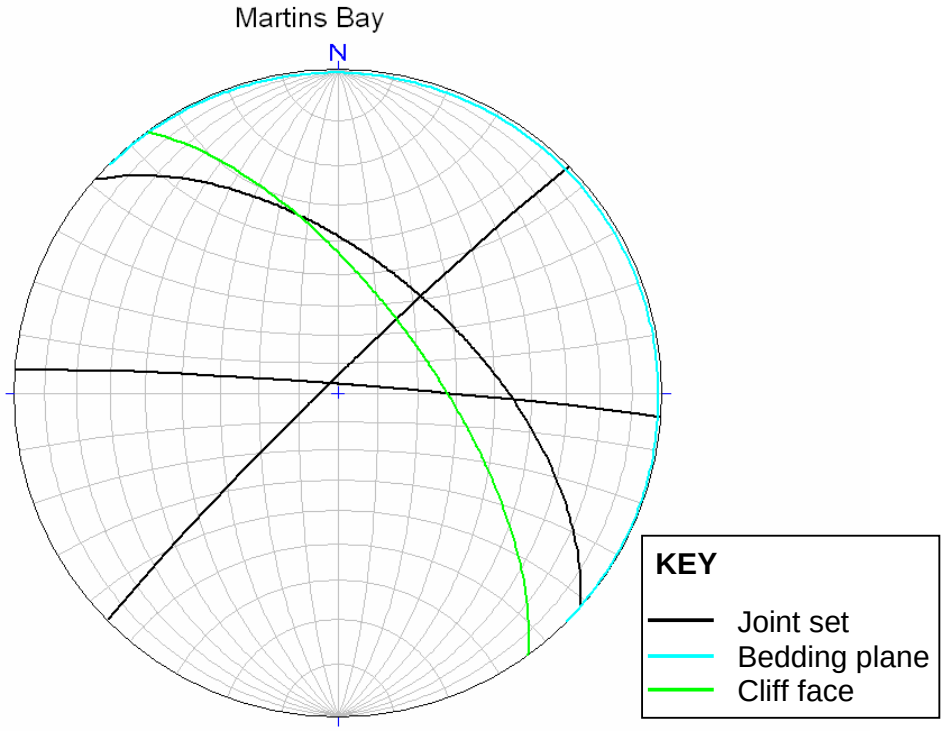
Martins Bay
N
KEY
Joint set
Bedding plane
Cliff face

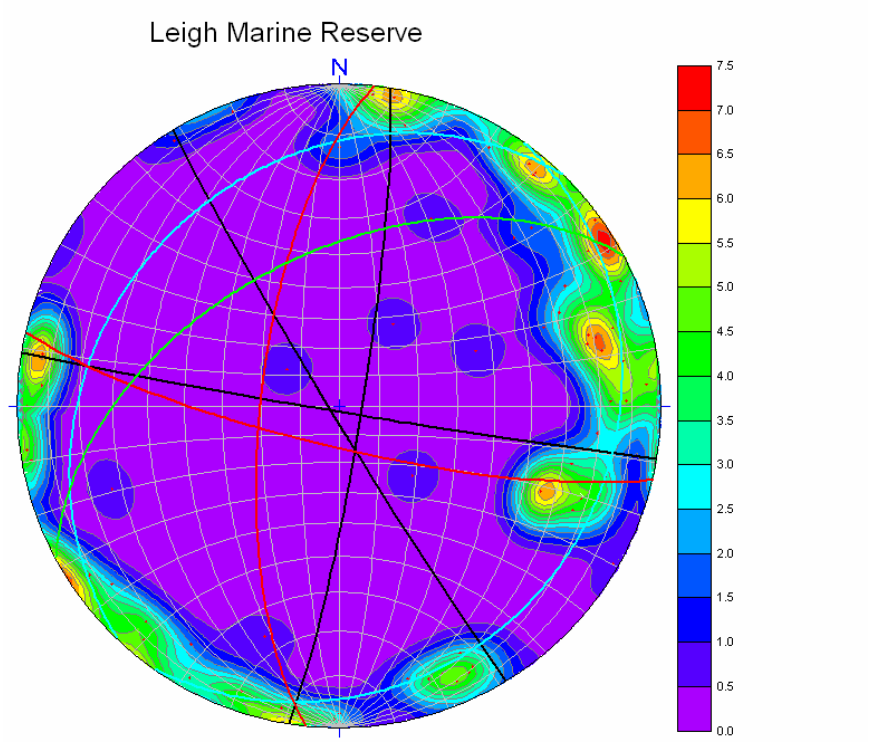
Leigh Marine Reserve
N
7.5
7.0
6.5
6.0
5.5
5.0
4.5
4.0
3.5
3.0
2.5
2.0
1.5
1.0
0.5
0.0

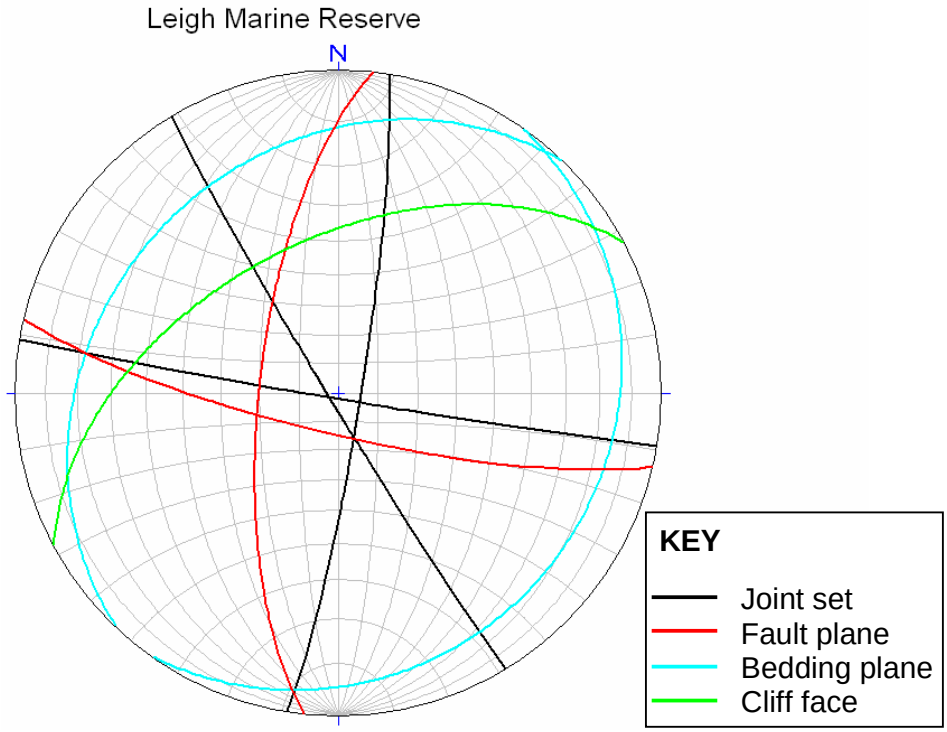
Leigh Marine Reserve
N
KEY
Joint set
Fault plane
Bedding plane
Cliff face

APPENDIX FIVE

GEOMORPHOLOGY PARAMETERS

- **Shore platform width**
- **Erosion rate**
- **Cliff angle and height**

Shore platform widths

SITE	Strike of cliffs	Correlation coefficient	Search width of 20 m	Platform reset to (m)	Mean width (m)	Median width (m)	Std deviation (m)	Min width (m)	Max width (m)
Cockle Bay	158 to 338	0.969	too small	24	8.29	7.64	3.30	2.69	13.76
Eastern Beach	156 to 336	0.981	yes	~	377.6	377.84	1.23	375.16	378.74
Musick Point	016 to 196	0.954	too small	38	165.43	163.55	36.32	94.28	234.02
Achilles Point	029 to 209	0.977	yes	~	28.35	29.63	7.92	14	39.60
Narrowneck Beach	129 to 309	0.938	yes	~	18.67	19.05	4.56	12.87	25.30
St Leonard's Beach	148 to 328	0.995	too small	26	33.79	31.33	9.06	22.76	50.84
Castor Bay	152 to 332	0.987	too small	132	100.82	101.68	4.45	92.74	109.12
Mairangi Bay	146 to 326	0.983	yes	~	58.58	58.75	3.46	54.07	64.62
Waiake Bay	168 to 348	0.989	yes	~	53.08	53.51	22.49	11.82	96.05
Army Bay	28 to 208	0.966	yes	~	140.74	142.35	21.03	110.04	173.63
Waiwera Beach	153 to 333	0.902	too small	40	73.23	73.05	22.1	31.94	121.37
Opahi Bay	152 to 332	0.938	too small	26	112.08	114.57	8.24	94.85	125.71
Martins Bay	154 to 334	0.987	too small	66	137.84	140.89	19.84	104.09	162.2
Buckleton Beach	021 to 201	0.954	yes	~	29.45	31.05	6.06	13.97	38.46
Matheson Bay	011 to 191	0.990	yes	~	90.32	90.61	5.44	82.37	100.52
Leigh Marine Reserve	078 to 258	0.994	yes	~	131.61	130.75	5.39	124.37	144.19

Predicted erosion rates

Site	n	Mean Platform Width (m)	Std. dev.	Std. Error (m)	Time (y)	Std. Error (y)	Rate (m/yr)	Std. Error (m/yr)	Rate (mm/yr)	Std. Error (mm/yr)
Cockle Bay	42	8.29	3.30	0.51	7120	70	0.00116	0.000072	1.16	0.072
Eastern Beach	11	377.60	1.23	0.37	7120	70	0.05303	0.00052	53.03	0.52
Musick Point	23	165.43	36.32	7.57	7120	70	0.02323	0.0011	23.23	1.09
Achilles Point	33	28.35	7.92	1.38	7120	70	0.00398	0.00020	3.98	0.20
Narrowneck Beach	8	18.67	4.56	1.61	7120	70	0.00262	0.00023	2.62	0.23
St Leonard's Beach	20	33.79	9.06	2.03	7120	70	0.00475	0.00029	4.75	0.29
Castor Bay	33	100.82	4.45	0.77	7120	70	0.01416	0.00018	14.16	0.18
Mairangi Bay	10	58.58	3.46	1.09	7120	70	0.00823	0.00017	8.23	0.17
Waiake Bay	125	53.08	22.49	2.01	7120	70	0.00746	0.00029	7.46	0.29
Army Bay	23	140.74	21.03	4.39	7120	70	0.01977	0.00065	19.77	0.65
Waiwera Beach	42	73.23	22.1	3.41	7120	70	0.01029	0.00049	10.29	0.49
Opahi Bay	66	112.08	8.24	1.01	7120	70	0.01574	0.00021	15.74	0.21
Martins Bay	9	137.84	19.84	6.61	7120	70	0.01936	0.00095	19.36	0.95
Buckleton Beach	72	29.45	6.06	0.71	7120	70	0.00414	0.00011	4.14	0.11
Matheson Bay	136	90.32	5.44	0.47	7120	70	0.01269	0.00014	12.69	0.14
Leigh Marine Reserve	36	131.61	5.39	0.90	7120	70	0.01848	0.00022	18.48	0.22

Cliff angle and height

Parameter / SITE / Units	Distance B (m)	Cliff base angle C (°)	Angle at distance D (°)	Platform angle E (°)	Angle F (°)	Angle G (°)	Angle H (°)	Length I (m)	height J (m)
Cockle Bay	10.0	**65.0**	51.0	13.0	38.0	14.0	128.0	**25.45**	**23.06**
Error	0.2	**2.5**	2.5	2.5	5.0	3.5	3.5	**4.28**	**3.98**
Eastern Beach	9.5	**62.0**	49.0	12.0	37.0	13.0	130.0	**25.42**	**22.44**
Error	0.2	**2.5**	2.5	2.5	5.0	3.5	3.5	**4.72**	**4.27**
Musick Point	19.3	**79.0**	42.0	5.0	37.0	37.0	106.0	**19.30**	**18.95**
Error	0.2	**2.5**	2.5	2.5	5.0	3.5	3.5	**2.61**	**2.63**
Achilles Point	15.0	**65.0**	43.5	4.5	39.0	21.5	119.5	**25.76**	**23.34**
Error	0.2	**2.5**	2.5	2.5	5.0	3.5	3.5	**3.39**	**3.20**
Narrowneck Beach	14.0	**65.0**	38.0	5.5	32.5	27.0	120.5	**16.57**	**15.02**
Error	0.2	**2.5**	2.5	2.5	5.0	3.5	3.5	**2.57**	**2.40**
St Leonard's Beach	11.5	**61.0**	47.0	12.0	35.0	14.0	131.0	**27.27**	**23.85**
Error	0.2	**2.5**	2.5	2.5	5.0	3.5	3.5	**4.62**	**4.16**
Castor Bay	15.5	**73.0**	43.0	4.0	39.0	30.0	111.0	**19.51**	**18.66**
Error	0.2	**2.5**	2.5	2.5	5.0	3.5	3.5	**2.52**	**2.49**
Mairangi Bay	4.0	**79.0**	57.0	2.0	55.0	22.0	103.0	**8.75**	**8.59**
Error	0.2	**2.5**	2.5	2.5	5.0	3.5	3.5	**1.26**	**1.27**
Waiake Bay	15.0	**79.0**	53.0	8.0	45.0	26.0	109.0	**24.20**	**23.75**
Error	0.2	**2.5**	2.5	2.5	5.0	3.5	3.5	**2.73**	**2.79**
Army Bay	37.2	**62.0**	35.0	3.0	32.0	27.0	121.0	**43.42**	**38.34**
Error	0.2	**2.5**	2.5	2.5	5.0	3.5	3.5	**6.79**	**6.19**
Waiwera Beach	10.0	**67.0**	57.0	16.0	41.0	10.0	129.0	**37.78**	**34.78**
Error	0.2	**2.5**	2.5	2.5	5.0	3.5	3.5	**8.98**	**8.36**
Opahi Bay	23.0	**74.0**	38.0	4.0	34.0	36.0	110.0	**21.88**	**21.03**
Error	0.2	**2.5**	2.5	2.5	5.0	3.5	3.5	**3.22**	**3.18**
Martins Bay	24.0	**67.0**	37.0	5.0	32.0	30.0	118.0	**25.44**	**23.41**
Error	0.2	**2.5**	2.5	2.5	5.0	3.5	3.5	**3.98**	**3.77**
Buckleton Beach	11.7	**73.0**	48.0	2.0	46.0	25.0	109.0	**19.91**	**19.04**
Error	0.2	**2.5**	2.5	2.5	5.0	3.5	3.5	**2.24**	**2.24**
Matheson Bay	19.5	**51.0**	34.0	5.0	29.0	17.0	134.0	**32.33**	**25.13**
Error	0.2	**2.5**	2.5	2.5	5.0	3.5	3.5	**5.70**	**4.60**
Leigh Marine Reserve	19.0	**51.0**	31.0	11.0	20.0	20.0	140.0	**19.00**	**14.77**
Error	0.2	**2.5**	2.5	2.5	5.0	3.5	3.5	**4.78**	**3.78**

APPENDIX SIX

ROCK MASS CLASSIFICATIONS

Geological Strength Index

Structure:		
Jointed-	IOM	Intact or Massive
	B	Blocky
	VB	Very Blocky
	BDS	Blocky Disturbed Seamy
	D	Disintegrated
	LS	Laminated Sheared
Flysch-	A	Thick-bedded, very blocky sandstone
	B	Sandstone with thin interlayers of siltstone
	C	Sandstone and siltstone in similar amounts
	D	Siltstone with sandstone layers
	E	Weak siltstone with sandstone layers
	F	Intensely folded/faulted siltstone with broken sandstone layers
	G	Undisturbed siltstone with or without a few thin sandstone layers
	H	Tectonically deformed siltstone forming a chaotic structure
Surface:	VG	Very Good
	G	Good
	F	Fair
	P	Poor
	VP	Very Poor

Site	GSI for Jointed Sandstone				GSI for Jointed Siltstone				GSI for Heterogeneous Rock			
	GSI	±	Structure	Surface	GSI	±	Structure	Surface	GSI	±	Structure	Surface
Cockle Bay	60	5	IOM-B	F	37	5	VB-D	F	45	5	B	F
Eastern Beach	50	5	B-VB	F	37	5	VB-D	F	42	5	B	F
Musick Point	65	5	B	G	45	5	VB	F	45	5	B	F-G
Achilles Point	65	5	B	G	40	5	D	G	40	5	C	G
Narrowneck Beach	50	5	B	F	35	5	D	F-G	35	5	D	F-G
St Leonard's Beach	65	5	B	G	45	5	VB-D	F	40	5	C	F-G
Castor Bay	42	5	BDS	F-G	42	5	BDS	F-G	24	5	F	F-G
Mairangi Bay	65	5	B	G	45	5	VB	F	45	5	B	F-G
Waiake Bay Site 3	65	5	B	G	30	5	D	F	41	5	C	F-G
Waiake Bay Site 4	60	5	B	F-G	30	5	D	F-G	38	5	C	F-G
Army Bay	45	5	BDS	G	33	5	BDS-D	F	20	5	F	F
Waiwera Beach 1	37	5	BDS	F	45	5	BDS	G	24	5	F	F-G
Waiwera Beach 2	40	5	VB-BDS	F	41	4	BDS	F-G	24	5	F	F-G
Opahi Bay	55	5	VB-BDS	G	40	5	D	G	45	5	B	G
Martins Bay	65	5	B	G	45	5	VB	F	40	5	C	F-G
Buckleton Beach	65	5	B	G	45	5	BDS	G	48	5	B	G
Matheson Bay	45	5	VB	F	37	5	BDS	F	25	5	E-F	F
Leigh Marine Reserve	45	5	VB	F	45	5	VB	F	20	5	F	F

Rock Quality Designation

$$RQD = 100e^{-0.1\lambda}(0.1\lambda + 1)$$

Where: λ = average number of discontinuities (that persist >0.1 m) per meter.

RQD value	Classification
90-100	Excellent
75-90	Good
50-75	Fair
25-50	Poor
0-25	Very poor

SITE		L (m)	n (joints)	λ (joints m^{-1})	RQD	Classification	RMR rating
Musick	H	12.38	53	4.28	93.07	excellent	18.5
	V	3.44	14	4.07	93.66	excellent	18.8
Narrowneck	H	4.53	40	8.83	77.87	good	15.5
	V	3.00	22	7.33	83.24	good	16.4
Castor	H	3.21	58	18.07	46.08	poor	9.2
	V	1.16	34	29.31	20.97	very poor	5.3
Waiake	H	9.38	68	7.249	83.55	good	16.6
	V	1.71	21	12.28	65.25	fair	12.9
Army	H	2.87	73	25.44	27.85	poor	6.2
	V	0.74	41	55.41	2.57	very poor	3.3
Waiwera	H	6.75	74	10.96	70.03	fair	13.8
	V	1.07	16	14.95	55.93	fair	11.2
Martins	H	9.02	50	5.543	89.27	good	17.8
	V	1.82	20	10.99	69.95	fair	13.8
Leigh	H	2.62	72	27.48	24.01	very poor	5.8
	V	1.70	116	68.24	0.85	very poor	3.1

Rock Mass Rating

SITE		UCS	RQD	Spacing	Persistence	Aperture	Roughness	Infill	Weathering	Condition	Groundwater	Orientation
Musick	H	2.3	18.5	8.4	4	1	4	4	5	18	10	-25
	V	1.8	18.8	8.5	2	1	3	4	5	15	10	-25
Narrowneck	H	3.0	15.5	6.9	6	1	3	4	5	19	15	-5
	V	1.5	16.4	7.4	2	1	4	4	5	16	15	-5
Castor	H	3.8	9.2	5.9	6	4	2	5	5	22	10	-50
	V	1.9	5.3	5.5	4	4	3	5	5	21	10	-50
Waiake	H	2.1	16.6	7.4	6	1	3	4	5	19	8.5	-5
	V	1.8	12.9	6.3	2	4	4	6	5	21	8.5	-5
Army	H	3.7	6.2	5.7	6	4	3	4	4	21	15	-50
	V	2.0	3.3	5.1	6	4	4	4	4	22	15	-50
Waiwera	H	4.7	13.8	6.4	4	4	5	3	5	21	15	-50
	V	2.0	11.2	6.0	6	4	4	5	5	24	15	-50
Martins	H	3.3	17.8	7.8	6	1	5	5	5	22	10	-25
	V	2.0	13.8	6.4	2	4	5	6	5	22	10	-25
Leigh	H	8.0	5.8	5.6	6	4	3	4	3	20	8.5	-50
	V	2.2	3.1	5.3	6	4	2	5	3	20	8.5	-50

SITE		bRMR	Classification	aRMR	Classification
Musick	H	57.2	good	32.2	poor
	V	54.1	fair	29.1	poor
Narrowneck	H	59.4	fair	54.4	fair
	V	56.3	fair	51.3	fair
Castor	H	50.9	fair	0.9	very poor
	V	43.7	fair	-6.3	very poor
Waiake	H	53.6	fair	48.6	fair
	V	50.5	fair	45.5	fair
Army	H	51.6	fair	1.6	very poor
	V	47.4	fair	-2.6	very poor
Waiwera	H	60.9	fair	10.9	very poor
	V	58.2	fair	8.2	very poor
Martins	H	60.9	fair	35.9	poor
	V	54.2	fair	29.2	poor
Leigh	H	47.9	fair	-2.1	very poor
	V	39.1	poor	-10.9	very poor

Slope Mass Rating

		bRMR	Slope dip βs	Slope dip direction αs	Joint dip βj	Joint dip direction αj	F1 Pαj-αs	rating	F2 βj	rating	F3 βj-βs	rating	F4	SMR	Description
Musick	H	57.2	79	346	10	277	-69	0.15	10	0.15	-69	-60	15	71	good
	V	54.1	79	346	10	277	-69	0.15	10	0.15	-69	-60	15	68	good
Narrowneck	H	59.4	65	010	15	202	192	0.15	15	0.15	-50	-60	15	73	good
	V	56.3	65	010	15	202	192	0.15	15	0.15	-50	-60	15	70	good
Castor	H	50.9	73	027	26	350	323	0.15	26	0.40	-47	-60	15	62	good
	V	43.7	73	027	26	350	323	0.15	26	0.40	-47	-60	15	55	normal
Waiake	H	53.6	79	059	06	221	162	0.15	6	0.15	-73	-60	15	67	good
	V	50.5	79	059	06	221	162	0.15	6	0.15	-73	-60	15	64	good
Army	H	51.6	62	300	25	300	0	1.00	25	0.40	-37	-60	15	43	normal
	V	47.4	62	300	25	300	0	1.00	25	0.40	-37	-60	15	38	bad
Waiwera	H	60.9	67	016	20	091	75	0.15	20	0.40	-47	-60	15	72	good
	V	58.2	67	016	20	091	75	0.15	20	0.40	-47	-60	15	70	good
Martins	H	60.9	67	054	03	042	-12	0.70	3	0.15	-64	-60	15	70	good
	V	54.2	67	054	03	042	-12	0.70	3	0.15	-64	-60	15	63	good
Leigh	H	47.9	51	332	10	302	-30	0.40	10	0.15	-41	-60	15	59	normal
	V	39.1	51	332	10	302	-30	0.40	10	0.15	-41	-60	15	51	normal

Rock Mass Strength

SITE		Intact rock strength	Weathering	Spacing	Orientation	Width	Continuity	Groundwater	RMS	Classification
Musick	H	5	9	15	14	5	5	4	57	Moderate
	V	5	9	15	14	5	5	4	57	Moderate
Narrowneck	H	5	9	15	18	5	6	6	64	Moderate
	V	5	9	15	18	5	6	6	64	Moderate
Castor	H	5	9	15	9	6	6	5	55	Moderate
	V	5	9	8	9	6	6	5	48	Weak
Waiake	H	5	9	15	18	5	6	4	62	Moderate
	V	5	9	15	18	6	5	4	62	Moderate
Army	H	5	8	8	9	6	5	5	46	Weak
	V	5	8	8	9	6	5	5	46	Weak
Waiwera	H	14	9	15	9	6	5	6	64	Moderate
	V	5	9	8	9	6	5	6	48	Weak
Martins	H	5	9	15	14	5	5	3	56	Moderate
	V	5	9	15	14	6	5	3	57	Moderate
Leigh	H	20	7	8	9	6	6	4	60	Moderate
	V	5	7	8	9	6	6	4	45	Weak

Rock Mass parameters – Hoek-Brown etc

Hoek Brown Parameters

Code	Term and Description	Units
σ_{ci}	sigci – intact uniaxial compressive strength	MPa
Adj. σ_{ci}	Adjusted sigci for flysch type	MPa
GSI	Geological Strength Index	-
M_i	Material constant for intact rock masses	-
Adj. M_i	Adjusted material constant for flysch type	-
D	Disturbance factor	-
γ	Unit weight	MN m^{-3}
Adj. γ	Adjusted unit weight for flysch type	MN m^{-3}
h	Slope height	m
c	Cohesion	MPa
phi	Friction angle	degrees
σ_t	sigt - Tensile strength	MPa
σ_c	sigc - Uniaxial compressive strength	MPa
σ_{cm}	sigcm - Global strength	MPa
ε_m	Modulus of deformation	MPa

Rock mass parameters for heterogeneous rock masses

Site	c (MPa)	phi (deg)	σ_t (MPa)	σ_c(MPa)	σ_{cm} (MPa)	ε_m (MPa)
Cockle Bay	0.104	43.49	-0.010	0.294	1.428	1542.00
Eastern Beach	0.066	37.41	-0.004	0.112	0.624	1179.71
Musick Point	0.088	43.81	-0.007	0.240	1.200	1542.00
Achilles Point	0.090	40.76	-0.007	0.206	1.202	986.17
Narrowneck Beach	0.046	39.29	-0.004	0.104	0.700	628.98
St Leonard's Beach	0.095	41.40	-0.008	0.229	1.338	986.17
Castor Bay	0.033	32.04	-0.002	0.047	0.491	232.62
Mairangi Bay	0.070	52.05	-0.006	0.267	1.604	1542.00
Waiake Bay	0.072	37.70	-0.004	0.131	0.760	986.17
Army Bay	0.045	25.39	-0.002	0.035	0.450	161.86
Waiwera Beach	0.055	29.11	-0.003	0.060	0.627	232.62
Opahi Bay	0.216	53.36	-0.020	0.923	5.533	1542.00
Martins Bay	0.100	42.02	-0.009	0.260	1.521	986.17
Buckleton Beach	0.288	57.16	-0.039	1.709	8.976	2012.50
Matheson Bay	0.074	38.22	-0.007	0.154	1.613	254.68
Leigh Marine Reserve	0.034	36.09	-0.003	0.067	0.873	161.86

Rock mass parameters

Rock mass parameters for heterogeneous rock masses

Site	Flysch type	Original σ_{ci}		Adjusted σ_{ci}		Averaged σ_{ci}	GSI	Original M_I		Adjusted M_I		Averaged M_I	D	Original γ		Adjusted γ		Averaged γ	h
		S	Z	S	Z			S	Z	S	Z			S	Z	S	Z		
Cockle Bay	B-C	19.9	6.4	17.9	6.4	12.2	45	17	7	15.3	7	11.2	0.5	0.019	0.016	0.017	0.016	0.0165	23.1
Eastern Beach	B-C	6.8	5.5	6.1	5.5	5.8	42	17	7	15.3	7	11.2	0.5	0.017	0.016	0.015	0.016	0.0155	22.4
Musick Point	B	12.9	6.8	12.9	-	12.9	45	17	7	17	-	12.0	0.5	0.018	0.016	0.018	-	0.0180	19.0
Achilles Point	C	23.9	5.5	19.1	5.5	12.3	40	17	7	13.6	7	10.3	0.5	0.021	0.016	0.017	0.016	0.0165	23.3
Narrowneck Beach	D	21.7	5.1	13.0	5.1	9.1	35	17	7	10.2	7	8.6	0.5	0.018	0.016	0.011	0.016	0.0135	15.0
St Leonard's Beach	C	25.0	7.4	20.0	7.4	13.7	40	17	7	13.6	7	10.3	0.5	0.020	0.016	0.016	0.016	0.0160	23.8
Castor Bay	F	32.4	8.1	13.0	8.1	10.5	24	17	7	6.8	7	6.9	0.5	0.022	0.016	0.009	0.016	0.0125	18.7
Mairangi Bay	B	11.1	7.0	11.1	-	11.1	45	17	7	17	-	12.0	0.5	0.019	0.016	0.019	-	0.0190	8.6
Waiake Bay	C	11.4	6.4	9.1	6.4	7.8	40	17	7	13.6	7	10.3	0.5	0.018	0.016	0.014	0.016	0.0150	23.8
Army Bay	F	31.1	10.2	12.4	10.2	11.4	20	17	7	6.8	7	6.9	0.5	0.021	0.016	0.008	0.016	0.0120	38.3
Waiwera Beach	F	41.3	10.2	16.5	10.2	13.4	24	17	7	6.8	7	6.9	0.5	0.022	0.016	0.009	0.016	0.0125	34.8
Opahi Bay	B	38.3	7.0	38.3	-	38.3	45	17	7	17	-	12.0	0.5	0.022	0.016	0.022	-	0.0220	21.0
Martins Bay	C	25.5	10.7	20.4	10.7	15.6	40	17	7	13.6	7	10.3	0.5	0.022	0.016	0.018	0.016	0.0170	23.4
Buckleton Beach	B	57.3	9.5	57.3	-	57.3	48	17	7	17	-	12.0	0.5	0.023	0.016	0.023	-	0.0230	19.0
Matheson Bay	E-F	98.9	13.0	49.5	13.0	31.2	25	17	7	8.5	7	7.8	0.5	0.024	0.016	0.012	0.016	0.0140	25.1
Leigh Marine Reserve	F	79.0	12.7	31.6	12.7	22.1	20	17	7	6.8	7	6.9	0.5	0.024	0.016	0.010	0.016	0.0130	14.8

Rock mass parameters for sandstone jointed rock masses

Site	σ_{ci}	GSI	M_i	D	γ	h (m)	c (MPa)	phi (deg)	σ_t (MPa)	σ_c(MPa)	σ_{cm} (MPa)	ε_m (MPa)
Cockle Bay	19.9	60	17	0.5	0.019	23.1	0.248	54.31	-0.038	1.362	4.291	5689.36
Eastern Beach	6.8	50	17	0.5	0.017	22.4	0.104	44.43	-0.006	0.233	1.124	2400.94
Musick Point	12.9	65	17	0.5	0.018	19.0	0.206	54.96	-0.038	1.239	3.188	8588.44
Achilles Point	23.9	65	17	0.5	0.021	23.3	0.356	56.11	-0.070	2.296	5.906	8588.44
Narrowneck Beach	21.7	50	17	0.5	0.018	15.0	0.147	54.82	-0.018	0.745	3.586	2400.94
St Leonard's Beach	25.0	65	17	0.5	0.020	23.8	0.363	56.52	-0.073	2.402	6.178	8588.44
Castor Bay	32.4	42	17	0.5	0.022	18.7	0.167	52.26	-0.013	0.628	4.311	1179.71
Mairangi Bay	11.1	65	17	0.5	0.019	8.6	0.149	57.90	-0.033	1.067	2.743	8588.44
Waiake Bay	11.4	63	17	0.5	0.018	23.8	0.200	51.84	-0.028	0.957	2.666	7299.60
Army Bay	31.1	45	17	0.5	0.021	38.3	0.261	48.49	-0.016	0.749	4.493	1542.00
Waiwera Beach	41.3	39	17	0.5	0.022	34.8	0.251	48.15	-0.013	0.641	5.050	901.50
Opahi Bay	38.3	55	17	0.5	0.022	21.0	0.307	56.51	-0.048	1.861	7.228	3714.16
Martins Bay	25.5	65	17	0.5	0.022	23.4	0.378	56.19	-0.075	2.450	6.302	8588.44
Buckleton Beach	57.3	65	17	0.5	0.023	19.0	0.660	61.01	-0.168	5.506	14.160	8588.44
Matheson Bay	98.9	45	17	0.5	0.024	25.1	0.401	57.56	-0.052	2.382	14.289	1542.00
Leigh Marine Reserve	79.0	45	17	0.5	0.024	14.8	0.277	59.50	-0.042	1.903	11.414	1542.00

Rock mass parameters for siltstone jointed rock masses

Site	σ_{ci}	GSI	M_I	D	γ	h (m)	c (MPa)	phi (deg)	σ_t (MPa)	σ_c(MPa)	σ_{cm} (MPa)	ε_m (MPa)
Cockle Bay	6.4	37	7	0.5	0.016	23.1	0.056	31.37	-0.004	0.085	0.471	753.13
Eastern Beach	5.5	37	7	0.5	0.016	22.4	0.051	30.49	-0.004	0.073	0.405	753.13
Musick Point	6.8	45	7	0.5	0.016	19.0	0.064	36.61	-0.009	0.164	0.633	1542.00
Achilles Point	5.5	40	7	0.5	0.016	23.3	0.057	31.47	-0.005	0.092	0.443	986.17
Narrowneck Beach	5.1	35	7	0.5	0.016	15.0	0.037	31.98	-0.003	0.058	0.353	628.98
St Leonard's Beach	7.4	45	7	0.5	0.016	23.8	0.076	35.54	-0.009	0.178	0.688	1542.00
Castor Bay	8.1	42	7	0.5	0.016	18.7	0.063	36.80	-0.008	0.157	0.691	1179.71
Mairangi Bay	7.0	45	7	0.5	0.016	8.6	0.045	42.57	-0.009	0.169	0.651	1542.00
Waiake Bay	6.5	30	7	0.5	0.016	23.8	0.046	28.17	-0.002	0.050	0.382	400.46
Army Bay	10.3	33	7	0.5	0.016	38.3	0.081	29.40	-0.005	0.100	0.668	525.14
Waiwera Beach	10.2	43	7	0.5	0.016	34.8	0.102	34.30	-0.011	0.213	0.896	1290.05
Opahi Bay	7.0	40	7	0.5	0.016	21.0	0.060	34.01	-0.006	0.117	0.563	986.17
Martins Bay	10.7	45	7	0.5	0.016	23.4	0.090	38.39	-0.014	0.258	0.995	1542.00
Buckleton Beach	9.5	45	7	0.5	0.016	19.0	0.076	39.05	-0.012	0.229	0.884	1542.00
Matheson Bay	13.0	37	7	0.5	0.016	25.1	0.080	35.98	-0.008	0.173	0.956	753.13
Leigh Marine Reserve	12.6	45	7	0.5	0.016	14.8	0.079	42.90	-0.016	0.304	1.172	1542.00

APPENDIX 7

DATABASE

See attached CD inside back cover of thesis:

- **Definition of parameters**
- **Database of Waitemata Group coastal cliff properties**
- **Correlation matrix**
- **Student t-test results**